The effect of ablation and acute inhibition of plasma membrane calcium ATPase 4 (PMCA4) with a novel inhibitor on isolated mouse mesenteric resistance arterial contractility

A thesis submitted to The University of Manchester for the degree of Doctor of Philosophy (PhD) in the Faculty of Medical and Human Sciences

Year of Submission: 2012

Sophronia Amabel Lewis

School of Medicine

Table of Contents

List of Figures

Chapter 1 Introduction

Chapter 2 Methods

Chapter 3 Results

Chapter 4 Discussion

Conclusion

List of Tables

Abstract

THE UNIVERSITY OF MANCHESTER

ABSTRACT OF THESIS submitted by Sophronia Amabel Lewis for the degree of Doctor of Philosophy (PhD), entitled 'The effect of ablation and acute inhibition of plasma membrane calcium ATPase 4 (PMCA4) with a novel inhibitor on isolated mouse mesenteric resistance arterial contractility'

December 2012

Plasma membrane calcium ATPase 4 (PMCA4) is a calcium extrusion pump which may also modulate Ca^{2+}-triggered signal transduction pathways. Previous studies postulate that PMCA4 modulates signalling via an interaction with neuronal nitric oxide synthase (nNOS) in localised plasmalemmal microdomains. The effect of PMCA4 on vascular contractility is unclear. This project has utilised PMCA4 ablated mice (PMCA4 KO $^{(-/-)}$) and a novel specific PMCA4 inhibitor (termed AP2) to study the role of PMCA4 in mouse resistance artery contractility.

Immunohistochemistry, Western blotting and polymerase chain reaction (PCR) confirmed the absence of PMCA4 in the brain, vasculature and ear snips obtained from PMCA4 KO $^{(-/-)}$ mice whereas it was present in those from wild type (WT $^{(+/+)}$) mice. Pressure myography was employed to assesss contractile function of isolated, pressurised (to 60 mmHg) mesenteric resistance arteries from 3 months old male PMCA4 KO $^{(-/-)}$ and WT $^{(+/+)}$ mice, in response to high K^+ physiological salt solution (KPSS) (40mM & 100mM) and noradrenaline (NA) (Log[NA] -9.0 to -5.0M). Passive lumen diameter and left and right wall thicknesses of arteries from PMAC4 KO $^{(-/-)}$ and WT $^{(+/+)}$ mice were taken at transmural pressures of 5-140 mmHg. Effects of acute PMCA4 inhibition with AP2 (10µM and 1µM), nitric oxide synthase (NOS) inhibition with LNNA (100µM) and specific nNOS inhibition with Vinyl-L-Nio (10µM) were also investigated. Effects of PMCA4 ablation and AP2 (10µM) on global intracellular Ca^{2+} changes ($[Ca^{2+}]_i$) in pressurised mesenteric arteries were assessed after loading arteries with the Ca^{2+}-sensitive indicator indo-1.

PMCA4 ablation had no effect on the magnitude of arterial constrictions or on the changes of $[Ca^{2+}]_i$ in response to KPSS (40mM & 100mM) or to noradrenaline. The passive intra-lumen diameter, wall thickness, wall to lumen diameter and cross sectional area of mesenteric arteries across the intravascular pressure range studied were also not modulated by PMCA4 ablation. A leftwards shift in the stress to strain relationship and significant increase in beta elastic modulus (β) were revealed in arteries from PMCA4 KO $^{(-/-)}$ mice compared to those from WT $^{(+/+)}$ mice, suggesting that PMCA4 ablation reduces mesenteric arterial distensibility. Acute PMCA4 inhibition with AP2, significantly reduced arterial constrictions and the increase in $[Ca^{2+}]_i$ in response to noradrenaline in arteries from WT $^{(+/+)}$ mice, but had no effect on arterial constrictions elicited by arteries from PMCA4 KO $^{(-/-)}$ mice. Inhibitory effects of AP2 were not present in arteries after NOS inhibition by LNNA and also after nNOS inhibition with Vinly-L-Nio. Hence, PMCA4 inhibition with AP2 reduces vascular constriction by a nNOS-dependent mechanism.

In conclusion, the main findings of the study were that ablation and acute inhibition of PMCA4 with AP2 have different effects on mouse mesenteric resistance arterial contractility. This study provides more insight into PMCA4 as a significant modulator of signalling within the vasculature via effects on nNOS.

Declaration

No portion of the work referred to in this thesis has been submitted in support of an application for another degree or qualification of this or any other university or other institute of learning.

Copyright Statement

i. The author of this thesis (including any appendices and/or schedules to this thesis) owns certain copyright or related rights in it (the "Copyright") and she has given The University of Manchester certain rights to use such Copyright, including for administrative purposes.

ii. Copies of this thesis, either in full or in extracts and whether in hard or electronic copy, may be made **only** in accordance with the Copyright, Designs and Patents Act 1988 (as amended) and regulations issued under it or, where appropriate, in accordance with licensing agreements which the University has from time to time. This page must form part of any such copies made.

iii. The ownership of certain Copyright, patents, designs, trade marks and other intellectual property (the "Intellectual Property") and any reproductions of copyright works in this thesis, for example graphs and tables ("Reproductions"), which may be described in this thesis, may not be owned by the author and may be owned by third parties. Such Intellectual Property and Reproductions cannot and must not be made available for use without the prior written permission of the owner(s) of the relevant Intellectual Property and/or Reproductions.

iv. Further information on the conditions under which disclosure, publication and commercialisation of this thesis, the Copyright and any Intellectual Property Rights and/or Reproductions described in it may take place is available from the University IP Policy (see http://www.campus.manchester.ac.uk/medialibrary/policies/interllectual-property.pdf), in any relevant Thesis restriction declarations deposited in the University Library, The University Library's regulations (see

http://www.manchester.ac.uk/library/aboutus/regulations) and in The University's policy on presentation of Theses.

Dedication

This thesis is dedicated to my dearest and loving mother the Late Mrs Moira, Gladys, Lois Lewis who passed away on the 15th December 2002 due to a heart condition. You will always be my insipiration.

Acknowledgements

First I would like to express my sincerest gratitude to my supervisors Dr Clare Austin and Dr Elizabeth Cartwright for all their valuable advice, patience, academic guidance and supervision over the last four years. I am truly grateful for their approachability and genuine concern shown to me during the course of my study. I acknowledge the support given to me by my advisor the late Dr Stephen O'Neil and would like to thank Dr Yvonne Alexander for stepping in as my advisor towards the end of my study.

I would like to extend a special thankyou to past and present members of Dr Clare Austin's Lab and Professor Ludwig Neyses' Lab, in particular Dr Natasha Hausman, Ms Lucy Walton, Mr Christopher Cobb, Dr Sarah Withers, Dr Fiona Lynch, Dr Mohamed Shaheen, Dr Tamer Mohamed and Ms Florence Baudoin for their technical support and help with experimental techniques.

To my family and friends who have been an unending source of moral support and encouragement I am truly grateful. To my brothers, sister and father, thankyou for always believing in me and inspiring me to always do better. Special thank you to all the wonderful friends I have become acquainted with at the University of Manchester who made my PhD experience thoroughly enjoyable and unforgettable.

Finally I would like to thank the British Heart Foundation for providing the funding that has made this project possible.

Abbreviations

ACh	Acetylcholine
ADP	Adenosine diphosphate
AM	Acetoxymethylester
AMP	Adenosine monophosphate
ANOVA	Analysis of Variance
ATP	Adenosine trisphosphate
BCA	Bicinchoninic acid
BK_{Ca}	Large conductance calcium-activated potassium channel
BSA	Bovine serum albumin
BSU	Biological Services Unit
bp	Base pairs
Ca^{2+}	Calcium
$Ca^{2+}Cl_2.2H_2O$	Calcium chloride dihydrate
CaM	Calmodulin
CaM-BD	Calmodulin bidning domain
Cav-1	Caveolin-1
cAMP	Cyclic-adenosine monophosphate
cGMP	Cyclic-guanosine monophosphate
CICR	Calcium induced calcium release
CPI-17	Protein kinase C-potentiated protein phosphatase inhibitor protein 17kDa

CSA	Cross sectional area
CVD	Cardiovascular disease
DAG	Diacylglycerol
DAPI	N,N'-4-xylylenebis (pyridium)
DPX	4',6-diamidino-2-phenylindole dihydrochloride
DMSO	Dimethyl sulfoxide
DNA	Deoxyribonucleic acid
dNTP	Deoxyribonucleotide triphosphate
EC	Endothelial cell
ECM	Extracellular matrix
ECL	Enhanced chemiluminescent solution
EDHF	Endothelium derived hyperpolarising factor
EDTA	Ethylene diamine tetra-acetic acid
EET	Epoxyeicosatrienoic acid
EGTA	Ethylene glycol tetra-acetic acid
Em	Membrane potential
eNOS	Endothelial nitric oxide synthase
FITC	Fluorescence isothiocynate
GAPDH	Glyceraldehyde 3-phosphate dehydrogenase
GPCR	G-protein coupled receptor
Gαq/11	Guanine nucleotide binding protein alpha q 11
Gαq 12/13	Guanine nucleotide binding protein alpha q 12/13

HCl	Hydrochloric acid
H&E	Hematoxylin & eosin
HEPES	4-(2-Hydroxyethyl)-1-piperazineethanesulfonic acid
HRP	Horseradish peroxidase
Ht $^{(+/-)}$	Heterozygote
IgG	Immunoglobulin G
IP_3	Inositol 1,4,5 trisphosphate
IP_3R	Inositol 1,4,5 trisphosphate receptor
IMS	Industrial methylated spirit
iNOS	Inducible nitric oxide synthase
K^+	Potassium ion
K_{Ca}	Calcium-activated potassium channel
KCl	Potassium chloride
kDa	Kilo dalton
K_2EDTA	Ethylenediaminetetraacetic acid dipotassium salt
$KHPO_4$	Potassium dihydrogen orthophosphate
KO $^{(-/-)}$	Knockout
KPSS	Potassium physiological salt solution
L-NAME	N^G-nitro-L-arginine methyl ester
LNNA	N^G-nitro-L-arginine
LQTS	Long QT syndrome

MAGUK	Membrane-associated guanylate kinase
mβcd	Methly-beta-cyclodextrin
MLC_{20}	Myosin (at serine residue 19 of the 20kDa regulatory myosin light chain)
$MLC2_V$	Myosin light chain kinase promoter
MLCK	Myosin light chain kinase
MLCP	Myosin light chain phosphatase
NA	Noradrenaline
NaCl	Sodium chloride
$NaHCO_3$	Sodium hydrogen carbonate
NADPH	Nicotinamide adenine dinucleotide phosphate
NCX	Sodium-calcium exchanger
NFAT	Nuclear factor of activated T-cell
NKA	Sodium-potassium ATPase
nNOS	Neuronal nitric oxide synthase
NO	Nitric oxide
NOS	Nitric oxide synthase
NS	Not significant
PBS	Phosphate buffer solution
PCR	Polymerase chain reaction
PDVF	Polyvinylidene fluoride
PDZ-BD	PSD 95, drosophila discs large protein and zone occludens-1 binding domain

PGI_2	Prostacyclin
PKA	Protein kinase A
PKC	Protein kinase C
PKG	cGMP-dependent protein kinase
PL	Activatory acidic phospholipid
PL-BD	Activatory acidic phospholipid binding domain
PLC	Phospholipase C
PLN	Phospholamban
PMCA	Plasma membrane calcium ATPase
PMT	Photon multiplier tube
PSS	Physiological salt solution
RASSF-1	Ras-associated factor 1
RhoA	Ras homolog gene family member A
Rho-GEF	Rho-guanine nucleotide exchange factor
Rho-K	Rho-associated protein kinase
ROCC	Receptor-operated calcium channel
ROCE	Receptor-operated calcium entry
ROS	Reactive oxygen species
RT-PCR	Real time- polymerase chain reaction
SDS	Sodium dodecyl sulphate
SDS-PAGE	Sodium dodecyl sulphate polyacrylamide gel electrophoresis
SEM	Standard error mean

SERCA	Sarco-endoplasmic reticulum calcium ATPase
sGC	Soluble guanylyl cyclase
SOCC	Store-operated calcium channel
SOCE	Store-operated calcium entry
SM	Smooth muscle
SNP	Sodium nitroprusside
SR	Sarco-endoplasmic reticulum
STIM1	Stromal interacting molecule 1
TAC	Transverse aortic constriction
TAE	Tris-acetate-ethylene diamine tetra-acetic acid
TBS	Tris buffered saline
TBST	Tris buffered saline plus Tween
TM	Transmembrane domain
TNF	Tumour necrosis factor
TRPC	Transient receptor potential channel
VLN	Vinyl-L-Nio
VOCC	Voltage-operated calcium channel
VSM	Vascular smooth muscle
WT	Wall thickness
WT $^{(+/+)}$	Wild type

Preface

My scientific research experience began while studying for my BSc in Biochemistry with molecular biology at Cardiff University where I completed a six weeks laboratory project for my final year dissertation entitled 'Protein engineering of an intracellular subtilisin protease' in 2005. Later on in 2008, I graduated from the University of Bristol with an MSc in Biomedical research which ecompassed lecture-based modules and a twelve week practical project with the Department of Anatomy. This was entitled 'Analysis of changes in glutamate receptors in the brain in type II diabetes'.

Experimental data presented in this thesis was obtained during the course of my PhD study which commenced in January 2009. All practical work was performed within the Cardiovascular Research Group at The University of Manchester.

Presentations derived from this thesis

Oral presentation

Ablation and acute inhibition of plasma membrane calcium ATPase 4 (PMCA4) with a novel inhibitor have different effects on isolated mouse mesenteric resistance arterial contractility. **S. Lewis**, C. Cobb, L. Neyses, E.J. Cartwright and C. Austin. The Physiological Society's vascular & smooth muscle themed meeting, (*Proc Physiol Soc* 25; 2011 (C06)), Edinburgh, UK, December 2011**. Awarded travel grant from the Physiological Society.**

Poster presentations

Different effects of plasma membrane calcium ATPase 4 (PMCA4) ablation and acute inhibition on contractility of isolated mouse mesenteric arteries. (*Artery Research* (2011), 5 (4) pg 183-184). **S. Lewis**, C. Cobb, L. Neyses, E.J. Cartwright and C. Austin. Artery 11 meeting, Paris, France, October 2011. **Awarded travel grant from the University of Manchester.**

The different effects of plasma membrane calcium ATPase 4 (PMCA4) ablation and acute inhibition with a novel inhibitor on constriction of isolated mouse mesenteric resistance arteries. **S. Lewis**, C. Cobb, L. Neyses, E. Cartwright and C. Austin. Northern Cardiovascular research group (NCRG) meeting, Hull, UK, April 2011.

Plasma membrane calcium ATPase 4 (PMCA4) ablation and acute inhibition; the differing effects on the contractile function of isolated mouse mesenteric arteries. **S. Lewis**, C. Cobb, L. Neyses, E. Cartwright and C. Austin. British Heart Foundation (BHF) fellow day meeting, Cambridge, UK, April 2011.

Paper in preparation

Title: 'Different effects of plasma membrane calcium ATPase 4 (PMCA4) ablation and acute inhibition on contractility of isolated mouse mesenteric arteries'. **S. Lewis**, C. Cobb, L. Neyses, E. Cartwright and C. Austin.

Chapter 1

Introduction

1.1 Impact of cardiovascular diseases (CVD) in the UK

Cardiovascular diseases (CVDs) encompass both cardiac and circulatory diseases and are a predominant cause of death in the UK as well as in other high-income countries (American Heart Association (AHA) 2008; Capewell *et al.*, 2008; Scarborough *et al.*, 2010; Young *et al.*, 2010). CVD is estimated to cause close to 200,000 deaths per year in the UK and there are more than three million individuals living with CVD in the UK (Scarborough *et al.*, 2010). CVD is also emerging as a significant cause of premature deaths, i.e. death before the age of 75 (Capewell *et al.*, 2008; Scarborough *et al.*, 2010). The current incidence of CVD is also a global issue and is set to increase given the rise in the aging population with predicted consequences to healthcare systems worldwide (American Heart Association (AHA) 2008; World Health Organisation (WHO); Dalton *et al.*, 2011; Heidenreich *et al.*, 2011). The overall cost implications of CVD to the UK economy has been recorded as over £30 billion (according to 2006 prices) and around £14.4 billion to the National Health Service (NHS) (an equivalent of 21% of all NHS expenditure) (Scarborough *et al.*, 2010). Therefore taking into consideration the significant consequences of CVDs (on mortality rates, public health and financial burden to the NHS and UK economy), there is a need for the improvement and development of effective CVD treatments and strategies aimed at targeting high CVD risk factors; one such risk factor is elevated blood pressure or hypertension.

The incidence of hypertension has increased over recent years and indeed a health survey for England has revealed an increase estimated at around 50% in the incidence of controlled hypertension between 2003 and 2010 with a prevalence of 31.5% and 29% among men and women respectively in 2010 (Health Survey for England 2010). However the true incidence is probably higher due to undiagnosed hypertension and it is suggested that there are as many as five million men and women in the UK with undiagnosed high blood pressure (Health Survey for England 2010). Developing and/or improving CVD treatments are heavily reliant upon an understanding of the mechanisms that govern homeostasis in the cardiovascular system. Though the underlying mechanisms responsible for the development and/or progression of CVDs are likely to be multiple and varied, functional and/or structural changes in the contractility of small resistance vessels associated with subsequent alterations in vascular resistance and blood flow are believed to be of prime importance (Feihl *et al.*, 2008; Mulvany, 2008; Schofield *et al.*, 2002). Indeed functional and structural changes in the small resistance vasculature are evident in numerous pathological conditions such as hypertension and diabetes (Feihl *et al.*, 2008; Mulvany, 2002; Sachidanandam *et al.*, 2009; Schofield *et al.*, 2002). Therefore, understanding the mechanisms that regulate contractility and structure in these resistance vessels will be extremely beneficial in the identification of new treatments for CVDs.

1.2 The importance of the resistance arteries in the cardiovascular system

The vascular network is comprised of arteries, arterioles, capillaries, venules and veins which are of crucial importance in the cardiovascular system. Together the small arteries and arterioles represent the resistance vessels. Resistance arteries are generally considered to have lumen diameters between 100 and 300 µm (Christensen *et al.*, 1993; Christensen *et al.*, 2001; Mulvany, 1987; Mulvany *et al.*, 1990; Rosei *et al.*, 2005). According to Poiseuille's law, resistance is inversely proportional to the radius of a vessel to the fourth power (*R (resistance) α 1/r (radius)* ^{4}*)* (Wheeler *et al.*, 1995), therefore even small changes in the diameter of resistance arteries may have a large impact on vascular resistance to blood flow. Importantly, in the cardiovascular system it is the diameter of resistance arteries which controls vascular resistance and this may affect the distribution blood flow in microvessels as well as the regulation of systemic blood pressure (Martinez-Lemus *et al.*, 2009; Simonsen *et al.*, 2012).

With the exception of the capillaries and smallest venules, the vascular walls of all other blood vessels, including the resistance arteries, are defined by three distinct layers starting with the inner most tunica intima layer, the middle tunica media and the outermost tunica adventitia (Martinez-Lemus, 2012; Martinez-Lemus *et al.*, 2009; Mulvany *et al.*, 1990; Rhodin *et al.*, 1980; Simonsen *et al.*, 2012) (figure 1.2.1). The tunica intima contains the delicate endothelium whereas the media is mainly comprised of smooth muscle cells and elastin fibres (figure 1.2.1). The outer most layer of the vessel wall, the adventitia, contains collagen fibres (figure 1.2.1). Both the vascular smooth muscle (VSM) and the endothelium are most crucial to the contractile function of resistance arteries whereas the collagen and elastin fibres contribute most to the structural integrity of vascular walls as well as to their mechanical properties (Briones *et al.*, 2003; Gonzalez *et al.*, 2005; Mulvany *et al.*,

1990; Simonsen *et al.*, 2012). The relative components of these layers may be different depending on the size of the blood vessel (figure 1.2.1). The intima of small resistance arteries is similarly arranged to the intima of larger conduit arteries, where a thin layer of endothelial cells form the endothelium (Megens *et al.*, 2007; Mulvany *et al.*, 1990; Rhodin *et al.*, 1980). The main differences in vascular wall arrangements exist in the tunica media and adventitia. The media of small resistance arteries have a higher proportion of smooth muscle cells when compared to elastin fibres and are often referred to as small muscular arteries (Megens *et al.*, 2007) (figure 1.2.1). The large smooth muscle component of resistance arteries is related to their function whereby they need to be able to rapidly constrict and relax in response to physiological factors in order to alter their lumen and thus resistance to blood flow (Martinez-Lemus *et al.*, 2009; Mulvany *et al.*, 1990; Simonsen *et al.*, 2012) (figure 1.2.1). On the other hand the adventitia is thicker in the larger conduit arteries, (also known as elastic arteries) than in the small arteries because these larger arteries have a major role in distribution of arterial blood (Megens *et al.*, 2007; Mulvany *et al.*, 1990; Rhodin *et al.*, 1980) (figure 1.2.1). The elastic nature of larger conduit arteries (usually exposed to high pulsatile pressures resulting from the intermittent outflow of blood from the heart) enables them to rapidly distend and accommodate high pressures thereby dampening the pressure fluctuations in downstream resistance arteries. It is the contractile state of the VSM that governs the diameter of resistance arteries which influences blood flow to peripheral tissues by modulating vascular resistance. Indeed changes in both the contractility and structure of resistance arteries, evident in some CVD diseased states for example hypertension, can modulate vascular resistance (Folkow, 1956; Folkow *et al.*, 1958). As such, it is

important that we understand the mechanisms which control and modulate resistance arterial diameter.

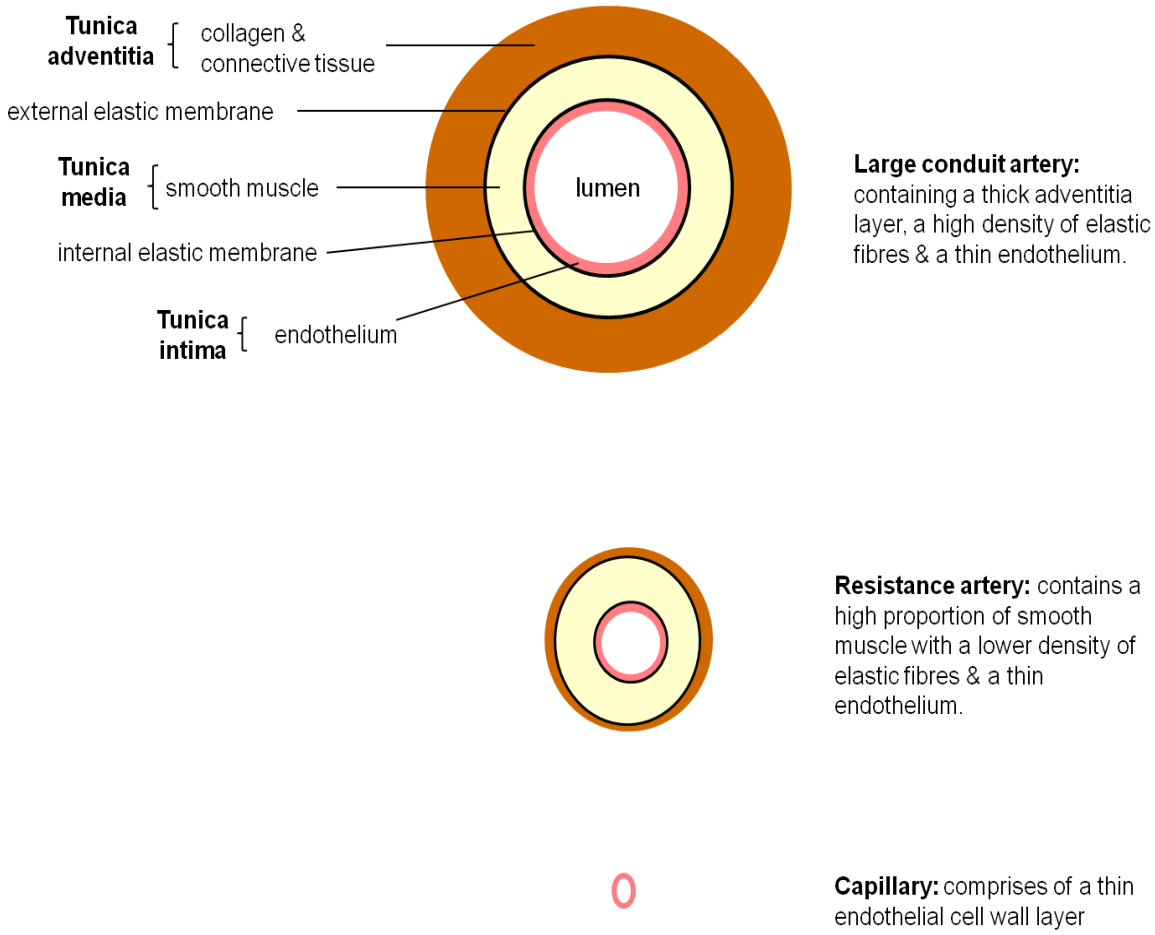

Figure 1.2.1: A schematic representation of arteries of the systemic circulation and their structural components. The larger arteries function to distribute blood pumped from the heart to the arteries downstream facilitated by their high elastic densities which allows them to distend and recoil in response to outflow from the heart. The resistance arteries possess a large smooth muscle component which mediates changes in diameter (in response to physiological factors) and thus regulates vascular resistance and blood flow. The capillaries have thin walls to allow for the exchange of material between blood and interstitial fluid.

1.3 Regulation of arterial diameter

The active diameter of arteries (i.e. the vascular tone) is governed by the contractile state of VSM cells and these can be modulated by chemical stimuli (for example hormones and neurotransmitters) or physical stimuli (for example alterations in flow and intraluminal pressure). These stimuli may induce modulations in the arterial diameter by acting directly on VSM cells or on the endothelium which releases vasoactive factors (discussed in section 1.3.2).

1.3.1 Mechanisms underlying modulation of VSM contractility; the role of calcium

Calcium plays a key role in modulation of VSM contractility and thus in modulation of arterial diameter (Berra-Romani *et al.*, 2008; Berridge, 1995; House *et al.*, 2008; Matchkov *et al.*, 2012; Somlyo *et al.*, 2003; Wamhoff *et al.*, 2006). Ultimately, an increase in intracellular free Ca^{2+} ($[Ca^{2+}]_i$) results in VSM constriction whereas a decrease results in VSM relaxation (Akata, 2007; Somlyo *et al.*, 1994a). Contractile stimuli (including both chemical and physical factors) can result in an increase in VSM cell $[Ca^{2+}]_i$ causing the cytosolic protein calmodulin (CaM) to bind four Ca^{2+} ions (Means *et al.*, 1991; Orallo, 1996). A conformational change induced in CaM encourages the $4Ca^{2+}$-CaM complex to bind to and activate myosin light chain kinase (MLCK) resulting in phosphorylation of myosin (at serine residue 19 of the 20kDa regulatory myosin light chain (MLC_{20})) (Sweeney *et al.*, 1994; Zhi *et al.*, 1994) (figure 1.3.1.1). This phosphorylation of MLC_{20} facilitates the activation of myosin adenosine triphosphatase (ATPase) by actin, causing the VSM to contract as a result of MgATP-dependent crossbridge cyclic interactions between myosin and

actin (Itoh *et al.*, 1989; Kamm *et al.*, 1989; Pfitzer, 2001; Somlyo *et al.*, 1994a; Somlyo *et al.*, 1994b).

While increases in $[Ca^{2+}]_i$ play a key role in VSM cell constriction, both chemical and physical stimuli are known to facilitate constriction by affecting the Ca^{2+} sensitivity of the actin-myosin contractile machinery (Himpens *et al.*, 1989; Hirano, 2007; Pfitzer, 2001; Ratz *et al.*, 2009). At a given $[Ca^{2+}]_i$, Ca^{2+} sensitisation causes and/or maintains the contractile force of the actin-myosin cross bridges by regulating the phosphorylation of MLC_{20} independently of MLCK signalling (Ganitkevich *et al.*, 2002; Martinez-Lemus *et al.*, 2009; Somlyo *et al.*, 2003).

Agonist activation of G-protein coupled receptors (GPCRs) on VSM cell membrane have been reported to increase the Ca^{2+} sensitisation of VSM via the Rho-associated protein kinase (RhoK) pathway (figure 1.3.1.1). RhoK, in turn, mediates the phosphorylation of MLC_{20} via inactivating myosin light chain phosphatase (MLCP) (discussed later) (Hirano, 2007; Ratz *et al.*, 2009; Sakurada *et al.*, 2001; Sakurada *et al.*, 2003). Dephosphorylation of MLC_{20} may be inhibited independently of the RhoK pathway by the activation of protein kinase C-potentiated protein phosphatase inhibitor protein 17kDa (CPI-17) (an inhibitor of MLCP), although this is thought to have a minor role in Ca^{2+} sensitisation (Eto *et al.*, 1995) (figure 1.3.1.1).

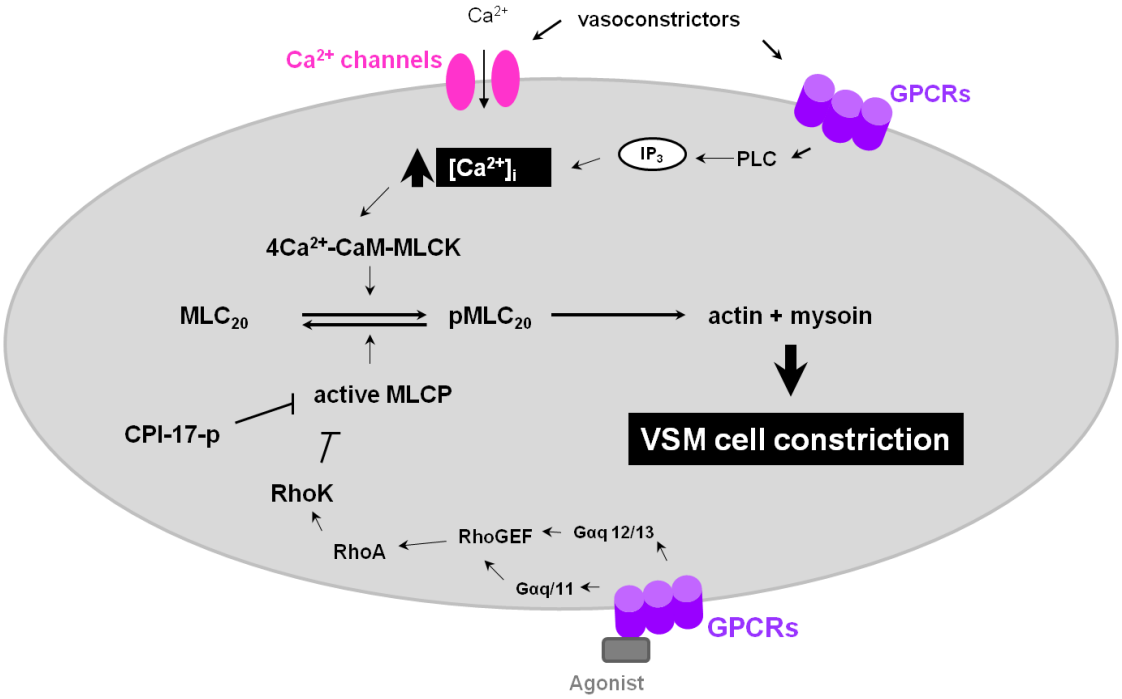

Key: CaM - calmodulin; **CPI-17-p** - (phosphorylated) protein kinase C-potentiated protein phosphatase inhibitor protein 17kDa; **GPCR** - G-protein coupled receptor; **Gαq/11** - guanine nucleotide binding protein alpha q 11; **Gαq 12/13** - guanine nucleotide binding protein alpha q 12/13; **IP_3** - inositol 1,4,5 trisphosphate; **MLCK** - myosin light chain kinase; **MLCP** - myosin light chain phosphatase; **(p)MLC_{20}** - (phosphroylated) myosin (at serine residue 19 of the 20kDa regulatory myosin light chain); **PLC** - phospholipase C; **RhoA** - Ras homolog gene family, member A; **RhoK** - Rho-associated protein kinase; **Rho GEF** - Rho-guanine nucleotide exchange factor; **VSM** - vascular smooth muscle

Figure 1.3.1.1: Mechanisms involved in VSM cell constriction. This may arise as a result of increases in $[Ca^{2+}]_i$ levels and/or enhanced Ca^{2+} sensitisation of the contractile machinery within the VSM cell due to stimulation of the VSM cell by a contractile stimuli. Increases in $[Ca^{2+}]_i$ facilitate VSM constriction via myosin light chain kinase (MLCK) dependent phosphorylation of myosin (at serine residue 19 of the 20kDa regulatory myosin light chain (MLC_{20})). Activation of the Rho-associated protein kinase (RhoK) pathway or phosphorylation of protein kinase C-potentiated protein phosphatase inhibitor protein 17kDa (CPI-17) leads to inactivation of the myosin light chain phosphatase (MLCP) and mediates phosphorylation of MLC_{20} as the VSM cell becomes sensitised to Ca^{2+}.

Relaxation of VSMCs is induced by a significant decrease in elevated $[Ca^{2+}]_i$ levels. The decrease in $[Ca^{2+}]_i$ may be either by $[Ca^{2+}]_i$ extrusion to the extracellular space and/or reuptake into intracellular Ca^{2+} stores (discussed in more detail in section 1.5). A decrease in available $[Ca^{2+}]_i$ allows CaM to be dissociated from the $4Ca^{2+}$-CaM-MLCK complex thereby inactivating MLCK, activating MLCP and resulting in dephosphorylation of MLC_{20} (independently of Ca^{2+}) (Orallo, 1996; Somlyo *et al.*, 2003; Somlyo *et al.*, 1994a). In turn dephosphorylated MLC_{20} inactivates the acto-myosin ATPase consequently causing relaxation of VSM (Orallo, 1996; Somlyo *et al.*, 1994a). The activity of MLCP is independent of any further changes to $[Ca^{2+}]_i$ and is involved in the Ca^{2+} desensitisation process of the contractile filaments in VSM cells (Somlyo *et al.*, 2003). While Ca^{2+} sensitisation may be important in reducing the energy used by the VSM contractile machinery in order to efficiently sustain vasoconstriction (Somlyo *et al.*, 2003) as time progresses the contractile machinery becomes desensitised to $[Ca^{2+}]$ favouring relaxation (Yagi *et al.*, 1988).

1.3.2 Role of the endothelium in the regulation of arterial contractility

The contractile state of the VSM, which ultimately determines arterial diameter, can also be modulated by vasoactive factors released from the endothelium (in the tunica intima layer). As such the endothelium has a major role in regulating vascular tone (Furchgott *et al.*, 1987; Furchgott *et al.*, 1980).

The endothelium, in response to various stimuli (for e.g. increased flow/shear stress, acetylcholine, serotonin and bradykinin), may release endothelium-derived vasodilators including nitric oxide (NO), prostacyclin (PGI_2) (a signalling product of prostaglandin) and endothelium-derived hyperpolarising factors (EDHF) which act on the VSM (Babiluri, 2009; Feletou *et al.*, 2006b; Furchgott, 1983; Furchgott *et al.*, 1980; Pohl *et al.*, 1986). An important vasoactive molecule that can be released by the endothelium is NO (discussed in detail in section 1.3.3). Also released by endothelial cells is PGI_2 which activates specific PGI_2 receptors on VSM which, via coupling to adenylate cyclase, increases cyclic-adenosine monophosphate (cAMP) levels and as such stimulate VSM relaxation (Abe *et al.*, 1992; Coleman *et al.*, 1994; Kukovetz *et al.*, 1979; Mombouli *et al.*, 1999; Moncada *et al.*, 1979). However, PGI_2 release may also lead to opening of endothelial cell potassium channels, resulting in hyperpolarisation of the underlying VSM which promotes arterial relaxation (Feletou *et al.*, 2006a; Feletou *et al.*, 2006b; Moncada *et al.*, 1979). Another endothelium derived vasoactive prostanoid, thromboxane A_2 (which is derived from the metabolism of arachadonic acid) conversely, has been shown to mediate vascular constriction and abnormalities in its activity are associated with CVDs (including thrombotic stroke, peripheral artery disease and embolism) (Flower, 2006; Moncada, 1982; Ogletree, 1987; Patrono *et al.*, 1990; Whittle *et al.*, 1981). It is now evident

that EDHF mediated pathways are of crucial importance in mediating endothelial-dependent dilatory responses in many arteries (Busse *et al.*, 2002; Chen *et al.*, 1989; Feletou *et al.*, 2006b; Waldron *et al.*, 1999). The identity of EDHFs remains controversial. It has been proposed that K^+ ions themselves may act as an EDHF. K^+ ions released from endothelial potassium channels (i.e. small and intermediate conductance Ca^{2+}-sensitive K^+ channels (SK_{Ca}) and (IK_{Ca})) accumulate in intercellular spaces, which activate K^+ channels on VSM cells eventually resulting in their membrane hyperpolarisation (Bradley *et al.*, 1999a; Bradley *et al.*, 1999b; Edwards *et al.*, 1998a; Edwards *et al.*, 1998b; Edwards *et al.*, 2004; Feletou *et al.*, 2009; Feletou *et al.*, 2006b; Haddy *et al.*, 2006). The spread of hyperpolarisation from the endothelium to the VSM, and thus VSM relaxation, is facilitated by electrical coupling through myoendothelial gap junctions (Beny *et al.*, 1994; Emerson *et al.*, 2000; Yamamoto *et al.*, 1999). In addition to K^+ ions, reactive oxygen species (ROS) and metabolites of arachidonic acids, epoxyeicosatrienoic acids (EETs), have all been proposed as EDHFs which can modulate arterial tone (Edwards *et al.*, 1998a; Ellis *et al.*, 2003; Feletou *et al.*, 2009; Feletou *et al.*, 2006b; Haddy *et al.*, 2006; Oltman *et al.*, 1998; Quilley *et al.*, 2000; Widmann *et al.*, 1998).

It is appreciated that although all three endothelium-derived vasoactive substances (i.e. NO, PGI_2, EDHF) are known to contribute to the regulation of vascular tone, their relative contributions may depend on the type of stimuli, size of the vessel and/or the species (Andresen *et al.*, 2006; Luksha *et al.*, 2009; You *et al.*, 1999). For example in larger mammalian arteries like the aorta it is NO that is responsible for endothelial-dependent vasodilations in response to acetylcholine (ACh) (Furchgott *et al.*, 1980). In the smaller resistance arteries, endothelium dependent relaxations to ACh are mediated largely by EDHF-mediated membrane hyperpolarisations of VSM

cells (Buus *et al.*, 2000; Furchgott *et al.*, 1987; Garland *et al.*, 1992; Sandow *et al.*, 2000).

1.3.3 Sources of NO and NO-mediated signalling in the vasculature

NO is an important vasoactive factor that is synthesised by three distinct NO synthase (NOS) enzymes, i.e. endothelial NOS (eNOS), neuronal NOS (nNOS) and inducible NOS (iNOS) and can be released by the vascular endothelium as well as other tissues of the body. All NOSs catalyse the oxidation of a guanidino nitrogen atom of L-arginine to NO and L-citrulline utilising molecular O_2 and NADPH as co-substrates (Boucher *et al.*, 1999; Forstermann *et al.*, 1995; Kerwin *et al.*, 1995; Stuehr *et al.*, 1991b). The constitutively expressed eNOS and nNOS were first characterised in mammalian vascular endothelial cells and neurons respectively and are dependent on Ca^{2+}-CaM (Boucher *et al.*, 1999; Forstermann *et al.*, 1995; Forstermann *et al.*, 1990; Forstermann *et al.*, 1991; Pollock *et al.*, 1993). However iNOS was first identified in murine macrophages and is mainly independent of Ca^{2+} due to its high affinity for CaM (Boucher *et al.*, 1999; Hevel *et al.*, 1991; Stuehr *et al.*, 1991a).

In the vasculature eNOS is mainly found in the endothelium and it is known to have important roles in the regulation of vascular tone, blood flow as well as systemic blood pressure (Furchgott *et al.*, 1989; Moncada *et al.*, 1991; Shimokawa, 1999; Vanhoutte, 1989). The nNOS enzyme is present in both the endothelium and VSM layers of arteries and, while there is still very little known about the localisation of iNOS within the vasculature, some have suggested it is present in VSM (Bachetti *et al.*, 2004; Boulanger *et al.*, 1998; Buchwalow *et al.*, 2002; Buchwalow *et al.*, 2004;

Segal *et al.*, 1999). NO sourced from nNOS and iNOS has been linked to vasodilation and vascular protection against lesion formation under certain pathological conditions (Huang *et al.*, 2002; Lamping *et al.*, 2000; Yogo *et al.*, 2000). Studies which have used arteries from nNOS and eNOS knockout animal models and/or the use of selective inhibitors have confirmed that nNOS and eNOS may modulate vascular tone (Gros *et al.*, 2003; Ichihara *et al.*, 1998; Melikian *et al.*, 2009; Seddon *et al.*, 2009; Waldron *et al.*, 1999). The NOS system is important to the maintenance of normal vascular function as an over or under-production of NO is present in certain pathologies, and a reduced NO bioavailability has been shown in vascular disease states including hypertension and atherosclerosis (Hobbs *et al.*, 1999; Mombouli *et al.*, 1999; Moncada *et al.*, 2006; Shimokawa, 1999). Furthermore, it has been shown that the n/i/eNOS knockout mice (in which all NOSs were ablated) may spontaneously develop vascular diseases such as hypertension and other cardiovascular pathologies (Nakata *et al.*, 2008).

NO modulates vascular tone by mediating increases in cyclic-guanosine monophosphate (cGMP) levels through its interaction and activation of soluble guanylyl cyclase (sGC) (Lincoln *et al.*, 1994; Mombouli *et al.*, 1999; Rapoport *et al.*, 1983). Elevated levels of cyclic nucleotides, mainly cGMP, in the cytoplasm of VSM cells are crucial to the relaxation of pre-constricted VSM (Morgado *et al.*, 2012; Orallo, 1996). cGMP can modulate vascular tone by activation of cGMP-dependent protein kinases which in turn reduce the sensitivity of the contractile machinery to Ca^{2+} and/or decrease levels of intracellular free Ca^{2+} ($[Ca^{2+}]_i$) ultimately causing VSM cells to relax (Lee *et al.*, 1997; Orallo, 1996). NO may also hyperpolarise the underlying VSM cells by activating potassium channels in a cyclic GMP-dependent manner (Bolotina *et al.*, 1994; Feletou *et al.*, 2006b; Plane *et al.*,

1998). Additionally NO can modulate vascular tone independently of the NO/cGMP signalling cascade because it can interact with other ionic channels of VSM cells and influence VSM cell membrane potential through mechanisms involving hyperpolarisations (Bolotina *et al.*, 1994; Feletou *et al.*, 2006b). Therefore the contractile state of VSM cells and thus arterial diameter and vascular resistance can be modulated both by factors acting directly on the VSM layer or by endothelium-derived factors acting on the VSM. A further process, via which resistance arterial diameter and vascular resistance can be modulated, evident in certain CVD pathologies is via structural remodelling of the resistance vasculature.

1.3.4 Structural remodelling of resistance arteries

Vascular remodelling of the small resistance arteries has been found in hypertension and may influence peripheral resistance and blood pressure as well as in other pathologies predisposed to developing CVD i.e. diabetes, obesity and acromegaly (Grassi *et al.*, 2010; Mulvany, 2012; Paisley *et al.*, 2009; Rizzoni *et al.*, 2001; Rizzoni *et al.*, 2009b; Simonsen *et al.*, 2012).

In essential hypertension inward eutrophic remodelling is evident (Aalkjaer *et al.*, 1987; Falloon *et al.*, 1994; Heagerty *et al.*, 1993; Rizzoni *et al.*, 1996; Schiffrin *et al.*, 1992). Eutrophic remodelling is characterised by a rearrangement of existing wall material around a smaller diameter resulting in an increased media-to-lumen ratio with no change in wall cross sectional area (CSA) (Bakker *et al.*, 2004; Korsgaard *et al.*, 1993; Mulvany, 1999; Mulvany *et al.*, 1996). In contrast, hypertrophic remodelling has been found in patients with secondary hypertension, diabetes mellitus and obesity (Grassi *et al.*, 2010; Rizzoni *et al.*, 2012; Rizzoni *et al.*,

2001; Schofield *et al.*, 2002). Vascular hypertrophic remodelling is manifested by thickening of the vessel wall (i.e. increased CSA), increased wall-to-lumen ratio arising from VSM cells contributing to wall growth and a reduced lumen diameter (Mulvany, 1999; Rizzoni *et al.*, 1996). While eutrophic remodelling is thought to be protective in maintaining wall stress near normal, hypertrophic remodelling is thought to be detrimental and has been suggested to contribute to target end-organ damage (Mulvany, 2002; Mulvany, 2008; Simonsen *et al.*, 2012; Strain *et al.*, 2005).

Changes to the structural mechanical properties of arteries i.e. distensibility, have also been shown in certain vascular disease states such as hypertension. While a decrease in arterial distensibility (i.e. increased arterial stiffness) has been shown in the large arteries (Hajdu *et al.*, 1994), an increase in distensibility has been observed in small arteries from hypertensive subjects (Baumbach *et al.*, 1989; Bund, 2001; Hajdu *et al.*, 1994; Heagerty *et al.*, 1993; Schofield *et al.*, 2002) although this is not a universal finding (Hayoz *et al.*, 1992; Intengan *et al.*, 1999; Laurent *et al.*, 1994). Changes in arterial distensibility are thought to be related to modifications in the components of the vascular wall extracellular matrix mainly elastin, collagen and fibronectin (Martinez-Lemus *et al.*, 2009; Rizzoni *et al.*, 2009a; Silver *et al.*, 2001; Touyz, 2003; VanBavel *et al.*, 2003).

Thus, CVD high risk pathologies may be associated with changes in arterial contractility, structure and distensibility. As such an understanding of the mechanisms by which these may be modulated is of prime importance.

1.4 Ca^{2+} mobilisation in VSM cells

The mechanisms involved in the alteration of $[Ca^{2+}]_i$ levels within VSM cells play crucial roles in regulating the contractile state of arterial VSM cells, and hence, arterial blood pressure and blood flow. The major processes in regulating $[Ca^{2+}]_i$ homeostasis within VSM cells involve the participation of factors which mobilise Ca^{2+} through Ca^{2+} entry across the plasma membrane and/or release from intracellular stores as well as those which reduce $[Ca^{2+}]_i$ by Ca^{2+} extrusion to the extracellular space or re-sequestering Ca^{2+} into intracellular stores within VSM cells.

At rest a Ca^{2+} gradient is evident across the plasma membrane of VSM cells (around 1-2mM in the extracellular space and around ~0.1µM in the cytoplasm (Akata, 2007; Bolton, 1979; Floyd *et al.*, 2007; McCarron *et al.*, 2006)). $[Ca^{2+}]_i$ levels may be variable across the cell's cytoplasm and can be significantly higher in compartmentalised intracellular regions than in the cytoplasm. For example, $[Ca^{2+}]_i$ in the sarco-endoplasmic reticulum (SR) of VSM cells has been measured at around 75 to 130µM (Sugiyama *et al.*, 1995).

Ca^{2+} can be mobilised from either of two sources; the extracellular space and from intracellular Ca^{2+} stores such as the SR (Marchand *et al.*, 2012). Under physiological conditions, vasoconstrictor stimuli may activate VSM cells to increase $[Ca^{2+}]_i$ as the result of a change in membrane potential (E_m), E_m of resting VSM cells ~ -40 to -65mV; this is also known as electro-mechanical coupling and/or binding of an agonist to a specific receptor (or pharmaco-mechanical coupling) (Marchand *et al.*, 2012; Orallo, 1996; Somlyo *et al.*, 1994a; Yamazaki *et al.*, 1998).

1.4.1 Ca^{2+} mobilisation: Ca^{2+} entry across the plasma membrane of VSM cells

Plasma membrane Ca^{2+} channels provide the major routes for Ca^{2+} entry into VSM cells and include the voltage-operated Ca^{2+} channels (VOCCs), receptor-operated Ca^{2+} channels (ROCCs) and store-operated Ca^{2+} channels (SOCCs) (Hughes, 1995) (figure 1.4.1.1).

There is evidence for the existence of six different types of VOCCs of which 'transient' (T-type) and 'long-lasting' (L-type) are the most important for voltage-gated Ca^{2+} entry into VSM cells (Hughes, 1995; Kuga *et al.*, 1996; Thakali *et al.*, 2010; Tsien *et al.*, 1990). L-type Ca^{2+} channels are dihydropyridine-sensitive channels which are slow to inactivate but may be activated by high voltage (between ~ -30mV to full activation at around +15mV) (Firth *et al.*, 2011; Hughes, 1995; Tsien *et al.*, 1991). $Cav_{1.2}$ is the most abundant of the L-type Ca^{2+} channels in arterial smooth muscle cells, widely expressed in the plasma membrane as single or small clusters, creating high $[Ca^{2+}]$ microdomain regions during influx, (called Ca^{2+} sparklet sites) which may contribute to local and global $[Ca^{2+}]_i$ under physiological conditions (Amberg *et al.*, 2007; Navedo *et al.*, 2007; Zhang *et al.*, 2007). Depolarisation of the VSM cell membrane increases the open probability of L-type channels and hence Ca^{2+} influx. The Ca^{2+} entering VSM cells from the extracellular space via these channels is believed to be the main source of Ca^{2+} influx related to VSM cell constriction (Akata, 2007; Orallo, 1996).

The T-type Ca^{2+} channels offer another route for Ca^{2+} entry and are low voltage activated (in the approximate range between ~ -40mV to full activation at ~ -10mV) but fast-inactivating channels (Firth *et al.*, 2011; Perez-Reyes, 2003). Out of the

three types of T-type Ca^{2+} channels identified in VSM cells ($Cav_{3.1}$, $Cav_{3.2}$ and $Cav_{3.3}$), $Cav_{3.3}$ is the most common (Perez-Reyes, 1998). The precise function of the T-type Ca^{2+} channels in VSM cells is unclear but arteries from $Cav_{3.2}$ knockout mice exhibited attenuated vasorelaxation, attributed to coupling between T-type and large-conductance Ca^{2+}-activated K^+ (BK_{Ca}) channels (Chen *et al.*, 2003) suggesting that T-type channels may regulate vascular tone. T-type channels are also believed to play a role in electrochemical coupling within the vasculature (Chen *et al.*, 2003; Marchand *et al.*, 2012). A third VOCC found in VSM cells is the 'resting' (R-type) Ca^{2+} channel. This has been suggested to be involved in sustaining slow Ca^{2+} entry during high K^+-induced membrane depolarisation, however, its physiological role remains incompletely understood (Bkaily *et al.*, 1995; Claing *et al.*, 1994; Orallo, 1996). Other types of voltage-dependent Ca^{2+} entry channels associated with stretch-induced VSM constriction (e.g. increases in intraluminal pressure) are also present in VSM cells (Baek *et al.*, 2011; Kuriyama *et al.*, 1995; Marin *et al.*, 1999). Examples of such stretch-activated Ca^{2+} entry channels are TRPM4 (melastatin) and TRPV1 (vanilloid) which were shown to contribute to regulation of vascular tone of cerebral and mesenteric arteries (Earley *et al.*, 2007; Gonzalez-Cobos *et al.*, 2010).

The ROCCs and SOCCs provide voltage-independent routes for Ca^{2+} entry across the plasma membrane. The majority of vasoconstrictor stimuli (including noradrenaline, angiotensin and ATP) provoke VSM constriction by binding to phospholipase C (PLC)-coupled membrane receptors thus activating Ca^{2+} influx (Bylund *et al.*, 1994; Dalziel *et al.*, 1994; Marchand *et al.*, 2012; Orallo, 1996). Stimulation of PLC-coupled receptors activates G-proteins and subsequently PLC, which sets off the phosphatidyl inositol cascade, resulting in the production of two second messengers inositol 1,4,5 trisphosphate (IP_3) and diacylglycerol (DAG)

(Berridge, 1993) (figure 1.4.1.1). DAG stimulates opening of ROCCs on the plasma membrane leading to Ca^{2+} influx and increased $[Ca^{2+}]_i$, in a process generally referred to as receptor-operated Ca^{2+} entry (ROCE) (figure 1.4.1.1) (Kuhr *et al.*, 2012; Large, 2002; Marchand *et al.*, 2012). In addition DAG may also activate protein kinase C (PKC), forming the PLC/DAG-regulated PKC complex which may phosphorylate VOCC, causing them to open up to Ca^{2+} influx (Marin, 1993; Schuhmann *et al.*, 1994). The other second messenger IP_3 diffuses from the membrane to the cytosol where it induces Ca^{2+} release from IP_3 sensitive intracellular Ca^{2+} stores (more details in section 1.4.2). As Ca^{2+} becomes depleted in intracellular stores, a Ca^{2+} deficiency signal is transmitted via stromal interacting molecule 1 (STIM 1) to activate SOCCs on the VSM plasma membrane (such as Orai1 and transient receptor potential channels (TRPCs)), which in turn open and allow Ca^{2+} influx from the extracellular space (Gonzalez-Cobos *et al.*, 2010; Leung *et al.*, 2008; Trebak, 2012; Walker *et al.*, 2001). This process is described as store-operated Ca^{2+} entry (SOCE) (previously known as capacitative Ca^{2+} entry) (Leung *et al.*, 2008; Putney *et al.*, 1993) (figure 1.4.1.1). The SOCCs are recognised to be important in replenishing internal Ca^{2+} stores, in Ca^{2+} entry and in regulating VSM cell contractility of vessels including mesenteric resistance arteries (Brueggemann *et al.*, 2006; Park *et al.*, 2008; Zhang *et al.*, 2002; Zhang *et al.*, 2010b). TRPCs can be dependent on store depletion of Ca^{2+} (i.e. the SOCCs) or independent of Ca^{2+} depletion (i.e. the ROCCs) (Akata, 2007; Gonzalez-Cobos *et al.*, 2010; Walker *et al.*, 2001) and are known to participate in both SOCE and ROCE mechanisms (Kuhr *et al.*, 2012; Kumar *et al.*, 2006; Large, 2002; Marchand *et al.*, 2012) (figure 1.4.1.1). When acting in reverse mode, the sodium-calcium exchanger (NCX) on the VSM cell membrane is also another mechanism for Ca^{2+} entry however the NCX is

discussed in more detail in section 1.5.2. In short there are many different Ca^{2+} entry mechanisms on the plasma membranes of VSM cells that can participate in vasoconstrictor-stimulated Ca^{2+} influx or mobilisation.

Even in the resting state, negligible amounts of Ca^{2+} may permeate the plasma membrane from the extracellular space, down the electrochemical gradient and into a resting VSM cell (Akata, 2007; Hughes, 1995; Orallo, 1996). While there is very little known about this mechanism of Ca^{2+} entry it is believed to be of less importance than the other aforementioned VSM cell Ca^{2+} influx mechanisms (Akata, 2007; Hughes, 1995; Orallo, 1996).

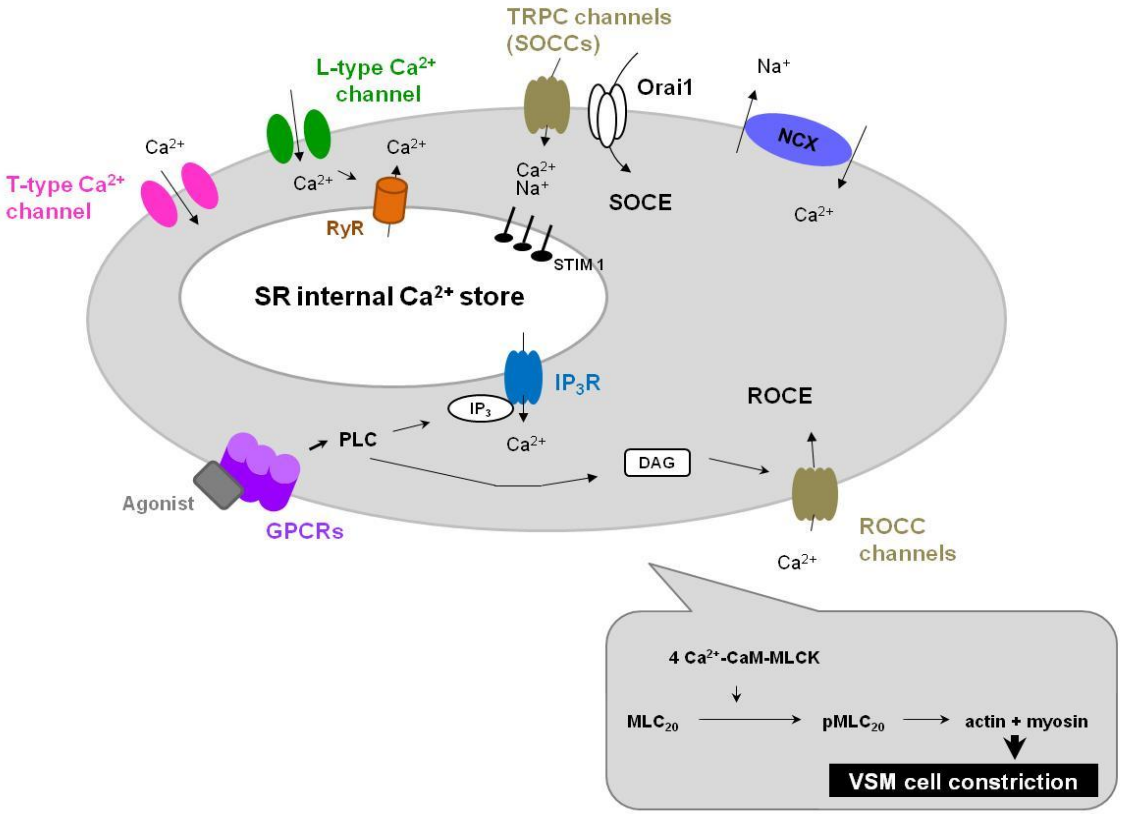

Key: **CaM** - calmodulin; **DAG** - diacylgycerol; **GPCR** - G-protein coupled receptor; **IP_3** - inositol 1,4,5 trisphosphate; **IP_3R** - inositol 1,4,5 trisphosphate receptor; **MLCK** - myosin light chain kinase; **(p)MLC_{20}** - (phosphroylated) myosin (at serine residue 19 of the 20kDa regulatory myosin light chain); **NCX** - sodium-calcium exchanger; **PLC** - phospholipase C; **ROCC** - receptor-operated Ca^{2+} channel; **ROCE** - receptor-operated Ca^{2+} entry; **RyR** - ryanodine sensitive receptor; **SOCC** - store-operated Ca^{2+} channel; **SOCE** - store-operated Ca^{2+} entry; **SR** - sarco-endoplasmic reticulum; **STIM1** - stromal interacting molecule 1; **TRPC** - transient receptor potential channels; **VSM** - vascular smooth muscle

Figure 1.4.1.1: Illustration of the various Ca^{2+} mobilisation mechanisms present in VSM cells that contribute to increases in $[Ca^{2+}]_i$ and therefore VSM cell constriction. Among those localised to the plasma membrane are the L- and T- type Ca^{2+} channels (which are voltage-dependent), the store and receptor-operated Ca^{2+} channels (SOCCs & ROCCs) which may be involved store/receptor operated Ca^{2+} entry (SOCE/ROCE) pathways and the sodium-Ca^{2+} exchanger (NCX) (in reverse mode, section 1.5.2). Those shown on the internal sarco-endoplasmic reticulum (SR) membrane are the inositol 1,4,5 trisphosphate receptor (IP_3R) and ryanodine sensitive receptor (RyR) channels (section 1.5.1.2) and stromal interacting molecule 1 (STIM1), the Ca^{2+} depleting sensor protein (which is part of SOCE pathway).

1.4.2 Ca^{2+} mobilisation: Ca^{2+} release from intracellular calcium stores within VSM cells

VSM cells store Ca^{2+} intracellularly in storage compartments such as the SR which contain Ca^{2+} binding proteins (i.e. calsequestrin and/or calreticulin) (Gordienko *et al.*, 2001; Laporte *et al.*, 1997; Orallo, 1996; Somlyo *et al.*, 1994a; van Breemen *et al.*, 1989). As an endo-membrane system, the SR consists of a peripheral portion in close proximity to the internal surface of VSM cell membrane and a deep or central portion located close to the nucleus (Devine *et al.*, 1972; Gordienko *et al.*, 2001; Laporte *et al.*, 1997). There are at least two distinct Ca^{2+} release mechanisms on the SR membrane of VSM cells, namely the IP_3 sensitive and ryanodine sensitive receptor channels (IP_3R and RyR respectively) (McGeown, 2004). Both IP_3R and RyR operate in a voltage-independent manner, are spatially distributed in SR membranes and have been identified in small resistance arteries (Lamont *et al.*, 2004; Lesh *et al.*, 1998; McGeown, 2004).

IP_3Rs are activated by bound IP_3 (generated by agonist activation of PLC-coupled membrane receptors) and may release large amounts of Ca^{2+} from the SR lumen into the cytosol. Hence, IP_3Rs play a crucial role in Ca^{2+} mobilisation within VSM cells. This interaction between IP_3 and its receptor is regulated by $[Ca^{2+}]_i$, as increases up to 300nM, can enhance the effectiveness of IP_3R to bind IP_3 consequently releasing Ca^{2+} from SR stores (Akata, 2007; Laporte *et al.*, 1997; Marin *et al.*, 1999; McGeown, 2004). Such local bursts of Ca^{2+} from clustered IP_3Rs on the SR membrane may be described as Ca^{2+} puffs which have been identified in VSM cells (Boittin *et al.*, 2000; Dargan *et al.*, 2003; Shuai *et al.*, 2002). These may lead to localised increases in $[Ca^{2+}]_i$ in VSM cells which in turn may induce further Ca^{2+} release through the RyR (also localised on SR membranes) in a Ca^{2+} induced Ca^{2+}

release (CICR) positive feedback mechanism (Jaggar *et al.*, 1998; Lesh *et al.*, 1998; McGeown, 2004). Therefore, the opening of single or clustered RyRs on SR membrane can amplify the Ca^{2+} signal within VSM cells via this CICR system (alongside IP_3Rs). CICR may trigger RyR to produce local Ca^{2+} transients called Ca^{2+} sparks which may also occur in VSM cells (Brenner *et al.*, 2000; Collier *et al.*, 2000; Guerrero-Hernandez *et al.*, 2002; Nelson *et al.*, 1995). A major role for Ca^{2+} sparks in VSM cells is believed to be in the activation of Ca^{2+}-activated K^+ (K_{Ca}) channels causing membrane hyperpolarisation, closure of VOCCs and VSM relaxation (Nelson *et al.*, 1995). Other Ca^{2+} transients which propagate through the cytoplasm as Ca^{2+} waves originate at IP_3R clusters on SR membrane and in turn these may stimulate CICR at RyRs (Berridge *et al.*, 2000; Iino *et al.*, 1994; McCarron *et al.*, 2006).

In summary Ca^{2+} is mobilised in VSM cells through influx across the plasma membrane and/or through release from internal Ca^{2+} stores. This contributes significantly to the rise in the bulk average cytoplasmic $[Ca^{2+}]_i$ as well as high $[Ca^{2+}]$ in local microdomain regions within the VSM cell and thus plays an essential role in the regulation of VSM contractility under physiological conditions.

1.5 The mechanisms present in VSM cells which reduce $[Ca^{2+}]_i$

Within VSM cells several mechanisms may reduce high levels of $[Ca^{2+}]_i$ promoting relaxation of pre-constricted VSM as well as maintaining Ca^{2+} homeostasis under basal conditions. These mechanisms include: the SR Ca^{2+}-ATPase pump (SERCA), the plasma membrane Ca^{2+} ATPase pump (PMCA), the Na^+/Ca^{2+} exchanger (NCX) as well as the mitochondrial uniporter (illustrated in figure 1.5.0.1) and cytoplasmic Ca^{2+}-binding proteins which are important in buffering free Ca^{2+} (Oloizia *et al.*, 2008). Also important in the process of Ca^{2+} removal from the cytoplasm of VSM cells are phospholamban (an endogenous inhibitor of SERCA) and the Na^+-K^+ ATPase (NKA) which couples to NCX promoting Ca^{2+} extrusion to the extracellular space (Oloizia *et al.*, 2008).

1.5.1 SR and the SR Ca^{2+} ATPase (SERCA)

SERCA (~110kDa) is localised to the intracellular SR membrane within VSM cells and actively uptakes Ca^{2+} from the cytosol into the SR lumen in response to store depletion (Gonzalez *et al.*, 1996; Missiaen *et al.*, 1991). SERCA is a member of the P-type ATPase family and is considered electroneutral because for every Ca^{2+} ion pumped into the SR lumen one K^+ and one H^+ ion are extruded from the SR lumen into the cytosol, while utilising high energy supplied from the hydrolysis of ATP to ADP (Grover *et al.*, 1992; Levy *et al.*, 1990). Three SERCA genes encode the SERCA1, SERCA2, and SERCA3 isoforms (Gonzalez *et al.*, 1996; Marin *et al.*, 1999; Missiaen *et al.*, 1991). Alternative splicing adds more variation for example the SERCA2 gene encodes SERCA2a and SERCA2b alternatively spliced transcripts (Zarain-Herzberg *et al.*, 1990), both of which have been found to be present in VSM

(Clark *et al.*, 2010; Eggermont *et al.*, 1990; Oloizia *et al.*, 2008). SERCA2b isoform is generally regarded as a ubiquitously expressed housekeeping pump and is thought to be the major SR Ca^{2+} pump in VSM (Lytton *et al.*, 1989; Oloizia *et al.*, 2008; Wu *et al.*, 1993).

Since SERCA lacks an auto-inhibitory CaM-binding domain it is not regulated by CaM, but instead is regulated by phospholamban (PLN) (Eggermont *et al.*, 1990; Grover *et al.*, 1992; James *et al.*, 1989; Marin *et al.*, 1999). PLN is thought to inhibit SERCA activity by a physical interaction which promotes a conformational state which is catalytically unfavourable or by interfering with the SERCA catalytic site itself (Eggermont *et al.*, 1990; James *et al.*, 1989; Mahaney *et al.*, 1991; Orallo, 1996; Voss *et al.*, 1991). Arterial smooth muscle derived from PLN-deficient mice exhibited reduced contractile responsiveness, effects which were abolished by pharmacological SERCA inhibitors, demonstrating an effect of PLN on arterial contractility (Lalli *et al.*, 1997; Oloizia *et al.*, 2008).

The use of different inhibitors to SERCA has demonstrated that SERCA participates in the regulation of $[Ca^{2+}]_i$ and in smooth muscle (including VSM) contractility (Gomez-Pinilla *et al.*, 2007; Liu *et al.*, 2006; Nazer *et al.*, 1998). SERCA's contribution to Ca^{2+} extrusion has been shown to be 31% in guinea pig bladder smooth muscle (Gomez-Pinilla *et al.*, 2007), 20% in mouse bladder smooth muscle (Liu *et al.*, 2006) and in VSM the rate of $[Ca^{2+}]_i$ clearance after SERCA inhibition was reduced by 23% (Nazer *et al.*, 1998). Therefore SERCA is believed to be a contributor to $[Ca^{2+}]_i$ clearance in both VSM and non-vascular smooth muscles.

1.5.2 The sodium-calcium exchanger (NCX)

NCX has been identified in small mesenteric arteries as well as in other blood vessels (O'Donnell *et al.*, 1994; Orallo, 1996; Zhang *et al.*, 2010a). The NCX (~ 112-116kDa) has a low affinity for Ca^{2+} and a high capacity to produce Ca^{2+} efflux which is driven by the transmembrane Na^{+} gradient, transporting one Ca^{2+} ion out of the cell into the extracellular space in exchange for three Na^{+} ions (Philipson *et al.*, 2000; Szewczyk *et al.*, 2007). There are three distinct mammalian NCX isoforms, NCX1 to 3 of which NCX1 is ubiquitously expressed and abundant in the heart and VSM, whereas NCX2 and NCX3 are restricted to brain and skeletal muscle (Blaustein *et al.*, 1999; Lytton, 2007; Oloizia *et al.*, 2008; Quednau *et al.*, 2004; Szewczyk *et al.*, 2007). These isoforms give rise to various alternative splice variants and importantly in VSM, NCX1 gives rise to predominantly NCX1.3 and NCX 1.7 spliced variants (Nakasaki *et al.*, 1993; Oloizia *et al.*, 2008; Quednau *et al.*, 2004; Quednau *et al.*, 1997). A study using smooth muscle-specific NCX1 overexpressing mice, showed agonist-induced decreases in $[Ca^{2+}]_i$ and tension were greater in arteries from transgenic mice, differences which were abolished by NCX inhibitors, supporting the notion that NCX can contribute to Ca^{2+} extrusion in VSM cells (Karashima *et al.*, 2007).

In VSM cells the NCX is the only $[Ca^{2+}]_i$ extrusion mechanism known to be bidirectional, contributing to either Ca^{2+} efflux or influx depending on $[Ca^{2+}]$ or $[Na^{+}]$ (Akata, 2007; Blaustein *et al.*, 1999; Marin *et al.*, 1999; Orallo, 1996; Yao *et al.*, 1998). Under circumstances of high $[Ca^{2+}]_i$ levels NCX is driven into forward mode, extruding $[Ca^{2+}]_i$ to the extracellular space in exchange for Na^{+}, mediating VSM relaxation (Philipson *et al.*, 2000). However, exposing smooth muscle to Na^{+} pump inhibitors (such as ouabain) or to K^{+}-free medium, affects the transmembrane

Na^+ gradient, and produces vasoconstriction as a result of intracellular Na^+ accumulation which is exchanged by Ca^{2+}, i.e. NCX is in the reverse mode (Karaki *et al.*, 1997; Marin, 1995; Marin *et al.*, 1999). It has also been suggested that reverse mode NCX activity may account for agonist-induced Ca^{2+} influx by local coupling between NCX and SOCE (i.e. TRPC and Orai1) (Baryshnikov *et al.*, 2009) however, the importance of the NCX in reverse mode to Ca^{2+} homeostasis is still under debate (Iwamoto *et al.*, 2004; Karaki *et al.*, 1997; Marin *et al.*, 1999; Zhang *et al.*, 2010a). In the forward mode NCX has been suggested to contribute to 30 to 35% of Ca^{2+} efflux in mouse uterine smooth muscle (Matthew *et al.*, 2004; Taggart *et al.*, 1997) and 70% in mouse bladder smooth muscle (Liu *et al.*, 2006). Its contribution in VSM cells is unclear and is yet to be quantified.

1.5.3 The sodium-potassium exchanger (NKA)-NCX coupling

NCX couples to the sodium-potassium exchanger (NKA) (which is essential in establishing both membrane potential and the Na^+ gradient) in VSM cell plasma membranes (figure 1.5.0.1) (Moore *et al.*, 1993; Shelly *et al.*, 2004). As a P-type ATPase NKA transports three Na^+ ions out of the cell in exchange for two K^+ ions with the hydrolysis of ATP, thus maintaining the Na^+ electrochemical gradient which drives Ca^{2+} extrusion by the NCX (Lingrel *et al.*, 1994; Oloizia *et al.*, 2008). NKA α_2 deficient mice are hypertensive and isolated arteries elicited increased contractile activity (similar responses in controls were also elicited after NKA inhibition by ouabain) (Zhang *et al.*, 2005). It has also been shown that transgenic mice overexpressing the α_2-trangene were hypotensive with increased NKA activity

(Pritchard *et al.*, 2007). These provide emerging evidence for NKA α_2 being specifically coupled to contractile pathways in the VSM.

1.5.4 The mitochondria

The mitochondria is believed to act as an intracellular Ca^{2+} store, decreasing high levels of $[Ca^{2+}]_i$ in cardiac cells, but its role in VSM cells is still not fully understood (Dedkova *et al.*, 2008; Kamishima *et al.*, 2002; Poburko *et al.*, 2004b). Generally the role of the mitochondria is widely accepted to be less important than that of the SR and in VSM cells it may be activated during pathologically high $[Ca^{2+}]_i$ levels (Broderick *et al.*, 1987; Oloizia *et al.*, 2008; Somlyo *et al.*, 1989) as well as during physiological cellular Ca^{2+} signalling events (David, 1999; Girard *et al.*, 1991). Ca^{2+} can be retained within the mitochondrial luminal space by high capacity buffers (Chalmers *et al.*, 2003). Mitochondria may be located close to internal SR stores within VSM cells (Nixon *et al.*, 1994) potentially resulting in the formation of microdomain regions and modulation of local Ca^{2+} signalling (McCarron *et al.*, 2006; Poburko *et al.*, 2004a; Poburko *et al.*, 2004b). The route for Ca^{2+} transport from the cytosol into mitochondria is via an electrophoretic uniporter which possesses a low affinity for Ca^{2+} (Akata, 2007; Cox *et al.*, 1993; Orallo, 1996). This uniporter is closely coupled to oxidative phosphorylation and utilises the electrochemical gradient across the inner mitochondrial membrane to drive Ca^{2+} into the mitochondria (Orallo, 1996; Pozzan *et al.*, 1994). In normal VSM cells the rate of Ca^{2+} influx into the mitochondria is slow so that intra-mitochondrial Ca^{2+} concentrations still remain low regardless of transient increases in $[Ca^{2+}]_i$, consistent

with the unimportance of the mitochondrial uniporter as major method for reducing $[Ca^{2+}]_i$ at least in VSM cells (Missiaen *et al.*, 1992; Orallo, 1996).

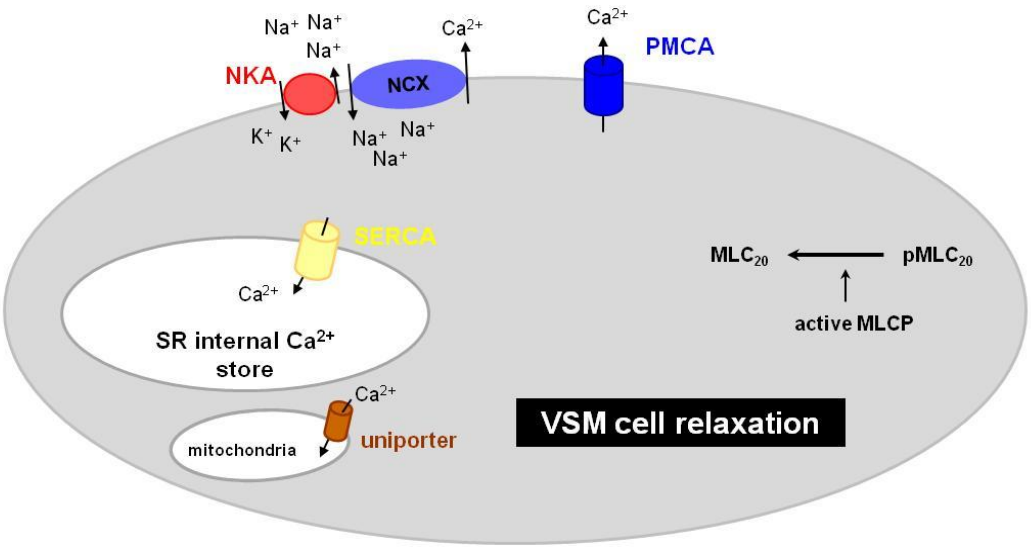

Key: **(p)MLC$_{20}$** - (phosphroylated) myosin (at serine residue 19 of the 20kDa regulatory myosin light chain); **NCX** - sodium-calcium exchanger; **NKA** - sodium-potassium exchanger; **PMCA** - plasma membrane calcium ATPase; **SERCA** - sarco-endoplasmic reticulum calcium ATPase; **SR** - sarco-endoplasmic reticulum; **VSM** - vascular smooth muscle

Figure 1.5.0.1: Schematic illustrating the different mechanisms that can reduce $[Ca^{2+}]_i$ within VSM cells. Among those shown on the VSM cell plasma membrane are the sodium-potassium exchanger (NKA), the sodium-Ca^{2+} exchanger (NCX) and the plasma membrane Ca^{2+} ATPase (PMCA), all of which extrude Ca^{2+} from the intracellular to the extracellular space. The SR Ca^{2+} ATPase (SERCA) is on the internal SR membrane of the VSM cell and is responsible for Ca^{2+} uptake from the cytosol.

The fifth important mechanism associated with a reduction of $[Ca^{2+}]_i$, also shown to be present in VSM cells, is the plasma membrane Ca^{2+} ATPase (PMCA). This Ca^{2+} ATPase pump will be fully discussed in detail below in the next section 1.6, as this protein is the primary focus of the present study.

1.6 Plasma membrane Ca^{2+} ATPase (PMCA)

Traditionally, the plasma membrane Ca^{2+} ATPase pump (PMCA) is thought to be an essential part of the cellular Ca^{2+} homeostatic machinery regulating $[Ca^{2+}]_i$ by exporting Ca^{2+} from the cytosol to the extracellular space (Brini, 2009; Carafoli, 1994; Di Leva *et al.*, 2008). Though, it is evident that it may also have other additional roles in cellular signalling.

Mammalian PMCA belongs to a multigene family of four different genes (named ATP2B1 to 4 in humans) encoding for the protein isoforms PMCA1 through to PMCA4 (with molecular masses between ~125 and 140kDa) (Stauffer *et al.*, 1995; Stauffer *et al.*, 1993; Strehler *et al.*, 2007; Strehler *et al.*, 2001). Additional isoform diversity is introduced by alternative splicing raising more than 20 splice variants (Stauffer *et al.*, 1995; Stauffer *et al.*, 1993; Strehler *et al.*, 2007; Strehler *et al.*, 2001).

1.6.1 The structure of PMCA

The principal structural components of the PMCA pump are organised on the cytoplasmic side and into: the intracellular N- and C-terminal tails, ten transmembrane domains (TM), and four loops of which the first two are of major importance to the function of the pump (figure 1.6.1.1). The N-terminal tail is important as it is the most variable portion of the pump (in the four isoforms) encompassing the first 80-90 amino acids (Brini, 2009; Di Leva *et al.*, 2008). Alternative splicing may occur at two major 'hot spots' of the pump called sites A and C (shown in figure 1.6.1.1) resulting in PMCA splice variants which may differ in the length of the first intracellular loop or in the C-terminal tail or in their affinity

for CaM (figure 1.6.1.1) (Keeton *et al.*, 1993; Santiago-Garcia *et al.*, 1996; Stauffer *et al.*, 1993; Strehler *et al.*, 2007; Strehler *et al.*, 2001).

The first intracellular loop (between TM 2 and 3), also called the transducer domain, contains one of the two sites for binding activatory acidic phospholipid (PL) (Brodin *et al.*, 1992; Zvaritch *et al.*, 1990), the alternative splice site A as well as one of the recipient sites for autoinhibitory interaction with CaM-binding domain (CaM-BD) (figure 1.6.1.1) (Chicka *et al.*, 2003; Di Leva *et al.*, 2008; Falchetto *et al.*, 1992). The other recipient site is located on the second intracellular loop (between TM 4 and 5) (Falchetto *et al.*, 1991; Zvaritch *et al.*, 1990), which also encompasses the catalytic core including the conserved lysine (K) and phosphorylated aspartate (D) residues, and is involved in ATP binding and hydrolysis (figure 1.6.1.1) (Di Leva *et al.*, 2008).

The cytosolic C-terminal tail of PMCA is longer than in other Ca^{2+} ATPases and is functionally important as it contains the CaM-BD and Ca^{2+} affinity binding sites as well as the alternative splice site C (figure 1.6.1.1) (Brini, 2009; Di Leva *et al.*, 2008; Hofmann *et al.*, 1993; James *et al.*, 1988; Keeton *et al.*, 1993; Kessler *et al.*, 1992). In the absence of Ca^{2+}/CaM, the CaM-BD associates with the CaM-BD recipient sites (of the first and second intracellular loops), holding the pump in an inactive (autoinhibitory) state (shown in figure 1.6.1.1). The second binding site of activatory acidic PLs is in the CaM-BD (Brodin *et al.*, 1992). It is worth mentioning that present in both the C-terminal and second intracellular loop are sequence binding regions that interact with molecular partners of PMCA (discussed in more detail later on in section 1.7).

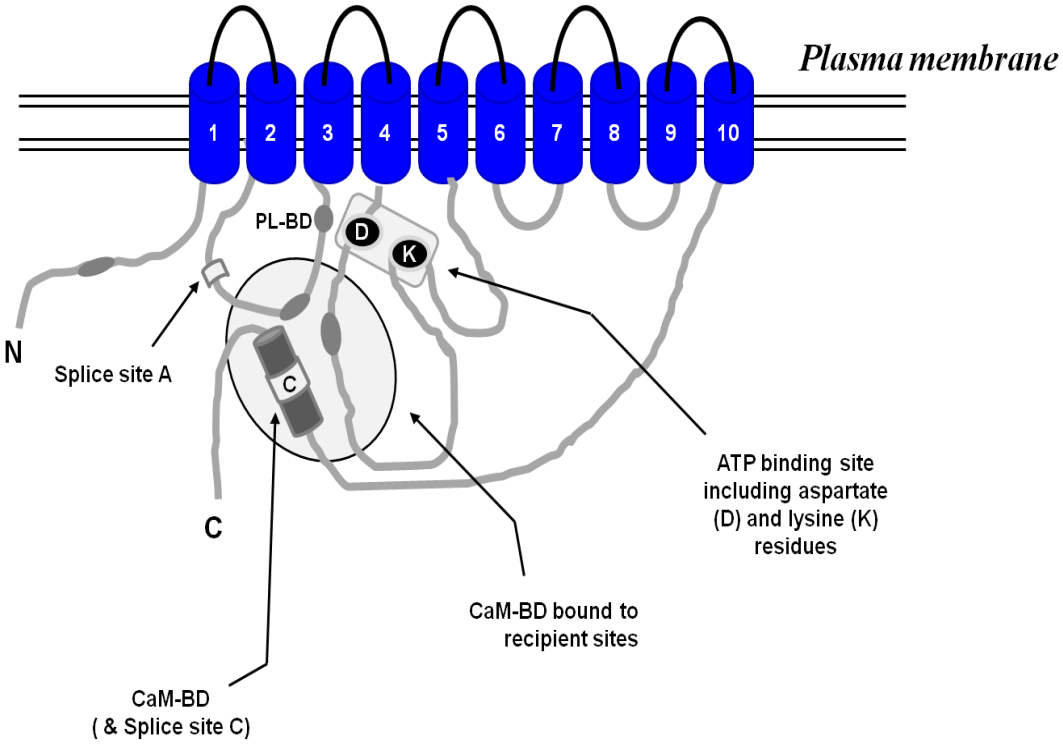

Key: **C** - C-terminal tail; **CaM-BD** - calmodulin binding domain; **D** - aspartate residue; **K** - lysine residue; **N** - N-terminal tail; **PL-BD** - activatory acidic phospholipid binding domain; **TM** - transmembrane domain

Figure 1.6.1.1: Schematic of the PMCA structure. The N-terminal, first intracellular loop (between transmembrane domain (TM) 2 & 3) and second (between TM 4 & 5) and the C-terminal region are all located on the cytoplasmic side (adapted from (Di Leva et al., 2008). The pump is in an autoinhibitory state as the calmodulin binding domain (CaM-BD) (on the C-terminus) is bound to recipient sites in the main body of the pump (on first and second loop). The ATP binding and hydrolysis domain (or the catalytic core) which includes phosphorylated aspartate and lysine residues are shown as well as the important sites of alternative splicing sites A & C (on the first loop and C-terminal tail) and the binding domain for acidic phospholipids (PL-BD) on the first cytosolic loop.

1.6.2 PMCA expression

The expression of the PMCA genes may be modulated during development and may be tissue or cell specific, however, PMCA1 and PMCA4 are ubiquitously expressed (Di Leva *et al.*, 2008; Keeton *et al.*, 1995; Stauffer *et al.*, 1995). PMCA2 and 3 have more tissue specific patterns of expression for example PMCA2 has been detected in mammalian brain, mammary glands and in hair cells of the auditory system and PMCA3 mainly in brain, liver and skeletal muscle (Furuta *et al.*, 1998; Greeb *et al.*, 1989; Reinhardt *et al.*, 2000; Stauffer *et al.*, 1995). Though PMCA1 is ubiquitous it is the most abundantly expressed isoform in the brain, lung and intestine (De Jaegere *et al.*, 1990; Di Leva *et al.*, 2008; Greeb *et al.*, 1989; Stauffer *et al.*, 1995; Strehler *et al.*, 2001). Significant PMCA4 expression has been identified in tissues including the kidney, erythrocytes, skeletal muscle, intestinal mucosa, spermatozoa, brain and heart and it is an important and abundant isoform in VSM (Brandt *et al.*, 1992; Pande *et al.*, 2006; Schuh *et al.*, 2004; Stauffer *et al.*, 1995; Strehler *et al.*, 2001; Szewczyk *et al.*, 2007).

1.6.3 PMCA1 isoform

There have been attempts made to develop a PMCA1 null mutant mouse model by targeted sequence deletion in the PMCA1 gene. However, PMCA1 null mutants are embryonically lethal early in development, between 3.5 to 8.5 days of pregnancy, after which only PMCA1 heterozygous mutants (PMCA1 Ht $^{(+/-)}$) and wild types were detectable. This observation suggests PMCA1 has a housekeeping function during embryogenesis (Brini, 2009; Okunade *et al.*, 2004; Prasad *et al.*, 2007; Shaheen, 2010). Loss of one copy of the PMCA1 gene does seem to have some

physiological consequences. Although PMCA1 Ht $^{(+/-)}$ mice appear visibly normal, bladder smooth muscle from these mice exhibited prolonged relaxation times after depolarisation with KCl suggesting a role for PMCA1 in Ca^{2+} extrusion (Liu *et al.*, 2006). In addition, PMCA1 may compensate, in some circumstances, for the loss of PMCA4. For example, in some mice, ablation of PMCA4 reduced portal vein contractility and apoptosis only when one copy of the PMCA1 gene was ablated i.e. PMCA4 $^{(-/-)}$/PMCA1 $^{(+/-)}$ mice (Okunade *et al.*, 2004).

In the last two years studies have begun to address the effects of PMCA1 on physiological functions by generating conditional tissue-specific knockout mice including PMCA1 cardiac specific knockout mice (Shaheen, 2010) and PMCA1 VSM specific knockout mice (Kobayashi *et al.*, 2012). PMCA1 cardiac specific knockout mice exhibited a decreased cardiac systolic function and reduced rate of relaxation *in vivo* (Shaheen, 2010) suggesting that PMCA1 can modulate cardiac function. PMCA1 VSM specific knockout mice exhibited increased systolic blood pressure and arterial contractility which was attributed to the Ca^{2+} handling effects of PMCA1 (i.e. clearance), (Kobayashi *et al.*, 2012) and indeed our group has also found increased systolic blood pressure in PMCA1 Ht $^{(+/-)}$ mice (unpublished data by Ludwig Neyses, Elizabeth Cartwright and Clare Austin's groups). Recent data generated in genome-wide association studies have identified single nucleotide polymorphisms present in the PMCA1 gene (ATP2B1) in association with blood pressure variance and hypertension (Cho *et al.*, 2009; Levy *et al.*, 2009; Tabara *et al.*, 2010; Takeuchi *et al.*, 2010). Taken together this recent data suggests that PMCA1 may play an important role in the regulation of cardiovascular homeostasis but currently there are few studies in which this has been investigated.

1.6.4 PMCA 2 and 3 isoforms

The PMCA2 gene is the only PMCA gene that has been causally linked to a genetic disease i.e. deafness and ataxia in deafwaddler and Wriggle Mouse Sagami mice (naturally occurring mutants with a spontaneous point mutation in PMCA2 gene) (Mammano, 2011; Prasad *et al.*, 2007; Street *et al.*, 1998; Takahashi *et al.*, 1999). Similarly, loss of hearing was observed in mouse models deficient in PMCA2 (Ficarella *et al.*, 2007; Kozel *et al.*, 2002; Kozel *et al.*, 1998; Prasad *et al.*, 2007). PMCA2 null mutants were profoundly deaf even at a young age and PMCA2 heterozygous mice were susceptible to noise induced hearing loss or developed a significant hearing deficit with age, effects attributed to loss of hair cell function (Brini, 2009; Kozel *et al.*, 2002; Kozel *et al.*, 1998). In humans, even though mutations occurring in the PMCA2 gene (ATP2B2) alone do not cause hearing loss, this has been shown to enhance the severity of hearing deficits due to other factors (Giacomello *et al.*, 2012; Schultz *et al.*, 2005). Balance defects have also been observed in PMCA2 null mutant mice which have been attributed to effects in cerebellar Purkinje cells (Stahl *et al.*, 1992).

PMCA2 also plays an important role in the secretion of high levels of Ca^{2+} in milk in lactating females (Reinhardt *et al.*, 2000; Reinhardt *et al.*, 2004). Lactating PMCA2 null mutant female mice exhibited around a 60% reduction of Ca^{2+} in their milk (Reinhardt *et al.*, 2004). Studies on an experimental autoimmune encephalomyelitis animal model (which reproduces features of multiple sclerosis such as neuronal degeneration and neuron pathology) demonstrated a downregulation of PMCA2 in spinal neurons (Nicot *et al.*, 2003), while a reduction in the number of spinal cord motor neurons was found in PMCA2 deficient mouse models (Kurnellas *et al.*, 2005). In the same study, inhibition of PMCA activity was also shown to delay Ca^{2+}

clearance in neuronal cell cultures (Kurnellas *et al.*, 2005). Taken in concert, these studies suggest that PMCA2 may also have an important role in neural function potentially by regulating Ca^{2+} homeostasis. Recently PMCA2 has been implicated in the control of Ca^{2+} dynamics in neurons supporting this notion (Gomez-Varela *et al.*, 2012). PMCA2 mRNA has also been shown to be highly overexpressed in breast cancer cells (Lee *et al.*, 2005) suggesting this isoform may play a role in tumourgenesis. In summation, our current understanding of PMCA2 is that it is involved in a number of different physiological and pathological functions including hearing and balance, the secretion of Ca^{2+} in milk of lactating mammals, neuronal function and tumorigenesis. Although the precise mechanisms of action are not yet fully known, effects on Ca^{2+} homeostasis have been suggested.

There have been no reports to date of PMCA3 gene targeted animal models. Miss-sense mutations in the PMCA3 gene have been identified in pancreatic tumours (Brini, 2009; Tempel *et al.*, 2007) while PMCA3 has been shown to be highly expressed (above PMCA2) in some, but not all, breast cancer cell types (Lee *et al.*, 2002; Lee *et al.*, 2005). These observations suggest that, like PMCA2, PMCA3 expression may play a role in tumour development. In neuronal cells, suppression of PMCA3 and 2 has been shown to affect the cell morphology (Zylinska *et al.*, 2007) and phenotype in adaptation to increases in $[Ca^{2+}]_i$ (Boczek *et al.*, 2012). Moreover, in human placenta PMCA3 gene (mRNA) expression has been shown to predict neonatal whole body bone mineral content (Martin *et al.*, 2007) although the exact mechanism is not yet fully understood. Thus, it would appear that both PMCA2 and 3 can have profound effects on specific physiological functions, however, more investigations into the role of PMCA3 and 2 particularly in the tissues where they

are specifically expressed are necessary as their roles have still not been fully clarified.

1.6.5 PMCA4 isoform

The majority of our current understanding of the roles and actions of PMCA has come from research focusing on the PMCA4 isoform. PMCA4 is thought to be ubiquitously expressed and has been identified as an essential isoform with important physiological roles in mammalian testes, heart, smooth muscles of bladder, uterus and blood vessels (Liu *et al.*, 2007; Okunade *et al.*, 2004; Schuh *et al.*, 2004).

PMCA4 null mutant (or PMCA4 KO $^{(-/-)}$) mice are viable and appear visibly healthy however, the males are infertile due to impaired hyper-activated sperm motility (Okunade *et al.*, 2004; Schuh *et al.*, 2004). PMCA4 was found to account for over 90% of the PMCA protein in sperm and testis (Okunade *et al.*, 2004; Ren *et al.*, 2001; Schuh *et al.*, 2004) where it is thought to co-localise with caveolin (Post *et al.*, 2010). The requirement of both PMCA4 and the Ca^{2+} influx channel, CatSper for hyper-activated sperm motility and their expression in the principle piece of the sperm tail, would suggest that PMCA4 also participates in Ca^{2+} regulation in sperm, as does CatSper (which is a Ca^{2+} channel responsible for cAMP-stimulated Ca^{2+} influx in sperm tails) (Okunade *et al.*, 2004; Ren *et al.*, 2001). The physiological importance of PMCA4 extends to platelets where it seems to play a role in regulating Ca^{2+}-dependent signalling events during platelet activation as suggested by reduced platelet aggregation responses in PMCA4 KO $^{(-/-)}$ mice (Jones *et al.*, 2010). Recently, PMCA4 has also been associated with Ca^{2+} dysregulation in the brains of patients

diagnosed with Alzheimer's disease (Mata *et al.*, 2011). Alterations in PMCA4 expression have been associated with remodelling of Ca^{2+} homeostasis in some types of cancers (Aung *et al.*, 2009) with changes in the expression of PMCA4 being reported in a variety of colon, gastric and breast cancer cell lines (Aung *et al.*, 2007; Aung *et al.*, 2009; Lee *et al.*, 2005; Ribiczey *et al.*, 2007). The exact changes in expression appear variable and while in some cancer cell lines PMCA4 expression was upregulated (Aung *et al.*, 2009), in others expression was downregulated (Aung *et al.*, 2009; Lee *et al.*, 2005). There seems to be a correlation between PMCA4 and cell death because it has been demonstrated in cellular systems that recombinant expression of a non-cleavable PMCA4 mutant prevents disturbances in Ca^{2+} handling and delays the kinetics of apoptosis and cell death by necrosis (Schwab *et al.*, 2002). Furthermore, the absence of PMCA4 reduced tumour necrosis factor (TNF)-induced cell death in a fibroblast-like cell line (Ono *et al.*, 2001), thus PMCA4 was suggested to be required for TNF-induced cell death. Therefore, the modified expression of some isoforms of PMCA observed in certain cancer types (as mentioned), might be important for tumour development and progression by encouraging an adaptive mechanism to regulate cell death, however this idea is speculative and has not yet been proven.

1.7 PMCA4 in the heart

Though PMCA4 is one of the most represented PMCA isoforms in the heart, interestingly PMCA4 activity has not been shown to be significantly involved in global $[Ca^{2+}]_i$ homeostasis of cardiomyocytes. Evidence from cardiomyocytes overexpressing PMCA4, showed global $[Ca^{2+}]_i$ and the activation or inactivation behaviour of L-type Ca^{2+} current (i.e. Ca^{2+} influx) was not different from controls (Hammes *et al.*, 1998), thus implying PMCA4 does not play a central role in regulating global $[Ca^{2+}]_i$ levels in these cells.

Current data, regarding PMCA4 in the heart indicates that it regulates signalling in cardiomyocytes via specific interactions with partner molecules. PMCA4 acts as a signalling protein in the heart, by interacting with Ca^{2+}/CaM-dependent enzymes such as calcineurin and nNOS and over 11 years ago *in vitro* experiments demonstrated a physical interaction between PMCA4 and nNOS in a cellular system (figure 1.7.0.1) (Schuh K. *et al.*, 2001). This physical interaction between PMCA4b and nNOS is mediated by a PDZ domain (PSD 95, Drosophila Discs large protein and Zone occludens-1) on nNOS and a PDZ-binding domain on PMCA4 (DeMarco *et al.*, 2001; Kim *et al.*, 1998; Williams *et al.*, 2006) (figure 1.7.0.1).

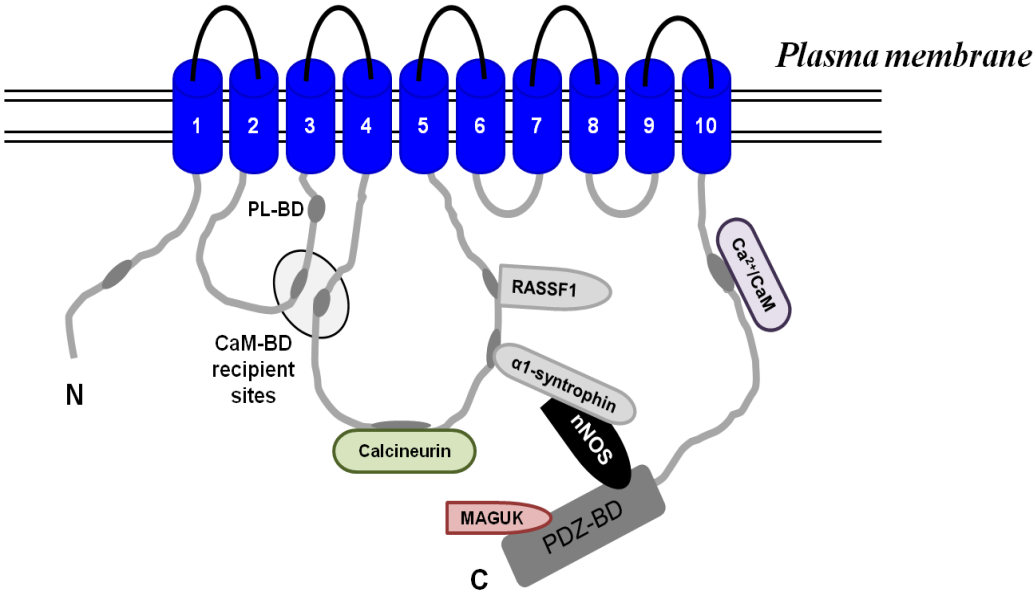

Key: **C** - C-terminal tail; **CaM** - calmodulin; **CaM-BD** - calmodulin binding domain; **MAGUK** - membrane-associated guanylate kinase; **N** - N-terminal tail; **nNOS** - neuronal nitric oxide synthase; **PDZ-BD** - PSD 95, drosophila discs large protein and zone occludens-1 binding domain; **PL-BD** - activatory acidic phospholipid binding domain; **RASSF1** - Ras-associated factor 1

Figure 1.7.0.1: Representation of the PMCA4 pump bound to its partner proteins at specific binding domains (BDs). A number of binding sites for the following PMCA4 interacting partner proteins: calcineurin, α1-syntrophin and Ras-associated factor 1 (RASSF1) are within the second intracellular loop (between transmembrane domain (TM) 4 & 5). PMCA4 becomes activated when Ca^{2+}/CaM is bound to its CaM-BD in the C-terminal region and also within this region is the important (PSD 95, Drosophila Discs large protein and Zone occludens-1) PDZ-binding domain (PDZ-BD), the main site of interaction between PMCA4 and neuronal nitric oxide synthase (nNOS) as well as other membrane-associated guanylate kinase (MAGUK) proteins. This schematic was adapted from (Di Leva *et al.*, 2008).

The functionality of the PMCA4-PDZ mediated nNOS interaction was demonstrated when PMCA4 was overexpressed in a cellular system, dramatically downregulating nNOS activity, however, expression of mutant PMCA4 (lacking the PDZ-binding domain which interacts with nNOS) did not impair nNOS activity (Schuh *et al.*, 2001). Currently the accepted theory in cardiac research is that, since nNOS is a Ca^{2+}/CaM-dependent enzyme, Ca^{2+} extrusion by PMCA4 lowers $[Ca^{2+}]_i$ in the vicinity of nNOS in the complex and thus downregulates the nNOS activity in cardiomyocytes (Cartwright *et al.*, 2007; Oceandy *et al.*, 2007). This has, however, not been directly demonstrated. PMCA1, the other PMCA isoform, expressed in the heart, has also been shown to interact with nNOS, though this interaction appears to be weaker than PMCA4-nNOS, with PMCA1 demonstrating less nNOS inhibitory capacity than PMCA4 (Williams *et al.*, 2006).

Immunoprecipitation studies in cardiac cells identified endogenous PMCA4b and nNOS in a ternary complex with α-1 syntrophin (figures 1.7.0.1 & 1.7.2.1). Overexpression of α-1 syntrophin and PMCA4 in a cellular system resulted in a reduction of nNOS activity over and above that of PMCA4 alone therefore suggesting PMCA4 and α-1 syntrophin may act synergistically to negatively regulate nNOS (Williams *et al.*, 2006). PMCA4 has also been reported to form protein-protein interactions with several proteins including calcineurin, Ras-associated factor 1 (RASSF1) and syntrophin but through other domains of PMCA4 distinct from the PDZ-binding region (Armesilla *et al.*, 2004; Buch *et al.*, 2005; Mohamed *et al.*, 2011b; Williams *et al.*, 2006) (shown in figure 1.7.0.1). For example, PMCA4 interacts with calcineurin in the PMCA4 catalytic domain (Buch *et al.*, 2005). Overexpression of PMCA4 in mammalian cells has shown calcineurin functionally interacts with PMCA4 causing inhibition of calcineurin activity (Buch *et al.*, 2005;

Wu *et al.*, 2009). This has potentially important consequences as calcineurin is a Ca^{2+}/CaM activated serine/threonine phosphatase which, when activated, binds to and dephosphorylates nuclear factor of activated T-cell (NFAT) which then translocates to the nucleus where it activates several hypertrophic genes (Crabtree, 1999; Kubis *et al.*, 2003; Molkentin *et al.*, 1998) (figure 1.7.2.1). Therefore, PMCA4 has been suggested to be an organiser of macromolecular protein complexes, in addition to its role in modulating signal transduction pathways in the heart. In fact most recently PMCA4 was found to have a structural role in tethering nNOS to a highly compartmentalised domain within the cardiac cell membrane (Mohamed *et al.*, 2011b). Thus, in the heart PMCA4 would appear to play a more important role in signal transduction/tethering rather than in the regulation of global $[Ca^{2+}]_i$ homeostasis as suggested in other cell types/tissues (previously mentioned). PMCA4 has been implicated in several patho-physiological conditions of the heart including cardiac hypertrophy, reduced β-adrenergic responsiveness and long QT syndrome (Mohamed *et al.*, 2009; Oceandy *et al.*, 2007; Ueda *et al.*, 2008; Wu *et al.*, 2009).

1.7.1 Role of PMCA4 in cardiac hypertrophy

Cardiac hypertrophy, is characterised by enlargement of the heart and increased cell volume in response to either exercise (non-pathological) or pathological stimuli including hypertension, ischemic heart or infectious agents (Lorell *et al.*, 2000). There is substantial evidence to suggest that PMCA4 overexpression has anti-hypertrophic effects in the heart (Wu *et al.*, 2009).

Increased cardiac hypertrophy was observed in PMCA4 gene deficient mice after pressure overload induced by transverse aortic constriction (TAC) (Wu *et al.*, 2009).

Conversely, hypertrophy of the heart, or cardiomyocytes, was suppressed in transgenic mice overexpressing PMCA4, after TAC and/or stimulation by hypertrophic agents (Wu *et al.*, 2009). The mechanism proposed was that PMCA4 overexpression reduces calcineurin/NFAT signalling in the heart (figure 1.7.2.1). This calcineurin/NFAT signalling pathway is well associated with cardiac hypertrophy and heart failure (Colella *et al.*, 2008; Wilkins *et al.*, 2004). In fact, hypertrophy and the associated NFAT nuclear translocation were inhibited in neonatal rat cardiomyocytes treated with the calcineurin inhibitor, cyclosporin A (Colella *et al.*, 2008). In the same study, hypertrophic agents resulted in increased cell size as well as NFAT nuclear translocation in cardiomyocytes (Colella *et al.*, 2008). Thus, the anti-hypertrophic effects of PMCA4 are likely mediated by PMCA4 forming a functional interaction with calcineurin which inhibits its activity and subsequently suppresses NFAT translocation to the nucleus, to induce the hypertrophic genes.

1.7.2 Role of PMCA4 in cardiac β-adrenergic response

In the heart the β-adrenergic receptors are of crucial importance for myocardial contraction and, when activated, lead to increased contractile force and heart rate. Studies in PMCA4b overexpressing mice (human PMCA4b under the control of myosin light chain kinase (MLC2v) promoter) have demonstrated a significantly reduced cardiac β-adrenergic contractile response which was not observed with mice overexpressing a mutant form of PMCA4 (Oceandy *et al.*, 2007). As the mutant PMCA4 (PMCA4 ct 120) is unable to interact with/ modulate nNOS due to lack of PDZ-binding domain but still retains its Ca^{2+} pumping activity, this suggests that the

PMCA4-nNOS interaction is important in the β-adrenergic cardiac function in mice (Oceandy *et al.,* 2007). Treatment of PMCA4 ct120 transgenic mice or wild type mice with a specific inhibitor of nNOS resulted in the attenuation of the β-adrenergic contractile response (Oceandy *et al.,* 2007). Hence data generated in this study suggests the modulated β-adrenergic contractile response observed in PMCA4 overexpressing animals was mediated by nNOS dependent mechanisms (Oceandy *et al.*, 2007).

A subsequent study using cardiomyocytes from hPMCA4b overexpressing mice elucidated downstream effectors of PMCA4-nNOS signalling pathway involved in the reduced cardiac β-adrenergic response (as was observed by (Mohamed *et al.,* 2009; Oceandy *et al.,* 2007)). A significant reduction in nNOS activity due to PMCA4 inhibition of nNOS, led to a cascade of events in which NO levels and cyclic GMP (cGMP) production by soluble guanylyl cyclase (sGC) were reduced (Mohamed *et al.,* 2009). Reduction in cGMP levels translates into a decrease in phosphodiesterase activity, which prevents cyclic AMP (cAMP) degradation (figure 1.7.2.1). Elevated cAMP levels activate increased protein kinase A (PKA) activity resulting in an attenuated response to β-adrenergic agonists through phosphorylation of proteins (i.e. phospholamban and cardiac troponin I (cTnI)) involved in excitation-contraction coupling (Mohamed *et al.,* 2009). Hence, PMCA4 has been shown to be crucial in the modulation of β-adrenergic cardiac function owing to its role in regulating nNOS activity and subsequently NO signalling in cardiac cells (figure 1.7.2.1).

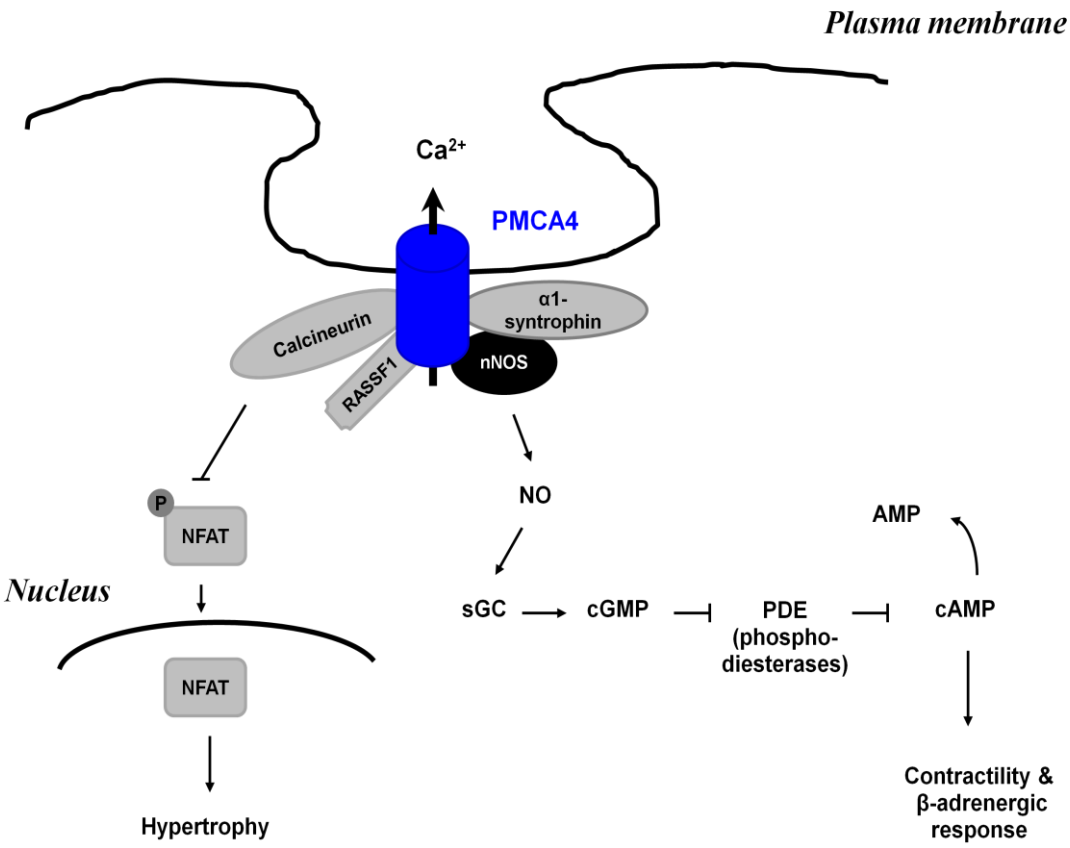

Key: **AMP** - adenosine monophosphate; **cAMP** - cyclic-adenosine monophosphate; **cGMP** - cyclic-guanosine monophosphate; **NFAT** - nuclear factor of activated T cells; **nNOS** - neuronal nitric oxide synthase; **NO** - nitric oxide; **PDE** - phosphodiesterase; **PMCA4** - plasma membrane Ca^{2+} ATPase 4; **RASSF1** - Ras-associated factor 1; **sGC** - soluble guanylyl cyclase

Figure 1.7.2.1: A schematic representation of a PMCA4 molecule localised to a cardiomyocyte plasma membrane bound to its partner molecules, calcineurin, Ras-associated factor 1 (RASSF1), neuronal nitric oxide synthase (nNOS) and α1-syntrophin (adapted from (Cartwright *et al.*, 2011b). Illustrated are intracellular signal transductions pathways leading up to cardiomyocyte hypertrophy (mediated by calcineurin/nuclear factor of activated T-cell (NFAT) signalling) as well as cardiomyocyte β-adrenergic signal transmission (mediated by nNOS signalling) dependent on the formation of functional protein-protein interactions between PMCA4 and partner molecules.

1.7.3 Role of PMCA4 in long QT syndrome

PMCA4 has been linked to long QT syndrome (LQTS) (a condition associated with sudden cardiac death due to arrhythmias) through the macromolecular complex it forms with nNOS and α1-syntrophin in cardiomyocyte plasma membranes (Ueda *et al.*, 2008) (illustrated in figure 1.7.0.1 & 1.7.2.1). A rare missense mutation (A390V) found in the gene encoding α1-syntrophin (SNTA1) has been characterised in an LQTS patient (Ueda *et al.*, 2008). This mutation, present in the region of α1-syntrophin which binds to PMCA4, was shown to selectively disrupt α1-syntrophin interaction with both PMCA4 and nNOS. Since there is evidence of PMCA4 inhibiting nNOS activity (Mohamed *et al.*, 2009; Oceandy *et al.*, 2007; Williams *et al.*, 2006), and of PMCA4 and α-1 syntrophin acting synergistically to negatively regulate nNOS in the heart (Williams *et al.*, 2006), the disrupted association of PMCA4 with the nNOS complex as a result of the A390V mutation was concluded to release the inhibition of nNOS by PMCA4 (Ueda *et al.*, 2008).

Evidence from genome-wide association studies have also highlighted that disruption of PMCA4-nNOS regulation (potentially mediated by nNOS binding/adaptor proteins) may have patho-physiological consequences in the heart. Polymorphisms in CAPON (another adaptor protein like α1-syntrophin capable of interacting with both PMCA4 and nNOS) were associated with a hallmark of cardiac arrhythmia and LQTS (Aarnoudse *et al.*, 2007; Arking *et al.*, 2006; Beigi *et al.*, 2009). This supports the notion that genes encoding for nNOS binding (or adaptor) proteins may be suitable genetic candidates for susceptibility to LQTS-syndrome. Hence, in this case the importance of PMCA4 in modulating signal transduction in cardiac cells is mainly due to its interaction with adaptor and/or partner molecules.

At this juncture, it is clear that PMCA4 is important in the normal physiological function of the mammalian heart, principally due to a more important role in modulating signal transduction pathways facilitated by associations with specific partner/adaptor molecules, independent of regulating global $[Ca^{2+}]_i$. It would also appear that genetic modifications of PMCA4 itself or its associating molecules or perturbations in the downstream signalling effectors may result in pathological consequences for the heart (Williams *et al.*, 2006).

1.8 PMCA4 in smooth muscle

In mouse bladder smooth muscle, protein analyses have established that PMCA4 is one of the major PMCA isoforms expressed (Liu *et al.*, 2006). Functional analysis of bladder contractility from PMCA gene targeted mice (deficient in PMCA4) suggested PMCA4 is significant to both excitation-contraction coupling and in Ca^{2+} extrusion-relaxation in this tissue (Liu *et al.*, 2006).

Bladder smooth muscle from PMCA4 ablated mice displayed shortened relaxation times in Ca^{2+} free solution after contraction to KCl, showing that ablation of PMCA4 impeded bladder smooth muscle relaxation. Although NCX was found to be the predominant contributor to relaxation in this smooth muscle, overall PMCA activity (of bladders from both PMCA4 and PMCA1 deficient mice) was quantified to contribute around ~25-30% to relaxation (Liu *et al.*, 2006). In contrast, in uterine smooth muscle, the contribution of PMCA4 towards Ca^{2+} efflux was quantified at around ~70%, (Matthew A *et al.*, 2004; Matthew *et al.*, 2004). Hence the contribution of PMCA4 to Ca^{2+} extrusion-relaxation may depend on the type of smooth muscle tissue. Furthermore, in mouse intestinal smooth muscle tissues, PMCA4 inhibition increased agonist stimulated contractile responses (El-Yazbi *et al.*, 2008), an observation which is again consistent with a role for PMCA4 in modulating levels of $[Ca^{2+}]_i$ of smooth muscle cells. PMCA was shown to co-localise with caveolin-1 in plasma membranes of tracheal and intestinal smooth muscle tissues with the disruption of caveolae in tracheal smooth muscles preventing the effects of PMCA4 (El-Yazbi *et al.*, 2008). Thus, the spatial arrangement of PMCA4 and caveolin-1 in plasma membrane caveolae may be important for optimum PMCA4 activity (El-Yazbi *et al.*, 2008).

In addition to a role in relaxation of smooth muscle, there is also evidence to suggest that PMCA4 may influence contraction. Bladder smooth muscle obtained from PMCA4 gene targeted mice (deficient in PMCA4) elicited a prolonged contraction half time to KCl (Liu *et al.*, 2006). This was attributed to co-operation between PMCA and NCX in that enhanced sub-plasmalemmal $[Ca^{2+}]_i$ potentially due to loss of PMCA4, also stimulated NCX activity. This hypothesis was consistent with the significantly shortened contraction time observed in PMCA gene targeted bladders upon inhibition of NCX (Liu *et al.*, 2006). Additional effects of PMCA4 on receptor-mediated (carbachol) signalling in bladder smooth muscles have also been suggested (Liu *et al.*, 2007). Bladder smooth muscle from PMCA4 deficient mice exhibited reduced contractile responses to carbachol but an increased contractile response to KCl (that was specific to PMCA4 deficient mice, heterozygous for the PMCA1 gene) which could not simply be explained by effects on $[Ca^{2+}]_i$ (Liu *et al.*, 2007). The mechanisms for this are currently unknown but the data does suggest that PMCA4 can modulate smooth muscle contractility by mechanisms which are independent of changes in global $[Ca^{2+}]_i$. Thus, PMCA4 may be involved in the regulation of Ca^{2+} homeostasis at least in smooth muscle cells of mouse bladder, uterus, intestine and trachea although additional effects may also be evident.

1.9 PMCA4 in the vasculature

Despite the fact that the role of PMCA (in particular isoform 4) has started to become apparent in mammalian bladder, uterine, intestine and tracheal smooth muscles, much is still unclear about its physiological significance in vascular smooth muscle (VSM) function. There have been several reports of PMCA4 expression in VSM cells (Afroze *et al.*, 2003; Hammes *et al.*, 1994; Husain *et al.*, 1997; Stauffer *et al.*, 1995). Most recently, real-time PCR detected varied expression of PMCA isoforms in vascular smooth muscle and in vascular endothelium, with PMCA4 being the predominant isoform in VSM (Pande *et al.*, 2006).

Thus far, in attempts to provide more insight into the physiological effects of PMCA4 on contractile function of VSM two different approaches have been undertaken. One approach made use of transgenic mice overexpressing human PMCA4b (either under the control of the vascular-specific SM22α promoter, or specifically induced in SM by doxycline) (Gros *et al.*, 2003; Schuh *et al.*, 2003) whereas the other approach used inhibitor peptides to PMCA4 called caloxins (Pande *et al.*, 2006; Pande *et al.*, 2008).

Surprisingly, both transgenic mouse models overexpressing PMCA4 showed an increase in blood pressure (Gros *et al.*, 2003; Schuh *et al.*, 2003). Studies using isolated conduit arteries (aorta) from mice overexpressing PMCA4 demonstrated increased contractile responses to depolarisation with KCl (Schuh *et al.*, 2003), while those of isolated mesenteric resistance arteries showed a heightened extent of myogenic contractile response as well as an increased sensitivity to the vasoconstrictor, phenylephrine (Gros *et al.*, 2003). Such data, is unexpected if PMCA4 were acting primarily as a pump which regulates global Ca^{2+} extrusion; an

increased activity of a Ca^{2+} extrusion pump may be expected to increase Ca^{2+} removal, enhance smooth muscle relaxation and reduce blood pressure. Furthermore, the basal $[Ca^{2+}]_i$ levels of VSM cells were not significantly altered by overexpression of human PMCA4 in the mouse vasculature (Gros *et al.*, 2003). Thus, unlike the studies on uterine and bladder smooth muscles, these studies provided no direct evidence to support the notion that PMCA4 has a principal functional role in global Ca^{2+} extrusion-relaxation in the vasculature.

The increased arterial contractility and elevated blood pressure observed in PMCA4 overexpressing mice were attributed to negative regulation of nNOS activity by PMCA4 (Gros *et al.*, 2003; Schuh *et al.*, 2003) as has been well characterised in the heart as well as within *in vitro* cellular systems (Cartwright *et al.*, 2007; Schuh *et al.*, 2001; Williams *et al.*, 2006). Thus, while studies in PMCA4 overexpressing mice clearly show that PMCA4 can regulate vascular tone and blood pressure the results suggest that it does this, not by modulation of global $[Ca^{2+}]_i$, but by a role in signal transduction (Gros *et al.*, 2003; Schuh *et al.*, 2003).

In contrast, studies using caloxin 1b1, proposed to be specific for PMCA4, demonstrated an augmented vascular contractility elicited by rat aortic preparations in response to agonist stimulation. Moreover, caloxin 1b1 increased cytosolic $[Ca^{2+}]$ in cultured arterial smooth muscle cells derived from porcine aortas (Pande *et al.*, 2006). More recently, the use of another variant of the inhibitor caloxin 1c2, (deemed to have a greater than 10-fold selectivity for PMCA4 over the other PMCA isoforms) was shown to increase the basal tone of isolated coronary arteries (Pande *et al.*, 2008). Caloxin 1c2 also increased the force of contraction elicited by arteries when extracellular $[Ca^{2+}]$ ($[Ca^{2+}]_o$) was lowered to 0.05mM and other Ca^{2+} removal methods like NCX and SERCA were inhibited (Pande *et al.*, 2008). However, such

an increase was not seen at higher $[Ca^{2+}]_o$ of 1.6mM (Pande *et al.*, 2008). Collectively, these data from the caloxin studies, reflect the expectations of inhibiting a Ca^{2+} extrusion pump; $[Ca^{2+}]_i$ would be expected to increase within VSM cells (where PMCA4 is largely expressed), leading to enhanced vascular contractile effects. Hence, the data from these studies would seem consistent with PMCA4 functioning mainly as a Ca^{2+} extrusion pump in the vasculature.

Thus, while overexpression of PMCA4 in the vasculature, causes augmentation of arterial contractility by the downregulation of vascular nNOS activity (and thus NO production) mediated via the PMCA4-nNOS complex (Gros *et al.*, 2003; Schuh *et al.*, 2003), inhibition of PMCA4 with caloxins also increases arterial contractility via effects on global $[Ca^{2+}]_i$ (figure 1.9.0.1).

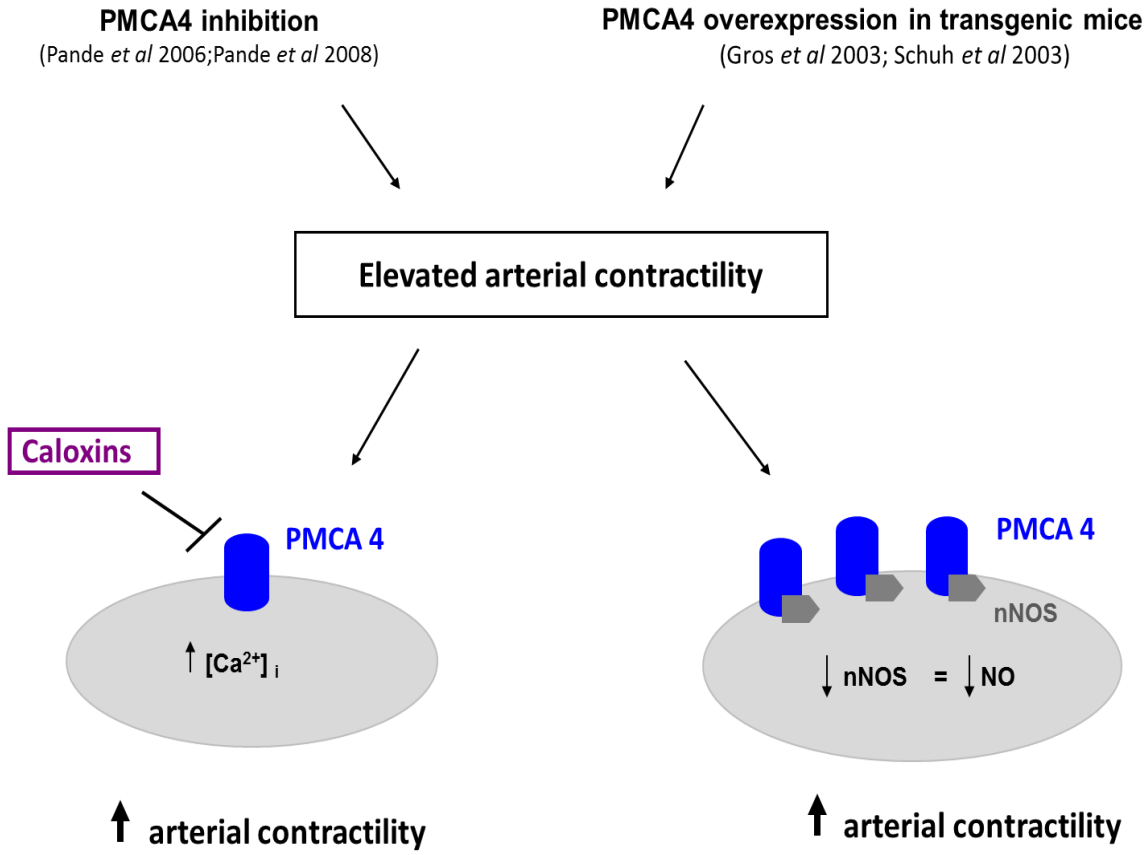

Figure 1.9.0.1: Proposed mechanisms within VSM cells responsible for the increase in vascular contractility observed when PMCA4 was inhibited or overexpressed. The enhanced vasocontractile effects seen in the PMCA4 inhibition studies were explained via modulation of global $[Ca^{2+}]_i$ (Pande *et al.*, 2006; Pande *et al.*, 2008), whereas in PMCA4 overexpressing mouse arteries, this was likely due to PMCA4 inhibiting nNOS, NO production owing to the PMCA4-nNOS functional interaction in the VSM plasma membrane (Gros *et al.*, 2003; Schuh *et al.*, 2003).

Currently, the effects of PMCA4 on vascular contractility remain incompletely understood and must be further investigated. Furthermore, there have been no studies to date which have investigated the effects of PMCA4 expression on vascular/arterial structure despite the fact that PMCA4 has been associated with VSM cell proliferation, with changes in PMCA4 mRNA expression levels being evident during cell cycle progression (Husain *et al.*, 1997). This is important as resistance arterial remodelling is a key feature of hypertension (Agabiti-Rosei, 2003; Feihl *et al.*, 2008; Izzard *et al.*, 2005; Mulvany, 1999) and PMCA4 has been associated with hypertension (Gros *et al.*, 2003; Schuh *et al.*, 2003).

1.10 Aims

The present study will aim to investigate further the role of PMCA4 in resistance arterial contractility by using two approaches i) the use of PMCA4 ablated mice and ii) a novel inhibitor of PMCA4. In addition, the effects of PMCA4 ablation on the structure of mouse arteries will also be investigated.

1.11 Hypothesis

The genetic ablation or inhibition of PMCA4 (with a novel PMCA4 inhibitor) will result in a decrease in the *in vitro* vascular contractile responses stimulated by exogenously added vasoconstrictors which may be associated with changes in nNOS activity and/or intracellular Ca^{2+} concentrations.

1.12 Objectives

The objectives of this study were i) to investigate the vascular contractile responses and ii) to investigate the passive structural characteristics of isolated mesenteric resistance arteries obtained from PMCA4 KO $^{(-/-)}$ mice in comparison to arteries from WT $^{(+/+)}$ mice in an *in vitro* pressure myograph system. Additional objectives were to iii) elucidate the effects of a novel PMCA4 inihibitor, AP2 on the vasocontractile responses of isolated mesenteric arteries from WT $^{(+/+)}$ mice and iv) to elucidate the effects of PMCA4 ablation and AP2 application on global $[Ca^{2+}]_i$ by loading arteries with the Ca^{2+}-sensitive dye, Indo-1.

Chapter 2

Methods

2.1 PMCA4 gene ablated mice

The PMCA4 gene ablated mice were provided by Professor Ludwig Neyses and Dr Elizabeth Cartwright's group at University of Manchester (Schuh *et al.*, 2004).

2.2 Breeding and maintenance of the PMCA4 gene targeted mice colony

Successful breeding of male with female mice heterozygous for the mutation maintained the colony. This resulted in wild type (PMCA4 WT $^{(+/+)}$), heterozygous (PMCA4 Ht $^{(+/-)}$) and PMCA4 knockout (PMCA4 KO $^{(-/-)}$) offspring born in the expected Mendelian ratio 25%, 50% and 25%. Homozygous PMCA4 mutant male mice are infertile.

Male PMCA4 WT $^{(+/+)}$, Ht $^{(+/-)}$ and KO $^{(-/-)}$ mice were kept and utilised at three months old in this study; other PMCA4 Ht $^{(+/-)}$ mice were used to breed the next generation (n was equal to the number of animals used in this study). Mouse husbandry and colony management were provided by the Biological Services Unit (BSU) at the University of Manchester. Mice were kept on a twelve hour light/dark cycle, room temperature of 18-23^{o}C and 40-60% humidity with *ad libitum* access to food, water and enrichment all in accordance to the UK Animals Act 1986.

2.3 Genotyping

There are no visible phenotype differences between the PMCA4 WT $^{(+/+)}$, Ht $^{(+/-)}$ and KO $^{(-/-)}$ mice at birth therefore identification of the genotype of pups was necessary. Each pup was given an identification number when small pieces of tissue were taken from their ears (ear snips) at the approximate weaning age of one month. DNA was prepared from this and polymerase chain reaction (PCR) was used to identify whether the mouse was WT $^{(+/+)}$, Ht $^{(+/-)}$ or KO $^{(-/-)}$ for the PMCA4 targeted allele. The protocol for genotyping included DNA extraction and PCR using the following primer pairs 11 & 12 and 11 & 13 (detailed in section 2.3.2). Whilst I did perform genotyping on several occasions, in the interest of good time management I must acknowledge the help from our research technician Florence Baudouin who carried this out on a routine basis.

2.3.1 DNA Extraction

Genomic DNA was extracted from the collected ear snips following the standardised DNA extraction protocol previously developed and optimised by Professor Ludwig Neyses and Dr Elizabeth Cartwright's group in Manchester, UK and Germany (Schuh *et al.*, 2004). Ear snips were incubated overnight at 56^{o}C in lysis buffer (1M Tris pH 8, 0.05M EDTA pH 8, and 10% (w/v) sodium dodecyl sulphate (SDS)), sterile autoclaved dH_2O and 0.5mg/ml proteinase K was used to break open the cells and expose the DNA within. This was spun in a micro centrifuge at 13,000rpm to separate out hair and cell debris. The supernatant containing genomic DNA was transferred into a new tube and isopropanol (150µl) was added causing DNA to aggregate. DNA was pelleted by centrifugation at 13,000 rpm for 5 minutes. The DNA pellet was washed in ice cold 70% ethanol to remove alcohol soluble salts, air

dried and re-suspended in TE buffer (10mM Tris pH 8 and 0.1mM EDTA). This was heated at 65^{o}C for 10 minutes to completely dissolve the DNA pellet. Each DNA sample was labelled with the unique mouse identification number and stored at 4^{o}C until PCR.

2.3.2 Polymerase Chain Reaction (PCR)

PCR was used to identify the wild type from the mutant PMCA4 allele (containing an intact neomycin nucleotide sequence which interrupted the PMCA4 gene sequence). Three different primers were specifically designed (by Professor Ludwig Neyses' group prior to commencement of this project) to work in pairs i.e. primers 11 and 13 amplified PMCA4 wild type DNA sequences while primers 11 and 12 amplified the mutant PMCA4 DNA sequences (figure 2.3.2.1). The exact primer nucleotide sequences are depicted in figure 2.3.2.1 (primers were supplied by Sigma-Genosystem, UK).

Primer 11:	CTGAGTAAAAGCCACATCG
Primer 13:	GGCTTGTCTTGATAGGTTG
Primer 12:	TATCGCCTTCTTGACGAGTT

A) PMCA4 WT $^{(+/+)}$ allele

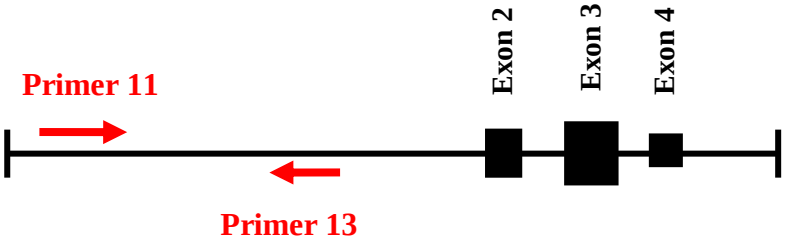

B) Mutant PMCA4 allele

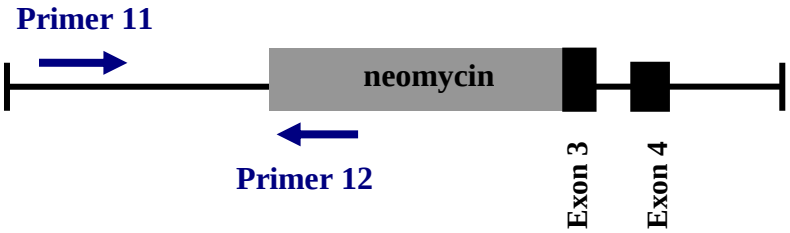

Figure 2.3.2.1: The specific nucleotide sequences of primers 11, 12 and 13. Schematic diagrams shown in A) and B) illustrate these primers (represented by small arrows in A) and B)) bound to PMCA4 target allele. A) Forward primer 11 and reverse primer 13 amplified PMCA4 WT $^{(+/+)}$ DNA sequences (2,500bp). While B) forward primer 11 and reverse primer 12 amplified mutant PMCA4 DNA sequences containing the neomycin marker found in the middle (2,500bp).

The composition of each PCR reaction mix was 15µl of Reddy mix Hi-Fidelity master mix^{TM} (ABgene, Epsom UK), forward and reverse primers (primers 11 and 12 or 13) each at 10pm/µl, 25mM magnesium acetate, sterile ddH_2O and ~50ng - 100ng of DNA. The Reddy mix Hi-Fidelity master mix^{TM} consisted of 210µM dNTPs, 1.35µM $MgCl_2$, 0.75U of DNA Taq polymerase, buffer and red inert gel loading dye.

For each experiment three control PCR mixes were set up: already identified PMCA4 WT $^{(+/+)}$, mutant PMCA4 samples and a negative control lacking DNA. Each isolated DNA sample was unique to a pup and was added to two different PCR reaction mixes, one including the PMCA4 WT $^{(+/+)}$ primer pair (11 and 13) and the other including the PMCA4 mutant primer pair (11 and 12). All PCR reaction mixes were gently vortexed and incubated on the lab bench for a few minutes then placed in a pre-programmed robocycler PCR machine (Stratagene, USA). The PCR conditions used were optimised by Professor Ludwig Neyses and Dr Elizabeth Cartwright's group at University of Manchester and the steps are listed as follows: initial denaturation at 95^{o}C (5 minutes), denaturation 95^{o}C (50 seconds), primers annealing 50^{o}C (50 seconds), extension 68^{o}C (3 minutes 10 seconds). 36 cycles were completed prior to termination 72^{o}C (10 minutes) (Schuh *et al.*, 2004).

2.3.3 Agarose gel electrophoresis

Following PCR, all samples were separated and visualised by DNA electrophoresis on a 1% agarose gel (agarose dissolved in TAE [40mM Tris, 1mM EDTA, 0.11% glacial acetic acid]) stained with 0.5µg/ml ethidium bromide. 1% agarose gel wells were loaded with 8µl of the molecular weight marker Hyper ladder I (Bioline, UK)

and 15µl of each PCR product sample. The loaded agarose gel was covered in TAE buffer solution and electrophoresed at 95 volts for 40 minutes using a Bio-Rad Power Pac. Visualisation by ultra violet light fluoresced ethidium bromide stained PCR DNA fragments as orange. Hyper ladder I molecular weight marker produced DNA bands of known molecular weights (~ 600 to 10,000bp), allowing for easy identification of the amplified PMCA4 DNA fragments sized 2,500bp. The presence of a 2500bp DNA fragment amplified with the WT primers (11&13) and its absence in PCR products generated with mutant primers (11 &12) represented a PMCA4 WT $^{(+/+)}$ mouse (figure 2.3.3.1). The reverse was observed in a PMCA4 KO $^{(-/-)}$ mouse and when a 2500bp DNA fragment was seen in the amplified products with WT (11&13) and in PCR products generated with mutant primers (11&12) this represented a PMCA4 Ht $^{(+/-)}$ mouse (figure 2.3.3.1).

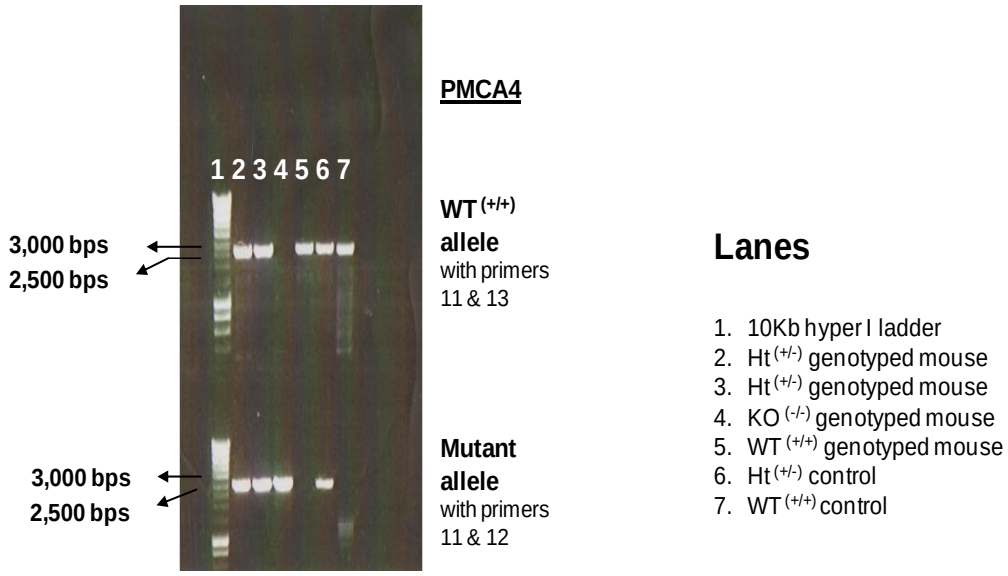

Figure 2.3.3.1: PCR genotyping of PMCA4 mice. The gel photograph shows in lane 1, molecular weight marker (hyper ladder I 600-10,000 bps) and in lanes 2 to 5 amplified PCR products (with PMCA4 WT $^{(+/+)}$ primers 11 &13 top row wells and with PMCA4 mutant primers 11 & 12 bottom row wells) sized 2500bps as separated on a 1% agarose gel. Lanes 6 to 7 shows previously identified PMCA4 Ht $^{(+/-)}$ and WT $^{(+/+)}$ amplicons (with both primer sets) from control PCR mixes. In lanes 2 to 3, mice were identified as PMCA4 Ht $^{(+/-)}$ due to the presence of both WT $^{(+/+)}$ and PMCA4 mutant amplicons identified with both primer sets. In lane 4 the single PMCA4 mutant identified by primer pair 11&12 indicated that this mouse was a PMCA4 KO $^{(-/-)}$ and in lane 5 the single WT $^{(+/+)}$ amplicon with primer pair 11&13 indicated a PMCA4 WT $^{(+/+)}$ mouse.

2.4 Dissection of arterial tissue

Male mice aged three months were humanely killed by cervical dislocation in accordance with University of Manchester guidelines and the UK Animals (Scientific Procedures) Act 1986. Immediately after death the entire mesenteric bed was removed from a mouse abdomen and placed into ice cold physiological salt solution (PSS) at pH 7.4 for transport to the lab. PSS composition was: NaCl 119mM, KCl 4.7mM, $MgSO_4.7H_2O$ 1.17mM, $NaHCO_3$ 25mM, KH_2PO_4 1.17mM, K_2EDTA 0.03mM, glucose 5.5mM and $CaCl_2.2H_20$ 1.6mM. On the lab bench, a freshly removed mesenteric bed was pinned out onto a silicon coated petri dish containing ice cold PSS (as shown in the photograph below) so that adherent adipose fatty tissue could be removed and third order mesenteric resistance arteries were cleanly isolated under a microscope (Zeiss, Stemi 1000 3.5x magnification). Cleaned third order mesenteric resistance arteries were segmented to 2mm in length for *in vitro* studies in the pressure myograph system (Living Systems Instrumentation, USA) as we have previously described (Hausman *et al.*, 2011; Shaw *et al.*, 2006; Withers *et al.*, 2009). From the same mouse mesenteric bed cleaned third order mesenteric arteries were processed for histology (section 2.4.1) and the rest of the cleaned arteries of the mesenteric bed were snap frozen in liquid nitrogen then kept at -80^0C until protein extraction (section 2.7.1).

From the same mouse, the thoracic aorta was also very cleanly dissected out, cleared of fat and adherent tissue (figure 2.4.1). Excess blood clots were removed from aortic tissue very carefully with dissection forceps and the tissue was immediately frozen in liquid nitrogen then stored at -80^oC for the extraction of protein (section 2.7.1) or otherwise the cleaned aortas were segmented to approximately 1.5cm segment lengths for further histological processing (section 2.5). On occasion, whole

brain tissue was also removed from PMCA4 WT $^{(+/+)}$ or KO $^{(-/-)}$ mice and immediately frozen in liquid nitrogen then stored at -80^{o}C for protein extraction.

A) Mouse mesenteric vascular bed B) Mouse thoracic aorta

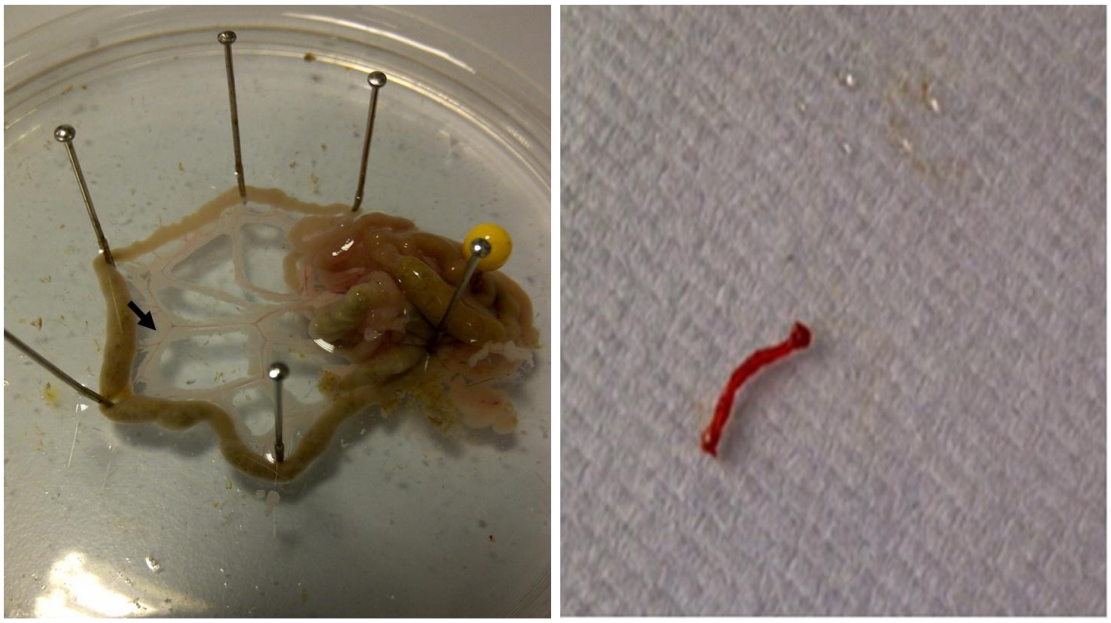

Figure 2.4.1: Photographic images of a mouse mesenteric vascular bed and a mouse aortic segement. In A) is the photograph of a freshly removed mouse mesenteric branched vascular bed pinned out on a silicon coated petri dish containing ice cold PSS solution. Blood vessels are encased in adipose fatty tissue (white spongy appearance) and the black arrow points to a third order resistance artery (approximately 100 to 200µm in diameter). Shown in B) is the photograph of a freshly removed mouse thoracic aorta (approximately 0.5 to 1mm in diameter), cleaned of connective tissue on a silicon coated petri dish.

2.5 Histology

Thoracic aortic segments (approximately 1.5cm in length) or third order mesenteric arterial segments (approximately 2mm in length) were fixed with 4% paraformaldehyde in 0.1M phosphate buffered saline (PBS) (Oxoid Ltd, UK) for at least 6 hours (in the case of aortic segments) or for 3 hours (in the case of mesenteric arterial segments) minimum at 4^{o}C ((Shaheen, 2010) adapted for mouse arterial sections). Fixed tissues were transferred into plastic histology cartridges in 50% industrial methylated spirit (IMS). The samples were then dehydrated and immersed in liquid paraffin wax using a Shandon Citadel 2,000 tissue processor. After being immersed in paraffin during the final step in tissue processor, samples were removed and aortic or mesenteric arterial segments were held by a pair of forceps perpendicular to the base of a metal mould containing liquid paraffin and cooled to -20^{o}C for 30 minutes to ensure that vessel segments were embedded in an upright position within the paraffin block. Transverse sections 5µm thick were cut on a microtome (Leitz 1512, (oil) Germany), mounted onto poly-l-lysine coated slides (VWR) and dried overnight at 37^{o}C. Prior to staining the sections were deparaffinised in xylene for 1 hour 30 minutes and then twice for 10 minutes, then dehydrated through descending grades of ethanol (100, 95, 90 and 70%). This was followed with a wash in running tap water for 5 minutes and distilled water for 1 minute. The many attempts made in the upright positioning of fixed mesenteric arteries within a paraffin block were not always successful owing to their very small size which meant that PFA-fixed arteries were lost during processing in the Shandon tissue processor. Otherwise, transverse mesenteric arterial sections fell from adhesive slides during deparaffinising, dehydration and rehydration steps and could

not be viewed with a microscope (Leica DM LB 100T, 60x, 40x, 20x & 10x objectives).

Haematoxylin and eosin (H&E) staining was used to examine gross morphology by identifying the cell nuclei, cytoplasm and extracellular matrix of cells present in the vascular walls of sectioned aortas (and on very rare occasions sectioned mesenteric arteries). The protocol was established by the Neyses group (Shaheen, 2010) although the timings were adapted for mouse aortic and mesenteric vessel sections. Slides were transferred into haematoxylin for 2 minutes then rehydrated under running tap water for 5 minutes. The sections were stained with eosin for 20 seconds, transferred to water and dehydrated through ascending grades of ethanol (70, 90, 95 and 100%). The sections were cleared in xylene to remove all traces of ethanol then mounted under coverslips with DPX mountant (N,N'-4-xylylenebis(pyridinium) (RA Lamb Ltd) and left to dry overnight at room temperature before examination using a microscope (Leica DM LB 100T, 10x, 20x & 40x objectives). Subsequently, the serial mouse aortic sections were used for immunostaining with primary antibodies as described below.

2.6 Immunohistochemistry

Immunohistochemistry was used to determine the expression and localisation of PMCA4 and nNOS within PMCA4 WT $^{(+/+)}$ and KO $^{(-/-)}$ mouse aortas by co-immunostaining (with antibodies to PMCA4 and nNOS, PMCA4 and α-actin VSM marker and PMCA4 and CD34 vascular endothelial marker) (Matsumoto *et al.*, 2003; Testa *et al.*, 2009). Aortic sections obtained from three PMCA4 WT $^{(+/+)}$ and

from three KO $^{(-/-)}$ mice aged 3 months (n=3) were analysed experimentally by immunohistochemistry. Experiments were repeated using different serial sections (at least 3 times) to minimise variability introduced by different aortic sections.

Slides containing aortic sections were incubated in 3% hydrogen peroxide for 15 minutes and washed twice with double distilled water for 10 minutes each before a final 10 minutes wash in phosphate buffered saline (PBS) (Oxoid Ltd, UK) composition: 137mM NaCl; 2.7mM KCl; 4.3mM Na_2HPO_4 and 1.47mM KH_2PO_4 at pH 7.4). Antigen retrieval was carried out using proteinase K in PBS (0.1mg/ml) for 10 minutes at room temperature in a humid chamber in order to minimise cross linking caused by tissue fixative. Sections were permeablised with Triton X-100 (BDH Ltd, UK) in PBS (0.1%) for 10 minutes and then washed in PBS twice for 10 minutes each. Non specific binding sites were blocked by incubation of tissue sections with 3% bovine serum albumin (BSA) in PBS for an hour at room temperature in a humid chamber.

The blocking agent (3% BSA in PBS) was removed by three 5 minute washes in PBS and followed by overnight incubation at 4^oC with the primary antibody (or antibodies in the case of co-staining). Initially, concentrations of primary antibodies were at 1:100 (in PBS); optimum results shown in chapter 3 were achieved at concentrations of 1:50 (in PBS) (table 2.6.1). For negative control(s), aortic sections were incubated with PBS instead of primary antibody using the same conditions.

Next day, three 5 minute PBS washes removed excess primary antibodies before incubation, at room temperature for 2 hours in the dark, with the appropriate secondary antibody (or antibodies in the case of co-staining) conjugated with texas red or FITC green fluorescent labels (Cell signaling Technology) at concentration of 1:500 (in PBS). Excess secondary antibody was washed away with PBS and sections

were stained with 3μM of 4', 6-diamidino-2-phenylindole dihydrochloride (DAPI), (Invitrogen Ltd, UK) at the concentration 1:100 (in PBS) for 5 minutes to identify the cell nuclei within the vascular walls of aortic tissue sections. Finally sections were washed in PBS then sterile water and mounted with coverslips using the Vectashield mounting medium (Vector Laboratories). Negative controls also underwent the same PBS washes, secondary antibody incubation(s) and mounting procedures as is described above. Aortas were visualised using a fluorescence (Olympus, (Ernst) fluorescence microscope: at 10x, 20x and 40x (oil) objectives) and an upright confocal fluorescence microscope (Nikon, Eclipse C1, Plus, at the listed (oil) objectives: 10x, 20x, 40x and 60x) with texas red, FITC green and blue filters using the EZ-C1 3.90 free viewer software.

Primary antibody	**Dilution (in PBS at 4^0C)**	**Supplier**
Mouse anti-PMCA4 monoclonal antibody	1/50	[JA9] Abcam plc
Rabbit anti-α-smooth muscle actin polyclonal antibody	1/50	Abcam plc
Rabbit anti-CD34 (endothelial cell marker) polyclonal antibody	1/50	Abcam plc
Rabbit anti-nNOS polyclonal antibody	1/50	Affinity Bioreagents (ABR)
Secondary antibody	**Dilution (in PBS at 4^0C)**	**Supplier**
Anti-mouse IgG texas red conjugate	1/500	Cell signaling Technology
Anti-rabbit IgG FITC conjugate	1/500	Cell signaling Technology

Table 2.6.1: Optimum conditions for the primary and secondary antibodies used to produce fluorescence images of aortic sections following immunohistochemistry.

2.7 Western blotting

Western blotting was used to further confirm the presence/ absence of PMCA4 protein in PMCA4 WT $^{(+/+)}$ and KO $^{(-/-)}$ mice and to determine whether ablation of PMCA4 modulated the expression of PMCA1, NCX and SERCA in the mouse vasculature (Ca^{2+} removal mechanisms present in VSM cells).

2.7.1 Protein extraction

Freshly isolated and frozen (to -80^{0}C) aortas and mesenteric arteries from 3 month old, male PMCA4 WT $^{(+/+)}$ and KO $^{(-/-)}$ mice were thawed on ice. Due to the abundant and ubiquitous expression of PMCA4 in mammalian brain (Stauffer *et al.*, 1995; Zylinska *et al.*, 2000), whole brain tissues removed from PMCA4 WT $^{(+/+)}$ and KO $^{(-/-)}$ mice were prepared in a similar method to vascular tissues. Thawed samples were homogenised in lysis buffer containing (1X PBS, 1% Igepal, 0.5% sodium deoxycholate, 0.1% SDS, 20µM PMSF, 500ng/ml leupeptin, 1µg/ml aprotium, 500ng/ml pepstatin). Initially an electric homogeniser was used but better protein extractions were achieved with a dounce homogeniser because samples could be kept on ice during homogenisation keeping protein degradation to a minimum. To separate debris from protein containing lysates, samples were centrifuged at 4^{0}C for 10 minutes at 3000rpm and the supernatant transferred to fresh microcentrifuge tubes and kept at -80^{0}C.

A standard bicinchoninic acid (BCA) protein assay (Thermo Scientific, Pierce protein research products, Illinois, USA) was used to determine the protein concentration in each supernatant sample. Diluted bovine serum albumin (BSA) standards at the listed descending concentrations: (µg/ml) 2000, 1500, 1000, 750,

500, 250, 125, 25 and 0 (or blank) and a reducing agent (containing sodium carbonate, sodium bicarbonate, bicinchoninic acid and sodium tartarate in 0.1M sodium hydroxide and 4% cupric sulphate) were prepared and incubated together in a micro well plate for 30 minutes, at 37^0C. On the same micro well plate, the reducing agent was also incubated with unknown aortic/brain tissue samples under the same conditions. Absorbance at or near 562nm were measured on a MultiSkan* Ex microplate photometer (Thermo Labsystems, Thermo Scientific) and analysed using the Ascent^{TM} computer software (Indigo Biosystems, USA) by plotting a standard curve of the blank corrected (for background) 562nm measurements of BSA standards against concentrations (in µg/ml) (as shown by figure). The standard curve generated was used to determine the final protein concentration of each unknown aortic sample for further analysis by Western blotting.

2.7.2 Protein separation, membrane blotting, blocking and antibody probing

Protein homogenates (50µg) were denatured in laemmli loading buffer (composition: 4% SDS, 10% 2-mercaptoethanol, 20% glycerol, 0.004% bromophenol blue and 0.125M Tris HCl) and separated by 8% Sodium Dodecyl Sulphate PolyAcrylamide Gel Electrophoresis (SDS-PAGE) at 120 volts for 1 hour 30 minutes using an electrophoresis cell (Mini Protean Tetra cell, Bio-Rad) filled with running buffer (composition: 25mM Tris HCl, 200mM glycine and 1% v/v 10% SDS). The separating gel was blotted to polyvinylidene fluoride (PDVF) membranes (Millipore-0.45 µm pore size) in a wet transfer procedure (wet transfer device, XCell SureLock™ Mini-Cell wet transfer device (Invitrogen)) at 30 volts for 2 hours (in

transfer buffer containing: 25mM Tris, 200mM glycine and 20% methanol) using a Bio-Rad Power Pac 200. Red ponceau staining for 2 minutes confirmed successful or unsuccessful protein transfer unto the PDVF membrane (figure 2.7.2.1).

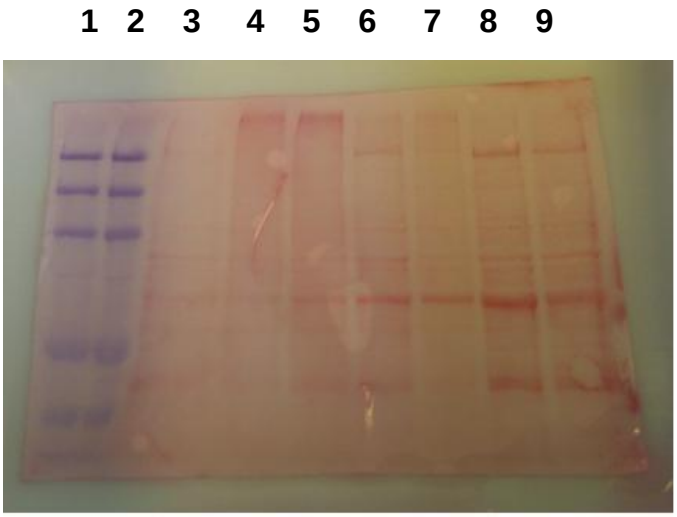

Figure 2.7.2.1: An example of a red ponceau stained PDVF membrane after SDS-PAGE and wet transfer of aortic protein extracts. All tissue samples were obtained from male PMCA4 WT $^{(+/+)}$ or KO $^{(-/-)}$ mice aged 3 months. The equal spread of pink bands down each lane (from lane 3 to 9) on the membrane are indicative of successful protein resolution by SDS-PAGE and transfer unto PDVF membrane prior to blocking and immunoblotting the with antibodies.

In order to prevent non specific antibody binding, membranes were blocked, initially in 3% non-fat dry milk in PBS-T (PBS with 0.05% Tween 20) for 2 hours 30 minutes, then overnight in 1% BSA in PBS-T (PBS with 0.05% Tween 20), then in 3% BSA in PBS-T (PBS with 0.05% Tween 20) for 2 hours 30 minutes however, the optimum visual results were achieved by blocking overnight in 3% BSA in PBS-T (PBS with 0.05% Tween 20) (refer to figure 2.7.2.2).

A) Blocking in 3% milk **B) Blocking in 1% BSA** **C) Blocking in 3% BSA**

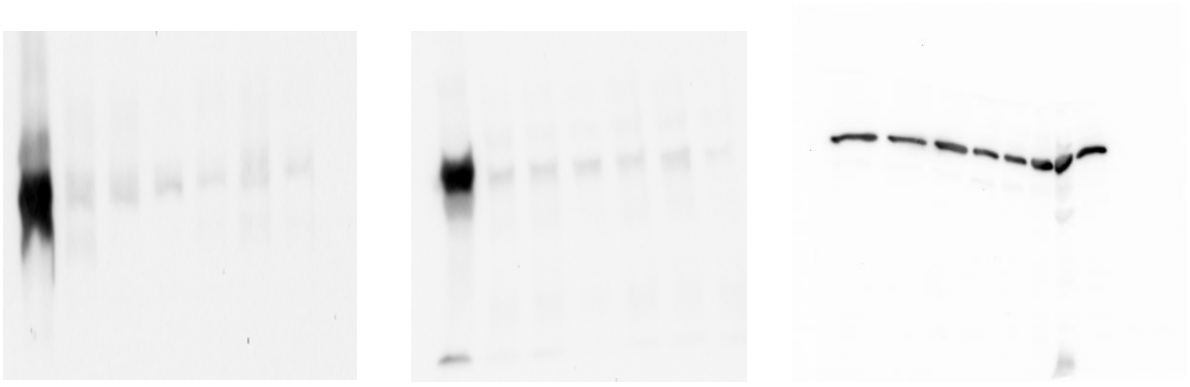

Figure 2.7.2.2: Optimisation of blocking agent used in Western blotting experiments. Chemiluminescence generated images of PDVF membranes blocked with different agents under different conditions. After immunoblotting membranes with GAPDH-HRP conjugated antibody used to assess whether protein loading was equal across the lanes. A) membrane blocked in 3% non-fat dry milk (in PBST) for 2 hours 30 minutes, at room temperature B) membrane blocked in 1% BSA (in PBST) overnight at 4^0C C) membrane blocked in 3% BSA for 2 hours and 30 minutes at room temperature. Optimum results were achieved in C).

The blotted membrane was probed with a primary antibody at 4^0C on a rocker (i.e. polyclonal anti-PMCA4, polyclonal anti-PMCA1, monoclonal anti-NCX1, polyclonal anti-nNOS, monoclonal anti-SERCA2 and loading controls i.e. monoclonal anti-GAPDH-horseradish peroxidise (HRP) conjugate and monoclonal anti-α-tubulin-HRP conjugate, supplied by Abcam plc, Affinity Bioreagents, Santa Cruz Biotechnology and Swant). The optimum incubation conditions and concentrations used to produce the immunoblotted membrane images shown in chapter 3 (results) after membrane immunoblotting with the above listed antibodies are listed in table 2.7.2.3 below.

After four washes with PBS-T, membranes were incubated with secondary anti-mouse or anti-rabbit HRP-coupled antibodies 1:2000 (Dako and Cell Signalling) for 2 hours on a rocker at room temperature and subsequently, washed three times with PBS-T. Proteins were detected with enhanced chemiluminescent solution (ECL™) (Fisher Scientific, ECL Plus, Western blotting Detection Reagents) in the dark, and visualised by a chemiluminescence detection system (Molecular Imager ChemiDocTM XRS, Bio-Rad) at various exposure times (in the range of 1 minute to 5 minutes until an unsaturated image was generated) in order to visualise the HRP-conjugated secondary antibody bound to primary antibody. Generated blot images by the chemiluminescence detection system showed protein bands of interest and band densities were quantified using the computer software Image J (Image Processing and Analysis in Java, free software) relative to GAPDH or α-tubulin loading controls.

Protein and molecular weight	**Primary antibody**	**Dilution (in TBST)**	**Incubation time**	**Supplier**
PMCA4 135kDa	Mouse anti-PMCA4 monoclonal antibody	1/1000	2hrs 30mins	[JA9] Abcam plc
PMCA1 140kDa	Rabbit anti-PMCA1 monoclonal anti body	1/1000	3hrs	Abcam plc
SERCA 110kDa	Mouse anti-SERCA monoclonal antibody	1/1000	3hrs	Affinity BioReagents (ABR)
NCX 120kDa	Rabbit anti-NCX monoclonal antibody	1/500	2hrs	Swant
α-tubulin 55kDa	Mouse anti-α-tubulin Monoclonal antibody - HRP conjugate	1/5000	2hrs	Abcam plc
GAPDH 37kDa	Mouse anti-GAPDH monoclonal antibody - HRP conjugate	1/5000	3 hrs	Santa Cruz Biotech
	Secondary antibody	**Dilution (in TBST)**	**Incubation time**	**Supplier**
Mouse IgG	Goat anti-mouse IgG-HRP conjugate	1/2000	2hrs	Dako
Rabbit IgG	Donkey anti-rabbit IgG-HRP conjugate	1/2000	2hrs	Cell Signalling Technology

Table 2.7.2.3: Optimised conditions for the primary and secondary antibodies in Western blotting experiments. Images of immunoblotted membranes are shown in results chapter 3.

2.8 Functional studies on isolated mouse mesenteric resistance arteries in a pressure myograph

To examine functional arterial responses, a freshly isolated and cleaned 2mm mesenteric artery segment (as described in tissue dissection section) was placed in a pressure myograph bath chamber (Living Systems Instrumentation (LSI), Burlington, USA) filled with 10mls of ice cold PSS.

The arterial segment was mounted between two glass micropipettes (50-70µm in diameter) and both ends of the artery were secured onto the micropipettes with two nylon ties. The bath chamber was placed on an inverted microscope (Leica DM IRB, by Leica Microsystems, Germany) and viewed with a 10x Fluor objective. The left micropipette end connected to a tap was closed off and the right micropipette end attached to a pressure servo control unit (LSI) remained open as pressure was slowly introduced into the lumen. Arteries were pressurised to a physiological pressure of 60mmHg and checked for the presence of leaks. This was done by switching the pressure servo unit to manual and pressure readings were monitored for any drop (refer to schematic and photograph of the system in figure 2.8.0.1 & 2.8.0.2).

Leak-free arteries maintained the intraluminal pressure of 60 mmHg and remained pressurised after switching the pressure servo unit from automatic to manual. Vessel lumen diameter and wall thicknesses (left and right walls) taken at a middle site along the length of the mounted artery, were measured by a video dimension analyser (supplied by LSI) and visualised on a video monitor screen (AD912A, CRT monitor B/W 12", American Dynamics) connected to video camera (CV-A50, JAI, Japan) (figure 2.8.0.2). Continuous traces of lumen diameters, left and right wall thicknesses were simultaneously recorded digitally by the computer software

program, WINDAQ data acquisition (Dataq Instruments, Ohio USA) and on a multitrace 4P 4-channel chart recorder (Lectromed, UK).

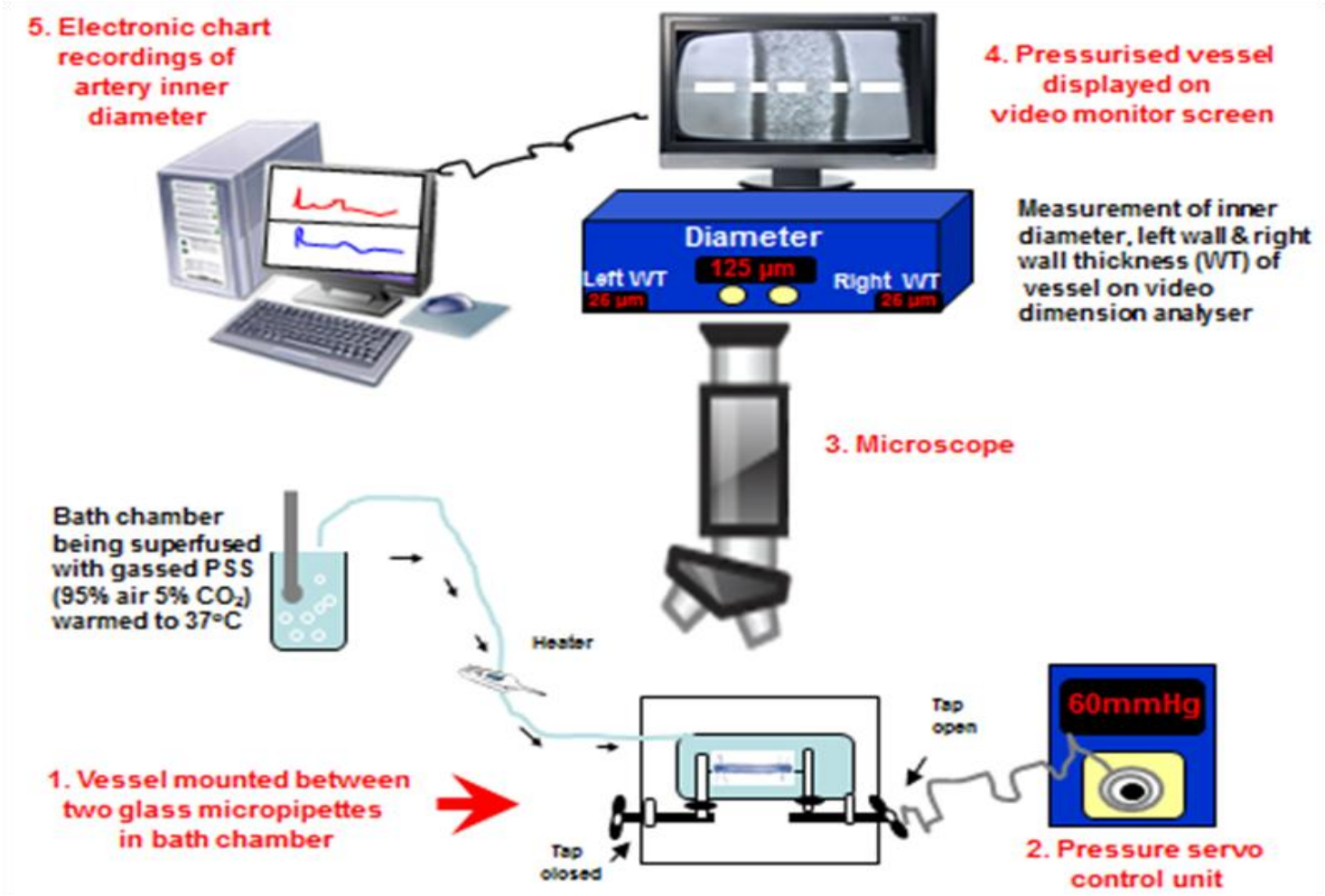

Figure 2.8.0.1: Cartooned illustration of a pressure myograph system. The illustration shows a cannulated and pressurised artery (to 60 mmHg) submerged in warmed PSS (37^0C) in the myograph bath chamber. The right tap is kept open and the pressure is controlled by the pressure servo unit and an image of the vessel as viewed under an inverted microscope is transmitted through a camera and displayed on a monitor screen. Readings (in µm) of the vessel's inner lumen diameter and left & right wall thicknesses are recorded by the video dimension analyser and electronically transmitted to a computer. Changes in vessel lumen diameter are processed by the computer software, (WINDAQ) and digitally recorded unto a chart.

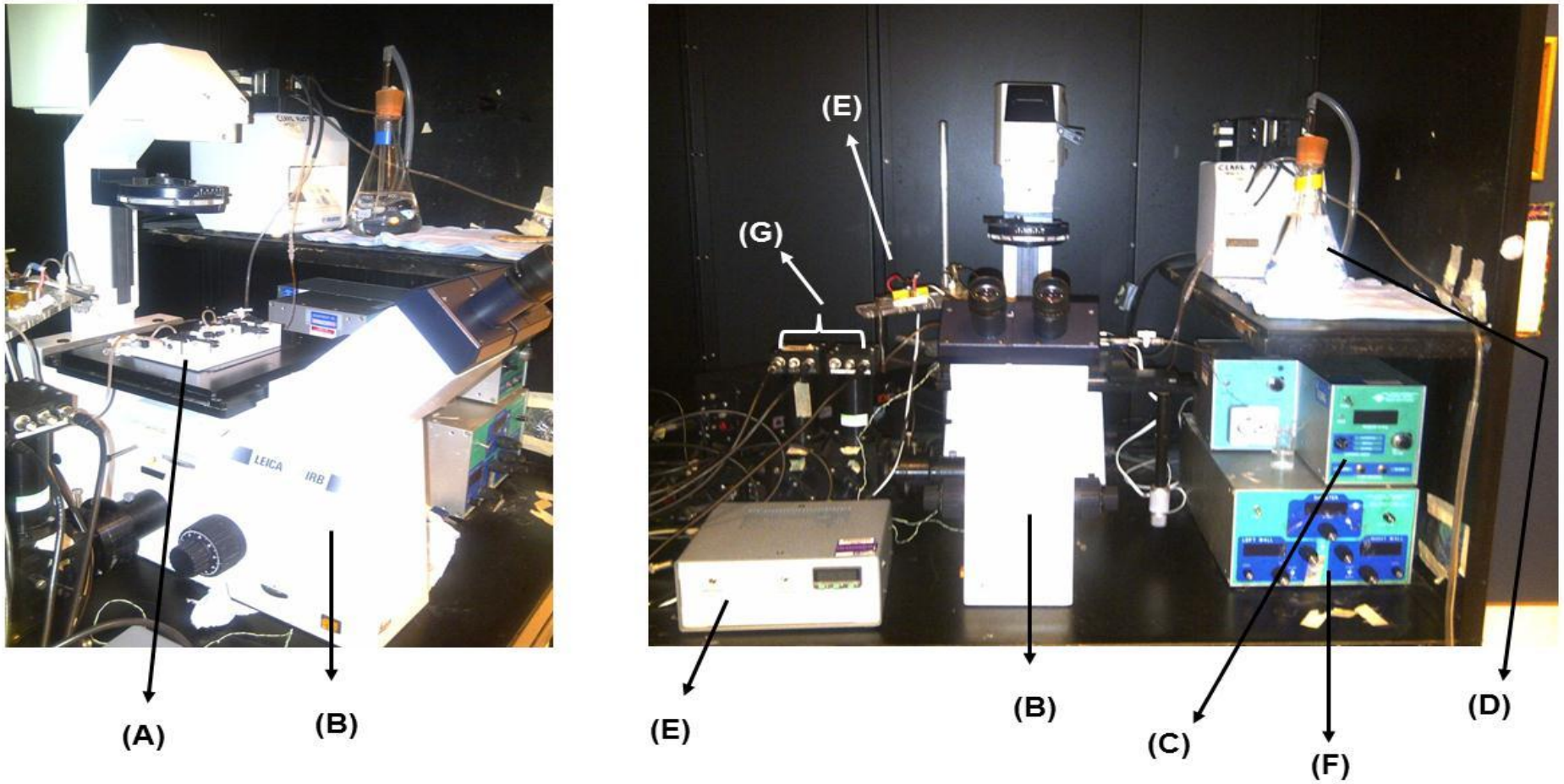

Figure 2.8.0.2: Photographs of the pressure myograph system used in this study. A) is the myograph bath chamber containing pressurised vessel submerged in PSS. This chamber is mounted on B) an inverted microscope with an attached camera. C) is the pressure servo control unit and D) shows PSS being gassed (with 95% air and 5% CO_2) and circulated around the system. E) points to the heater and temperature regulator and F) is the video dimension analyser which records the inner lumen diameter and left & right wall thicknesses of the pressurised vessel throughout an experiment. G) points to the two (400 and 500nm) photon multiplier tubes (PMT) for measuring signals emitted by Ca^{2+}-dye loaded vessels (as mentioned in section 2.9).

2.8.1 Drug preparations used in pressure myography experiments

Noradrenaline in the range (in M) $1x10^{-9}$- $3x10^{-5}$; acetylcholine, in the range (in M) $1x10^{-9}$ - $1x10^{-5}$ and sodium nitroprusside in the range (in M) $1x10^{-11}$ - $1x10^{-5}$ were prepared from serial stock concentrations of (in M): $1x10^{-2}$, 10^{-3}, 10^{-4}, 10^{-5} and 10^{-6} dissolved in PSS. N^{G}-nitro-L-Arginine (LNNA) 100µM was dissolved in PSS. A stock concentration of 0.01M AP2 was made in 100% DMSO which was diluted in PSS to reach final concentrations of 10µM and 1µM. (AP2 has an IC_{50} of 0.15µM for PMCA4 and 5µM for SERCA in cardiac tissue (Abou-Leisa *et al.*, 2011; Cartwright *et al.*, 2011a; Mohamed *et al.*, 2011a)). Vinyl-L-Nio (VLN) 10µM was prepared from a stock concentration of 0.01M diluted in de-ionised H_2O. Methyl-β-cyclodextrin (mβcd) 0.01M was prepared in PSS. Caloxin 1b1, 100µM was prepared from a stock concentration of 10mM dissolved in de-ionised H_2O. A stock concentration of 8mM Indol-1AM (in HEPES containing 20% pluronic acid, 80% DMSO) was diluted in HEPES to give a final concentration of 20µM.

2.8.2 Assessment of contractile responses:

Contractile responses were assessed in arteries isolated from the following animals: PMCA4 WT $^{(+/+)}$, KO $^{(-/-)}$, Ht $^{(+/-)}$ mice. In some experiments another strain of WT $^{(+/+)}$ mice were used mainly due to the limited availability of PMCA4 WT $^{(+/+)}$ mice. The other strain of WT $^{(+/+)}$ mice were bred purely from a 129/Sv non mixed background and the PMCA4 WT $^{(+/+)}$ mice were bred from a 129/Sv and C57Bl/6 mixed background (Schuh *et al.*, 2004). Mesenteric resistance arteries physiologically pressurised to 60 mmHg in the myograph system were subjected to a number of different experimental protocols to address the following:

2.8.2.1 Effects of PMCA4 ablation on arterial contractility

Pressurised arteries from PMCA4 mice were superfused in the bath with PSS at 37^{o}C, gassed with 95% air; 5% CO_2 for at least 20 minutes during equilibration time. Arteries were then exposed to 40mM potassium in PSS solution (KPSS) (composition: NaCl 83.7mM, KCl 40M, $MgSO_4.7H_2O$ 1.17mM, $NaHCO_3$ 25mM, KH_2PO_4 1.17mM, K_2EDTA 0.03mM, glucose 5.5mM and $CaCl_2.2H_20$ 1.6mM) (KCl being isosmotically substituted for NaCl)) and to 2 x 100mM potassium solution (KPSS) (composition: NaCl 23.7mM, KCl 100M, $MgSO_4.7H_2O$ 1.17mM, $NaHCO_3$ 25mM, KH_2PO_4 1.17mM, K_2EDTA 0.03mM, glucose 5.5mM and $CaCl_2.2H_20$ 1.6mM). Each KPSS exposure was removed by a PSS wash allowing arteries to fully relax to their starting diameter.

Following the start up protocol when vessels were established as alive and viable, arteries were incubated for at least 30 minutes in PSS and repeat exposures to 40mM KPSS and to 100mM KPSS were carried out and washed off with PSS. A cumulative concentration response curve to the adrenergic agonist noradrenaline (NA) was constructed over the range (in M) $1x10^{-9}$, $3x10^{-9}$, $1x10^{-8}$, $3x10^{-8}$, $1x10^{-7}$, $3x10^{-7}$, $1x10^{-6}$, $3x10^{-6}$, $1x10^{-5}$ and $3x10^{-5}$. Arteries were left to stabilise at the highest concentration ($3x10^{-5}$M noradrenaline) and a cumulative concentration response curve to the endothelial-dependent dilator acetylcholine (ACh) (over the range (in M) $1x10^{-9}$, $3x10^{-9}$, $1x10^{-8}$, $3x10^{-8}$, $1x10^{-7}$, $3x10^{-7}$, $1x10^{-6}$, $3x10^{-6}$ and $1x10^{-5}$) was constructed. Arteries were then washed with PSS until the pressurised vessel returned its stable resting diameter. Fully dilated arteries (in PSS) were then constricted with $3x10^{-5}$M noradrenaline and following stabilisation, a concentration response curve to the endothelium independent dilator sodium nitroprusside (SNP) (an exogenous NO donor) was constructed at the listed concentrations (in M): $1x10^{-}$

^{11}, 3x10^{-11}, 1x10^{-10}, 3x10^{-10}, 1x10^{-9}, 3x10^{-9}, 1x10^{-8}, 3x10^{-8}, 1x10^{-7}, 3x10^{-7}, 1x10^{-6}, 3x10^{-6} and 1x10^{-5}). The pressurised vessel was then returned to its stable resting diameter with a final PSS washout.

2.8.2.2 Effects of Nitric oxide synthase (NOS) inhibition by N^G-nitro-L-arginine (LNNA) on arterial contractility

Subsequent experiments investigated the effect of inhibition of nitric oxide synthase (NOS) by the NOS inhibitor N^G-nitro-L-arginine (LNNA) on contractile responses of mesenteric arteries from PMCA4 WT $^{(+/+)}$ and KO $^{(-/-)}$ mice. To determine this the experimental protocol above was repeated but, instead of incubating arteries for 30 minutes with PSS arteries were incubated with 100µM of the NOS inhibitor, LNNA (Hausman *et al.*, 2011). The following exposures to KPSS and cumulative concentrations of noradrenaline, acetylcholine and sodium nitroprusside were all carried out in the continued presence of 100µM LNNA.

2.8.2.3 Effects of PMCA4 ablation on the passive arterial properties of isolated pressurised mouse mesenteric arteries

At the end of each functional experiment arteries were superfused with calcium-free PSS (NaCl 119mM, KCl 4.7mM, $MgSO_4.7H_2O$ 1.17mM, $NaHCO_3$ 25mM, KH_2PO_4 1.17mM, K_2EDTA 0.03mM, glucose 5.5mM and ethylene glycol tetra-acetic acid (EGTA), 2mM) for at least 25 minutes to ensure the artery lost all form of vascular tone. The transmural pressure was reduced to 5 mmHg and subsequently increased to 10, 20, 40, 60, 80, 100, 120 and 140 mmMHg. Measurements of passive lumen

diameter and left and right wall thicknesses (taken from three sites along the length of a vessel and averaged) were taken at each pressure after stabilisation of diameter.

2.8.2.4 Effects of a novel PMCA4 specific inhibitor (AP2) on arterial contractility

Further experiments were performed to investigate the effects of the novel PMCA4 specific inhibitor (AP2) (Abou-Leisa *et al.*, 2011; Mohamed *et al.*, 2011a) on mesenteric arterial contractility.

Pressurised third order mesenteric resistance arteries from PMCA4 WT $^{(+/+)}$ and WT $^{(+/+)}$ as well as PMCA4 KO $^{(-/-)}$ mice were set up as described above and left to equilibrate in PSS for at least 20 minutes. Arteries were then exposed to 40mM and 100mM KPSS. PSS washes between each KPSS exposure allowed vessels to return to their stable resting diameter.

Arteries were then incubated for 30 minutes in either of the following solutions: 10µM AP2 (Abou-Leisa *et al.*, 2011; Mohamed *et al.*, 2011a) (in PSS containing 0.1% dimethyl sulfoxide (DMSO)) or in PSS containing 0.1% DMSO for the respective controls. The effect of a lower concentration 1µM of AP2 (Abou-Leisa *et al.*, 2011; Mohamed *et al.*, 2011a) (in PSS containing 0.1% DMSO) was also examined in separate experiments.

Following incubation, in the continued presence of AP2 or control (in PSS containing 0.1% DMSO), arteries were exposed to 40mM and 100mM KPSS which were each washed off with PSS. A cumulative concentration response curve to the agonist,

noradrenaline was constructed using the concentrations described above (section 2.8.2.1).

2.8.2.5 Effects of AP2, on arterial contractility in the presence of a non specific NOS or a specific nNOS inhibitor

To determine the effects of NOS inhibition on the effects of AP2, additional experiments were performed (using the protocol described above) where pressurised arteries from WT $^{(+/+)}$ mice were simultaneously incubated with either of the following solutions: 10μM AP2 (in PSS containing 0.1% DMSO) or 10μM AP2 together with 100μM LNNA a non specific NOS inhibitor (in PSS containing 0.1% DMSO) or 10μM AP2 (in PSS containing 0.1% DMSO) together with 10μM Vinyl-L-Nio (VLN), a specific nNOS inhibitor (Birenbaum *et al.*, 2008; Hatanaka *et al.*, 2006) (in de-ionised H_2O) for a period of 30 minutes. The experimental protocol described above was then performed. Experiments described in this section and section 2.8.2.4, were carried out concomitantly on allowing direct comparisons to be made.

2.8.2.6 Does methyl-β-cyclodextrin (mβcd), modulate the effects of AP2 on mouse mesenteric arterial contractility?

Further studies were carried out to investigate whether AP2 had effects on arterial contractility in the presence of methyl-β-cyclodextrin (mβcd) which disrupts of caveolae structure (Shaw *et al.*, 2006).

Arteries from WT $^{(+/+)}$ mice were exposed to 40mM, 100mM KPSS and following washing, were incubated for 30 minutes in the presence of 0.01M mβcd (in PSS) (Shaw *et al.*, 2006) or in 10μM AP2 (in PSS containing 0.1% DMSO) simultaneously with 0.01M mβcd (in PSS). Following incubation, arteries were exposed to 40mM and to 100mM KPSS before a cumulative concentration response curve to noradrenaline was constructed (see section 2.8.2.1 for full details of protocol).

2.8.2.7 What are the effects of caloxin 1b1 (a commercially available PMCA4 inhibitor) on mesenteric arterial contractility?

Further experiments were performed to investigate the effects of caloxin 1b1, a different PMCA4 inhibitor (Pande *et al.*, 2006), on mesenteric arterial contractility. Third order mesenteric resistance arteries from PMCA4 WT $^{(+/+)}$ mice were set up as described above. Following equilibration, arteries were exposed to 40mM, 100mM KPSS (see section 2.8.2.4). Arteries were then incubated for 30 minutes with 100μM caloxin 1b1 (Pande *et al.*, 2006) or PSS (for controls). Following incubation, responses to 40mM and 100mM KPSS and to cumulative concentrations of noradrenaline were obtained in a similar protocol to section 2.8.2.4. To examine the

specificity of caloxin 1b1 the experiments described above were also performed in mesenteric arteries from PMCA4 KO $^{(-/-)}$ mice. All experiments were carried out on separate arteries.

2.9 Measurement of global intracellular Ca^{2+} ($[Ca^{2+}]_i$) signals in pressurised mouse mesenteric arteries

PMCA4 has been suggested to have a role as a calcium extrusion pump in some tissues (Liu *et al.*, 2006; Matthew *et al.*, 2004; Matthew A *et al.*, 2004). To allow global $[Ca^{2+}]_i$ changes to be measured in intact arteries, third order mesenteric resistance arteries from freshly sacrificed mice (i.e. PMCA4 WT $^{(+/+)}$, KO $^{(-/-)}$ mice and the other strain of WT $^{(+/+)}$ mice), were isolated and cut to 2mm length segments (as previously described). These were loaded with 20µM of the acetoxymethylester (AM) form of the ratiometric Ca^{2+}-sensitive dye Indo-1 (Molecular Probes) (in HEPES containing 0.05% pluronic acid and 0.25% DMSO) in a 1.5µl micro-centrifuge tube for 1 hour 30 minutes at room temperature and subsequently for 30 minutes at 37^0C. Arteries were incubated in a HEPES-buffered salt solution (composition: NaCl 154mM, KCl 5.6mM, $MgSO_4$ 1.2mM, glucose 11.7mM, $CaCl_2$ 3mM and HEPES 11mM; pH 7.4 with NaOH) to ensure constant pH. Due to the sensitivity of the dye to photobleaching, incubation of arteries with Indo-1 AM occurred in the dark and light was kept to a minimum thereafter.

Each loaded 2mm segmented mesenteric artery was cannulated onto two glass micropipettes in a myograph bath chamber which was then mounted on an inverted microscope (Leica DM LB), viewed with a 10x Fluor objective and pressurised to 60mmHg as described in section 2.8. To minimise areas of visual field not occupied by the artery, a variable rectangular aperture on the side of the microscope was placed in front of camera and the two photomultiplier signal detectors. To enable arterial diameter and the Indo-1 Ca^{2+} signal ratio to be continuously and simultaneously measured a 600nm filter was positioned in front of the microscope incident light to weakly illuminate arteries. Leak-free Indo-1 AM loaded pressurised

arteries were equilibrated by circulating PSS (at 37^{o}C, gassed with 95% air; 5% CO_2) for a minimum of 15 minutes in a similar procedure to that described in section 2.8.2.1. Following equilibration, indo-1 loaded arteries were excited by light at 340nm using a 150W high intensity xenon light source (Ushio xenon short ARC lamp, Ushio inc., Japan).

Positioned within the inverted microscope was a filter cube with a 340nm excitation filter (15nm bandpass Cairn Research, UK) and a 360nm dichroic filter at 45^0 (15nm bandpass Cairn Research, UK). These ensured light passing through the 340nm excitation filter was directed up towards the artery and after excitation of the Indo-1 loaded artery, emitted light of >360nm was transmitted through the 360nm dichroic filter and directed towards the signal detectors (at the side port of the microscope). This emitted light was further directed through a second 45^0 dichroic filter (480nm, long transmission, LT, Cairn) allowing light <480nm upwards to an emission filter (405/30nm bandpass, BP, Cairn) positioned in front of the first photomultiplier tube (PMT, Cairn). Light >480nm passed through the dichroic filter to a third 45^0 dichroic filter (600nm, LT Cairn) which in turn, allowed light <600nm to be directed upwards to a 500nm emission filter (500nm, LT Cairn) placed in front of the second PMT. Thus the first PMT measured emission signals at 400nm and the second PMT signals at 500nm. Signals were relayed digitally using Model DI-220 analog I/O digital output converter and recorded via WINDAQ data acquisition (Dataq Instruments, Ohio USA) and on a multitrace 4P 4-channel chart recorder (supplied by Lectromed, UK).

At the end of every experiment, arteries were superfused with 10mM manganese chloride ($MnCl_2$) in HEPES for 20-25 minutes in order to quench the Indo-1 signals and this was used to determine tissue autofluorescence (or intrinsic fluorescence

emitted by the tissue). Tissue autofluorescence value was subtracted from 400nm and 500nm signals and a ratio of the corrected 400:500nm signals were calculated.

Due to recognised problems with calibration of indo-1 emission signals in intact tissues the ratio of the 400nm emission signal and 500nm emission signal of Indo-1 (i.e. 400nm:500nm emission ratio ($F4_{00}/F_{500}$)) were taken as a representation of $[Ca^{2+}]_i$. Previous studies by our group have shown that changes in the Indo-1 emission ratio (F_{400}/F_{500}) are representative of changes in $[Ca^{2+}]_i$ within mesenteric arteries (Austin *et al.*, 1995; Shaw *et al.*, 2003).

To address the effects of PMCA4 ablation on $[Ca^{2+}]_i$ within intact vessels, third order mesenteric arteries obtained from PMCA4 WT $^{(+/+)}$ and KO $^{(-/-)}$ mice aged 3 months were loaded with 20µM Indo-1 AM as described above. In experiments addressing the effects of PMCA4 inhibition with AP2 or effects of AP2 in the presence of nNOS inhibitor (VLN), isolated mesenteric artery segments obtained from WT $^{(+/+)}$ mice were incubated with 10µM AP2 (in HEPES containing 0.1% DMSO) or 10µM AP2 in the presence of 10µM VLN (in de-ionised H_20), while being loaded with 20µM Indo-1 AM. To measure arterial contractility in all experiments a startup protocol of 100mM KPSS constriction followed by a PSS wash was observed to check if mounted, pressurised arteries were alive. The following experimental protocol was then performed. Pressurised arteries were constricted with 40mM KPSS, 100mM KPSS and to $3x10^{-5}$M noradrenaline (in PSS) until maximum constrictions were maintained, with each exposure being followed by a PSS wash.

2.10 Quantitative analysis:

2.10.1 Contractile responsiveness

For each artery contractile responses to KPSS and noradrenaline (NA) were determined as a change in diameter with the stimulus and then normalised to resting diameter in PSS:

% constriction:

- (Δ in absolute diameter / resting diameter) x 100

Change in absolute arterial diameter (constriction) with each added concentration of noradrenaline was normalised to the maximal noradrenaline-induced constriction with $3x10^{-5}$M and expressed as a percentage. The noradrenaline concentration (in M) that produced half-maximal constriction was determined as the EC50 value (using the Graph Pad prism 5 software, USA) and was used as an indication of arterial sensitivity.

% constriction normalised to diameter Δ in max [NA]:

- ((Δ in absolute diameter with each added [NA]) / (maximal constriction to [NA] $3x10^{-5}$M)) x 100

Change in absolute arterial diameter (dilation) with each added concentration of acetylcholine (ACh) was normalised to the maximal noradrenaline-induced constriction with $3x10^{-5}$M and expressed as a percentage. Mesenteric arterial responses to sodium nitroprusside (SNP) concentrations were also normalised by using a similar method.

% dilation:

- ((Δ in absolute diameter with each added [dilator]) / (maximal constriction to [NA] $3x10^{-5}$M)) x 100

In this study, the **time (T) constriction** is defined as the time (in seconds) for a mesenteric artery resting in PSS to reach maximum and stabilised constriction to 40mM or 100mM KPSS (or in some cases to $3x10^{-5}$M noradrenaline) (figure 2.10.1).

The **time (T) relaxation** is defined as the time (in seconds) it took for a mesenteric artery constricted to 40mM or 100mM KPSS (or in certain cases to $3x10^{-5}$M noradrenaline) to fully dilate to resting diameter upon PSS washout (figure 2.10.1). Time zero was taken from initial point at which the artery began to display relaxation (figure 3.1.1).

Whereas $\mathbf{T_{1/2}}$ **relaxation** is defined as the time (in seconds) it took for a mesenteric artery pre-constricted to a vasoconstrictor stimulus (i.e. 40mM or 100mM KPSS or $3x10^{-5}$M noradrenaline) to relax by 50% upon PSS wash.

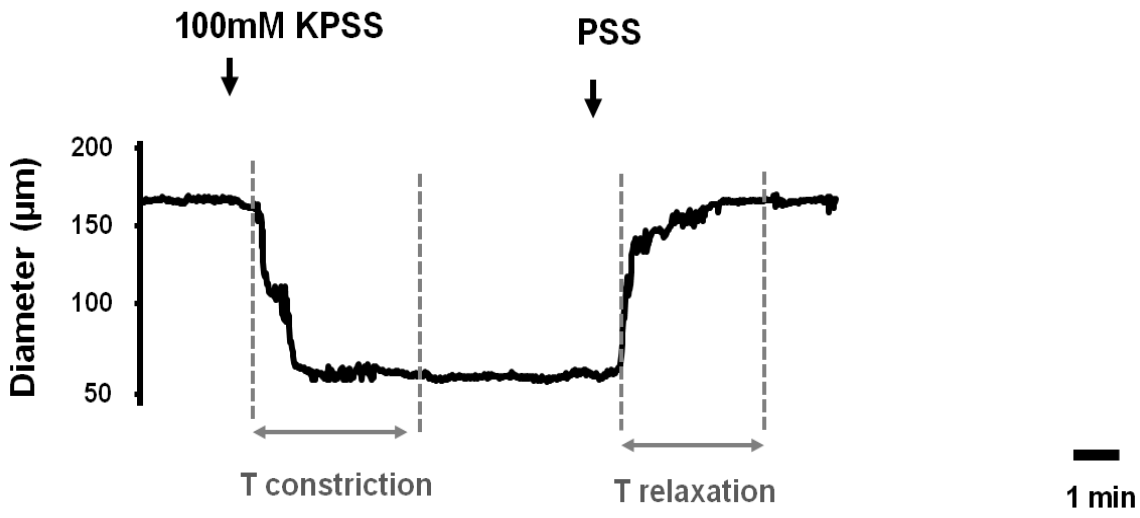

Figure 2.10.1: Example of an experimental trace recording showing diameter changes of a pressurised mouse mesenteric artery responding to 100mM KPSS and PSS. Data was recorded by WINDAQ data acquisition software. Depicted arrows show time points from which T constriction and T relaxation (in seconds) were determined.

2.11 Structural mesenteric arterial assessments

Measured passive lumen diameters and wall thicknesses at three sites along the length of the vessel were averaged for each intraluminal pressure.

Cross-sectional area was calculated from:

Cross-sectional area (CSA) μm^2 = $\pi (r_0^2 - r_1^2)$

(Where **r** defines the radius, r_1 is the radius of vessel lumen and r_0 is the external radius of vessel as shown below).

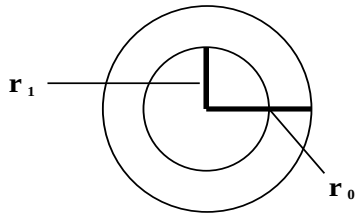

Stress and strain were calculated from:

Stress (dyne/cm^2) = (P x r_1) / WT

(Where **P** is intraluminal pressure (1mmHg = 1334 dyne/cm^2) and WT is arterial wall thickness mean of right and left walls) (Bund, 2001; Izzard *et al.*, 2006).

Strain = $(D-D_0) / D_0$

(Where **D** is diameter at each pressure and D_0 is diameter at 5 mmHg) (Bund, 2001; Izzard *et al.*, 2006).

Elastic modulus (β) was determined from $y = ae^{\beta x}$ of the stress-strain fitted curve (where **a** & **β** are constants and **e** is the base of natural logarithm). **a** is the stress at 5mmHg; **β** is the slope of the $\log_e$ stress-strain relationship defined as the elastic

modulus which is an index of distensibility; the higher the value of **β** the lower the arterial distensibility (Bund, 2001; Izzard *et al.*, 2006).

2.12 Indo-1 F_{400}/F_{500} Ca^{2+} emission ratio (taken as global $[Ca^{2+}]_i$) in resting and vasoconstrictor stimulated mesenteric arteries

Tissue autofluorescence was subtracted from the 400 and 500nm Indo-1 fluorescence emissions and the resultant F_{400}/F_{500} emission ratio was taken as an indication of $[Ca^{2+}]_i$ (F_{400}/F_{500} Ca^{2+} emission ratio). The change in F_{400}/F_{500} Ca^{2+} emission ratio (emitted by indo-1 loaded arteries) upon vasoconstrictor stimulation was calculated as the difference between baseline F_{400}/F_{500} emission ratio of Indo-1 and the stable maximum/peak ratio upon stimulation with a vasoconstrictor i.e. 40mM, 100mM KPSS or $3x10^{-5}$M noradrenaline (figure 2.12.1).

Time for increase in F_{400}/F_{500} Ca^{2+} emission ratio (upon vasoconstrictor stimulation**)** was determined as the time it took in seconds for resting arteries to increase their F_{400}/F_{500} Ca^{2+} emission ratio to a stable maximum (or peak) in response to a vasoconstrictor stimulus (figure 2.12.1).

The time for decrease in F_{400}/F_{500} Ca^{2+} emission ratio was determined as the time noted in seconds for the stabilised maximum/peak F_{400}/F_{500} Ca^{2+} emission ratio of pre-constricted arteries to fall to baseline upon PSS washout (figure 2.12.1). The **time half ($T_{1/2}$) for decrease in F_{400}/F_{500} Ca^{2+} emission ratio** was determined as the time noted in seconds for the maximum F_{400}/F_{500} Ca^{2+} emission ratio of arteries to fall by 50% upon PSS washout (figure 2.12.1).

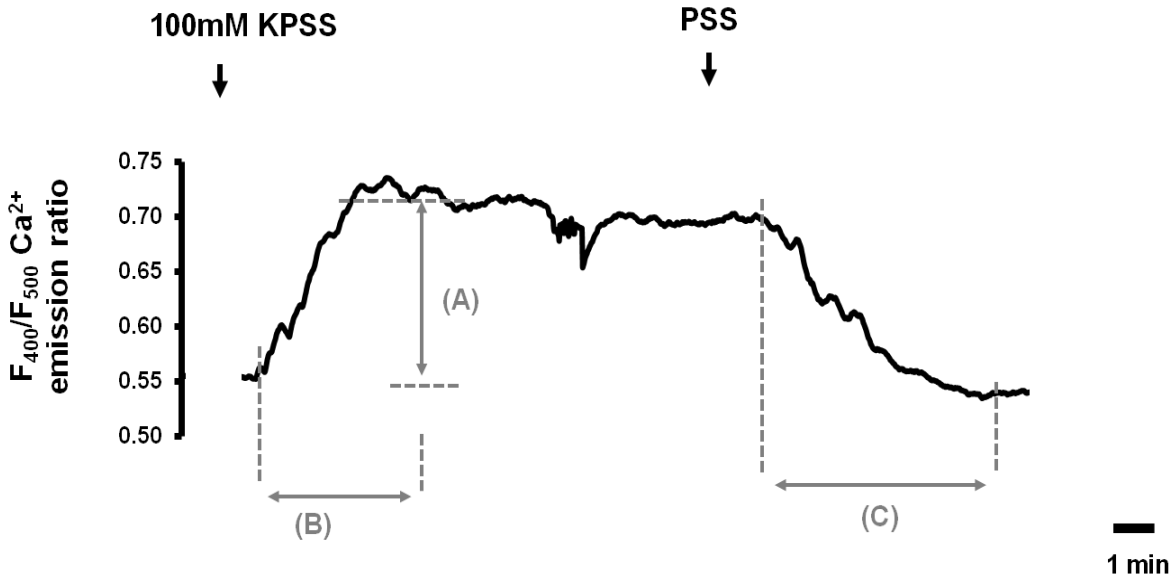

Figure 2.12.1: An experimental trace recording of a pressurised mouse mesenteric artery displaying changes in the F_{400}/F_{500} emission ratio of Indo-1 in response to 100mM KPSS and upon PSS washout. Data was recorded by WINDAQ data acquisition software. (A) is the **Δ F_{400}/F_{500} Ca^{2+} emission ratio (upon 100mM KPSS stimulation)**. Horizontal grey arrows depict time points from which (B) **time for increase in F_{400}/F_{500} Ca^{2+} emission ratio (upon 100mM KPSS stimulation)** and (C) the **time for decrease in F_{400}/F_{500} Ca^{2+} emission ratio (upon PSS washout)** were determined.

2.13 Statistical analysis

Results are expressed as means ± SEM (standard error mean) with n representing the number of animals. The number of repeats for each methodology to determine significance of the data was arrived at based upon power calculations and preliminary studies performed by previous lab members. Concentration response and pressure response curves were analysed by two-way analysis of variance (ANOVA) and for repeated measures with a p value <0.05 being considered statistically significant. This was followed by the Boneferroni post-hoc test to determine if p value was <0.05 (#). Statistical comparisons of all other data (including relative band intensity, % constriction to 40 or 100mM KPSS, T and $T_{1/2}$ relaxations, EC50s and β values already defined earlier in this chapter) were performed using an unpaired student's t test. The differences between means were considered significant at $p<0.05$ (*) and not significant at $p>0.05$ (NS). All statistical evaluations were performed using the Graph Pad Prism 5 computer software (USA).

Chapter 3

Results

3.1 Confirmation of the presence and absence of PMCA4 in tissues fr PMCA4 WT $^{(+/+)}$ and KO $^{(-/-)}$ mice respectively

The phenotype of PMCA4 WT $^{(+/+)}$ and KO $^{(-/-)}$ mice were identified by genotyping as described in the methods chapter section 2.3. Further confirmation of the presence or absence of PMCA4, in these mice were carried out by Western blotting and immunohistochemical analysis.

3.1.1 Brain tissues

PMCA4 is abundant in the mammalian brain (Guerini, 1998; Sepulveda *et al.*, 2006; Stahl *et al.*, 1992; Stahl *et al.*, 1994; Stauffer *et al.*, 1995; Zylinska *et al.*, 2000). Therefore freshly frozen whole brain homogenates from PMCA4 KO $^{(-/-)}$ and WT $^{(+/+)}$ mice (n=3 per group) were analysed by Western blotting using a PMCA4 antibody. This confirmed that PMCA4 expression was present in the brains obtained from PMCA4 WT $^{(+/+)}$ mice but was absent in those from KO $^{(-/-)}$ mice (figure 3.1.1.1).

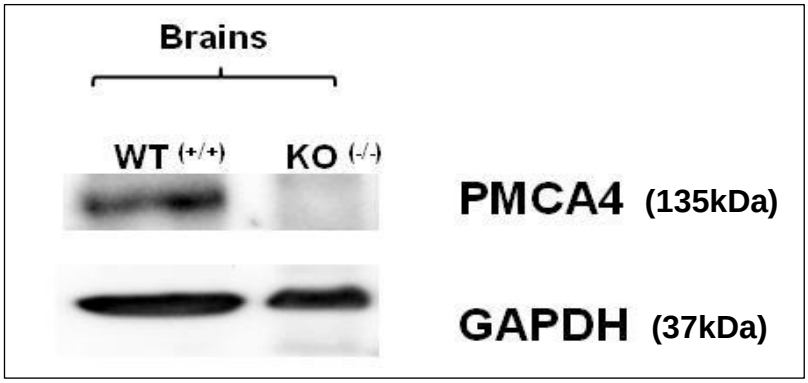

Figure 3.1.1.1: PMCA4 protein expression shown in a homogenised brain obtained from a PMCA4 WT $^{(+/+)}$ mouse and its absence in the brain of a KO $^{(-/-)}$ mouse. GAPDH was used as a protein loading control showing sufficient loading of brain tissue samples per well lane.

3.1.2 Vascular tissues

H&E staining of paraffin embedded arterial sections were performed in order to determine the quality of sections obtained from PMCA4 WT $^{(+/+)}$ and KO $^{(-/-)}$ mice. It was very difficult to obtain good quality mouse mesenteric arterial sections, largely because of their small size, and there was usually no staining visualised after treatment with H&E. However, in a small number of mesenteric arterial sections obtained from PMCA4 WT $^{(+/+)}$ and KO $^{(-/-)}$ mice, H&E staining was visible (figure 3.1.2.1). It was much easier to obtain quality sections from mouse aortas. Hence all immunohistochemical experiments were conducted on aortic sections. H&E staining of mesenteric arterial and aortic sections revealed that there were no gross morphological differences between those arteries obtained from PMCA4 KO $^{(-/-)}$ mice in comparison to those from WT $^{(+/+)}$ mice figure 3.1.2.1.

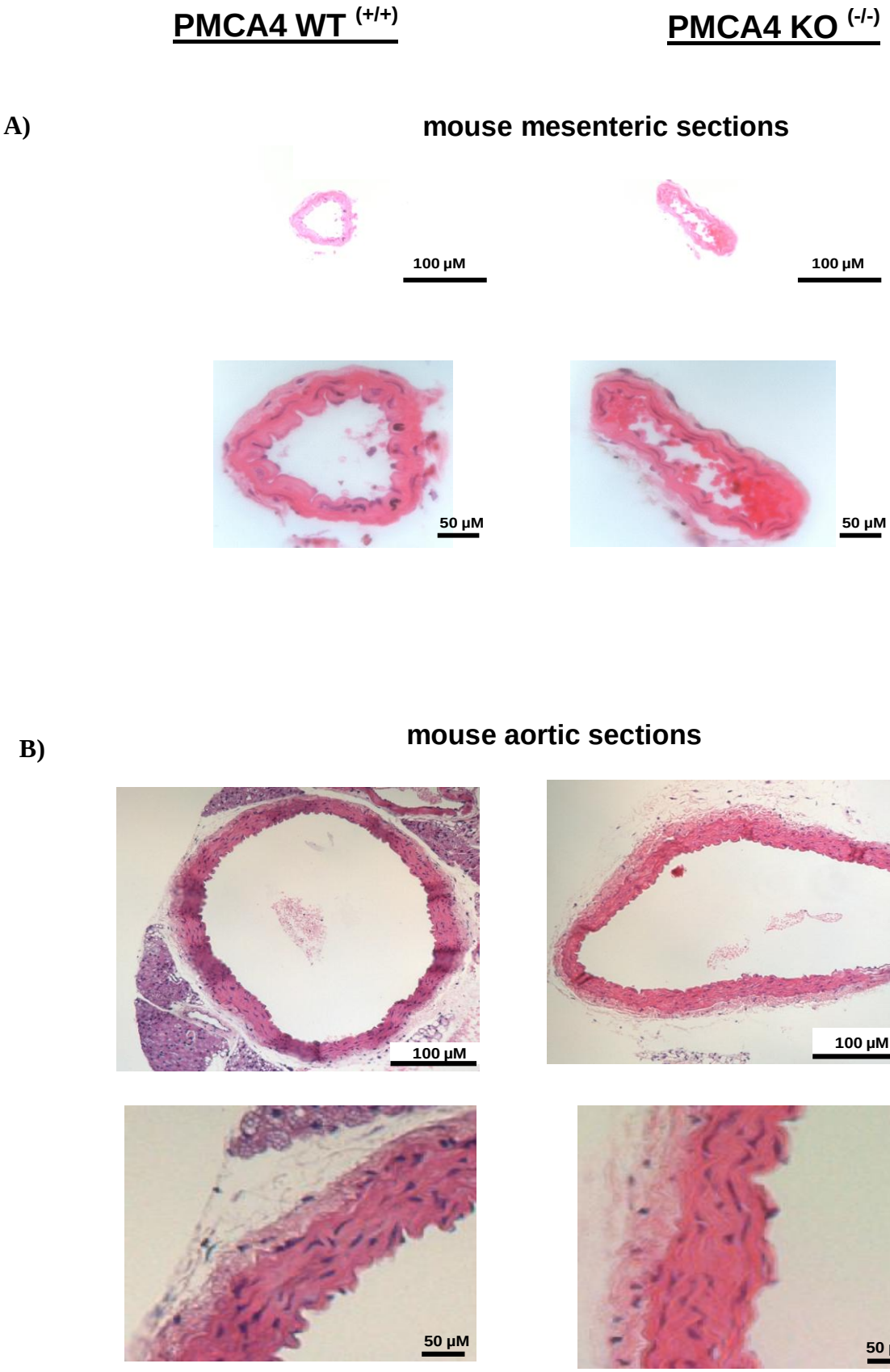

Figure 3.1.2.1: H&E stained histological images of transverse sections (5µm thick) of mouse mesenteric arteries and aortas. Shown in A) are mesenteric arteries and in B) aortas obtained from PMCA4 WT $^{(+/+)}$ and KO $^{(-/-)}$ mice taken at x40 and x10 objectives. Eosin stained the cytoplasm & extracellular matrix of arteries pink and haematoxylin stained the nuclei of cells present within the vessel walls dark purple. No gross morphological differences in the vessel structures were evident in the mesenteric arteries or aortas from PMCA4 WT $^{(+/+)}$ and KO $^{(-/-)}$ mice.

Aortic sections obtained from three PMCA4 WT $^{(+/+)}$ and three KO $^{(-/-)}$ mice (n=3) were investigated in immunohistochemical experiments using a primary antibody against PMCA4. Immunohistochemical data confirmed that PMCA4 was expressed in the aortas of PMCA4 WT $^{(+/+)}$ mice but was absent in those of KO $^{(-/-)}$ mice (figure 3.1.2.2).

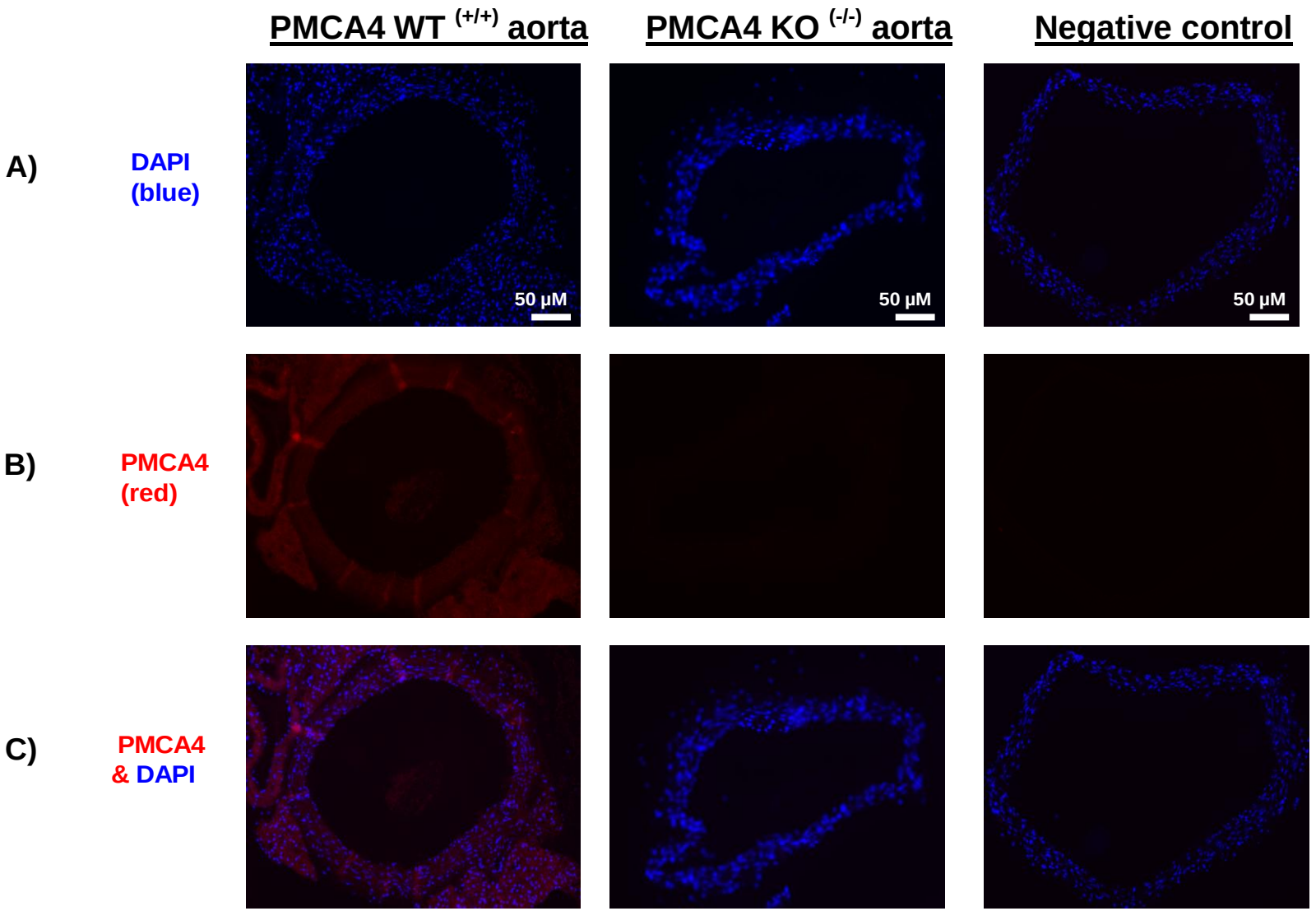

Figure 3.1.2.2: Immunofluorescence images of transverse aortic sections (5µm thick) showing the expression of PMCA4 in PMCA4 WT $^{(+/+)}$ mouse aorta and its absence in a PMCA4 KO $^{(-/-)}$ mouse aorta. In panel A) are DAPI fluorescence images showing the nuclei of cells within the vessel walls. In panel B) are the sections obtained from PMCA4 WT $^{(+/+)}$ and KO $^{(-/-)}$ mice stained with a PMCA4 antibody detected by texas red, and panel C) shows the overlay images of the DAPI and PMCA4 stained sections. All images shown were taken at 10x objective after 70 seconds exposure time.

3.2 Localisation of PMCA4 within the arterial wall

To determine the localisation of PMCA4 within the arterial wall, mouse aortic sections were simultaneously probed with antibodies against PMCA4 and smooth muscle α-actin (a VSM marker) or CD34 (a vascular endothelium marker). These experiments showed that in aortic sections obtained from PMCA4 WT $^{(+/+)}$ mice, PMCA4 was present in the VSM but not in the endothelium. However, PMCA4 expression was not found in either the VSM or endothelium of aortic sections from PMCA4 KO $^{(-/-)}$ mice (figures 3.2.1 & 3.2.2).

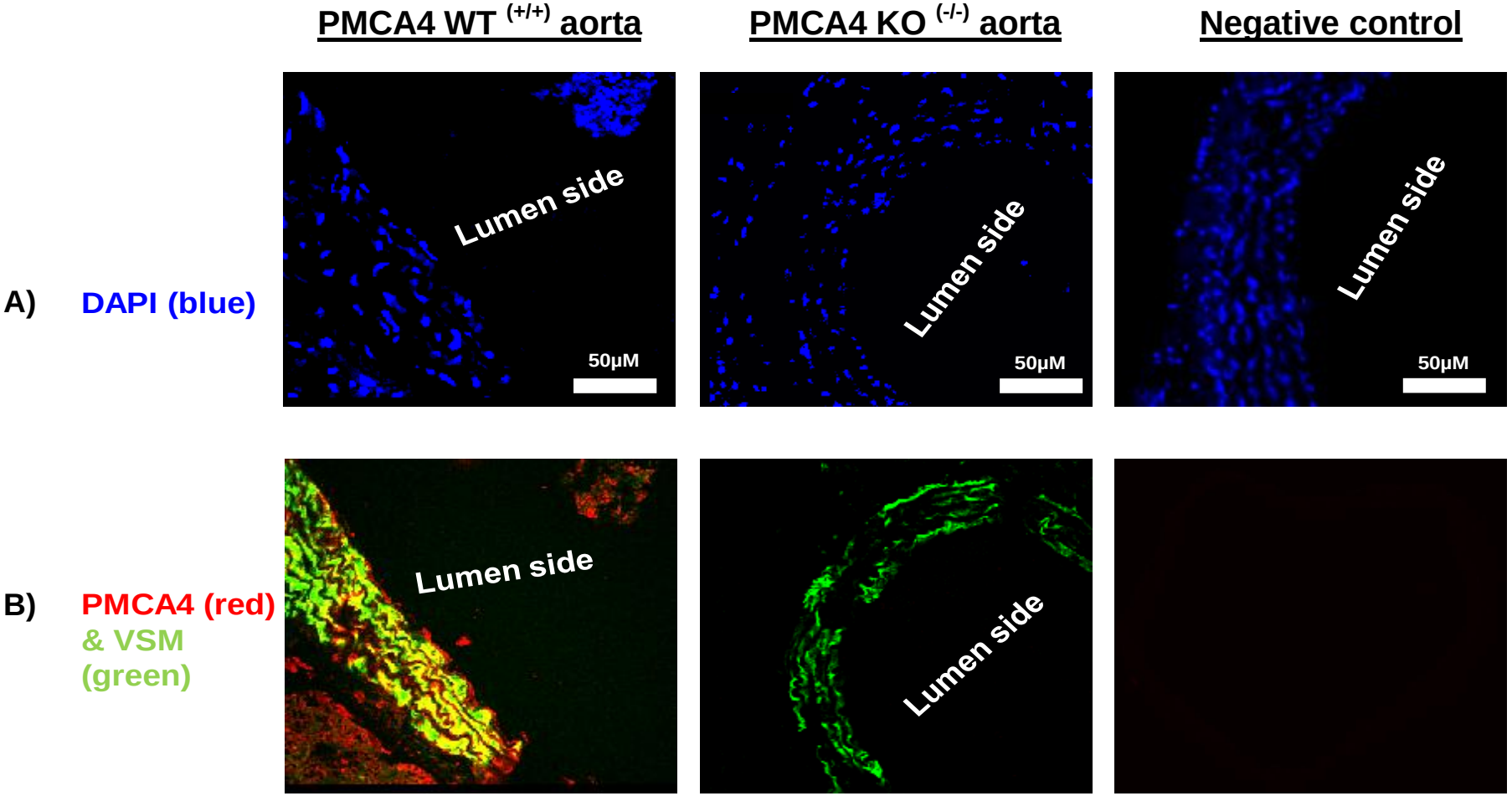

Figure 3.2.1: Immunofluorescence images of aortic sections showing the localisation of PMCA4 to the VSM of a PMCA4 WT $^{(+/+)}$ mouse aorta and its absence in a PMCA4 KO $^{(-/-)}$ mouse aorta. In panel A) are DAPI fluorescing cells detected in mouse aortic sections by immunofluorescence. Panel B) shows mouse aortic sections co-immunostained with a PMCA4 antibody (texas red) and a smooth muscle α-actin antibody (FITC green). Also shown is the aortic section obtained from PMCA4 WT $^{(+/+)}$ mice used as a negative control. All images shown were taken at x40 objective after 70 seconds exposure time.

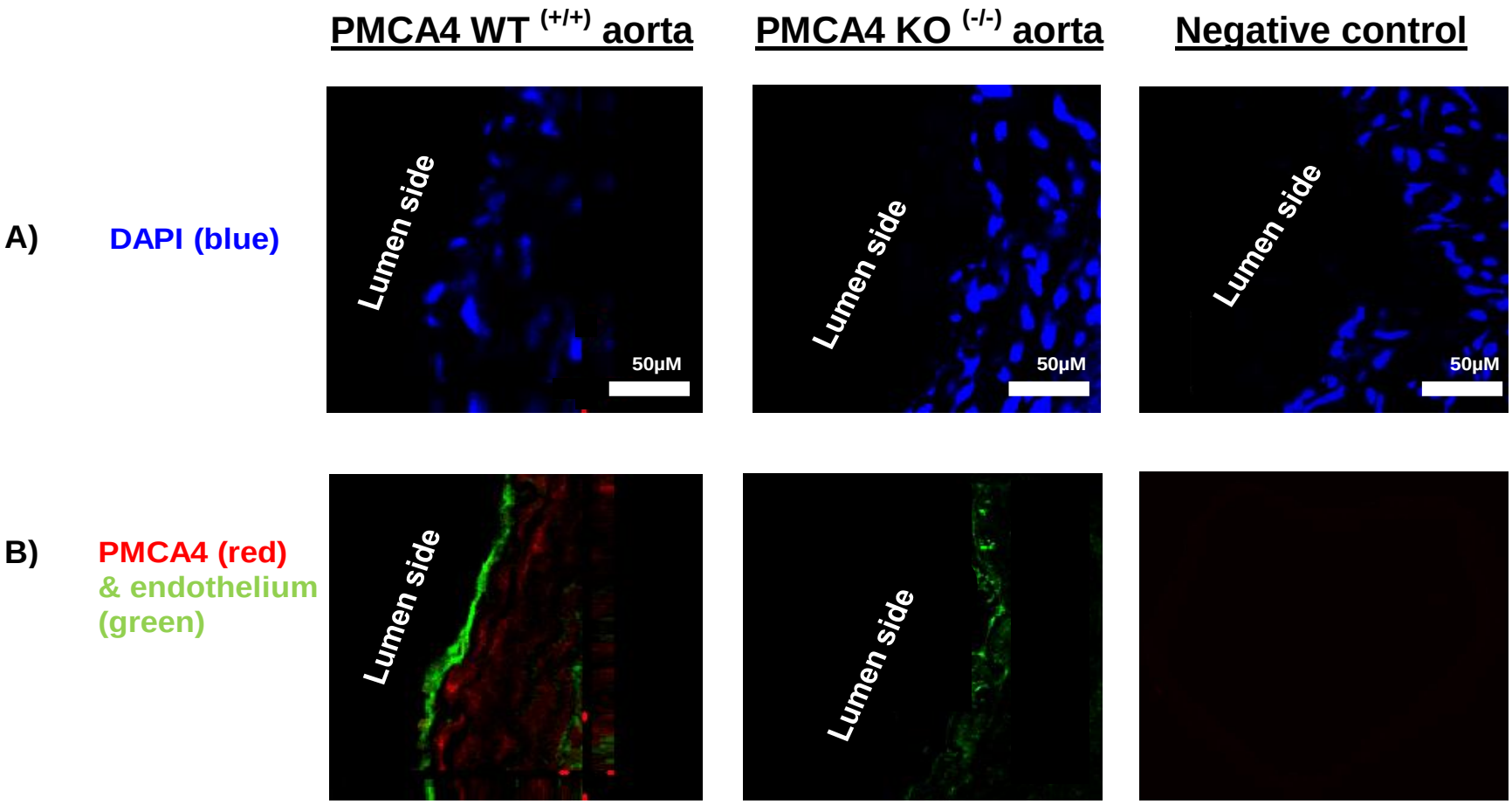

Figure 3.2.2: Immunofluorescence images of aortic sections showing PMCA4 is not in the endothelium layer of the vessel obtained from a PMCA4 WT $^{(+/+)}$ mouse and that it is completely absent in the aorta from a PMCA4 KO $^{(-/-)}$ mouse. In panel A) are fluorescing cell nuclei within mouse aortic walls stained with DAPI and detected by immunofluorescence. Panel B) shows mouse aortic sections co-immunostained with a PMCA4 antibody (texas red) and a CD34 endothelial marker antibody (FITC green). Aortic sections from PMCA4 WT $^{(+/+)}$ mice used as negative controls are also shown. All images shown were taken with a x40 objective after 70 seconds exposure time.

3.3 Does ablation of PMCA4 modify the protein expression levels of other Ca^{2+}-regulatory proteins in the mouse vasculature?

Further analysis in the mouse vasculature assessed whether ablation of PMCA4 modulated the expression of Ca^{2+}-regulatory proteins associated with $[Ca^{2+}]_i$ removal in VSM i.e. PMCA1, SERCA and NCX. This was performed by Western blotting experiments using freeze-snapped aortas freshly dissected from PMCA4 WT $^{(+/+)}$ and KO $^{(-/-)}$ mice immediately after sacrifice. No significant changes in the expression of PMCA1, SERCA2 and NCX1 in aortas of PMCA4 KO $^{(-/-)}$ mice in comparison to those of WT $^{(+/+)}$ mice were found. It is acknowledged that in this study only the expression of Ca^{2+}-regulatory proteins associated with $[Ca^{2+}]_i$ removal have been addressed in aortas of PMCA4 KO $^{(-/-)}$ and WT $^{(+/+)}$ mice, mainly due to time and financial constraints. Other Ca^{2+}-regulatory proteins such as ryanodine and IP_3 receptor channels and L-type Ca^{2+} channels involved in mobilising Ca^{2+} in VSM cells have not been investigated.

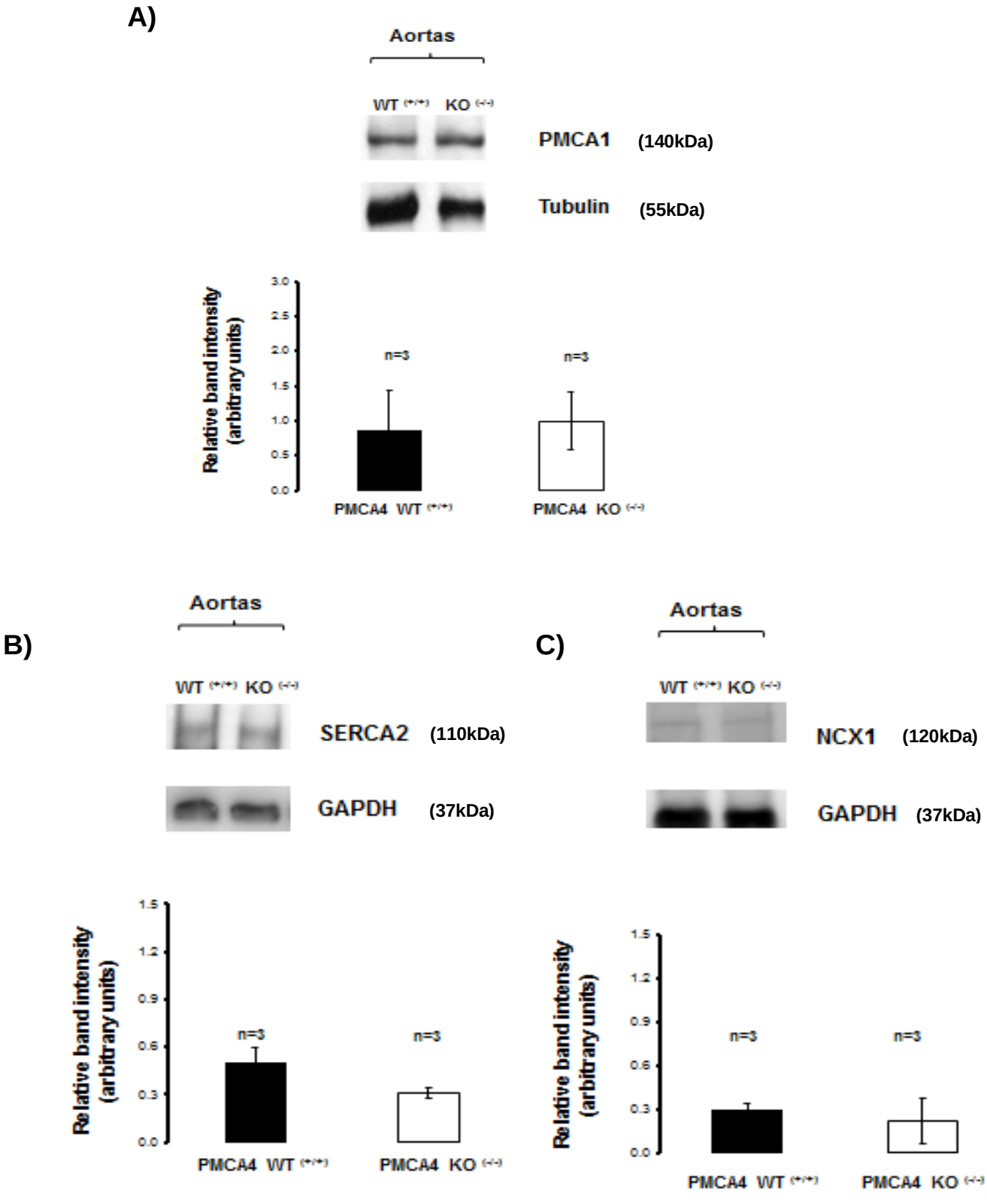

Figure 3.3.1: Expression of PMCA1, SERCA2 and NCX1 in aortic tissue homogenates from PMCA4 WT $^{(+/+)}$ and KO $^{(-/-)}$ mice. No significant differences were found in the protein expression of A) PMCA1, B) SERCA2 & C) NCX1 in aortas obtained from PMCA4 KO $^{(-/-)}$ mice in comparison to those from WT $^{(+/+)}$ mice after normalisation of the band density with the respective loading controls GAPDH or tubulin (n=3 in each group). Not significant according to unpaired student's t tests and the results are presented as ± SEM.

3.4 Effects of PMCA4 ablation on arterial contractility in response to:

3.4.1 High potassium solution (KPSS)

In order to investigate whether contractile responses of pressurised mesenteric resistance arteries to high potassium were affected by ablation of PMCA4, arteries were exposed to 40mM and/or 100mM KPSS for a minimum of 5 minutes and then washed out with PSS.

All arteries exhibited maintained constrictions in response to KPSS. Ablation of PMCA4 had no effect on the magnitude of constriction to either 40mM or 100mM KPSS (constriction (as % resting diameter) to 40mM KPSS = PMCA4 KO $^{(-/-)}$ 43.18 ± 5.06% (n=12), WT $^{(+/+)}$ 43.72 ± 4.66% (n=14), NS; and to 100mM KPSS = PMCA4 KO $^{(-/-)}$ 53.92 ± 3.53% (n=19), WT $^{(+/+)}$ 58.88 ± 2.57% (n=30), NS) (figure 3.4.1.1).

Isolated, pressurised mesenteric arteries from PMCA4 Ht $^{(+/-)}$ mice exhibited similar contractile responses to 100mM KPSS when compared with arteries from PMCA4 WT $^{(+/+)}$ or KO $^{(-/-)}$ mice (constriction (as % resting diameter) = PMCA4 Ht $^{(+/-)}$ 60.9 ± 2.7% (n=9), NS when compared to either PMCA4 WT $^{(+/+)}$ or KO $^{(-/-)}$ mice).

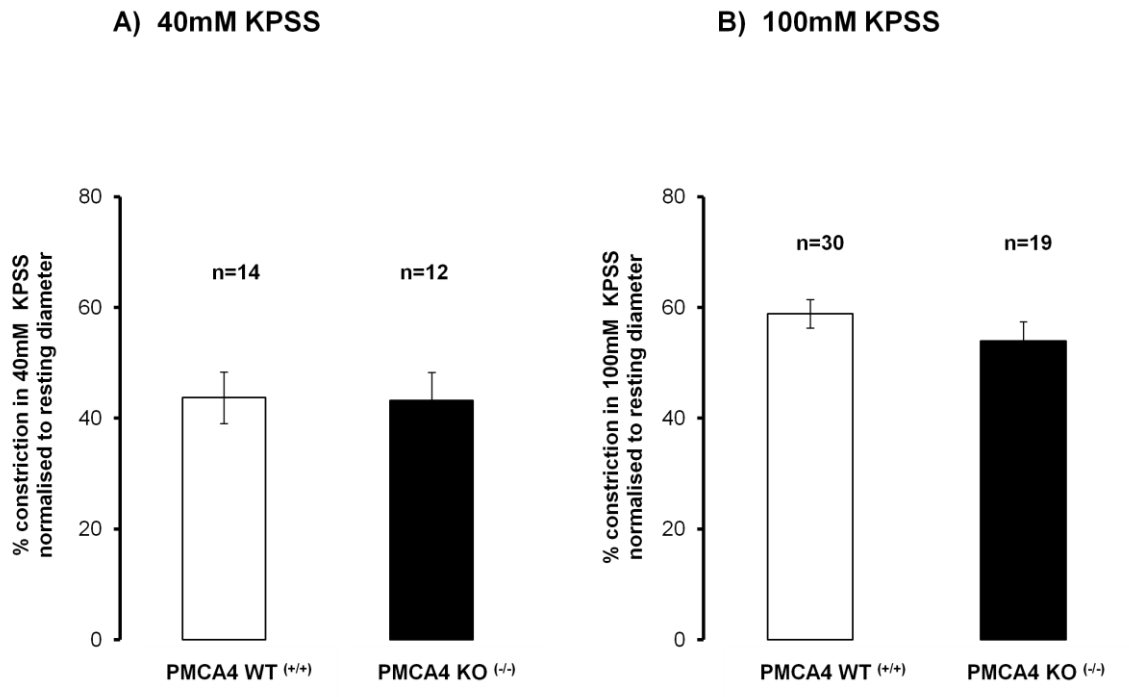

Figure 3.4.1.1: Effects of PMCA4 ablation on mesenteric arterial constriction in response to 40mM & 100mM KPSS. Contractile responses (expressed as % constriction normalised to starting diameter) of isolated and pressurised mesenteric arteries from PMCA4 WT $^{(+/+)}$ and KO $^{(-/-)}$ mice following membrane depolarisation with A) 40mM KPSS and B) 100mM KPSS. Data presented as mean ± SEM. Not significant according to an unpaired student's t test.

Following the washout of 40mM KPSS, the relaxation times (i.e. the time for pre-constricted arteries to return to starting diameter, defined by T relaxation and $T_{1/2}$ relaxation times) displayed by arteries were not modified by the ablation of PMCA4 (T relaxations = PMCA4 KO $^{(-/-)}$ 157.53 ± 9.77 seconds (n=12) and WT $^{(+/+)}$ 146.30 ± 8.85 seconds (n=14), NS; and the $T_{1/2}$ relaxations = PMCA4 KO $^{(-/-)}$ 55.34 ± 8.79 seconds (n=12) and WT $^{(+/+)}$ 42.40 ± 6.40 seconds (n=14), NS after 40mM KPSS washout) (figure 3.4.1.2).

The same was true of the arterial relaxation times following washout of 100mM KPSS (T relaxations exhibited by arteries = PMCA4 KO $^{(-/-)}$ 180.38 ± 10.82 seconds (n=19) and WT $^{(+/+)}$ 164.08 ± 6.27 seconds (n=30), NS; and for the $T_{1/2}$ relaxations = PMCA4 KO $^{(-/-)}$ 75.36 ± 7.01 seconds (n=19) and WT $^{(+/+)}$ 59.81 ± 4.41 seconds (n=30), NS) (figure 3.4.1.3).

Relaxation times after 100mM KPSS washout, observed in arteries from PMCA4 Ht $^{(+/-)}$ mice were similar to those observed in arteries from WT $^{(+/+)}$ or PMCA4 KO $^{(-/-)}$ mice (T relaxation = PMCA4 Ht $^{(+/-)}$ 153.92 ± 15.82 seconds (n=9), and for $T_{1/2}$ relaxation = PMCA4 Ht $^{(+/-)}$ 63.47 ± 8.51 seconds (n=9)).

The time for isolated, pressurised arteries to constrict in response to 40mM or 100mM KPSS (T constriction) was similar in arteries from PMCA4 KO $^{(-/-)}$ mice compared with arteries from WT $^{(+/+)}$ mice (T constriction for 40mM KPSS = PMCA4 KO $^{(-/-)}$ 124.8 ± 5.5 seconds (n=12); WT $^{(+/+)}$ 128.8 ± 8.3 seconds (n=14), NS and T constriction for 100mM KPSS = PMCA4 KO $^{(-/-)}$ 145.1 ± 10.9 seconds (n=19); WT $^{(+/+)}$ 141.8 ± 10.8 seconds (n=30), NS) (Figure 3.4.1.4). Arteries from PMCA4 Ht $^{(+/-)}$ mice also displayed similar constriction times (PMCA4 Ht $^{(+/-)}$ 135.3 ± 15.1 seconds (n=9).

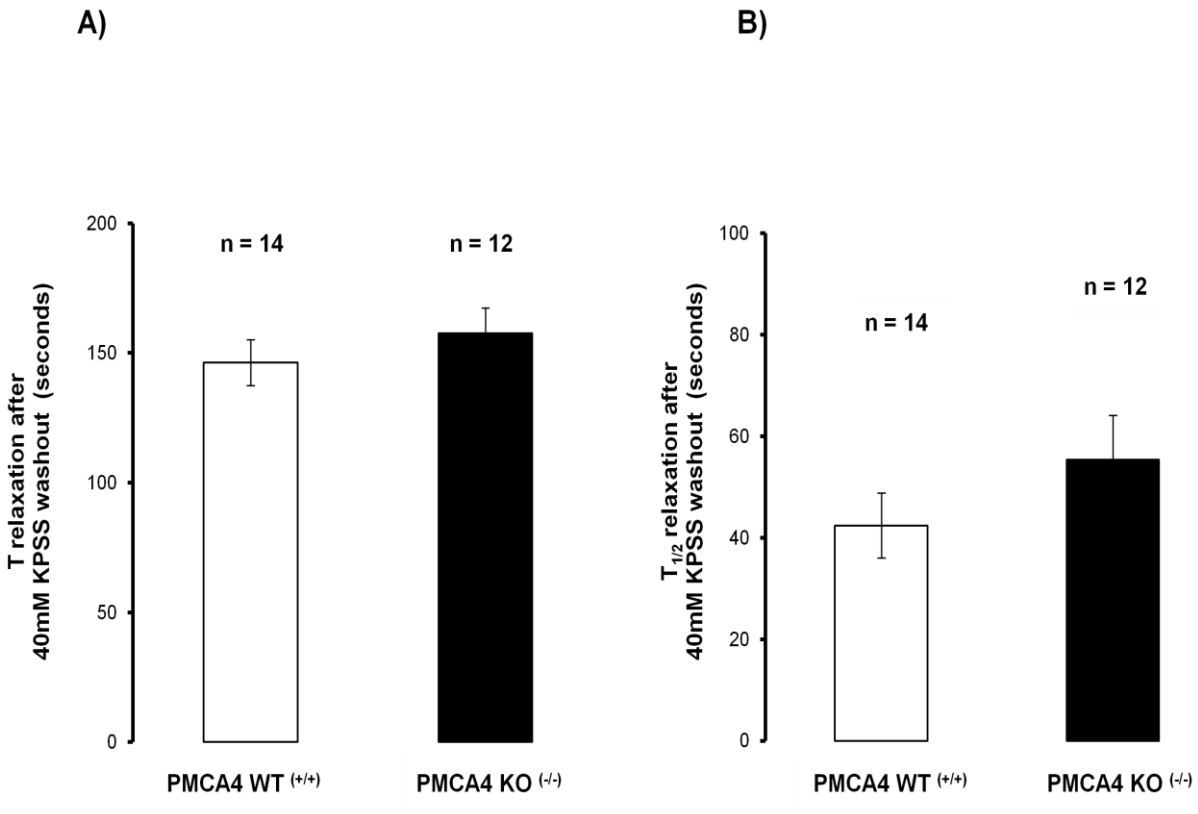

Figure 3.4.1.2: Effect of PMCA4 ablation on relaxation times of mesenteric arteries following washout of 40mM KPSS. A) T relaxation (T = time (seconds) isolated and pressurised arteries pre-constricted with KPSS returned to starting diameter following washout with PSS) and B) $T_{1/2}$ relaxation (defined as the time in seconds for arteries pre-constricted with KPSS to relax by 50% upon washout with PSS) following washout of 40mM KPSS. Data presented as mean $\pm$ SEM. There were no significance differences in relaxation times of arteries from PMCA4 KO $^{(-/-)}$ mice compared to WT $^{(+/+)}$ mice, according to an unpaired student's t test.

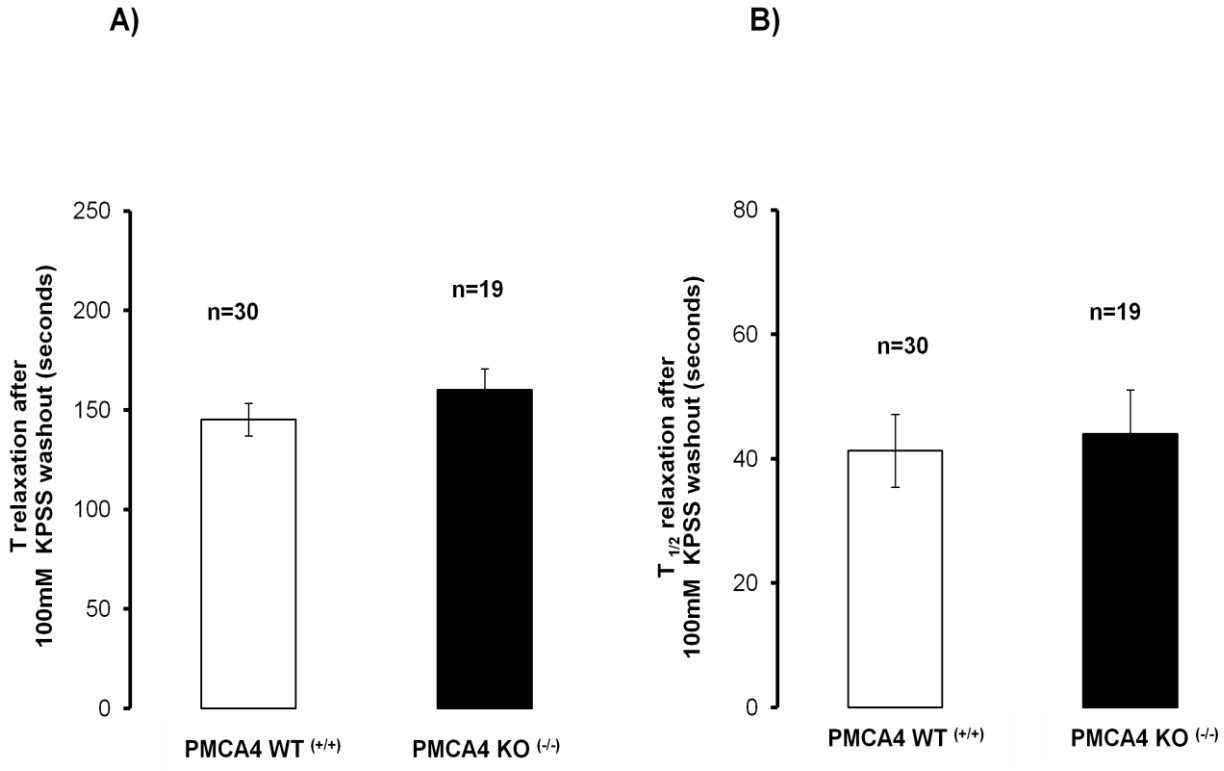

Figure 3.4.1.3: Effect of PMCA4 ablation on relaxation times displayed by mesenteric arteries following washout of 100mM KPSS. After 100mM KPSS washout A) T relaxation (T = time (seconds) isolated and pressurised arteries pre-constricted with KPSS to return to resting diameter following washout with PSS) and B) $T_{1/2}$ relaxation (defined as the time in seconds for arteries pre-constricted with KPSS to relax by 50% upon washout with PSS) were not significantly different in arteries from PMCA4 KO $^{(-/-)}$ mice compared to WT $^{(+/+)}$ mice, unpaired student's t test. Data presented as mean ± SEM.

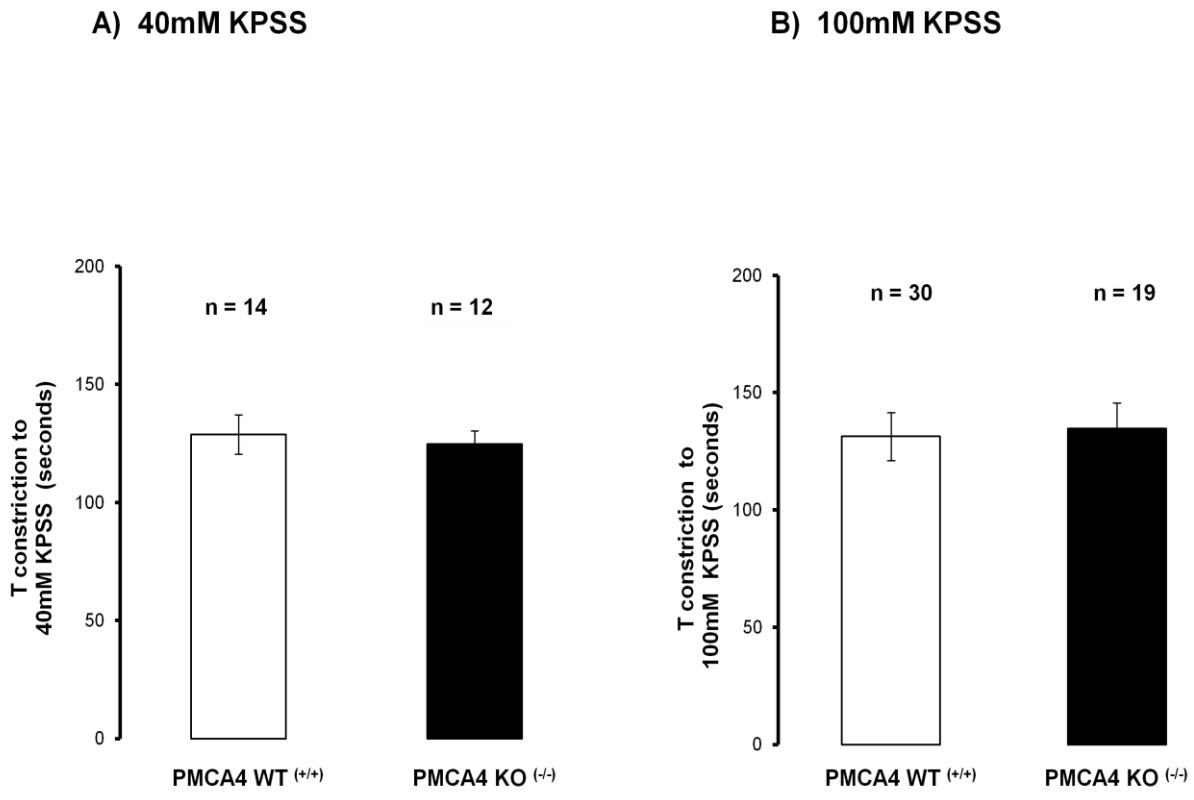

Figure 3.4.1.4: Effects of PMCA4 ablation on constriction times displayed by mesenteric arteries in response to 40mM & 100mM KPSS. T constriction (in seconds) was the time for arteries to reach a stable constriction in response to A) 40mM KPSS and B) 100mM KPSS. Data presented as mean $\pm$ SEM. No significant difference in constriction times of arteries from PMCA4 KO $^{(-/-)}$ mice were evident when compared to WT $^{(+/+)}$ mice, in response to 40mM or 100mM KPSS, unpaired student's t test.

3.4.2 Noradrenaline (NA)

In order to investigate whether adrenoreceptor agonist mediated contractile responses were altered by the ablation of PMCA4 dose response curves to noradrenaline were constructed. All isolated and pressurised mesenteric resistance arteries exhibited maintained concentration dependent constrictions to noradrenaline. However, similar to the results of KPSS, PMCA4 ablation had no effect on arterial constriction to noradrenaline (figure 3.4.2.1).

The noradrenaline induced contractile response exhibited by arteries from PMCA4 Ht $^{(+/-)}$ mice were similar to those from KO $^{(-/-)}$ and/or WT $^{(+/+)}$ mice (maximal responses = PMCA4 Ht $^{(+/-)}$ 59.6 ± 3.8% (n=8), KO $^{(-/-)}$ 59.5 ± 4.7% (n=11) and WT $^{(+/+)}$ 58.8 ± 2.5% (n=14), NS).

Sensitivity to noradrenaline, shown as EC50 values (i.e. the agonist concentration required to achieve half of the maximum arterial response to noradrenaline), was also analogous between groups (LogEC50 = PMCA4 KO $^{(-/-)}$ -6.241 ± 0.093 (n=11), WT $^{(+/+)}$ -6.485 ± 0.259 (n=14) and for Ht $^{(+/-)}$ mice -6.187 ± 0.176 (n=8), NS).

3.4.3 Acetylcholine (ACh)

Ablation of PMCA4 had no effect on the functional arterial responses to the endothelial-dependent dilator acetylcholine (maximal dilatory responses = PMCA4 WT $^{(+/+)}$ 24.8 ± 3.3% (n=13), KO $^{(-/-)}$ 23.1 ± 5.0% (n=11), NS) (figure 3.4.3.1).

Arteries from PMCA4 Ht $^{(+/-)}$ mice (27.5 ± 5.5% (n=6)) also exhibited similar responses to acetylcholine as did arteries from KO $^{(-/-)}$ and/or WT $^{(+/+)}$ mice. It was unreliable to calculate EC50 values for arterial sensitivity to acetylcholine, due to

uncertainty as to whether pressurised arteries achieved the maximal dilatory response. It is acknowledged that the magnitude of acetylcholine dependent dilations observed in all isolated, pressurised mouse mesenteric arteries were small with relatively low maximal arterial dilatory responses being achieved. The acceptable threshold for maximal dilatory responses to acetylcholine achieved by arteries from PMCA4 WT $^{(+/+)}$ mice was set at 8%. However no threshold could be set for the dilatory responses to acetylcholine achieved by arteries from PMCA4 KO $^{(-/-)}$ and PMCA4 Ht $^{(+/-)}$ mice as this was being investigated for the first time.

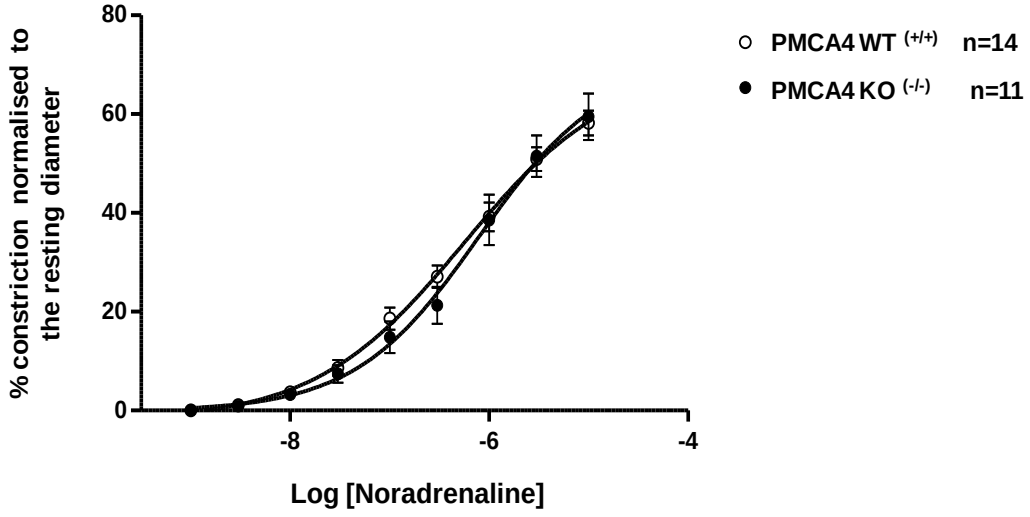

Figure 3.4.2.1: Effect of PMCA4 ablation on mesenteric arterial constriction in response to noradrenaline. Responses (expressed as % constriction normalised to resting diameter) of isolated, pressurised mesenteric arteries from PMCA4 WT $^{(+/+)}$ (n=14) and KO $^{(-/-)}$ (n=11) mice to cumulative concentrations (Log[NA] -9.0 to -4.5M) of noradrenaline. Data expressed as mean ± SEM. Not significant, repeated measurements analysis of variance (ANOVA).

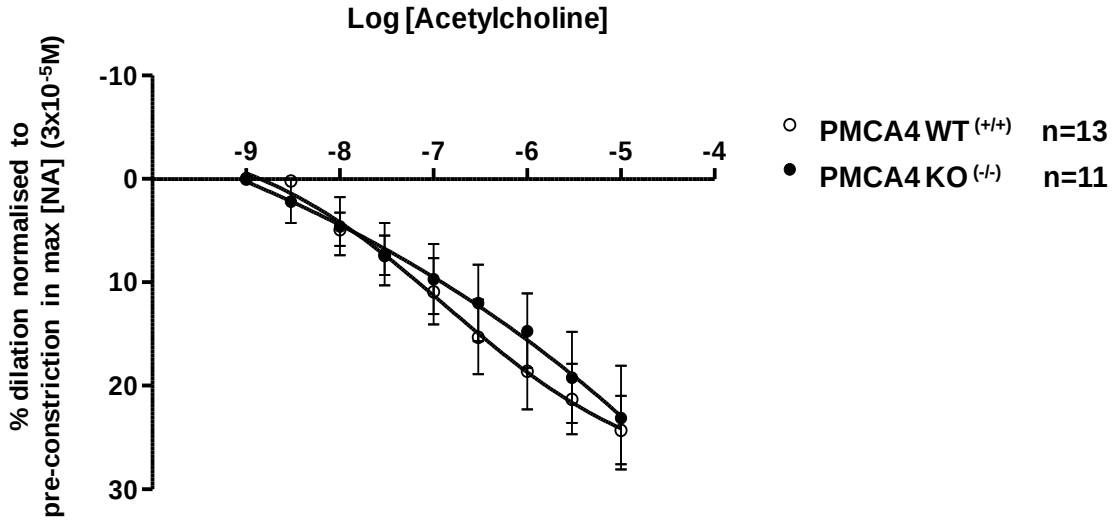

Figure 3.4.3.1: Effect of PMCA4 ablation on dilatory responses of mesenteric arteries in response to acetylcholine. Dilatory responses (expressed as % dilation normalised to the pre-constriction in $3x10^{-5}$M [NA]) of isolated, pressurised resistance arteries from PMCA4 KO $^{(-/-)}$ and from WT $^{(+/+)}$ mice to cumulative concentrations of acetylcholine (Log[ACh] -9.0 to -5.0M). Data expressed as mean ± SEM. No significant difference according to repeated measurements ANOVA.

3.4.4 Sodium nitroprusside (SNP)

Dilations in response to the exogenous nitric oxide donor, sodium nitroprusside were also similar between arteries from PMCA4 KO $^{(-/-)}$ and WT $^{(+/+)}$ mice (dilations to maximum sodium nitroprusside concentration, $1x10^{-5}$ M SNP = PMCA4 KO $^{(-/-)}$ 74.2 ± 6.8% (n=11) and WT $^{(+/+)}$ 67.3 ± 6.1% (n=12), NS) (figure 3.4.4.1).

Again EC50 values were not calculated due to uncertainty as to whether the maximal possible dilation was achieved. Responses exhibited by arteries obtained from PMCA4 Ht $^{(+/-)}$ mice were not significantly altered in comparison with arteries from PMCA4 KO $^{(-/-)}$ and WT $^{(+/+)}$ mice (maximal responses = PMCA4 Ht $^{(+/-)}$ 83.8 ± 4.0% (n=5)).

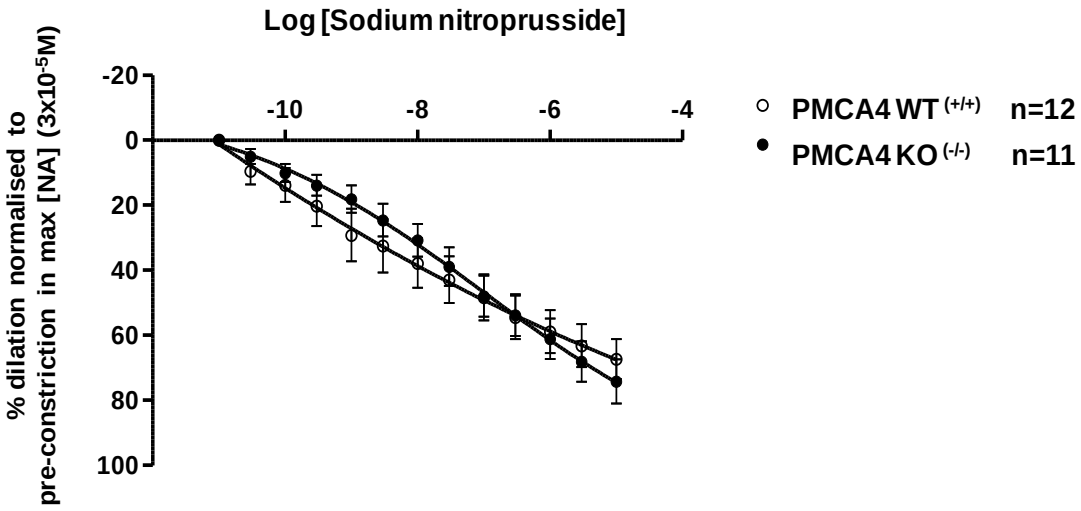

Figure 3.4.4.1: Effect of PMCA4 ablation on dilatory responses of mesenteric arteries in response to sodium nitroprusside. Dilatory responses (expressed as % dilation normalised to the pre-constriction in $3x10^{-5}$M [NA]) of isolated resistance arteries from PMCA4 KO $^{(-/-)}$ and from WT $^{(+/+)}$) mice to cumulative concentrations of sodium nitroprusside (Log[SNP] -11.0 to -5.0M). Data presented as mean ± SEM. Not significant according to repeated measurements ANOVA.

3.5 Effects of nitric oxide synthase (NOS) inhibition by LNNA on arterial contractility to:

Previous studies using PMCA4 overexpressing mice have shown that PMCA4 may modulate smooth muscle contractile function via the regulation of nNOS activity (Gros *et al.*, 2003; Schuh *et al.*, 2003). As such, the effect of NOS inhibition with LNNA (which inhibits all forms of NOS including nNOS) was investigated by incubating isolated pressurised mouse mesenteric arteries for 30 minutes in 100µM of LNNA or alternatively in PSS for controls.

3.5.1 High potassium solution (KPSS)

The NOS inhibitor LNNA, had no effect on the responses of vessels from PMCA4 WT $^{(+/+)}$ mice to 100mM KPSS (WT $^{(+/+)}$ arterial responses without LNNA treatment = 56.3 $\pm$ 3.6% (n=14)) and with LNNA treatment = 60.8 ± 4.9% (n=8), NS) (figure 3.5.1.1). Contractile responses of isolated arteries from PMCA4 KO $^{(-/-)}$ mice to 100mM KPSS were also unaffected by LNNA incubation (KO $^{(-/-)}$ responses = 52.3 $\pm$ 3.5% (n=11) and 50.5 ± 8.8% (n=5) in the absence and presence of LNNA respectively, NS) (figure 3.5.1.1).

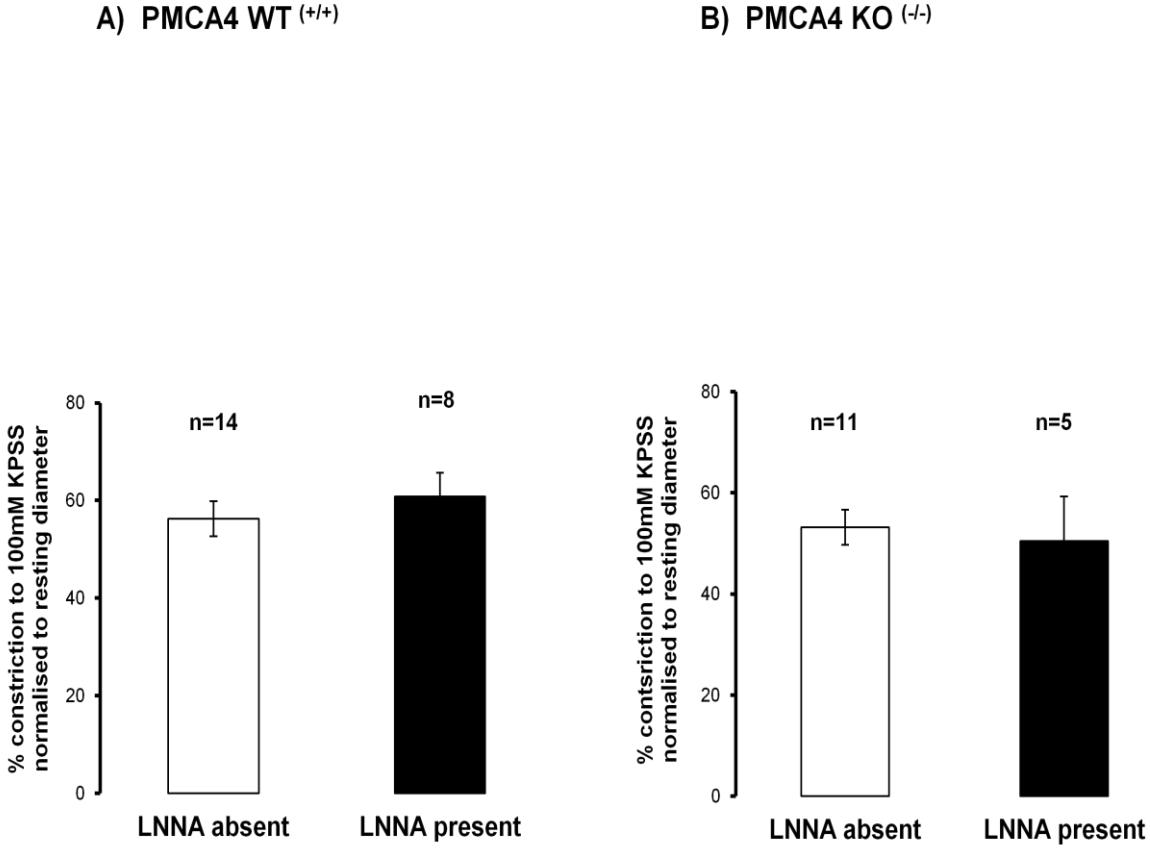

Figure 3.5.1.1: Effect of LNNA on constriction of mesenteric arteries from PMCA4 WT $^{(+/+)}$ & KO $^{(-/-)}$ mice in response to 100mM KPSS. Contractile arterial responses (as % constrictions to 100mM KPSS normalised to starting diameter) of isolated, pressurised resistance arteries from A) PMCA4 WT $^{(+/+)}$ mice and from B) KO $^{(-/-)}$ mice in the presence and absence of LNNA (100µM). Data presented as mean $\pm$ SEM. No significant difference between arterial responses generated in the absence and presence of LNNA, unpaired student's t test.

3.5.2 Noradrenaline (NA)

NOS inhibition with LNNA also had no significant effect on constrictions of arteries from PMCA4 WT $^{(+/+)}$ mice in response to noradrenaline (maximal responses (as % starting diameter) = 58.8 ± 2.5% (n=14) and 62.6 ± 1.7% (n=8) in the absence and presence of LNNA, NS) (figure 3.6.2.1). Likewise, there was no effect of LNNA on noradrenaline induced constrictions of isolated arteries from PMCA4 KO $^{(-/-)}$ mice (maximal response (as % starting diameter) = 59.5 ± 4.7% (n=11) and 56.2 ± 4.6% (n=5) in the absence and presence of LNNA respectively, NS) (figure 3.5.2.1).

The sensitivity of arteries from both PMCA4 WT $^{(+/+)}$ and KO $^{(-/-)}$ mice to noradrenaline (shown as EC50 values), were also unaffected by LNNA (logEC50 of arteries from PMCA4 WT $^{(+/+)}$ mice = -6.485 ± 0.259 (n=14) and -6.257 ± 0.144 (n=8), in the absence and presence of LNNA respectively, NS; for PMCA4 KO $^{(-/-)}$ mice = -6.241 ± 0.093 (n=11) and -6.139 ± 0.095 (n=5), in the absence and presence of LNNA respectively, NS; and for PMCA4 Ht $^{(+/-)}$ mice = -6.187 ± 0.176 (n=8) and -6.169 ± 0.050 (n=3), in the absence and presence of LNNA respectively, NS).

3.5.3 Acetylcholine (ACh)

Further investigations, showed that LNNA had no effect on the dose-dependent dilatory responses to acetylcholine exhibited by arteries from PMCA4 WT $^{(+/+)}$ mice (maximal responses (as % of arterial constriction to the highest noradrenaline dose) = 24.8 ± 3.3% (n=13) and 24.0± 9.1% (n=7) in the presence and absence of LNNA respectively, NS) (figure 3.5.3.1). LNNA had no effect on the dilatory responses to acetylcholine in arteries isolated from PMCA4 KO $^{(-/-)}$ mice pre-constricted with

noradrenaline (28.8 ± 17.7% (n=5) and 23.1 ± 5% (n=11) in the absence and presence of LNNA respectively, NS) (figure 3.5.3.1).

3.5.4 Sodium nitroprusside (SNP)

LNNA had no effect on the sodium nitroprusside induced dilatory responses of arteries from PMCA4 WT $^{(+/+)}$ mice (maximal responses (as % of arteries pre-constricted with the highest noradrenaline dose = 67.3 ± 6.1% (n=12) and 68.6 ± 10.5% (n=6) in the absence and presence of LNNA respectively, NS) (figure 3.6.4.1). Neither did LNNA have any effect on arterial responses of arteries from PMCA4 KO $^{(-/-)}$ mice to sodium nitroprusside (74.2 ± 6.8% (n=11) and 74.3 ± 5.0% (n=5) in the absence and presence of LNNA respectively, NS) (figure 3.5.4.1).

A) PMCA4 WT (+/+)

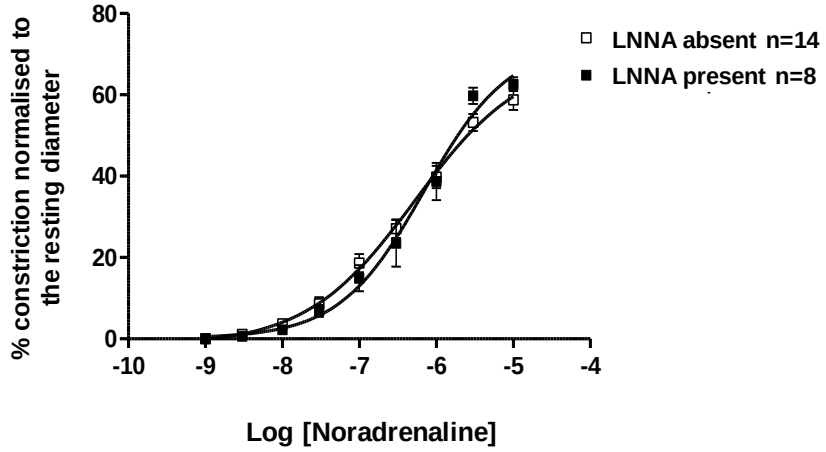

B) PMCA4 KO (-/-)

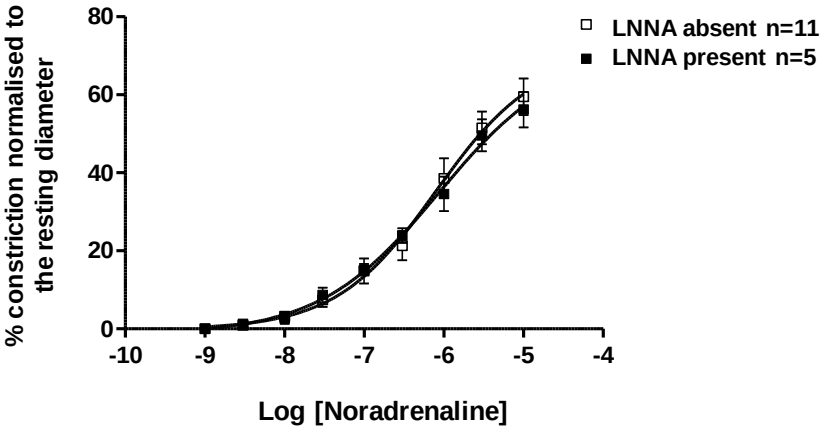

Figure 3.5.2.1: Effect of LNNA on constriction of mesenteric arteries from PMCA4 WT (+/+) & KO (-/-) mice in response to noradrenaline. Constrictions (as a % of the starting diameter) of isolated and pressurised mesenteric arteries to cumulative concentrations of noradrenaline (Log[NA] -9.0 to -4.5M) from A) PMCA4 WT (+/+) and from B) KO (-/-) mice without and with LNNA treatment. Data presented as mean ± SEM. No significant difference between responses generated in the absence and presence of LNNA, repeated measurements, ANOVA.

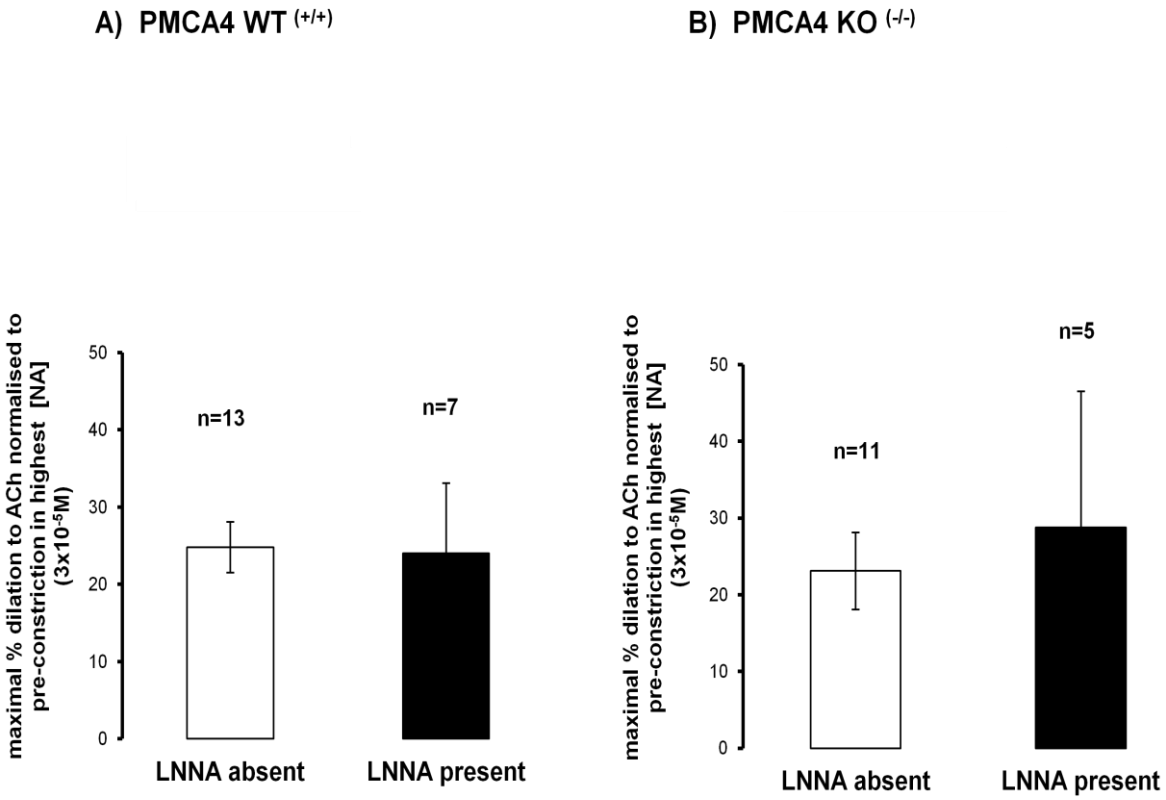

Figure 3.5.3.1: Effect of LNNA on dilatory responses of mesenteric arteries from PMCA4 WT $^{(+/+)}$ & KO $^{(-/-)}$ mice to acetylcholine. Maximal dependent dilations to Log[ACh] -5.0M acetylcholine (as % of pre-constriction in the highest [NA] dose) exhibited by arteries from A) PMCA4 WT $^{(+/+)}$ and from B) KO $^{(-/-)}$ mice in the absence and presence of LNNA treatment. Data presented as mean $\pm$ SEM. No significant difference between responses generated in the absence and presence of LNNA, unpaired student's t test.

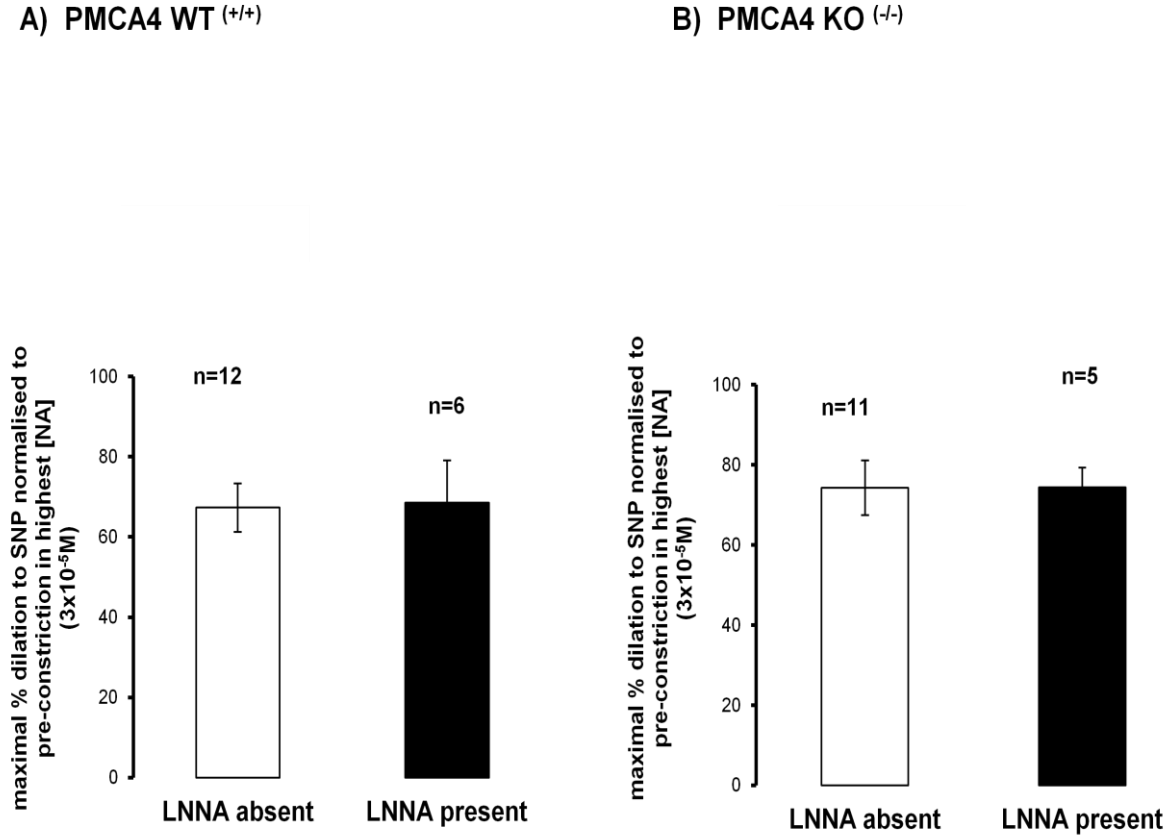

Figure 3.5.4.1: Effect of LNNA on dilatory responses of mesenteric arteries from PMCA4 WT $^{(+/+)}$ & KO $^{(-/-)}$ mice to sodium nitroprusside. Maximal dilations to Log[SNP] -5.0M (dilations as % pre-constriction in the highest [NA] dose) exhibited by arteries from A) PMCA4 WT $^{(+/+)}$ and from B) KO $^{(-/-)}$ mice in the absence and presence of LNNA treatment. Data presented as mean $\pm$ SEM. No significant difference between responses generated in the absence and presence of LNNA were evident, unpaired student's t test.

3.6 Effects of PMCA4 ablation on the concentration of intracellular free calcium ($[Ca^{2+}]_i$)

Since PMCA may act as a calcium extrusion mechanism we investigated the effect of PMCA4 ablation on basal and on stimulated global intracellular Ca^{2+} concentrations ($[Ca^{2+}]_i$) in isolated, pressurised resistance arteries. Global intracellular Ca^{2+} concentration within the mesenteric arterial wall was assessed with the use of the Ca^{2+} fluorescent dye, indo-1.

3.6.1 Effects on basal $[Ca^{2+}]_i$

Ablation of PMCA4 had no effect on the baseline 400:500 fluorescence (or F_{400}/F_{500}) Ca^{2+} emission ratio (representative of global intracellular $[Ca^{2+}]$) of isolated, pressurised arteries (Resting F_{400}/F_{500} Ca^{2+} emission ratio = PMCA4 KO $^{(-/-)}$ 0.64 ± 0.06 (n=6) and WT $^{(+/+)}$ 0.65 ± 0.06 (n=6), NS) (figure 3.6.1.1).

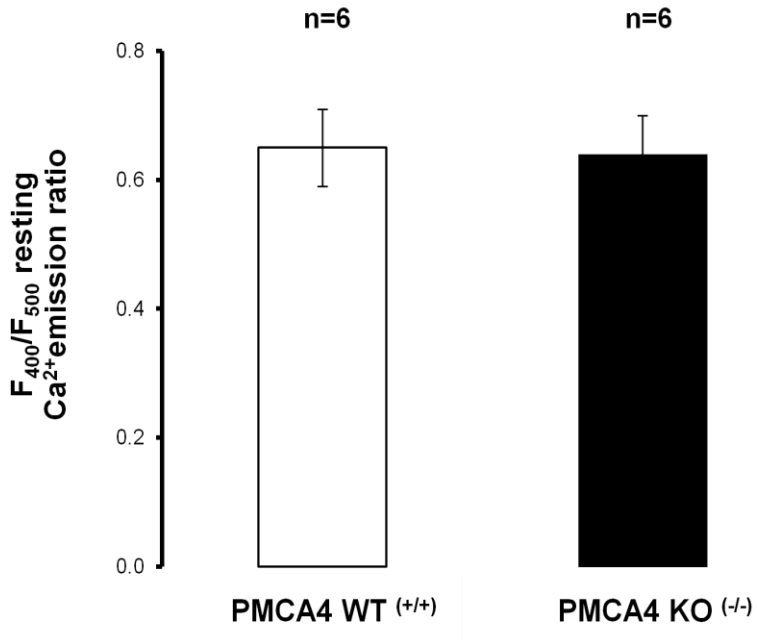

Figure 3.6.1.1: Effect of PMCA4 ablation on basal $[Ca^{2+}]_i$ of intact mesenteric arteries. Basal levels of $[Ca^{2+}]_i$ present within intact, pressurised mesenteric resistance arteries isolated from PMCA4 WT $^{(+/+)}$ and from KO $^{(-/-)}$ mice as was monitored by the resting F_{400}/F_{500} Ca^{2+} emission ratio. Data presented as mean $\pm$ SEM. No significant difference between arteries from PMCA4 KO $^{(-/-)}$ and WT $^{(+/+)}$ mice, unpaired student's t test.

3.6.2 Effects on elevations of $[Ca^{2+}]_i$ in response to 40mM KPSS

Arterial stimulation with 40mM KPSS resulted in an increase in the F_{400}/F_{500} Ca^{2+} emission ratio and maintained constriction of arteries from PMCA4 KO $^{(-/-)}$ and WT $^{(+/+)}$ mice. The ablation of PMCA4 had no effect on the magnitude of arterial constrictions to 40mM KPSS (constriction as % normalised to starting diameter = PMCA4 KO $^{(-/-)}$ 36.96 ± 6.44% (n=6) and WT $^{(+/+)}$ 33.20 ± 7.18% (n=6), NS) or on the magnitude of the change in the F_{400}/F_{500} Ca^{2+} emission ratio (Δ in F_{400}/F_{500} Ca^{2+} emission ratio = PMCA4 KO $^{(-/-)}$ 0.14 ± 0.04 (n=6) and WT $^{(+/+)}$ 0.13 ± 0.03 (n=6), NS) (figure 3.6.2.2).

T constriction, i.e. the time taken for isolated, pressurised arteries to reach maximum constriction in response to 40mM KPSS was also not significantly altered by PMCA4 ablation (PMCA4 KO $^{(-/-)}$ 143.93 ± 13.73 seconds (n=6) and WT $^{(+/+)}$ 140.63 ± 17.70 seconds (n=6), NS) (figure 3.6.2.3).

In all experiments, elevations in the F_{400}/F_{500} Ca^{2+} emission ratio preceded KPSS induced constrictions (time difference between the initial rise in F_{400}/F_{500} Ca^{2+} emission ratio and start of 40mM KPSS induced constriction = PMCA4 KO $^{(-/-)}$ 24.60 ± 6.55 seconds (n=6) and WT $^{(+/+)}$ 19.23 ± 3.47 seconds (n=6), NS). The maximal rise in the F_{400}/F_{500} Ca^{2+} emission ratio was reached before the maximal constriction, with times being similar between arteries from PMCA4 KO $^{(-/-)}$ and WT $^{(+/+)}$ mice (figure 3.6.2.3) (Time for maximal increase in F_{400}/F_{500} Ca^{2+} emission ratio upon 40mM KPSS stimulation = PMCA4 KO $^{(-/-)}$ 115.93 ± 7.65 seconds (n=6) and WT $^{(+/+)}$ 104.63 ± 13.78 seconds (n=6), NS).

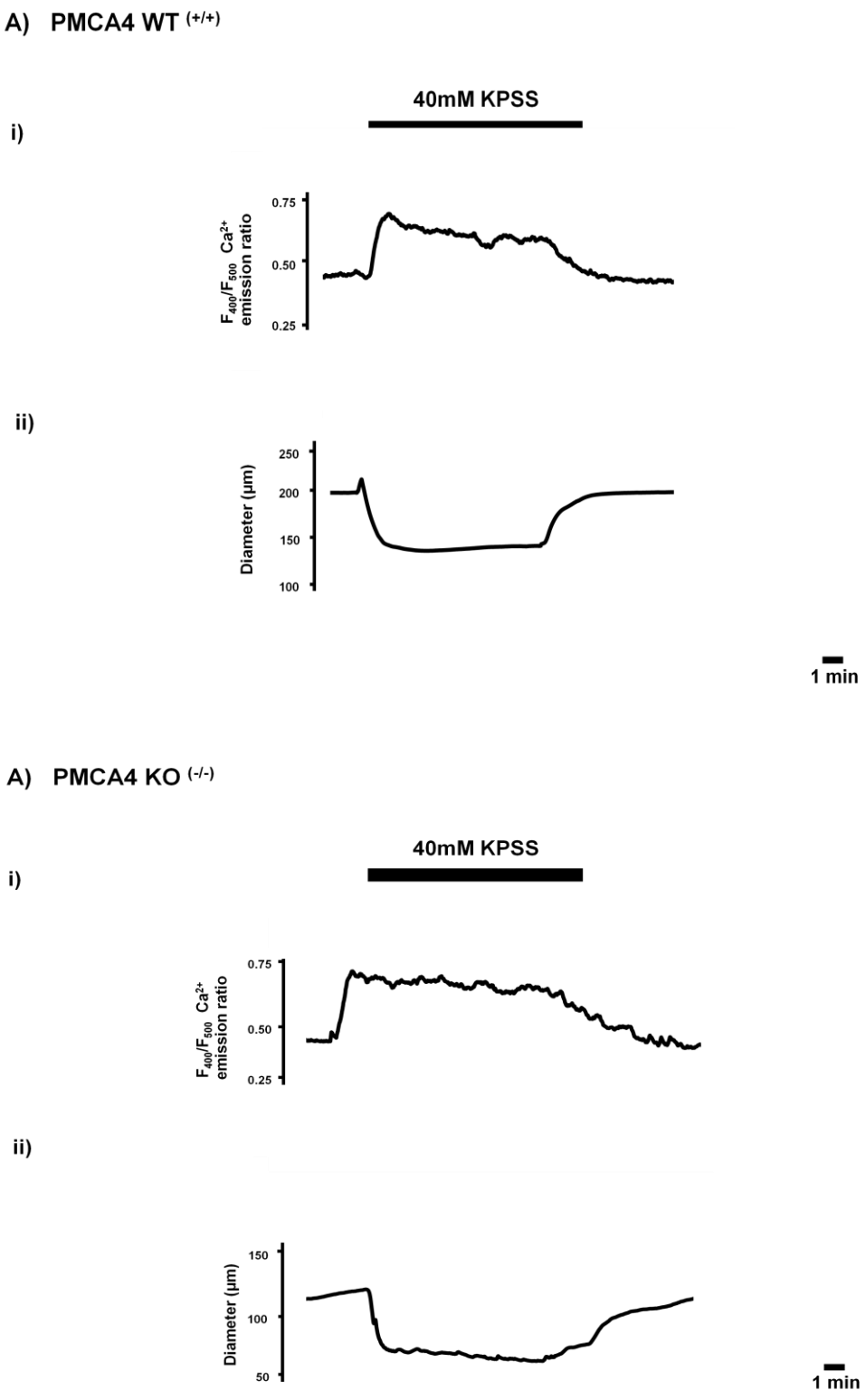

Figure 3.6.2.1: Experimental trace recordings of pressurised arteries simultaneously showing changes in the F_{400}/F_{500} Ca^{2+} emission ratio & diameter in response to 40mM KPSS. Data recorded by WINDAQ data acquisition software. Increases in the F_{400}/F_{500} Ca^{2+} emission ratio preceded arterial constrictions to 40mM KPSS as displayed by an artery from A) a PMCA4 WT $^{(+/+)}$ mouse and B) that from a PMCA KO $^{(-/-)}$ mouse.

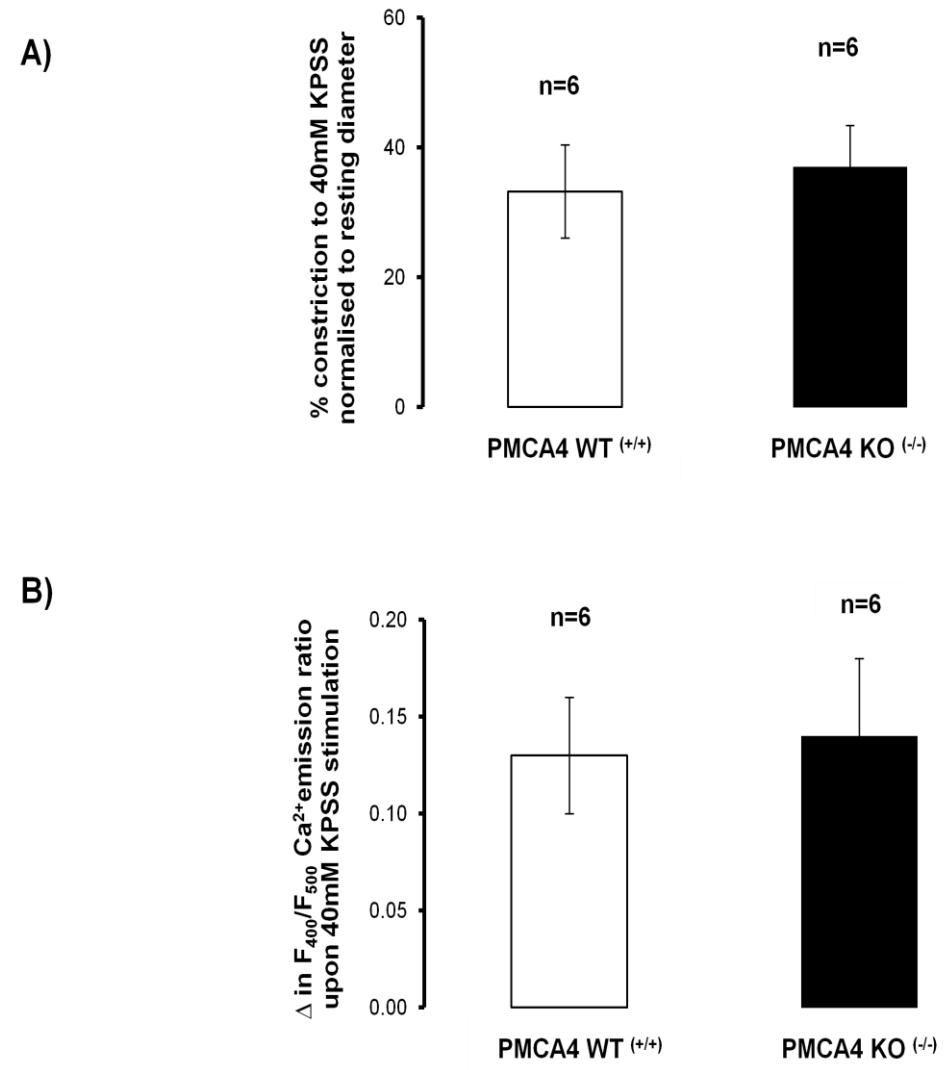

Figure 3.6.2.2: Effects of PMCA4 ablation on mesenteric arterial constrictions & on the F_{400}/F_{500} Ca^{2+} emission responses to 40mM KPSS. A) The arterial contractile response (as a % of starting diameter) and B) the change in F_{400}/F_{500} Ca^{2+} emission ratio (representative of global $[Ca^{2+}]_i$) to 40mM KPSS as was displayed by arteries isolated from PMCA4 WT $^{(+/+)}$ and KO $^{(-/-)}$ mice. Data presented as mean $\pm$ SEM. Not significant, unpaired student's t test.

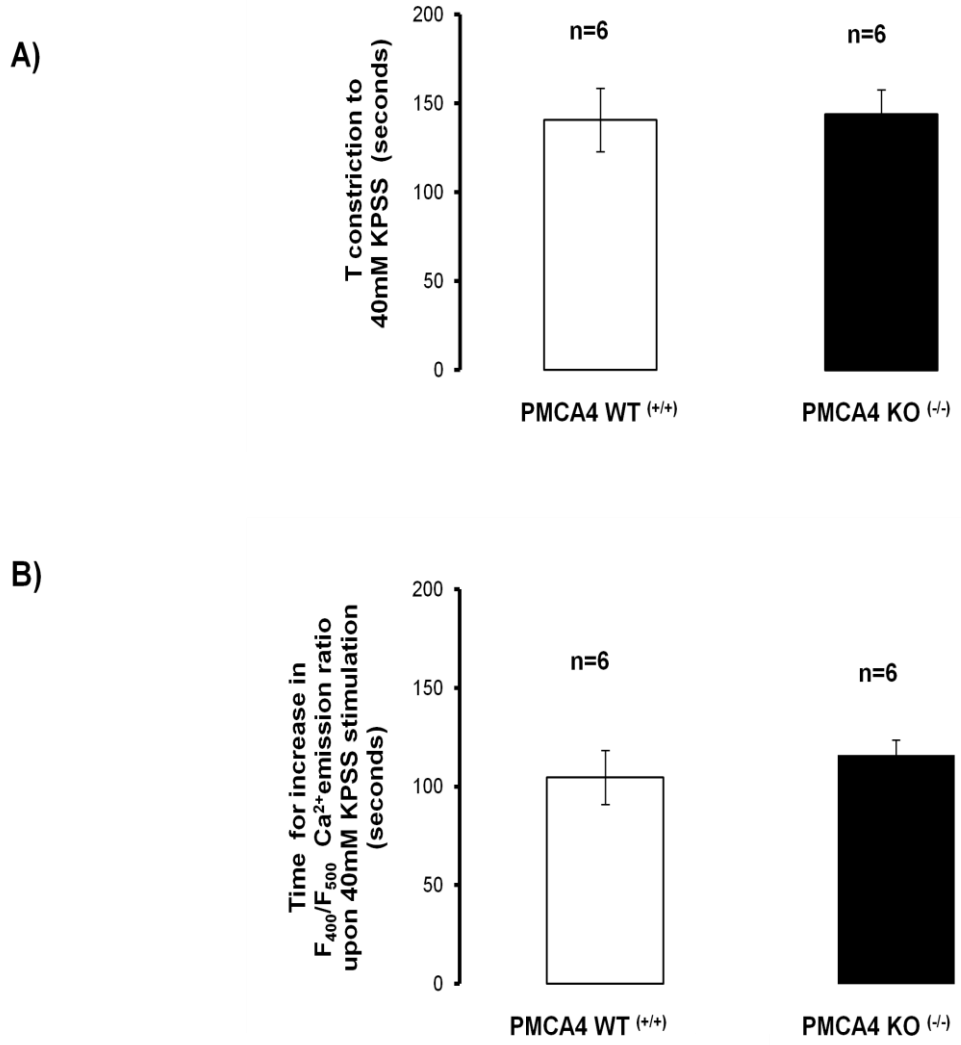

Figure 3.6.2.3: Effects of PMCA4 ablation on the constriction time & on the time for increase in the F_{400}/F_{500} Ca^{2+} emission responses of arteries to 40mM KPSS. A) The time (in seconds) for arteries from PMCA4 WT $^{(+/+)}$ and KO $^{(-/-)}$ mice to reach maximum stable constriction (or T constriction) and represented in B), is the time it took the same arteries to increase F_{400}/F_{500} Ca^{2+} emission ratio, (representative of global $[Ca^{2+}]_i$) to reach maximum upon 40mM KPSS stimulation. Data presented as mean $\pm$ SEM. Not significant, unpaired student's t test.

Relaxation times observed i.e. times for arteries to return to their stable resting diameters following washout of 40mM were not significantly altered by PMCA4 ablation (T relaxations = PMCA4 KO $^{(-/-)}$ 188.67 ± 27.00 seconds (n=6), WT $^{(+/+)}$ 185.07 ± 11.75 seconds (n=6), NS and $T_{½}$ relaxations, (i.e. the time noted for pre-constricted arteries to relax by 50%) after 40mM KPSS washout = PMCA4 KO $^{(-/-)}$ 57.07 ± 14.66 seconds (n=6), WT $^{(+/+)}$ 53.47 ± 7.45 seconds (n=6), NS) (figure 3.6.2.4).

Following washout of 40mM KPSS, the decrease in the F_{400}/F_{500} Ca^{2+} emission ratio of isolated arteries from PMCA4 KO $^{(-/-)}$ and WT $^{(+/+)}$ mice were similar (figure 3.6.2.4) (Time for decrease in F_{400}/F_{500} Ca^{2+} emission ratio upon 40mM KPSS washout = PMCA4 KO $^{(-/-)}$ 156.07 ± 25.81 seconds (n=6), WT $^{(+/+)}$ 152.47 ± 13.91 seconds (n=6), NS; and the $T_{1/2}$ (i.e. the time noted for the maximum F_{400}/F_{500} Ca^{2+} emission ratio to decrease by 50%) upon 40mM KPSS washout = PMCA4 KO $^{(-/-)}$ 62.83 ± 6.54 seconds (n=6), WT $^{(+/+)}$ 61.07 ± 9.64 seconds (n=6), NS).

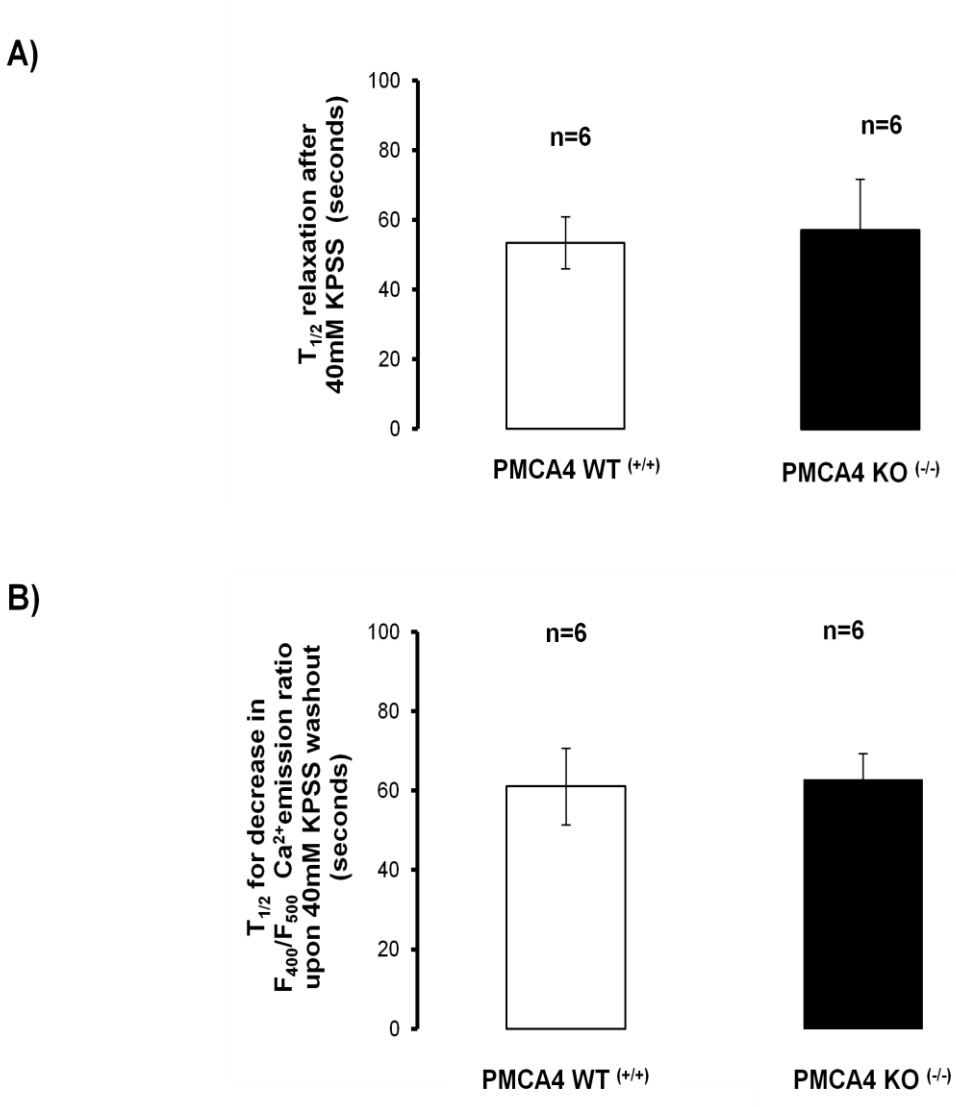

Figure 3.6.2.4: Effects of PMCA4 ablation on the $T_{1/2}$ relaxation times and on the $T_{1/2}$ for decrease in the F_{400}/F_{500} Ca^{2+} emission responses of arteries upon washout of 40mM KPSS. A) The time noted for isolated pressurised arteries from PMCA4 WT $^{(+/+)}$ and KO $^{(-/-)}$ mice pre-constricted to 40mM KPSS to relax by 50% upon PSS washout (or $T_{1/2}$ relaxation). B) The time noted for the maximum F_{400}/F_{500} Ca^{2+} emission ratio (representative of global $[Ca^{2+}]_i$) in the same arteries to decrease by 50% upon washout of 40mM KPSS. Data presented as mean ± SEM. All not significantly different from each other, unpaired student's t test.

3.6.3 Effects on elevations of $[Ca^{2+}]_i$ in response to 100mM KPSS

Stimulation of pressurised arteries from both PMCA4 KO $^{(-/-)}$ and WT $^{(+/+)}$ mice with 100mM KPSS also evoked elevations in the F_{400}/F_{500} Ca^{2+} emission ratio and maintained constrictions (figure 3.6.3.1).

The magnitude of constriction and change in F_{400}/F_{500} Ca^{2+} emission ratio were unaffected by ablation of PMCA4 (constriction as % normalised to starting diameter = PMCA4 KO $^{(-/-)}$ 56.29 ± 8.39% (n=6) and WT $^{(+/+)}$ 50.43 ± 5.69% (n=6), NS; and the Δ in F_{400}/F_{500} Ca^{2+} emission ratio = PMCA4 KO $^{(-/-)}$ 0.19 ± 0.03 (n=6) and WT $^{(+/+)}$ 0.17 ± 0.02 (n=6), NS) (figure 3.6.3.2).

The rise in F_{400}/F_{500} Ca^{2+} emission ratio preceded arterial constriction (time difference between the initial rise in F_{400}/F_{500} Ca^{2+} emission ratio and start of 100mM KPSS induced constriction = PMCA4 KO $^{(-/-)}$ 27.43 ± 6.40 seconds (n=6) and WT $^{(+/+)}$ 37.93 ± 17.74 seconds (n=6), NS). This reached a maximum before maximal arterial constriction was achieved (time for maximal increase in F_{400}/F_{500} Ca^{2+} emission ratio upon 100mM KPSS stimulation = PMCA4 KO $^{(-/-)}$ 151.90 ± 15.97 seconds (n=6) and WT $^{(+/+)}$ 153.80 ± 27.57 seconds (n=6), NS); and the time noted for arteries to reach maximal constriction (i.e. T constriction) to 100mM KPSS = PMCA4 KO $^{(-/-)}$ 190.80 ± 20.52 seconds (n=6) and WT $^{(+/+)}$ 200.53 ± 34.09 seconds (n=6), NS) (figure 3.6.3.3). There were no differences in these times between arteries from PMCA4 KO $^{(-/-)}$ and PMCA4 WT $^{(+/+)}$ mice.

.

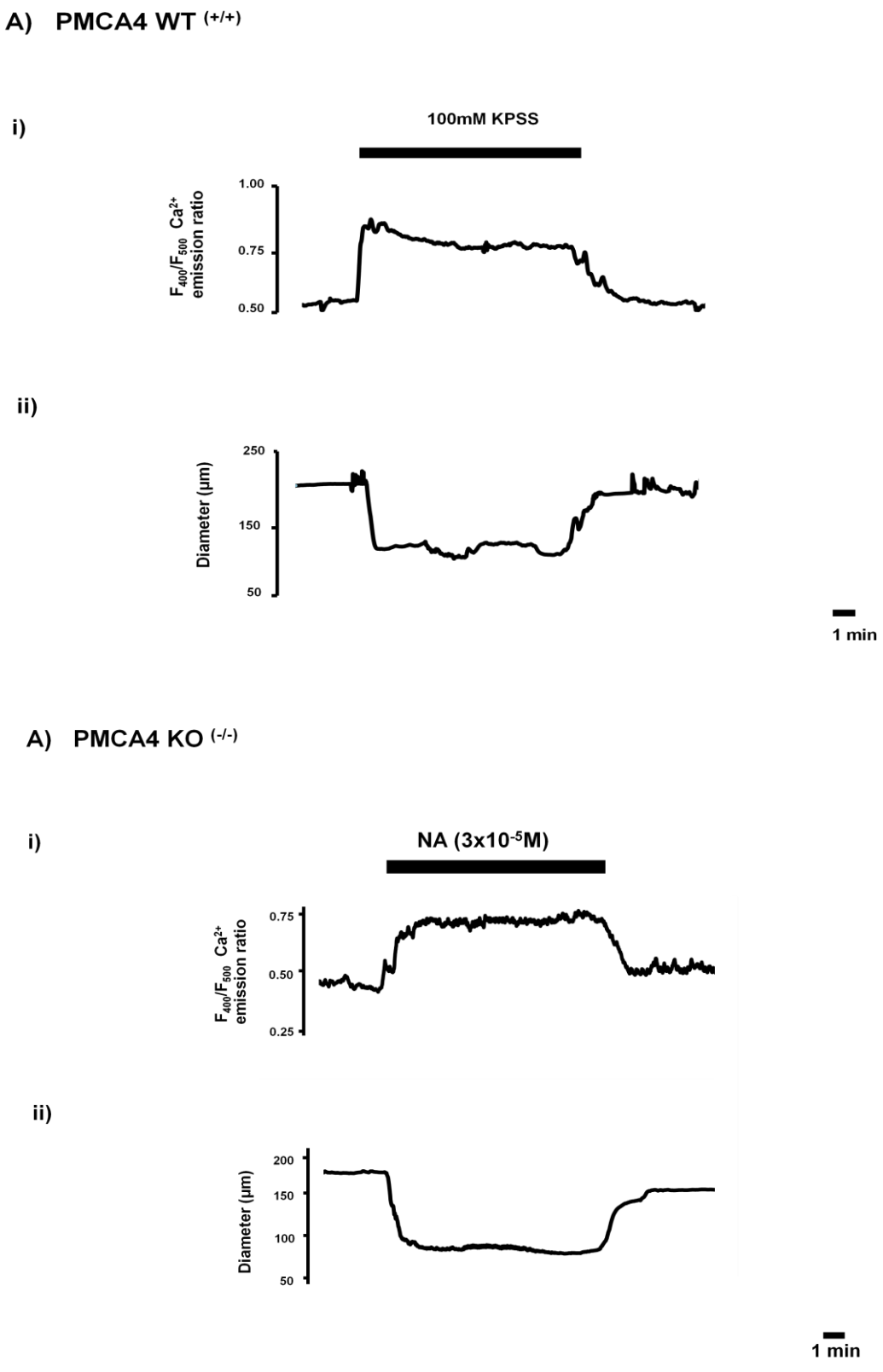

Figure 3.6.3.1: Experimental trace recordings of pressurised arteries simultaneously showing changes in the F_{400}/F_{500} Ca^{2+} emission ratio & diameter in response to 100mM KPSS. As recorded by WINDAQ data acquisition software. One artery was isolated from A) a PMCA4 WT $^{(+/+)}$ mouse and the other isolated from B) a PMCA4 KO $^{(-/-)}$ mouse. Elevations of the F_{400}/F_{500} Ca^{2+} emission ratio (Ai & Bi) preceded decreases in vessel diameter in response to 100mM KPSS as displayed by arteries from A ii) PMCA4 WT $^{(+/+)}$ and from B ii) PMCA4 KO $^{(-/-)}$ mice.

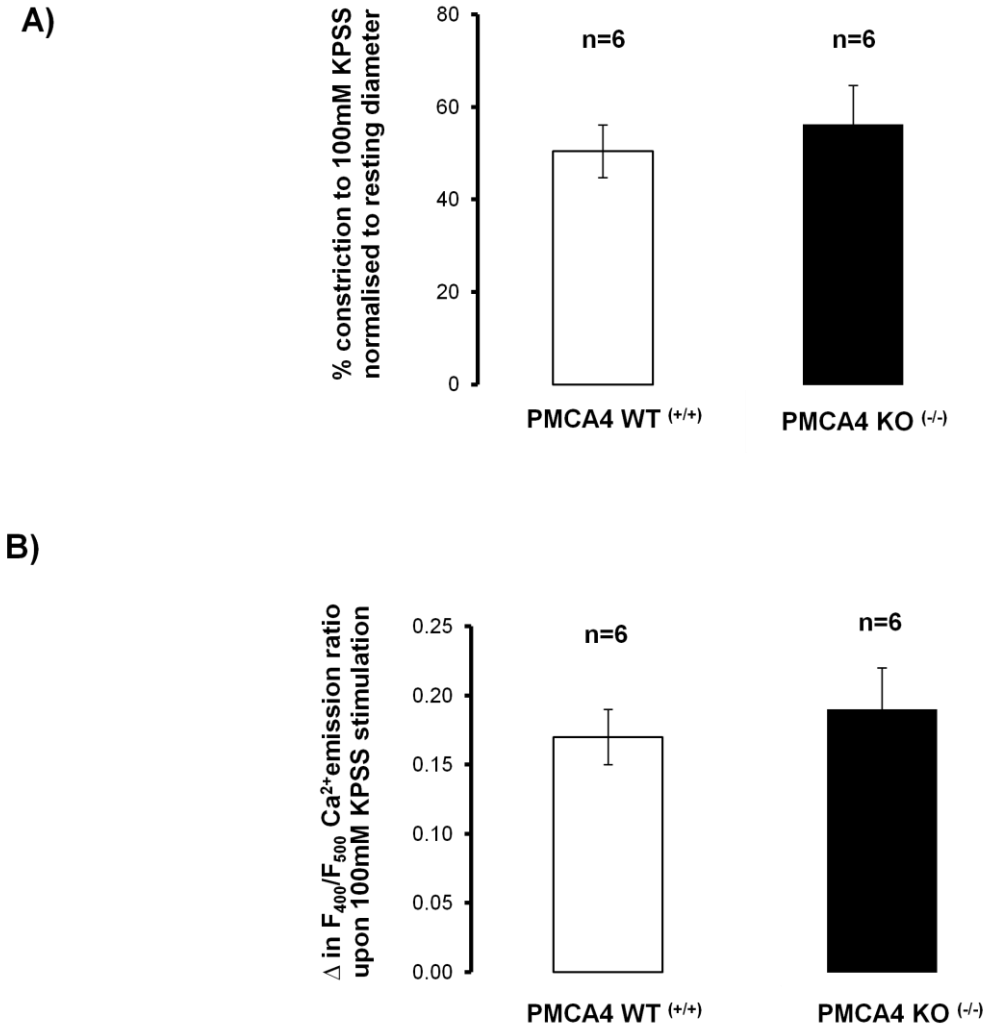

Figure 3.6.3.2: Effects of PMCA4 ablation on arterial constrictions and on the F_{400}/F_{500} Ca^{2+} emission responses to 100mM KPSS. A) The arterial contractile response (constriction as a % of resting diameter) and B) the change in the F_{400}/F_{500} Ca^{2+} emission ratio (representative of global $[Ca^{2+}]_i$) displayed by arteries from PMCA4 WT $^{(+/+)}$ and KO $^{(-/-)}$ mice responding to 100mM KPSS. Data presented as mean $\pm$ SEM. Not significant, unpaired student's t test.

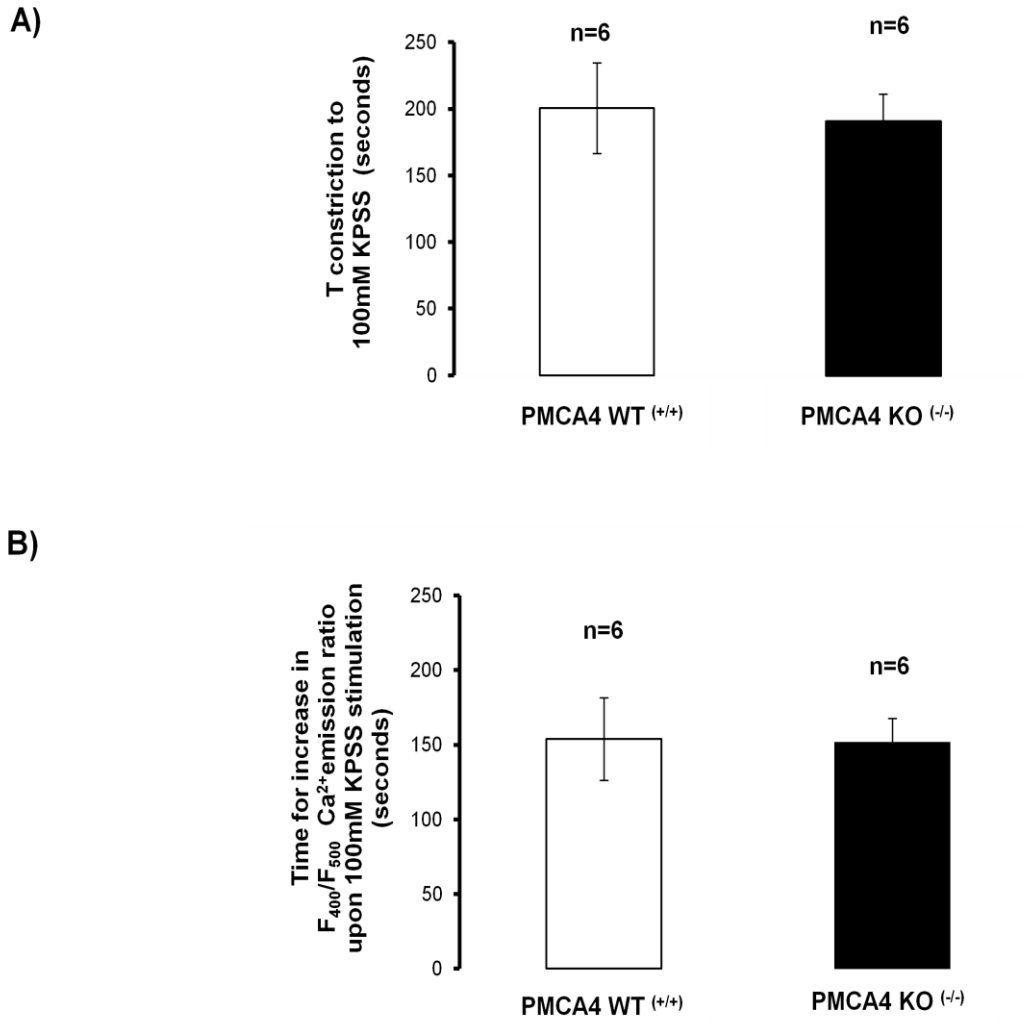

Figure 3.6.3.3: Effects of PMCA4 ablation on the constriction time and on the time for increase in the F_{400}/F_{500} Ca^{2+} emission responses of arteries to 100mM KPSS. A) The time (in seconds) isolated arteries from PMCA4 WT $^{(+/+)}$ and KO $^{(-/-)}$ mice achieved maximum constriction (T constriction) and B) the observed time, the same vessels maximally increased F_{400}/F_{500} Ca^{2+} emission ratio to 100mM KPSS stimulation. Data presented as mean $\pm$ SEM. Times exhibited by arteries from PMCA4 KO $^{(-/-)}$ and WT $^{(+/+)}$ mice were not significantly different, unpaired student's t test.

Relaxation times (i.e. T and $T_{1/2}$ relaxations) for arteries to return to their stable resting diameters following washout of 100mM KPSS were not significantly altered by PMCA4 ablation (T relaxation = PMCA4 KO $^{(-/-)}$ 317.37 ± 19.52 seconds (n=6), WT $^{(+/+)}$ 293.53 ± 31.39 seconds (n=6), NS; and T ½ relaxation after 100mM KPSS washout = PMCA4 KO $^{(-/-)}$ 42.73 ± 11.97 seconds (n=6), WT $^{(+/+)}$ 42.73 ± 4.09 seconds (n=6), NS) (figure 3.6.3.4).

The times observed for the decline in the F_{400}/F_{500} Ca^{2+} emission after 100mM KPSS washout were similar in arteries from PMCA4 KO $^{(-/-)}$ mice and from WT $^{(+/+)}$ mice (time for decrease in F_{400}/F_{500} Ca^{2+} emission ratio upon 100mM KPSS washout = PMCA4 KO $^{(-/-)}$ 240.53 ± 21.70 seconds (n=6), WT $^{(+/+)}$ 220.93 ± 29.93 seconds (n=6), NS; and for the $T_{1/2}$ (i.e. the time for the maximum F_{400}/F_{500} Ca^{2+} emission ratio to decrease by 50% upon 100mM KPSS washout) = PMCA4 KO $^{(-/-)}$ 98.30 ± 15.22 seconds (n=6), WT $^{(+/+)}$ 96.20 ± 16.26 seconds (n=6), NS) (figure 3.6.3.4).

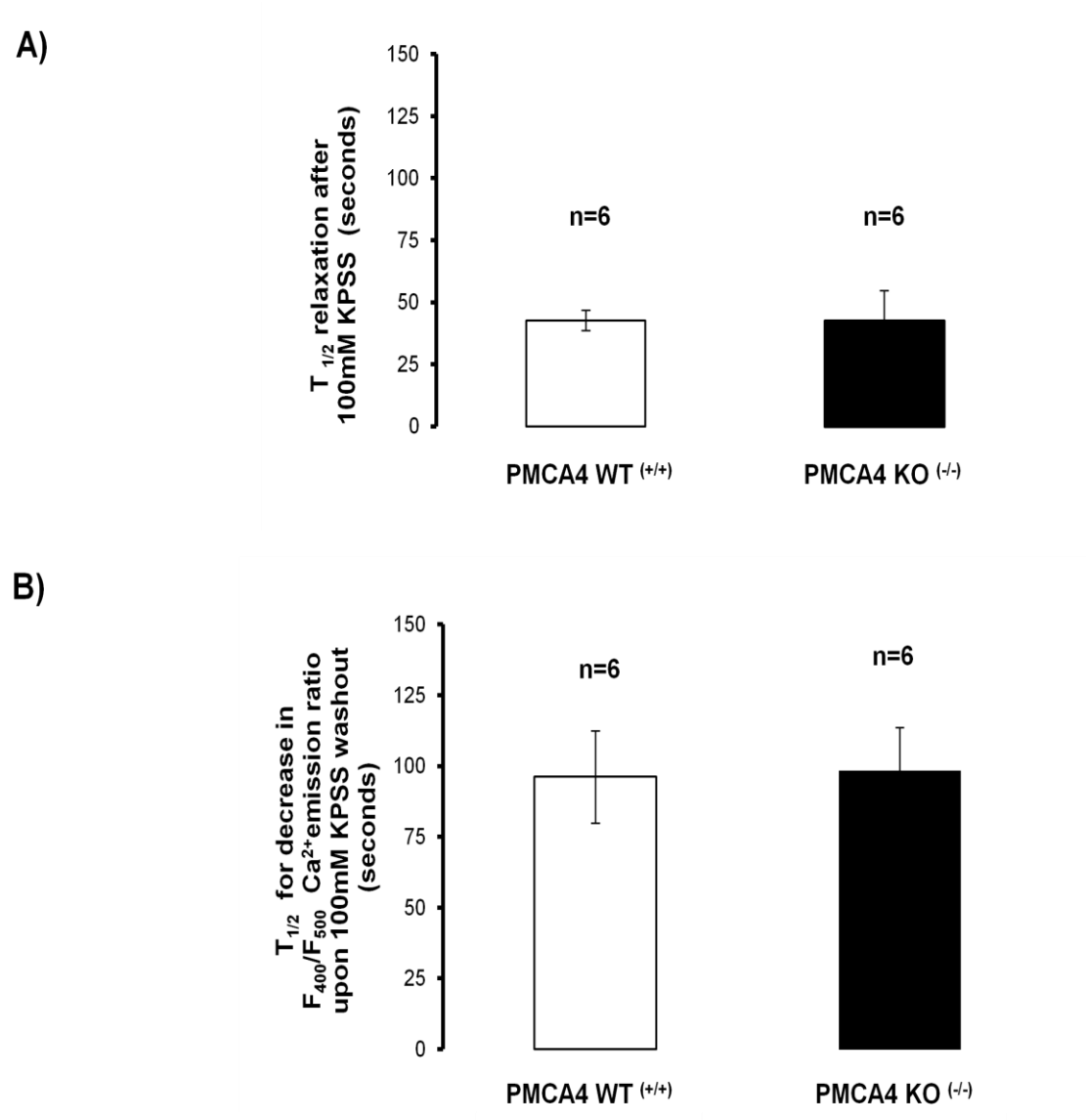

Figure 3.6.3.4: Effects of PMCA4 ablation on $T_{1/2}$ relaxation times and on the $T_{1/2}$ for decrease in the F_{400}/F_{500} Ca^{2+} emission responses of arteries upon washout of 100mM KPSS. A) The time for arteries isolated from PMCA4 WT $^{(+/+)}$ and KO $^{(-/-)}$ mice pre-constricted to 100mM KPSS to relax by 50% upon PSS washout ($T_{1/2}$ relaxation) and B) the time for the maximum F_{400}/F_{500} Ca^{2+} emission ratio displayed in the same vessels to decrease by 50% upon 100mM KPSS washout. Data presented as mean $\pm$ SEM. Not significant, unpaired student's t test.

3.6.4 Effects on elevation of $[Ca^{2+}]_i$ in response to noradrenaline

An increased F_{400}/F_{500} Ca^{2+} emission ratio and maintained constriction were observed following stimulation of pressurised arteries with $3x10^{-5}$M noradrenaline. Similar to the results from KPSS stimulation, PMCA4 ablation did not affect the magnitude of constrictions or the change in F_{400}/F_{500} Ca^{2+} emission ratio (constriction as % normalised to starting diameter = PMCA4 KO $^{(-/-)}$ 64.80 ± 4.55% (n=6) and WT $^{(+/+)}$ 60.75 ± 8.29% (n=6), NS; and the Δ in F_{400}/F_{500} Ca^{2+} emission ratio = PMCA4 KO $^{(-/-)}$ 0.16 ± 0.03 (n=6) and WT $^{(+/+)}$ 0.18 ± 0.02 (n=6), NS) (figure 3.6.4.2).

Noradrenaline induced elevations in the F_{400}/F_{500} Ca^{2+} emission ratio reached the maximum prior to achievement of maximal arterial constrictions. There was no significant modulation in the time difference between the initial rise in F_{400}/F_{500} Ca^{2+} emission ratio and start of noradrenaline induced constriction by ablation of PMCA4 (time difference for PMCA4 KO $^{(-/-)}$ = 16.00 ± 4.13 seconds (n=6) and for WT $^{(+/+)}$ = 11.47 ± 1.61 seconds (n=6), NS).

PMCA4 ablation also did not modulate the time for arteries to increase F_{400}/F_{500} Ca^{2+} emission ratio to maximum when stimulated by noradrenaline (time for maximal increase in F_{400}/F_{500} Ca^{2+} emission ratio upon noradrenaline stimulation = PMCA4 KO $^{(-/-)}$ 164.20 ± 31.07 seconds (n=6) and WT $^{(+/+)}$ 160.73 ± 11.83 seconds (n=6), NS) (figure 3.6.4.3). Neither did PMCA4 ablation have any effect on the time for arteries to reach maximal constriction (i.e. T constriction) to noradrenaline (T constriction = PMCA4 KO $^{(-/-)}$ 200.80 ± 32.21 seconds (n=6), WT $^{(+/+)}$ 191.20 ± 16.94 seconds (n=6), NS, upon noradrenaline stimulation) (figure 3.6.4.3).

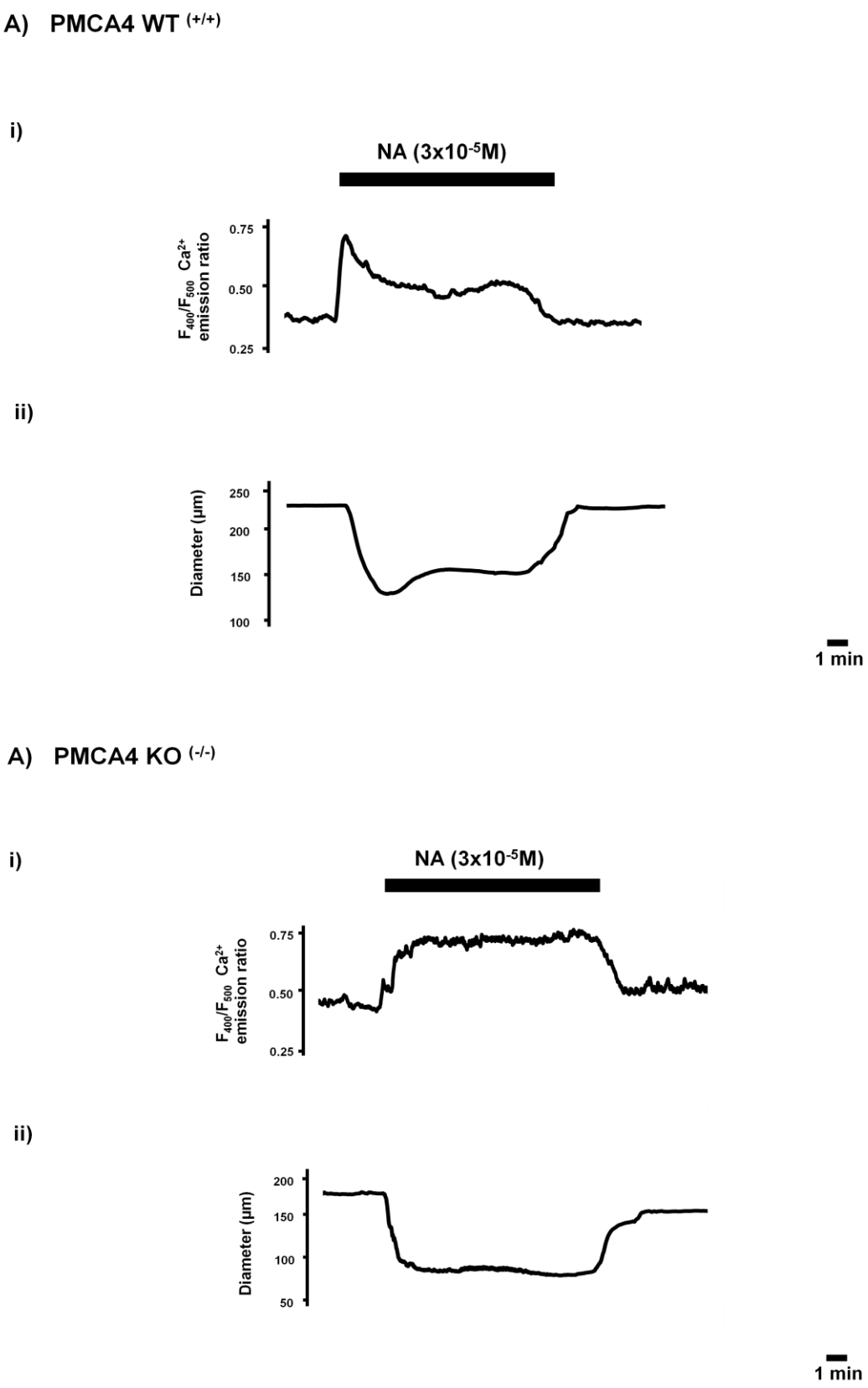

Figure 3.6.4.1: Experimental trace recordings of pressurised arteries simultaneously displaying changes in the F_{400}/F_{500} Ca^{2+} emission ratio & diameter in response to noradrenaline. Data was recorded by WINDAQ data acquisition software. Elevations in the F_{400}/F_{500} Ca^{2+} emission ratio preceded arterial constrictions to $3x10^{-5}$M noradrenaline shown in an artery from A) a PMCA4 WT $^{(+/+)}$ mouse and B) that from a PMCA KO $^{(-/-)}$ mouse.

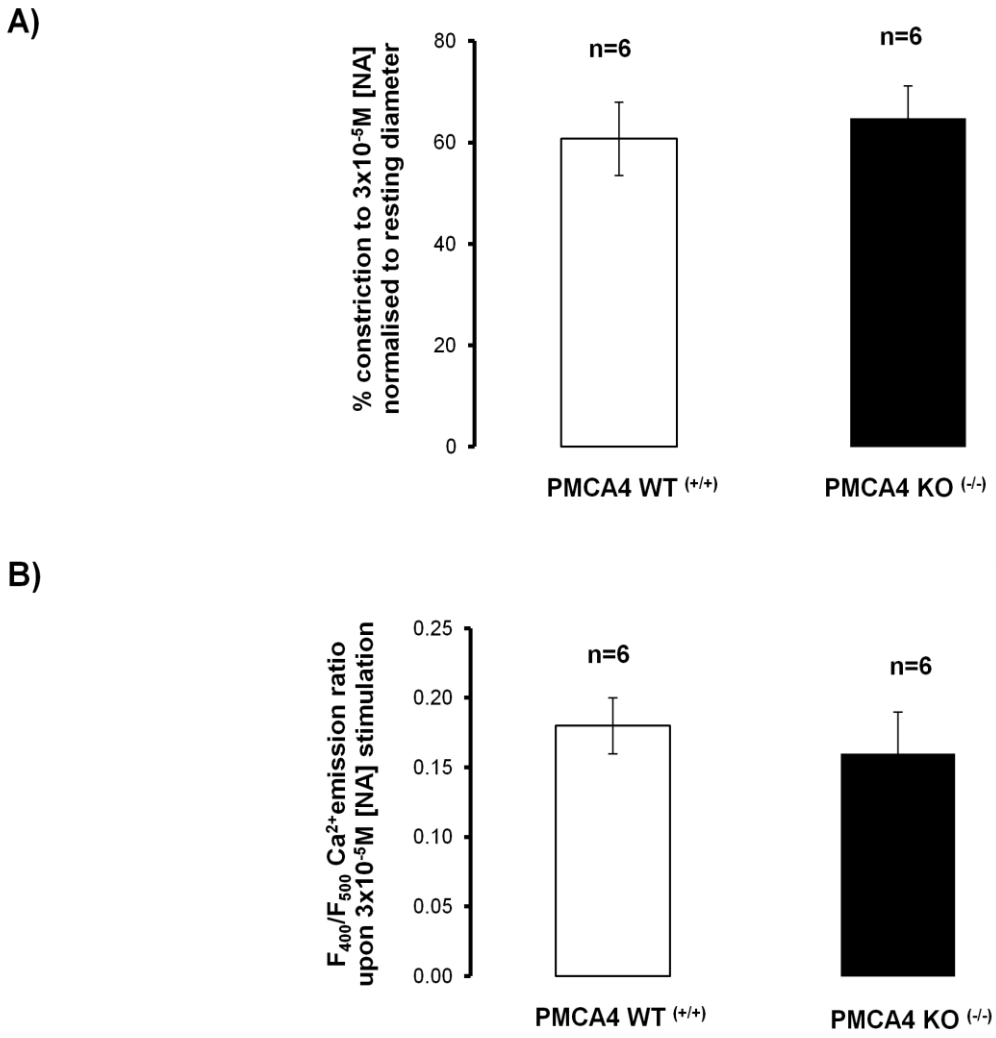

Figure 3.6.4.2: Effects of PMCA4 ablation on arterial constrictions and on the F_{400}/F_{500} Ca^{2+} emission responses to noradrenaline. A) Contractile arterial responses (as % of resting diameter) induced by $3x10^{-5}$M noradrenaline and B) differences in the F_{400}/F_{500} Ca^{2+} emission ratio, (representing global $[Ca^{2+}]_i$) as was present in arteries from PMCA4 WT $^{(+/+)}$ compared to arteries from KO $^{(-/-)}$ mice. Results presented as mean ± SEM. No significant difference apparent according to unpaired student's t test.

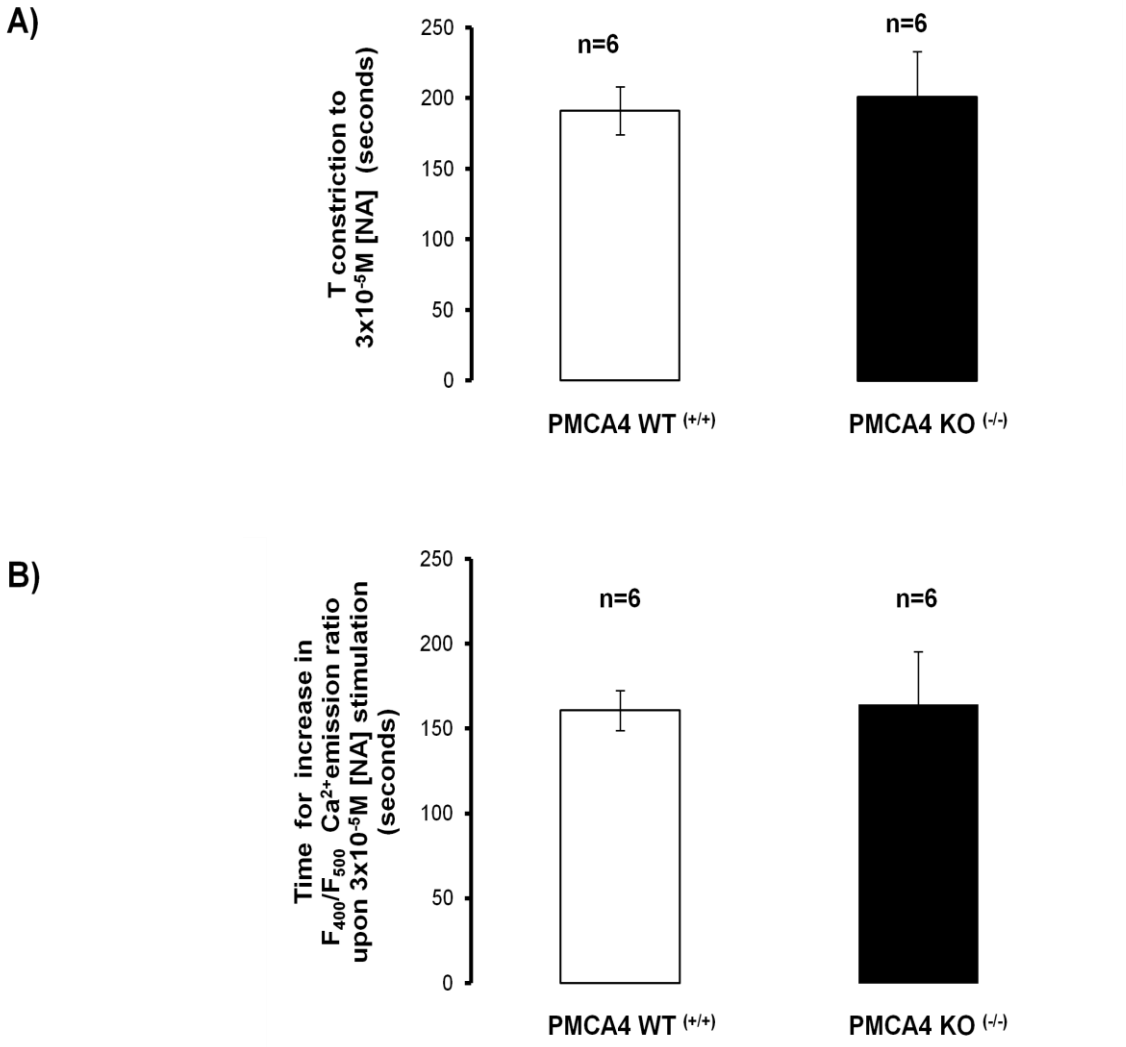

Figure 3.6.4.3: Effects of PMCA4 ablation on the constriction time and on the time for increase in the F_{400}/F_{500} Ca^{2+} emission responses of arteries to noradrenaline. A) The T constriction (i.e. the time in seconds to achieve stable maximum constriction) and B) time for increase in the F_{400}/F_{500} Ca^{2+} emission ratio to $3x10^{-5}$M noradrenaline, as displayed by arteries from PMCA4 WT $^{(+/+)}$ in comparison with KO $^{(-/-)}$ mice. Data presented as mean ± SEM. Not significant according to unpaired student's t test.

The relaxation times observed for arteries to return to stable resting diameters (i.e. the T and $T_{1/2}$ relaxation times) following the washout of noradrenaline were unaltered by the ablation of PMCA4 (T relaxation = PMCA4 KO $^{(-/-)}$ 251.20 ± 23.38 seconds (n=6), WT $^{(+/+)}$ 245.43 ± 9.09 seconds (n=6), NS; and $T_{1/2}$ relaxation after noradrenaline washout = PMCA4 KO $^{(-/-)}$ 108.60 ± 17.40 seconds (n=6), WT $^{(+/+)}$ 103.93 ± 9.70 seconds (n=6), PMCA4 KO $^{(-/-)}$, NS) ($T_{1/2}$ relaxation times shown in figure 3.6.4.4).

Decrease in the F_{400}/F_{500} Ca^{2+} emission ratio as a result of noradrenaline washout was analogous between arteries from PMCA4 KO $^{(-/-)}$ and WT $^{(+/+)}$ mice (time for decrease in F_{400}/F_{500} Ca^{2+} emission ratio upon noradrenaline washout = PMCA4 KO $^{(-/-)}$ 223.53 ± 21.51 seconds (n=6), WT $^{(+/+)}$ 212.03 ± 10.82 seconds (n=6), NS; and for the $T_{1/2}$ (i.e. the time for the maximum F_{400}/F_{500} Ca^{2+} emission ratio to decrease by 50%) upon noradrenaline washout = PMCA4 KO $^{(-/-)}$ 112.00 ± 10.31 seconds (n=6), WT $^{(+/+)}$ 110.00 ± 14.09 seconds (n=6), NS) (figure 3.6.4.4).

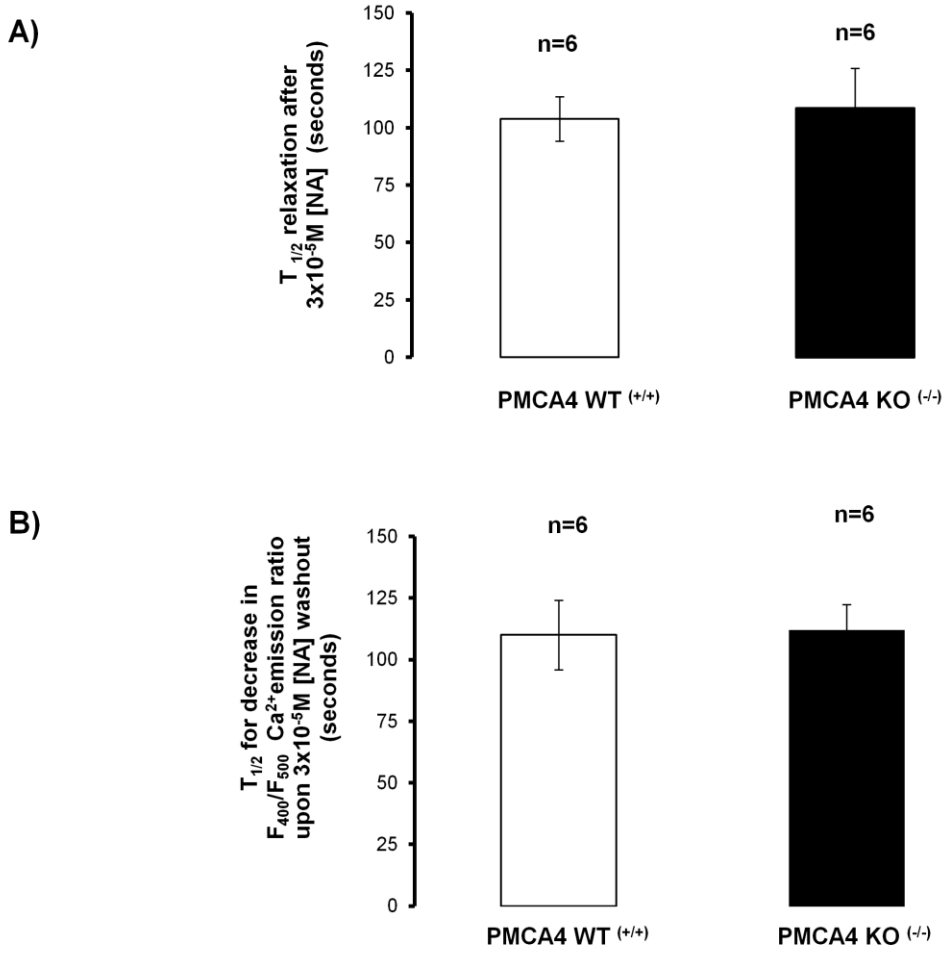

Figure 3.6.4.4: Effects of PMCA4 ablation on $T_{1/2}$ relaxation times and on the $T_{1/2}$ for decrease in the F_{400}/F_{500} Ca^{2+} emission responses of arteries upon washout of noradrenaline. A) The $T_{1/2}$ relaxation (the time in seconds for pre-constricted arteries to relax by 50% following washout of $3x10^{-5}$M noradrenaline) and B) $T_{1/2}$ (the time for the maximum F_{400}/F_{500} Ca^{2+} emission ratio in the same vessels to decrease by 50%) upon $3x10^{-5}$M noradrenaline washout, as exhibited in arteries from PMCA4 WT $^{(+/+)}$ mice compared with KO $^{(-/-)}$ mice. Data presented as mean ± SEM. No significant difference, according to unpaired student's t test.

3.7 Effects of PMCA4 ablation on passive arterial properties

In order to investigate whether the ablation of PMCA4 had effect(s) on the structural and/or on the passive characteristics of mesenteric resistance arterial walls, isolated vessels were pressurised across nine cumulative transmural pressures (between 5 to 140 mmHg) in a Ca^{2+} free PSS solution.

PMCA4 ablation had no effect on the passive arterial diameter, wall thickness, wall to lumen ratio or cross sectional area (CSA) of third order mesenteric arteries when isolated and pressurised mesenteric resistance arteries were fully dilated in a Ca^{2+} free solution (figure 3.7.1).

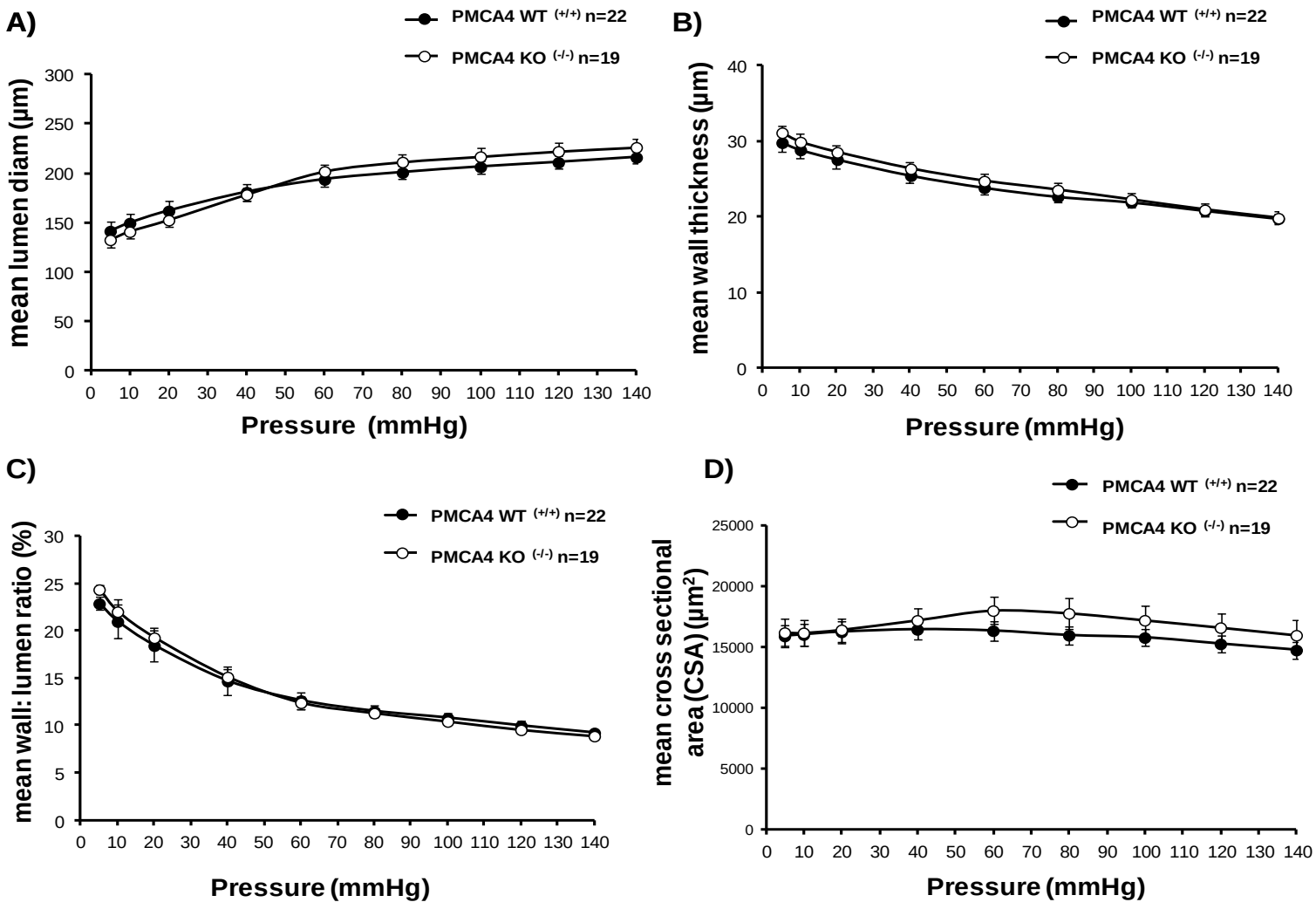

Figure 3.7.1: Passive arterial properties of mesenteric resistance arteries isolated from PMAC4 WT $^{(+/+)}$ and KO $^{(-/-)}$ mice. The mean lumen diameter in A), the mean wall thickness in B), the mean wall to lumen ratio in C), and the mean cross sectional area to pressure relationship in D) were similar in arteries from PMAC4 KO $^{(-/-)}$ compared with those from WT $^{(+/+)}$ mice. Data expressed as mean ± SEM. No significant difference was observed according to repeated measurements analysis of variance.

A leftwards shift in the stress to strain relationship was seen in arteries from PMCA4 KO $^{(-/-)}$ compared with arteries from WT $^{(+/+)}$ mice (figure 3.7.2). The mean elastic modulus (β) was significantly greater in arteries from PMCA4 KO $^{(-/-)}$ mice than those from WT $^{(+/+)}$ mice (PMCA4 KO $^{(-/-)}$ 10.03 ± 2.0 (n=19), WT $^{(+/+)}$ 5.75 ± 0.64 (n=21), $p<0.05$, according to an unpaired student's t test). Taken together these are indicative of decreased vessel distensibility in mesenteric resistance arteries from PMCA4 KO $^{(-/-)}$ mice.

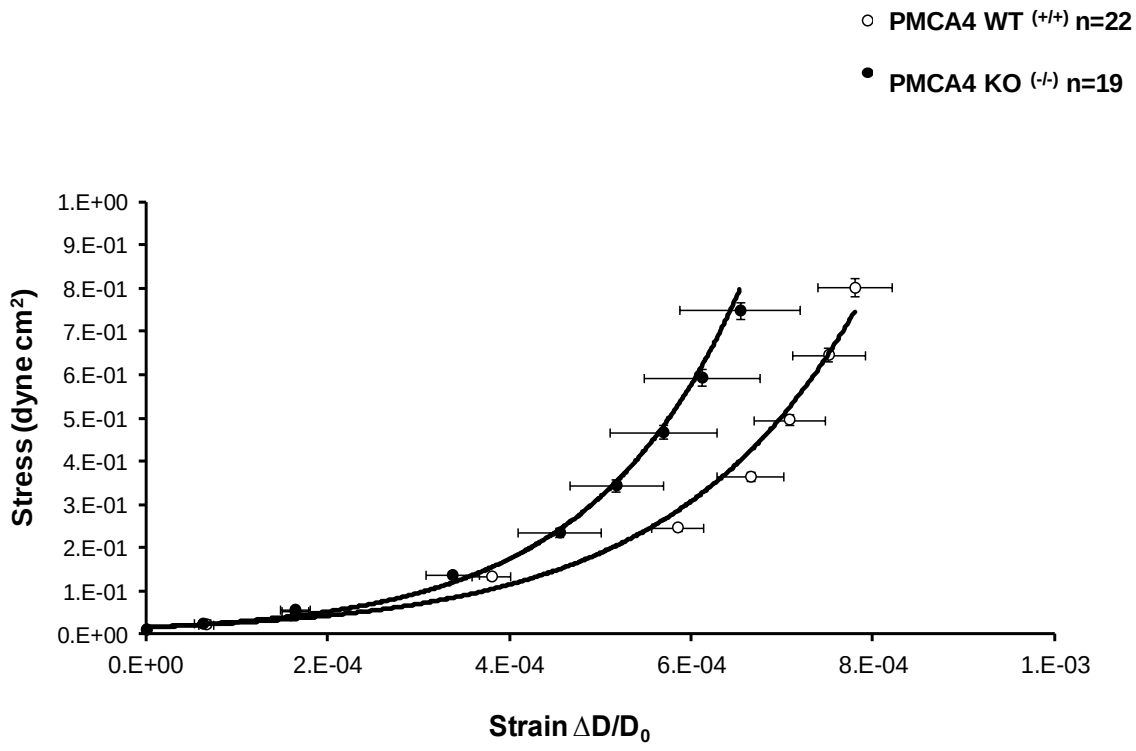

Figure 3.7.2: Effect of PMCA4 ablation on the stress, strain relationship of pressurised mouse mesenteric arteries. The stress (dyne cm^2), strain ($(D-D_0)/D_0$ (where D is diameter at each pressure and D_0 is diameter at 5 mmHg)) relationship of isolated and pressurised mesenteric resistance arteries from PMAC4 KO $^{(-/-)}$ mice was shifted to the left in comparison to the stress, strain relationship of arteries from WT $^{(+/+)}$ mice.

3.8 What are the effects of PMCA4 inhibition with AP2 on arterial contractility?

3.8.1 In response to high potassium solution (KPSS)

To investigate whether the inhibition of PMCA4 with the novel inhibitor AP2 had any effect on arterial contractility pressurised mesenteric arteries isolated from WT $^{(+/+)}$ mice were incubated for 30 minutes with/without 10µM of AP2.

In contrast to the effects of PMCA4 ablation, inhibition of PMCA4 with AP2 did modulate the contractility of isolated mesenteric arteries from WT $^{(+/+)}$ mice to depolarisation with KPSS. Incubation of arteries from WT $^{(+/+)}$ mice with 10µM AP2, significantly attenuated the contractile response to 100mM KPSS (constriction (as a % of starting diameter) = 69.1 ± 3.55% (n=8) and 53.5 ± 4.96% (n=9) in the absence and presence of AP2 respectively, $p<0.05$) (figure 3.8.1.1).

The contractile response of arteries from WT $^{(+/+)}$ mice to 40mM KPSS were not significantly reduced after incubation with 10µM of AP2 (constriction (as a % of starting diameter) = 53.4 ± 3.84% (n=8) in the absence of AP2 and 44.1 ± 5.38% (n=9) in the presence of AP2, NS) (figure 3.8.1.1).

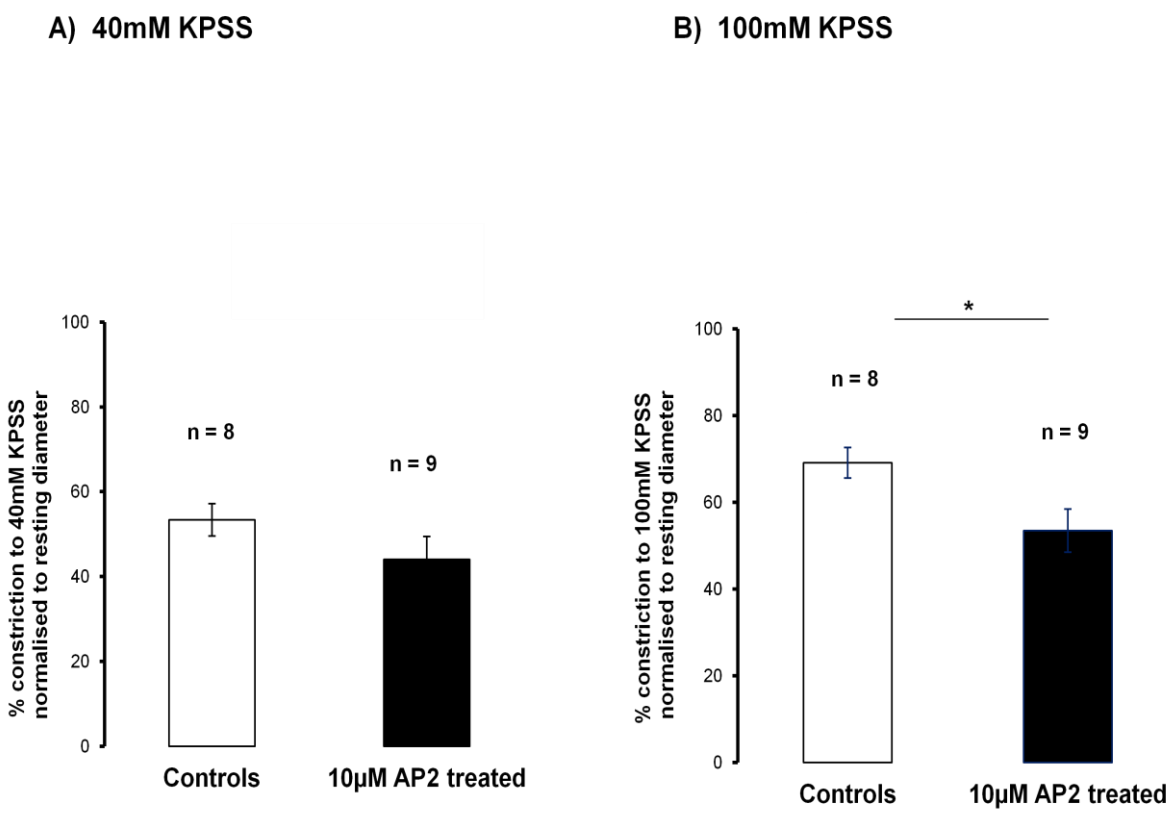

Figure 3.8.1.1: Effects of AP2 (10μM) on mesenteric arterial constrictions in response to 40mM & 100mM KPSS. The contractile response (as % of starting diameter) of isolated, pressurised mesenteric resistance arteries from WT $^{(+/+)}$ mice to A) 40mM and to B) 100mM KPSS stimulations. Data expressed as mean ± SEM. The arterial contractile response was significantly attenuated in the case of B) 100mM KPSS (* is $p<0.05$), according to an unpaired student's t test.

The relaxation times noted for mesenteric arteries to return to starting diameters (defined as T and $T_{1/2}$ relaxation) achieved by vessels from WT $^{(+/+)}$ mice after 40mM or 100mM KPSS washouts were not significantly altered after incubation with 10μM AP2. (T relaxation after 40mM KPSS washout = 175.4 ± 21.8 seconds (n=8) and 170.3 ± 21.4 seconds (n=9); and $T_{1/2}$ relaxation after 40mM KPSS washout = 41.3 ± 9.2 seconds (n=8) and 36.6 ± 6.6 seconds (n=9), in the absence and presence of 10μM AP2 respectively, NS, (not shown); the T relaxation after washout of 100mM = 215.5 ± 18.3 seconds (n=8) and 213.1 ± 25.4 seconds (n=9), and $T_{1/2}$ relaxation after washout of 100mM = 53.9 ± 7.5 seconds (n=8) and 42.9 ± 9.0 seconds (n=9) in the absence and presence of 10μM AP2 respectively, NS) (figure 3.81.2).

The effects of a lower concentration of AP2 (1μM) on the contractile function of mesenteric resistance arteries from WT $^{(+/+)}$ mice was also examined. The contractile responses observed to both 40mM and 100mM KPSS stimulations were not significantly decreased after incubation of arteries with 1μM AP2 (constriction (as a % of starting diameter) to 40mM KPSS = 55.6 ± 3.36% (n=11) and 47.2 ± 4.27% (n=4) in the absence and presence of AP2 respectively, NS) and to 100mM KPSS = 69.1 ± 2.97% (n=11) and 61.0 ± 6.02% (n=4) in the absence and presence of AP2 respectively, NS) (figure 3.8.1.3).

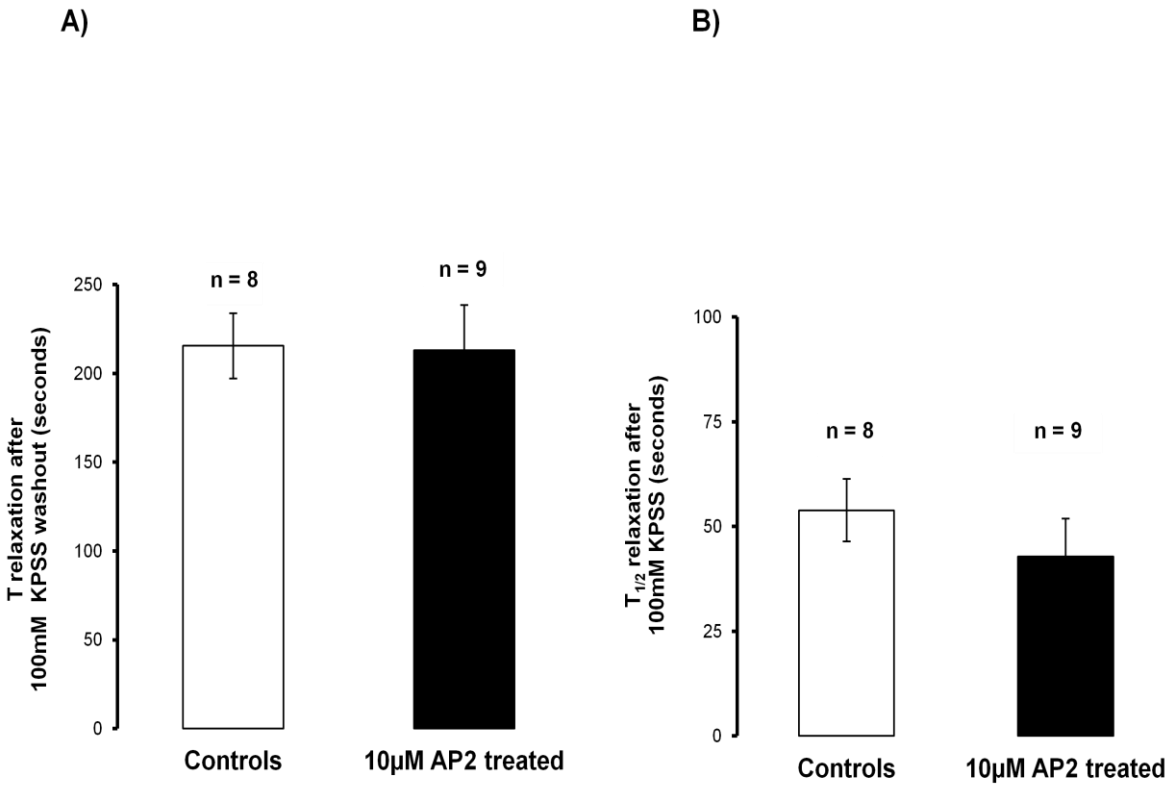

Figure 3.8.1.2: Effect of AP2 (10μM) on relaxation times of mesenteric arteries upon washout of 100mM KPSS. A) T relaxation (T = time (seconds) pressurised arteries pre-constricted with 100mM KPSS to return to resting diameter following washout with PSS) and B) $T_{1/2}$ relaxation (the time in seconds for arteries pre-constricted with 100mM KPSS to relax by 50% upon washout with PSS). Data presented as mean ± SEM. No significant difference between arteries incubated with 10μM AP2 compared to control vessels, unpaired student's t test. Time zero was taken from the beginning of the relaxation.

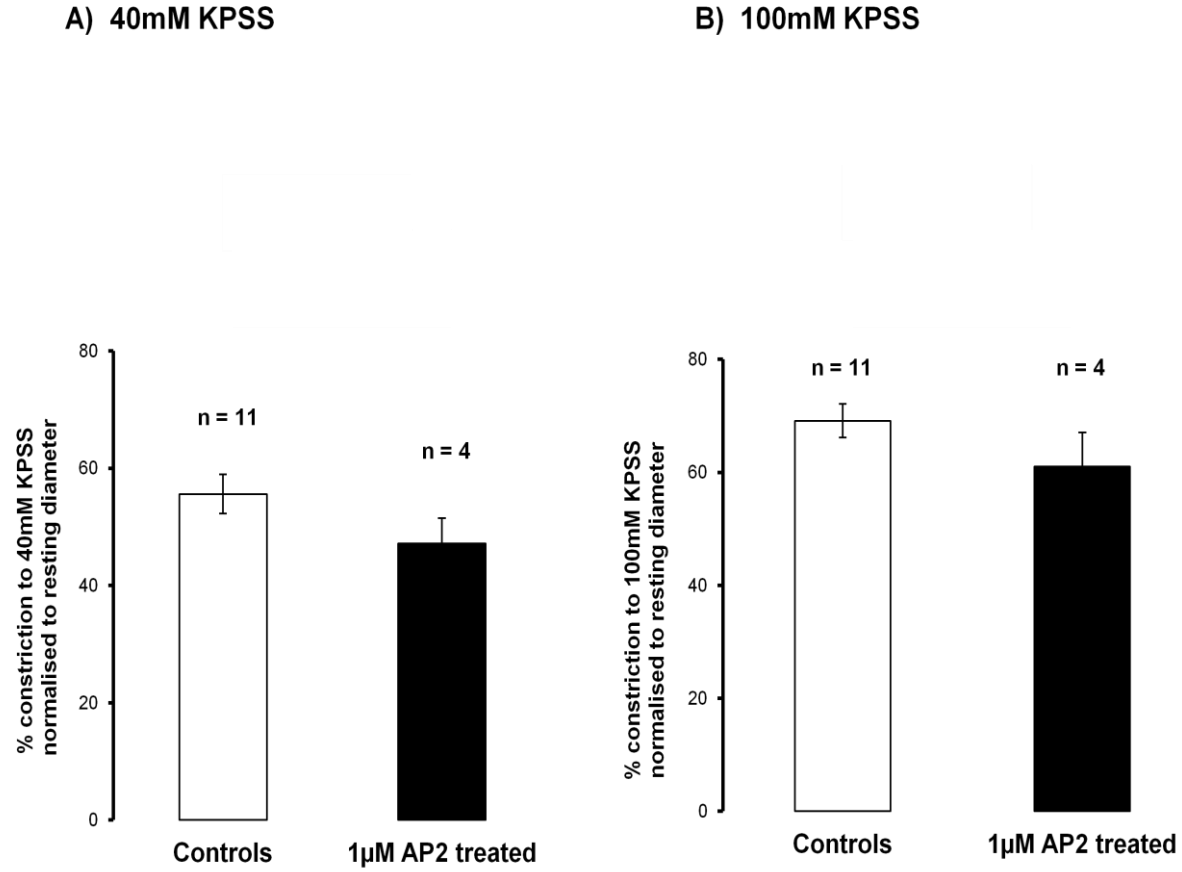

Figure 3.8.1.3: Effects of AP2 (1µM) on mesenteric arterial constrictions in response to 40mM & 100mM KPSS. Contractile responses (as % of starting diameter) of isolated arteries from WT $^{(+/+)}$ mice to A) 40mM and to B) 100mM KPSS stimulations in the presence and absence of 1µM AP2. Data presented as mean ± SEM. No significant difference according to an unpaired student's t test.

Unfortunately, due to technical difficulties in retrieving a few trace recorded files of the 1μM AP2 experiments the relaxation times (i.e. T and $T_{½}$ relaxations) of arteries isolated from WT $^{(+/+)}$ mice could not be calculated.

3.8.2 In response to noradrenaline (NA)

Further studies examined the effect of PMCA4 inhibition with AP2 on mouse mesenteric arterial contractility to cumulative doses of noradrenaline.

Incubation with 10μM AP2 significantly reduced constriction of arteries from WT $^{(+/+)}$ mice to noradrenaline (maximal response (as a % of starting diameter) to noradrenaline = 78.50 ± 2.29% (n=8) and 61.77 ± 4.00% (n=8) in the absence of and presence of AP2 respectively, $p<0.05$) (figure 3.8.2.1).

A reduction in the constriction to noradrenaline was also observed following incubation of arteries from WT $^{(+/+)}$ mice with a lower dose (1μM) of AP2 (max constriction = 78.60 ± 2.02% (n=11) and 61.69 ± 4.29% (n=3) in the absence of and presence of AP2 respectively, $p<0.05$) (figure 3.8.2.1).

A)

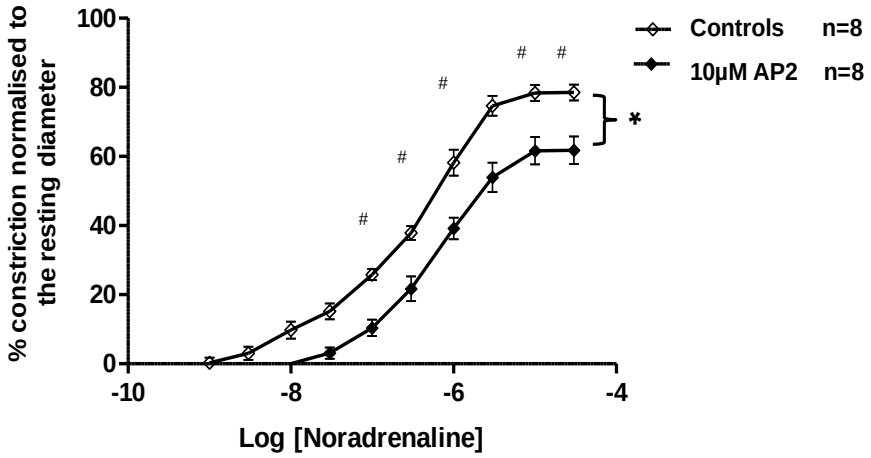

B)

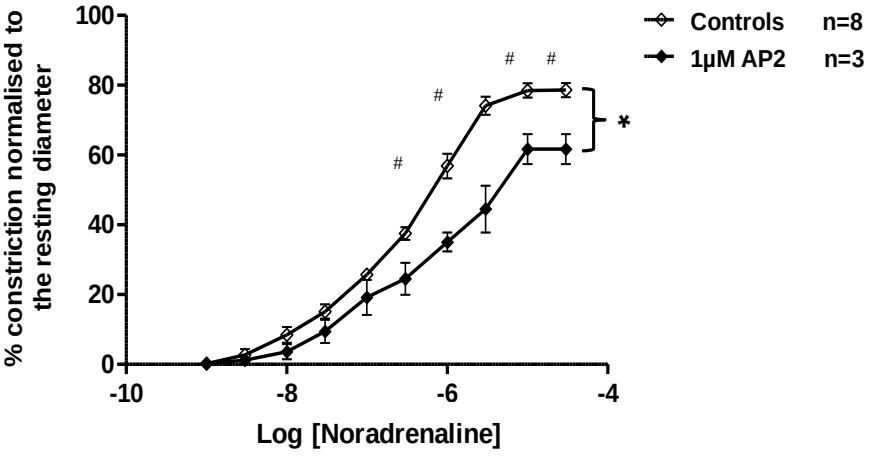

Figure 3.8.2.1: Effect of AP2 on arterial constrictions in response to noradrenaline. Constrictions (as a % of the starting diameter) of isolated and pressurised mesenteric arteries from WT $^{(+/+)}$ mice to cumulative concentrations of noradrenaline (Log[NA] -9.0 to -4.5 M) following incubation without and with A) 10µM AP2 or with B) 1µM AP2 were significantly reduced compared to controls. Data presented as mean ± SEM and * is $p<0.05$, according to repeated measures, ANOVA. Analysis by the bonferroni post test revealed levels of significance (# is $p<0.05$) at the following Log[NA] -4.0, -4.5, -5.0, -5.5 and -6.0 M present in A) and B).

3.9 Effects of AP2 on arteries isolated from PMCA4 KO $^{(-/-)}$ mice

In order to examine whether the novel inhibitor AP2 had an effect on the contractility of vessels in which PMCA4 had been ablated mesenteric arteries were isolated from PMCA4 KO $^{(-/-)}$ mice and incubated with 10μM of AP2 for 30 minutes.

Incubation with AP2 had no significant effect on arterial constrictions to either KPSS or noradrenaline displayed by arteries from PMCA4 KO $^{(-/-)}$ mice (constrictions (as % of resting diameter) to 40mM KPSS = 53.0 ± 4.1% (n=8) in absence of AP2 and 45.0 ± 3.0% (n=6) in the presence of AP2, NS; to 100mM KPSS = 77.3 ± 2.7% (n=8) in absence of AP2 and 74.1 ± 3.4% (n=6) in the presence of AP2, NS; and the maximal response (as a % of starting diameter) to noradrenaline = 74.5 ± 2.7% (n=8) and 73.1 ± 3.1% (n=6) in the absence of and presence of AP2 respectively, NS) (figures 3.9.0.1 & 3.9.0.2).

.

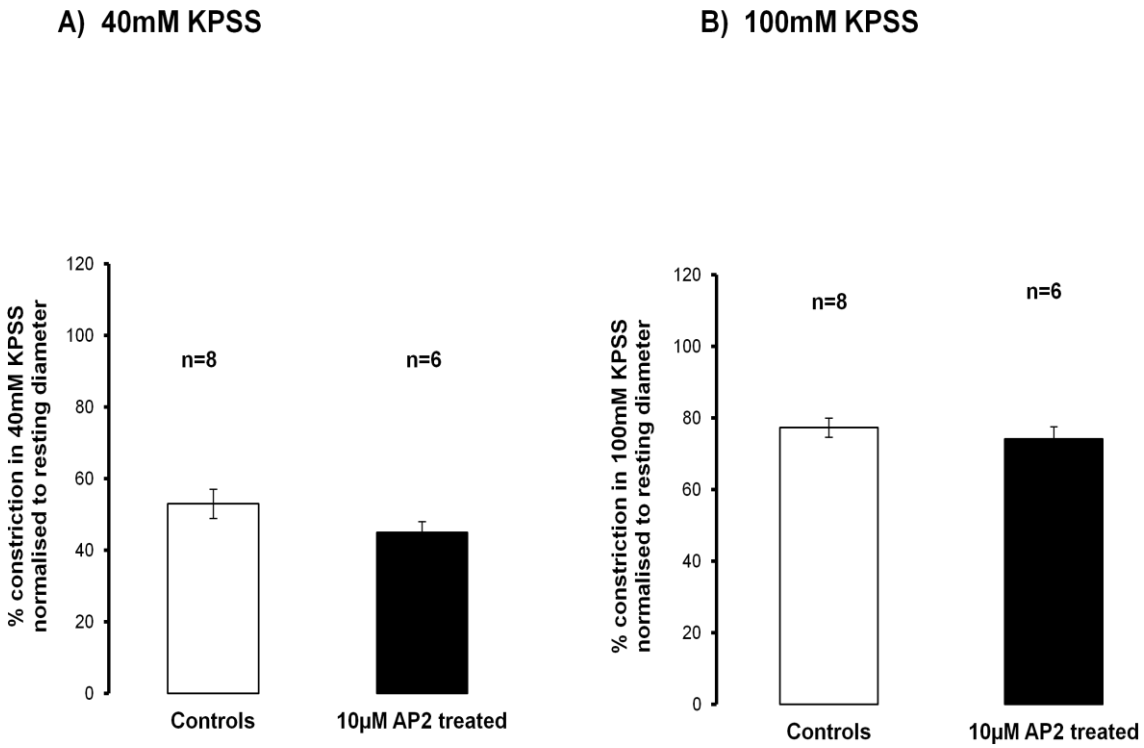

Figure 3.9.0.1: Effects of AP2 (10µM) on the contractility of mesenteric arteries from PMCA4 ablated mice in response to 40mM & 100mM KPSS. Constrictions (expressed as % of starting diameter) of isolated arteries from PMCA4 KO $^{(-/-)}$ mice in response to A) 40mM and to B) 100mM KPSS in the absence and presence of 10µM AP2 treatment. Data presented as mean ± SEM. No significant difference, according to unpaired student's t test.

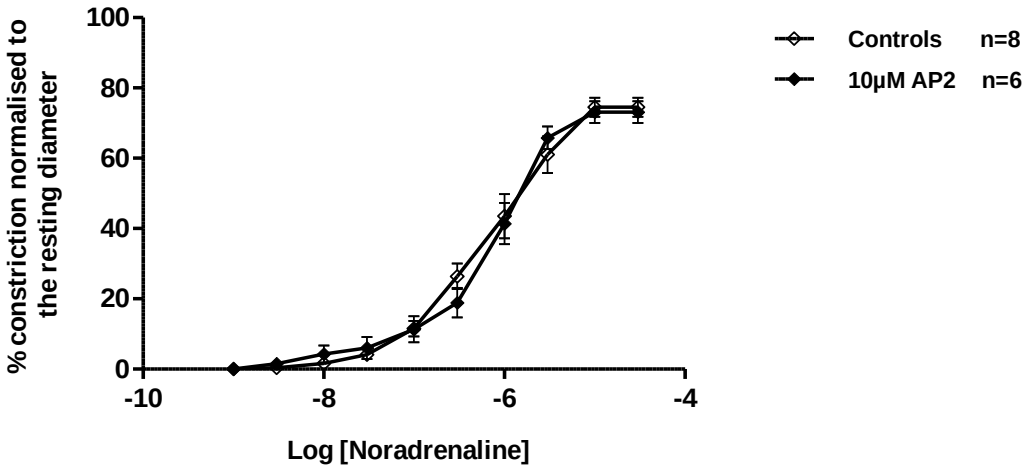

Figure 3.9.0.2: Effect of AP2 (10µM) on contractility of mesenteric arteries from PMCA4 ablated mice in response to noradrenaline. The contractile response (as a % of the starting diameter) of mesenteric arteries from PMCA4 KO $^{(-/-)}$ mice to cumulative concentrations of noradrenaline (Log [NA] -9.0 to -4.5 M) after incubation in the absence and presence of 10µM AP2. Data presented as mean ± SEM. Analysis by repeated measures, ANOVA found no significant difference.

3.10 What is the mechanism via which inhibition of PMCA4 with AP2 reduces contractility of mesenteric resistance arteries isolated from WT $^{(+/+)}$ mice?

Previously, studies using arteries isolated from mice which overexpress PMCA4 have shown that arterial contractility is enhanced by nNOS-dependent mechanisms (Schuh et al., 2003; Gros et al., 2003). To explore whether the reduced arterial contractility observed in the present study with PMCA4 inhibition by AP2 is NO-dependent, the effects of AP2 were examined in the absence and presence of both LNNA and Vinyl-L-Nio (VLN) to inhibit all NOS and nNOS respectively.

AP2 (10 µM) had no significant effect on contractile responses of arteries from WT $^{(+/+)}$ mice to 100mM KPSS when NOS was inhibited with LNNA (i.e. following simultaneous incubation with AP2 and LNNA) (constriction (as a % of starting diameter) = 69.1 ± 3.55% (n=8) in the absence of AP2, 53.5 ± 4.96% (n=9) and 71.5 ± 4.85% (n=8) in the presence of AP2 and AP2+LNNA respectively (controls vs AP2, $p<0.05$; controls vs AP2+LNNA, NS) (figure 3.10.1).

Similarly, AP2 in the presence of LNNA did not affect the contractile function of arteries from WT $^{(+/+)}$ mice in response to 40mM KPSS (constriction (as a % of starting diameter) = 53.4 ± 3.84% (n=8) in the absence of AP2, and 61.5 ± 2.14% (n=8) in the presence of AP2+LNNA, NS; contraction in the absence of AP2 = 44.1 ± 5.38% (n=9), NS) (figure 3.10.1).

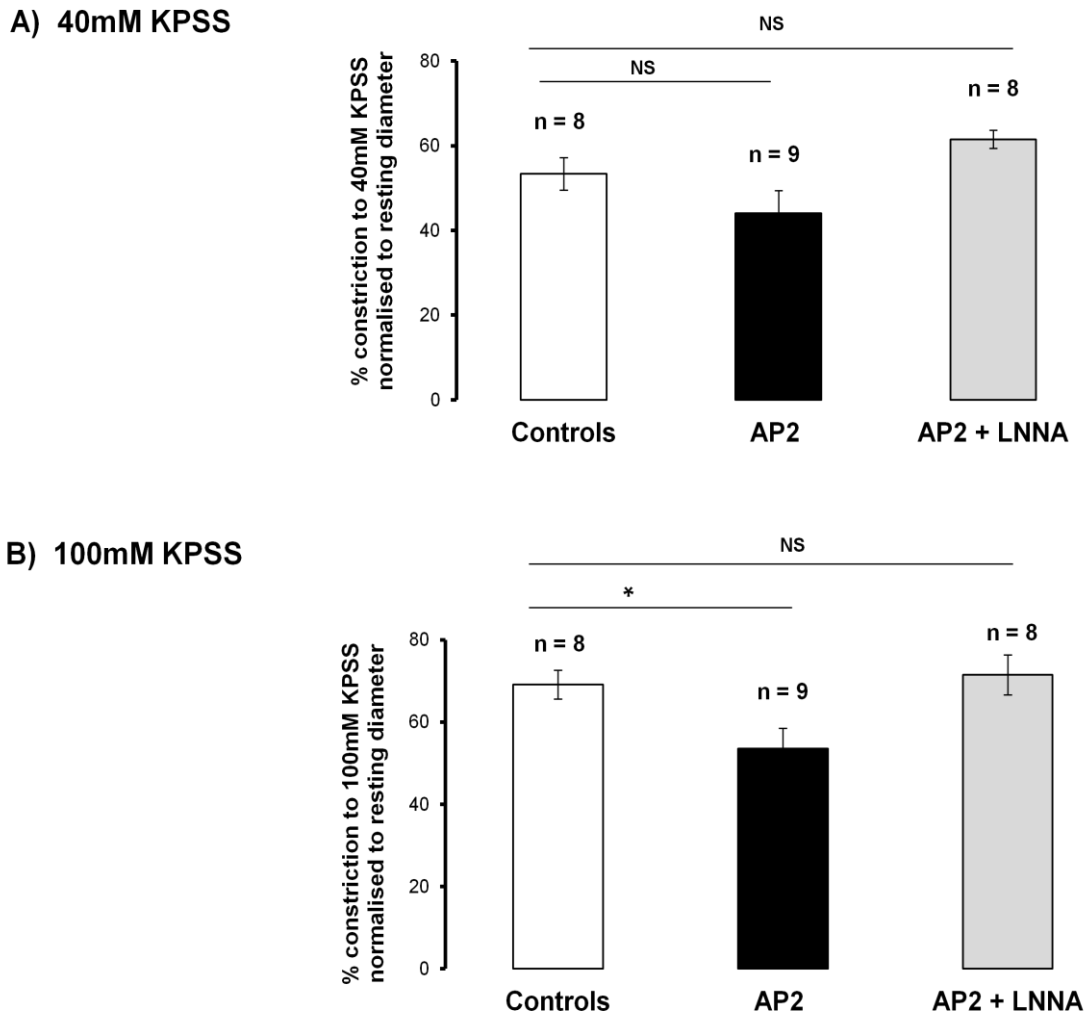

Figure 3.10.1: Effects of AP2 & AP2+LNNA on mesenteric arterial constrictions in response to 40mM & 100mM KPSS. Constriction of mesenteric resistance arteries from WT $^{(+/+)}$ mice to A) 40mM KPSS and to B) 100mM KPSS following vessel incubation in PSS (controls), in 10µM AP2 and in the presence of 10µM AP2 and 100µM LNNA. Reduced constriction of AP2 treated arteries to B) 100mM KPSS was not present in vessels treated with AP2+LNNA. Data presented as mean ± SEM, significant differences $p<0.05$ are shown as * and not significant differences as NS, according to statistical analysis via unpaired student's t test.

AP2 had no effect on constriction of arteries from WT $^{(+/+)}$ mice to noradrenaline in the presence of LNNA (maximal response (as a % of starting diameter) = 78.50 ± 2.29% (n=8) in the absence of AP2 and 70.48 ± 2.23% (n=8) in the presence of AP2+LNNA respectively, NS) (figure 3.10.2). The significant reduction in noradrenaline induced constriction after 10μM AP2 incubation was not present after simultaneous AP2 and LNNA incubation of arteries.

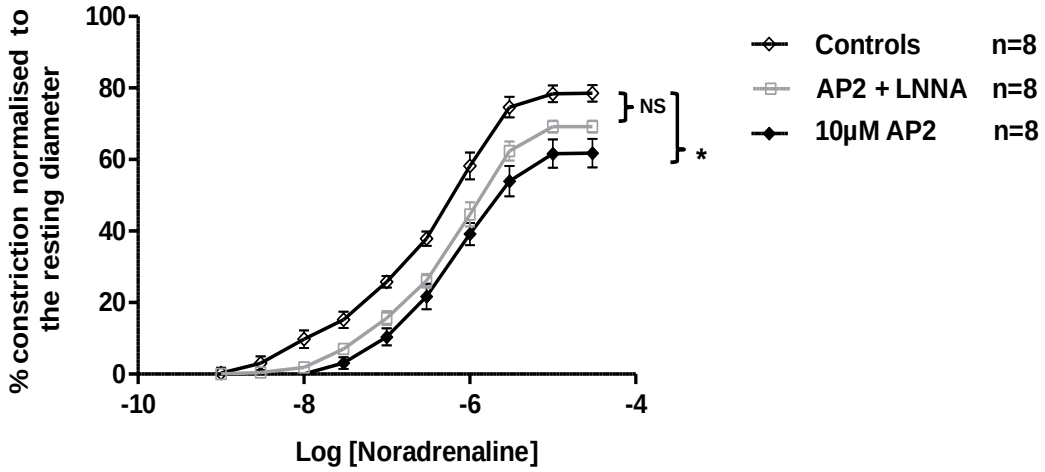

Figure 3.10.2: Effects of AP2 & AP2+LNNA on mesenteric arterial constrictions in response to noradrenaline. Constrictions to noradrenaline (Log[NA] -9.0 to -4.5 M) as exhibited by untreated, 10µM AP2 treated and 10µM and 100µM LNNA simultaneously treated arteries from WT $^{(+/+)}$ mice. The significantly reduced constriction (* is $p<0.05$) of arteries isolated from WT $^{(+/+)}$ mice to cumulative concentrations of noradrenaline (Log[NA] -9.0 to -4.5 M) as a result of 10µM AP2 incubation was not present following incubation of arteries with 100µM LNNA in the presence of AP2. Data expressed as mean ± SEM. Analysis by repeated measures, ANOVA showed no significant difference between response of arteries after AP2 and AP2+LNNA incubation.

Inhibition of nNOS by Vinyl-L-Nio (VLN) also abolished the significant effect of AP2 on 100mM KPSS induced constrictions of arteries from WT $^{(+/+)}$ mice (constriction (as a % of starting diameter) to 100mM KPSS = 69.1 ± 3.55% (n=8) in the absence of AP2 and 53.5 ± 4.96% (n=9) in the presence of AP2, $p<0.05$) after incubation of vessels with AP2 in the presence of VLN (constriction (as a % of starting diameter) = 69.1 ± 3.55% (n=8) in the absence of AP2 and 79.2 ± 2.62% (n=5) in the presence of AP2+VLN respectively, NS) (figure 3.10.3).

Constrictions of arteries to 40mM KPSS were not significantly different from control or AP2 incubated arteries in the presence of AP2 and VLN (constriction (as a % of starting diameter) = 53.4 ± 3.84% (n=8) in the absence of AP2 and 62.9 ± 4.15% (n=5) in presence of AP2+VLN, NS) (figure 3.10.3).

AP2 also had no significant effect on the contractile response of arteries from WT $^{(+/+)}$ mice to noradrenaline when nNOS was inhibited by VLN (maximal response to noradrenaline (as a % of starting diameter); 78.50 ± 2.29% (n=8) in the absence of AP2 and 75.18 ± 1.31% (n=5) in the presence of AP2+VLN respectively, NS) (figure 3.10.4).

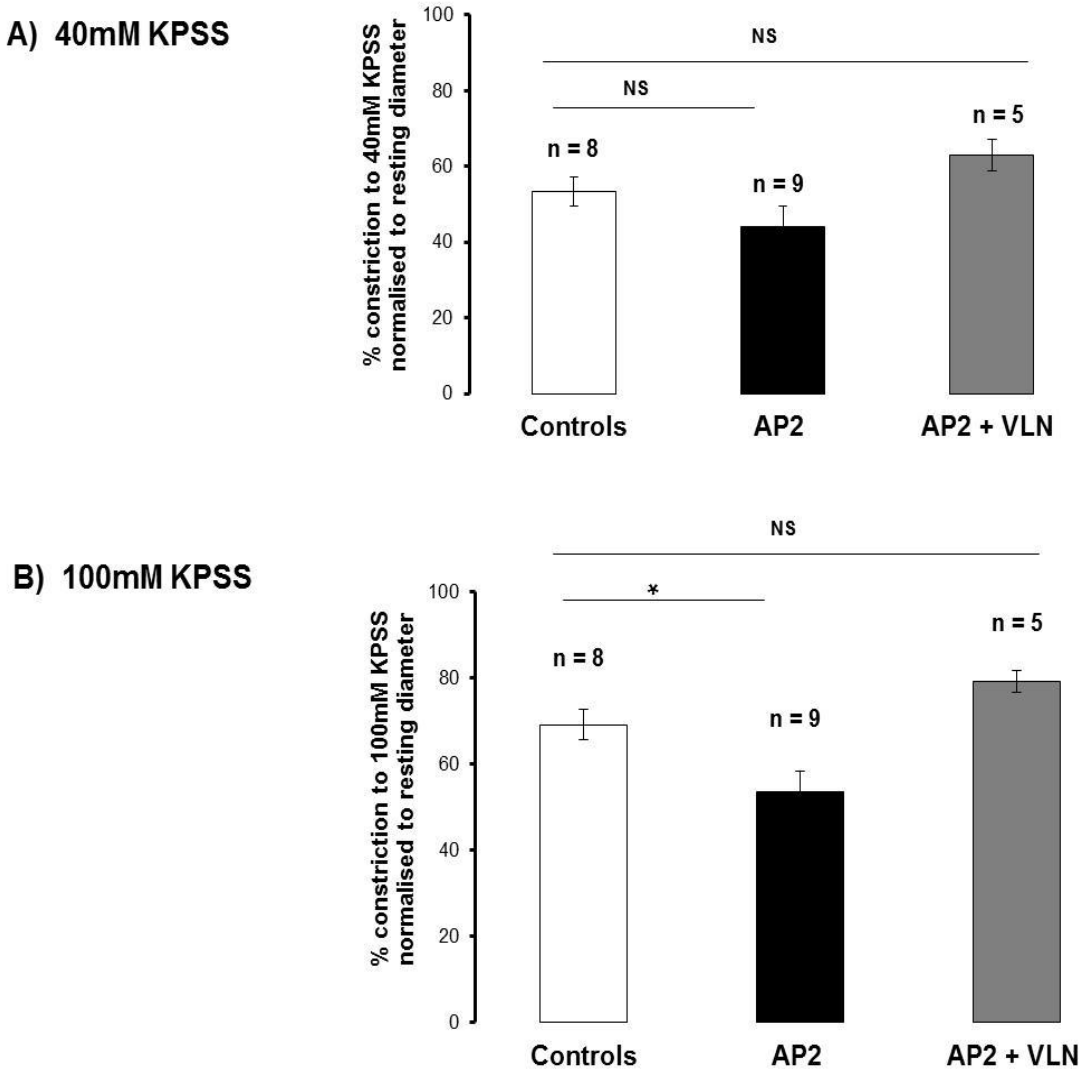

Figure 3.10.3: Effects of AP2 & AP2+Vinyl-L-Nio (VLN) on mesenteric arterial constrictions in response to 40mM & 100mM KPSS. Arterial constrictions of mesenteric arteries from WT $^{(+/+)}$ mice in response to A) 40mM KPSS and B) 100mM KPSS following incubations with PSS (controls), 10µM AP2 and 10µM VLN in the presence of 10µM AP2. Reduced constriction of AP2 treated arteries to B) 100mM KPSS was not present in vessels treated with AP2 + VLN. Data is expressed as mean ± SEM, * is $p<0.05$ and NS is not significantly different, after analysis by an unpaired student's t test.

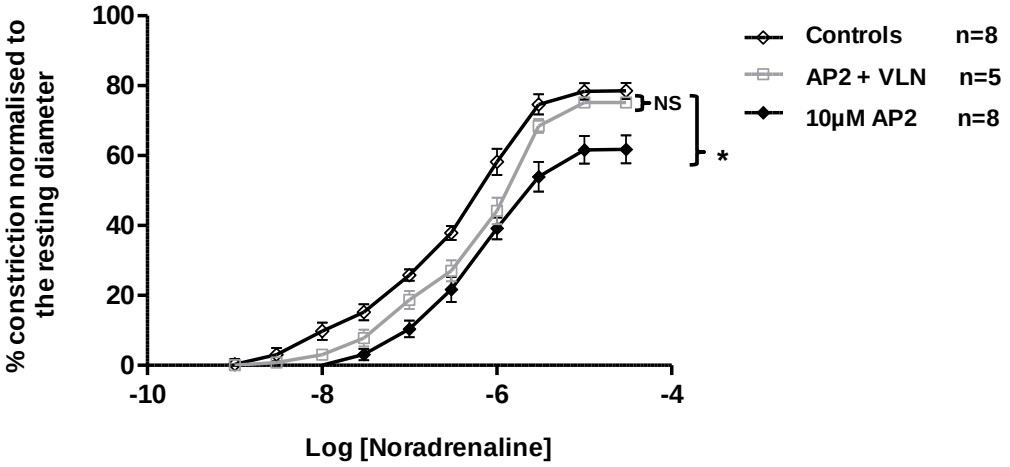

Figure 3.10.4: Effects of AP2 & AP2+Vinyl-L-Nio (VLN) on mesenteric arterial constrictions in response to noradrenaline. Constrictions to noradrenaline (Log[NA] -9.0 to -4.5 M) as exhibited by untreated, 10µM AP2 treated and 10µM and 10µM VLN simultaneously treated arteries from WT $^{(+/+)}$ mice. The significantly reduced contractile response (* is $p<0.05$) of mesenteric arteries from WT $^{(+/+)}$ mice to noradenaline (Log[NA] -9.0 to -4.5 M) as a result of 10µM AP2 incubation was not present after incubation of arteries with 10µM AP2 in the presence of 10µM VLN. Data expressed as mean ± SEM. Analysis by repeated measures, ANOVA showed no significant difference between response of arteries after 10µM AP2 and AP2 + VLN incubation.

3.11 Effects of PMCA4 inhibition with AP2; and of AP2 in the presence of nNOS inhibition by Vinyl-L-Nio (VLN) on the concentration of intracellular free calcium ($[Ca^{2+}]_i$)

To study whether AP2 modulated intracellular Ca^{2+} homeostasis, global levels of $[Ca^{2+}]_i$ were examined in pressurised mesenteric arteries from WT $^{(+/+)}$ mice following incubation with 10μM AP2 for 30 minutes. Further studies were also conducted to determine whether AP2 had any effect on intracellular Ca^{2+} homeostasis in the presence of nNOS inhibition with 10μM VLN.

3.11.1 Effects on basal $[Ca^{2+}]_i$

The inhibition of PMCA4 with AP2 had no effect on the baseline levels of F_{400}/F_{500} Ca^{2+} emission ratio (representative of global $[Ca^{2+}]_i$) in pressurised mesenteric arteries isolated from WT $^{(+/+)}$ mice (resting F_{400}/F_{500} Ca^{2+} emission ratio = 0.70 ± 0.14 (n=4) in the absence of AP2 and 0.65 ± 0.14 (n=4) in the presence of AP2, NS) (figure 3.11.1.1). Neither did the incubation of arteries with AP2 in the presence of nNOS inhibition by VLN affect the baseline F_{400}/F_{500} Ca^{2+} emission ratio (resting F_{400}/F_{500} Ca^{2+} emission ratio = 0.69 ± 0.17 (n=4) in the absence of AP2, and 0.75 ± 0.09 (n=5) in the presence of AP2+VLN respectively; NS) (figure 3.11.1.1).

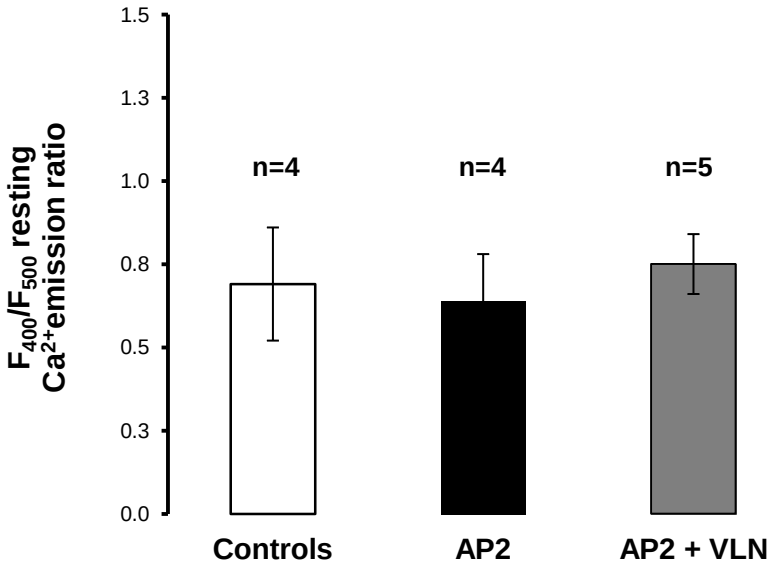

Figure 3.11.1.1: Effects of AP2 & AP2+Vinyl-L-Nio (VLN) on basal $[Ca^{2+}]_i$ of intact mesenteric arteries. Resting F_{400}/F_{500} Ca^{2+} emission ratio of untreated; 10µM AP2 treated and 10µM AP2 + 10µM VLN treated pressurised mesenteric resistance arteries obtained from WT $^{(+/+)}$ mice. Data expressed as mean ± SEM. AP2 or AP2+VLN treated vessels not significantly different from control vessels according to an unpaired student's t test.

3.11.2 Effects on elevations of $[Ca^{2+}]_i$ in response to 40mM KPSS

Addition of 40mM KPSS resulted in a maintained increase in the F_{400}/F_{500} Ca^{2+} emission ratio and sustained constriction of arteries from WT $^{(+/+)}$ mice. AP2 incubation of arteries had no significant effect on the magnitude of arterial constrictions to 40mM KPSS, (as % normalised to starting diameter = 38.41 ± 5.53% (n=4) and 27.25 ± 10.09% (n=4) in the absence and presence of AP2 respectively, NS) or in the magnitude of change in the F_{400}/F_{500} Ca^{2+} emission ratio (Δ in F_{400}/F_{500} Ca^{2+} emission ratio = 0.24 ± 0.07 (n=4) in the absence and 0.14 ± 0.02 (n=4) in the presence of AP2, NS) (figure 3.11.2.1). There were also no significant changes observed in the magnitude of constrictions or change in the F_{400}/F_{500} Ca^{2+} emission ratio between untreated arteries and AP2+VLN treated vessels (constrictions as % normalised to starting diameter = 38.41 ± 5.53% (n=4) in the absence of AP2 and 31.52 ± 10.30% (n=5) in the presence of AP2+VLN, NS; and Δ in F_{400}/F_{500} Ca^{2+} emission ratio = 0.24 ± 0.07 (n=4) in the absence of AP2, and 0.33 ± 0.04 (n=5) in the presence of AP2+VLN, NS) (figure 3.11.2.1).

The T constriction times, i.e. time taken for arteries to reach maximum constriction in response to 40mM KPSS, were similar between AP2 incubated and untreated arteries (201.10 ± 74.77 seconds (n=4) and 205.70 ± 46.46 seconds (n=4) in the absence and presence of AP2 respectively, NS) and between AP2+VLN and untreated arteries from WT $^{(+/+)}$ mice (201.10 ± 74.77 seconds (n=4) in the absence of AP2 and 211.36 ± 11.31 seconds (n=5) presence of AP2+VLN, NS) (figure 3.11.2.2).

Elevations in the F_{400}/F_{500} Ca^{2+} emission ratio preceded KPSS induced constrictions of all arteries from WT $^{(+/+)}$ mice. The differences in the time observed between the

initial elevation in the F_{400}/F_{500} Ca^{2+} emission ratio and start of 40mM KPSS induced constriction were not significantly altered as a result of AP2 treatment or AP2+VLN treatment of arteries (40.00 ± 22.19 seconds (n=4) in the absence of AP2; 49.80 ± 30.15 seconds (n=4) and 33.44 ± 4.46 seconds (n=5) in the presence of AP2 and AP2+VLN respectively; (controls vs AP2, NS), (controls vs AP2+VLN, NS)).

The time for F_{400}/F_{500} Ca^{2+} emission ratio to increase to maximum and the time for maximal constriction in response to 40mM KPSS was also not modified by AP2 in the presence/absence of VLN (time for maximal increase in F_{400}/F_{500} Ca^{2+} emission ratio = 169.60 ± 63.33 seconds (n=4) in the absence of AP2, 165.60 ± 28.32 seconds (n=4) and 173.20 ±10.37 seconds (n=5) in the presence of AP2 and AP2+VLN respectively, (controls vs AP2, NS) (controls vs AP2+VLN, NS); and the time for maximal constriction = 201.10 ± 74.77 seconds (n=4) in the absence of AP2, 205.70 ± 46.46 seconds (n=4) and 212.56 ± 12.40 seconds (n=5) in the presence of AP2 and AP2+VLN respectively, (controls vs AP2, NS) (controls vs AP2+VLN, NS); upon 40mM KPSS stimulation) (figure 3.11.2.2).

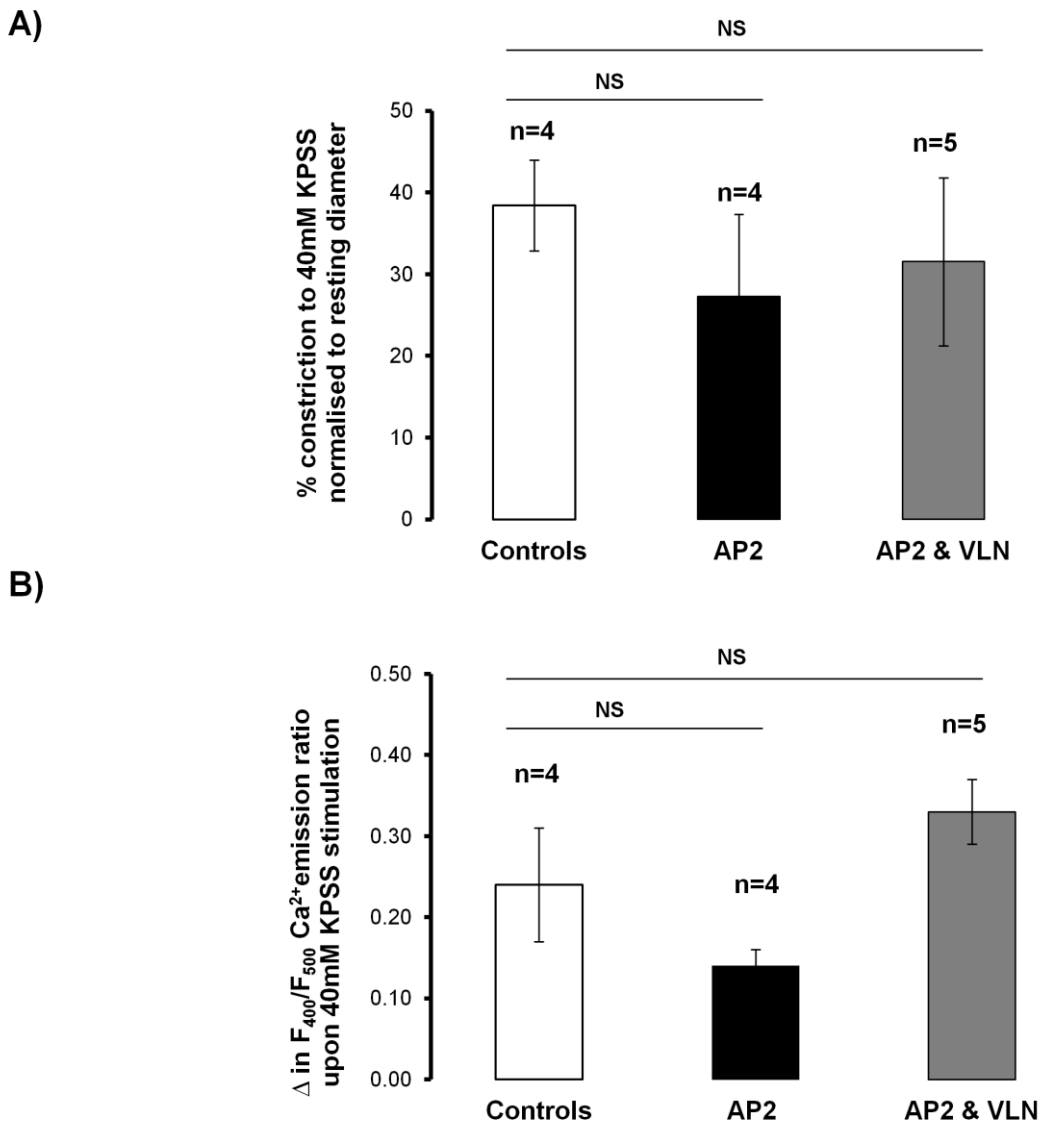

Figure 3.11.2.1: Effects of AP2 & AP2+Vinyl-L-Nio (VLN) on arterial constrictions and on the F_{400}/F_{500} Ca^{2+} emission responses to 40mM KPSS. A) Constrictions (as % of starting diameter) to 40mM KPSS of arteries from WT $^{(+/+)}$ mice without and after 10µM AP2 or 10µM AP2 + 10µM VLN incubation while B) is the change (i.e. increase) noted in the F_{400}/F_{500} Ca^{2+} emission ratio to addition of 40mM KPSS. Data expressed as mean ± SEM. No significant differences between control and AP2 treated arteries or control and AP2+VLN treated arteries, unpaired student's t tests.

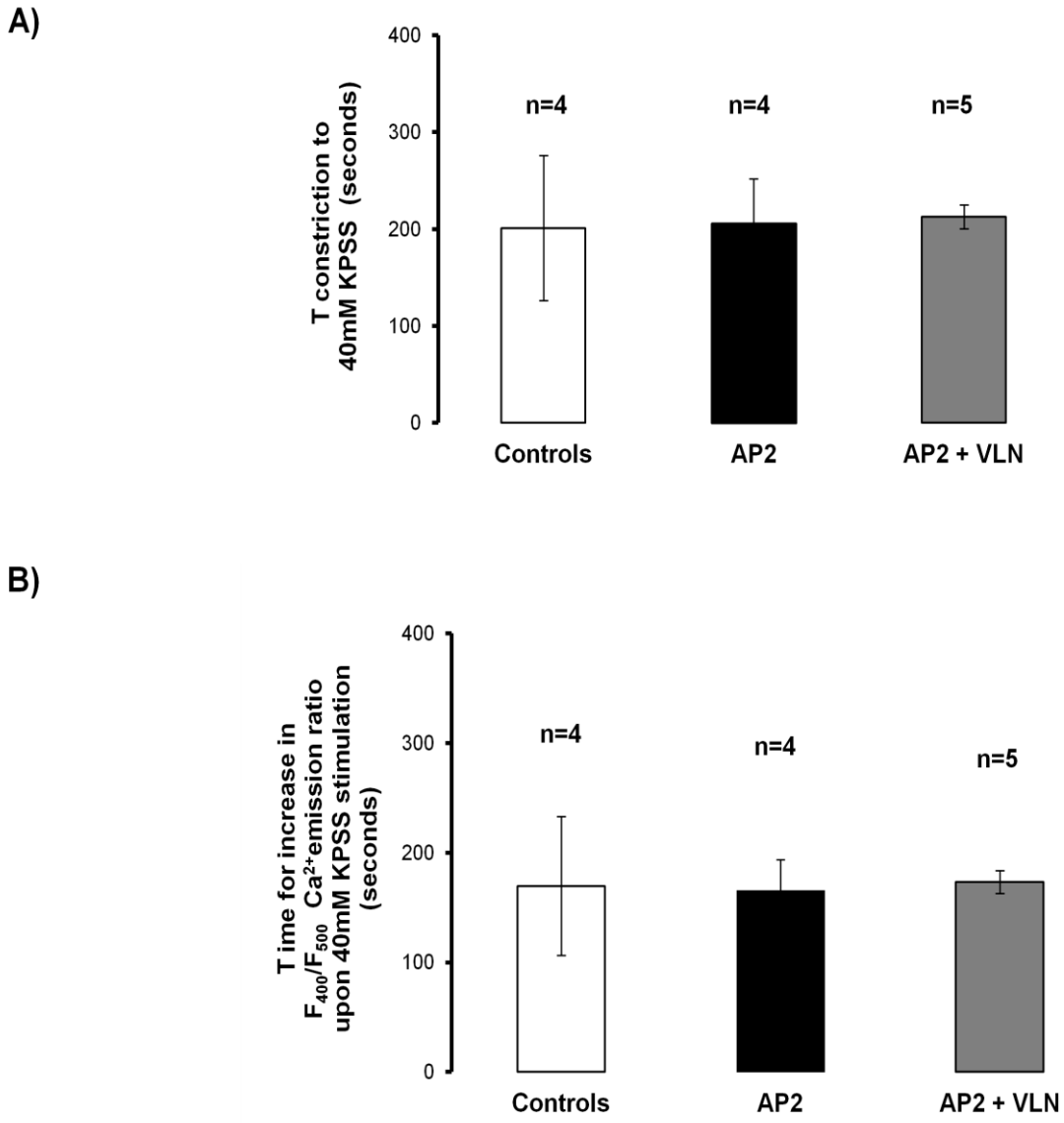

Figure 3.11.2.2: Effects of AP2 & AP2+Vinyl-L-Nio (VLN) on the constriction time and on the time for increase in the F_{400}/F_{500} Ca^{2+} emission responses of arteries to 40mM KPSS. A) The time for pressurised arteries from WT $^{(+/+)}$ mice to constrict maximally to 40mM KPSS and B) for the F_{400}/F_{500} Ca^{2+} emission ratio to increase to maximum following incubation without and with 10µM AP2 or with 10µM AP2 + 10µM VLN. Data presented as mean ± SEM. No significant difference between AP2 or AP2+VLN treated and control arteries, unpaired student's t test.

Incubation of arteries with AP2 or AP2+VLN did not alter the times it took vessels to return to their stable resting diameters (i.e. T and $T_{1/2}$ relaxations) following washout of 40mM KPSS (T relaxation = controls: 216.70 ± 30.18 seconds (n=4), AP2: 224.80 ± 75.78 seconds (n=4) and AP2+VLN: 243.04 ± 14.57 seconds (n=5); (controls vs AP2, NS) (controls vs AP2+VLN, NS); and $T_{1/2}$ relaxation = controls: 59.65 ± 30.39 seconds (n=4), AP2: 60.50 ± 13.39 seconds (n=4) and AP2+VLN: 61.82 ± 13.51 seconds (n=5); (controls vs AP2, NS) (controls vs AP2+VLN, NS); after 40mM KPSS washout) ($T_{1/2}$ relaxation times shown in figure 3.11.2.3).

Arterial treatment with AP2 or AP2 in the presence of nNOS inhibition by VLN also had no effect on the time recorded for the fall in the F_{400}/F_{500} Ca^{2+} emission ratio when 40mM KPSS was washed out (time for decrease in F_{400}/F_{500} Ca^{2+} emission ratio = controls: 171.50 ± 19.76 seconds (n=4), AP2: 176.40 ± 69.64 seconds (n=4) and AP2+VLN: 198.72 ± 19.61 seconds (n=5); (controls vs AP2, NS) (controls vs AP2+VLN, NS); and the $T_{1/2}$ (i.e. the time taken for the maximum F_{400}/F_{500} Ca^{2+} emission ratio to decrease by 50%) upon 40mM KPSS washout = controls: 74.28 ± 10.13 seconds (n=4), AP2: 79.03 ± 28.36 seconds (n=4) and AP2+VLN: 94.28 ± 10.39 seconds (n=5); (controls vs AP2, NS) (controls vs AP2+VLN, NS)) (figure 3.11.2.3).

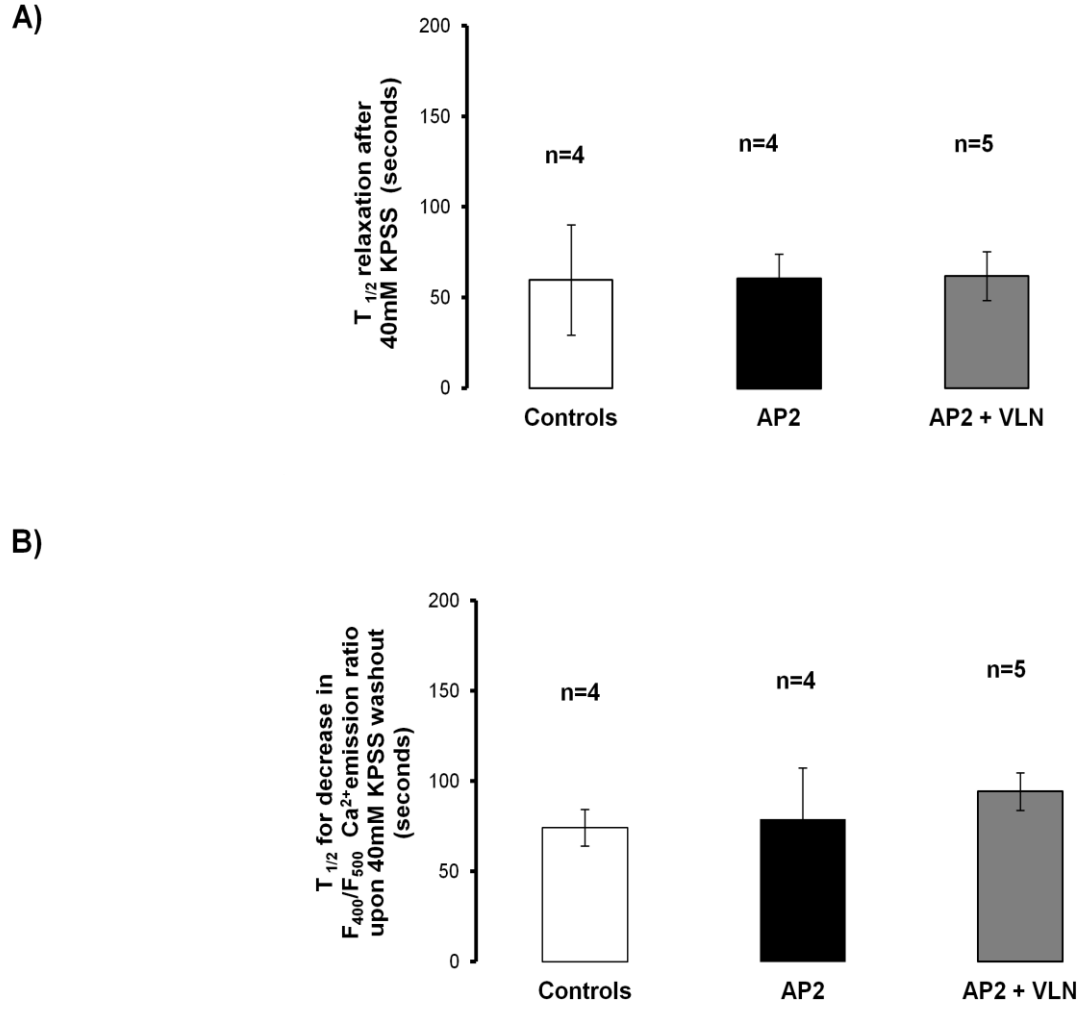

Figure 3.11.2.3: Effects of AP2 & AP2+Vinyl-L-Nio (VLN) on $T_{1/2}$ relaxation times and on the $T_{1/2}$ for decrease in the F_{400}/F_{500} Ca^{2+} emission responses of arteries upon washout of 40mM KPSS. A) The $T_{1/2}$ relaxation (time in seconds for arteries pre-constricted to 40mM KPSS to relax by 50% upon PSS washout) and B) $T_{1/2}$ for decrease in the F_{400}/F_{500} Ca^{2+} emission response (time taken for maximum F_{400}/F_{500} Ca^{2+} emission ratio to decrease by 50%), in the same vessels following washout of 40mM KPSS. As exhibited by arteries from WT $^{(+/+)}$ mice after incubation in PSS (controls) or 10µM AP2 or 10µM AP2 + 10µM VLN. Data presented as mean ± SEM. AP2 or AP2+VLN treated arteries not significantly different from controls, according to unpaired student's t test.

3.11.3 Effects on elevations of $[Ca^{2+}]_i$ in response to 100mM KPSS

Stimulation of pressurised mesenteric arteries from WT $^{(+/+)}$ mice with 100mM KPSS induced a steady increase in the F_{400}/F_{500} Ca^{2+} emission ratio prior to maintained vascular constriction. Incubation with AP2 did not significantly reduce the magnitude of constriction but significantly reduced the change in F_{400}/F_{500} Ca^{2+} emission ratio of arteries when stimulated with 100mM KPSS ((constriction as % normalised to starting diameter = 58.07 ± 9.97% (n=4) and 36.08 ± 14.61% (n=4), NS; and the Δ in F_{400}/F_{500} Ca^{2+} emission ratio = 0.26 ± 0.05 (n=4) and 0.15 ± 0.02 (n=4), $p<0.05$) in the absence and presence of AP2 respectively) in response to 100mM KPSS (figure 3.11.3.1).

In the presence of nNOS inhibition by VLN AP2 had no effect on the magnitude of arterial constriction to 100mM KPSS ((constriction as % normalised to starting diameter = 45.06 ± 10.98% (n=5) in the presence of AP2+VLN). However, the significant reduction in the change in F_{400}/F_{500} Ca^{2+} emission ratio to 100mM KPSS observed with AP2 alone was not present after AP2+VLN arterial treatment (the change in F_{400}/F_{500} Ca^{2+} emission ratio = AP2+VLN: 0.39 ± 0.04 (n=5)) (figure 3.11.3.1).

Time differences between the initial rise in F_{400}/F_{500} Ca^{2+} emission ratio and start of 100mM KPSS induced constriction were not significantly altered by AP2 or AP2+VLN incubation of arteries. These were recorded as follows 51.35 ± 25.81 seconds (n=4) as displayed by control arteries, 32.00 ± 13.45 seconds (n=4) and 31.44 ± 6.46 seconds (n=5) displayed by arteries incubated with AP2, and AP2+VLN respectively; (controls vs AP2, NS) (controls vs AP2+VLN, NS).

Times for maximal increase in F_{400}/F_{500} Ca^{2+} emission ratio were faster than times for maximal arterial constriction (i.e. T constriction) to 100mM KPSS and both were not significantly modified by AP2 or by simultaneous AP2+VLN incubation of arteries. (Time for maximal increase in F_{400}/F_{500} Ca^{2+} emission ratio = controls: 201.05 ± 38.78 seconds (n=4), AP2: 239.00 ± 36.48 seconds (n=4) and AP2+VLN: 234.04 ± 38.28 seconds (n=5); (controls vs AP2, NS) (controls vs AP2+VLN, NS); and T constriction = controls: 298.80 ± 70.66 seconds (n=4), AP2: 285.50 ± 32.96 seconds (n=4) and AP2+VLN: 328.08 ± 28.29 seconds (n=5) ; (controls vs AP2, NS) (controls vs AP2+VLN, NS) to 100mM KPSS) (figure 3.11.3.2).

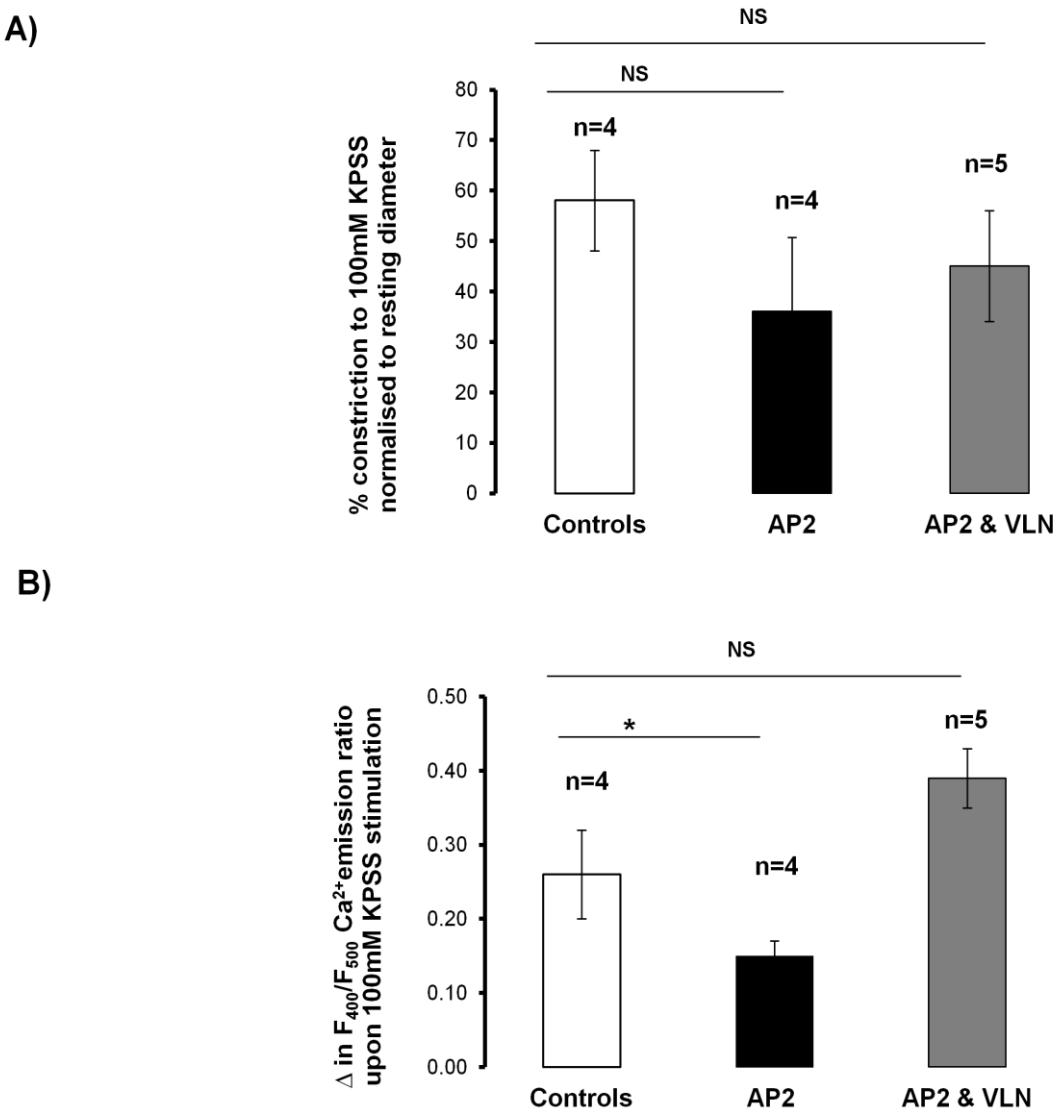

Figure 3.11.3.1: Effects of AP2 & AP2+Vinyl-L-Nio (VLN) on arterial constrictions and on the F_{400}/F_{500} Ca^{2+} emission responses to 100mM KPSS. A) Contractile response (constrictions as % of starting diameter) of pressurised arteries from WT $^{(+/+)}$ mice to 100mM KPSS and B) the change (i.e. increase) in the F_{400}/F_{500} Ca^{2+} emission ratio after incubation in PSS (controls) or with 10µM AP2 or 10µM AP2 + VLN. F_{400}/F_{500} Ca^{2+} emission responses of arteries to 100mM KPSS was significantly decreased after incubation with 10µM AP2 in comparison to controls (* is $p<0.05$, unpaired student's t test). There was no significant difference following incubation with 10µM AP2 +10µM VLN in comparison to controls (NS, is not significantly different, unpaired student's t test). Data presented as mean ± SEM.

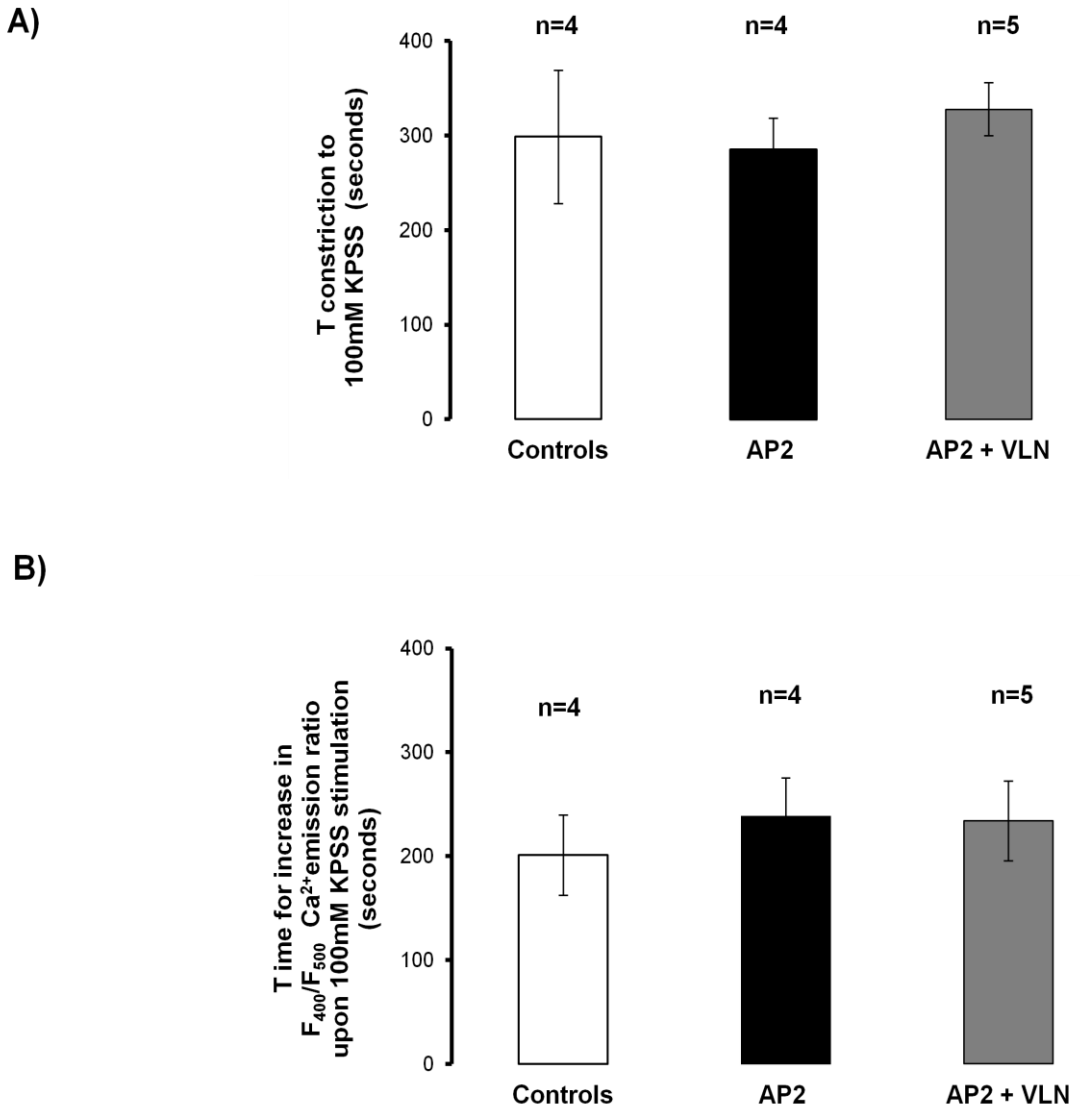

Figure 3.11.3.2: Effects of AP2 & AP2+Vinyl-L-Nio (VLN) on the constriction time and on the time for increase in the F_{400}/F_{500} Ca^{2+} emission responses of arteries to 100mM KPSS. A) The time (in seconds) for untreated, 10µM AP2 as well as 10µM AP2 + 10µM VLN incubated mesenteric arteries isolated from WT $^{(+/+)}$ mice to constrict maximally to 100mM KPSS and in the same vessels B) the time for increase in F_{400}/F_{500} Ca^{2+} emission ratio upon 100mM KPSS stimulation. Data expressed as mean ± SEM. No significant difference between AP2 or AP2+VLN treated and control arteries, analysis by an unpaired student's t test.

The relaxation times (i.e. T and $T_{1/2}$ relaxations) upon washout of 100mM KPSS were not modulated after AP2 or after AP2+VLN incubation of arteries (T relaxations = controls: 312.70 ± 94.01 seconds (n=4), AP2: 295.00 ± 70.00 seconds (n=4) and AP2+VLN: 314.56 ± 16.79 seconds (n=5); and the $T_{1/2}$ relaxations = controls: 110.68 ± 55.45 seconds (n=4), AP2: 99.60 ± 11.85 seconds (n=4) and AP2+VLN: 83.88 ± 14.80 seconds (n=5) to 100mM KPSS; (controls vs AP2, NS) (controls vs AP2+VLN, NS)) ($T_{1/2}$ relaxation times shown in figure 3.11.3.3). The same was true in relaxation times noted for F_{400}/F_{500} Ca^{2+} emission to decrease upon 100mM KPSS washout following incubation of arteries with AP2 or AP2+VLN (time for decrease in F_{400}/F_{500} Ca^{2+} emission ratio upon 100mM KPSS washout = controls: 239.30 ± 38.17 seconds (n=4), AP2: 233.30 ± 60.98 seconds (n=4) and AP2+VLN: 259.04 ± 16.91 seconds (n=5); and for the $T_{1/2}$ (i.e. time taken for the maximum F_{400}/F_{500} Ca^{2+} emission ratio to decrease by 50% upon 100mM KPSS washout) = controls: 99.83 ± 28.81 seconds (n=4), AP2: 93.73 ± 32.95 seconds (n=4) and AP2+VLN: 112.98 ± 4.81 seconds (n=5)); (controls vs AP2, NS) (controls vs AP2+VLN, NS) (figure 3.11.3.3).

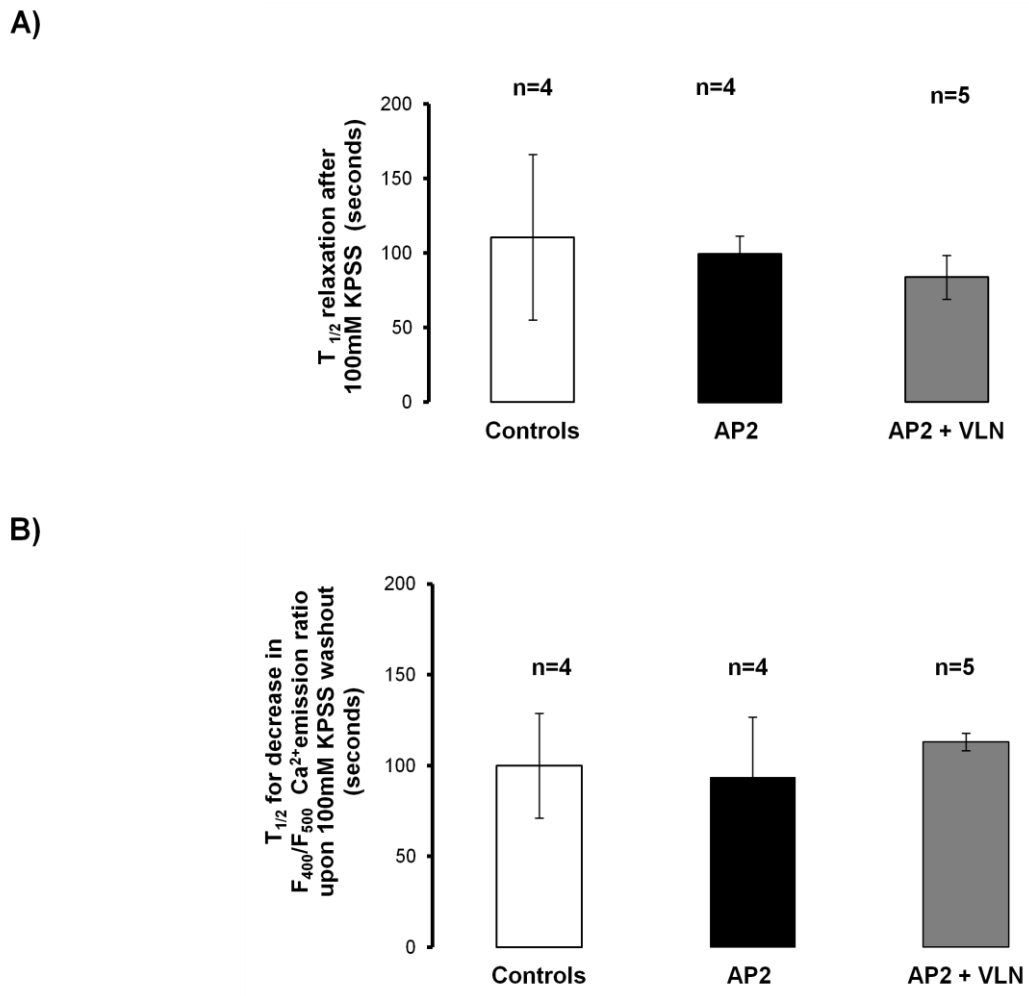

Figure 3.11.3.3: Effects of AP2 & AP2+Vinyl-L-Nio (VLN) on $T_{1/2}$ relaxation times and on the $T_{1/2}$ for decrease in the F_{400}/F_{500} Ca^{2+} emission responses of arteries upon washout of 100mM KPSS. A) $T_{1/2}$ relaxation (i.e. the time in seconds for pre-constricted arteries to KPSS relax by 50% upon PSS washout) and B) $T_{1/2}$ for decrease in the F_{400}/F_{500} Ca^{2+} emission response (time taken for the maximum F_{400}/F_{500} Ca^{2+} emission ratio to decrease by 50%) after the washout of 100mM KPSS, as observed in the same vessels obtained from WT $^{(+/+)}$ mice. Arteries were incubated in PSS (controls) or 10µM AP2 or 10µM AP2 + 10µM VLN. Data presented as mean ± SEM. Analysis by unpaired student's t test showed no significant difference between AP2 or AP2+VLN treated and control vessels.

3.11.4 Effects on elevation of $[Ca^{2+}]_i$ in response to noradrenaline

There was a steady increase in the F_{400}/F_{500} Ca^{2+} emission ratio prior to arterial constriction upon stimulation with $3x10^{-5}$M noradrenaline. Incubation of arteries from WT $^{(+/+)}$ mice with AP2 resulted in the significant reductions in both the magnitude of constriction as well as the change in F_{400}/F_{500} Ca^{2+} emission ratio in response to $3x10^{-5}$M noradrenaline ((constriction as % normalised to starting diameter = 57.46 ± 6.20% (n=4) in the absence of AP2 and 34.40 ± 7.08% (n=4) in the presence of AP2, $p<0.05$; and the Δ in F_{400}/F_{500} Ca^{2+} emission ratio = 0.23 ± 0.04 (n=4) and 0.12 ± 0.02 (n=4) in the absence and presence of AP2 respectively, $p<0.05$) upon $3x10^{-5}$M noradrenaline stimulation) (figure 3.11.4.1). These changes with AP2 alone were not present in arteries incubated with AP2 in the presence of nNOS inhibition by VLN (constriction as % normalised to starting diameter = 62.68 ± 7.71% (n=5) in the presence of AP+VLN; and the Δ in F_{400}/F_{500} Ca^{2+} emission ratio = AP2+VLN: 0.36 ± 0.07 (n=5); (controls vs AP2+VLN, NS)) (figure 3.11.4.1).

AP2 or AP2 together with VLN did not affect the time difference seen between the initial rise in F_{400}/F_{500} Ca^{2+} emission ratio and start of noradrenaline induced constriction (time difference noted in = controls: 58.90 ± 25.57 seconds (n=4), AP2: 36.95 ± 14.60 seconds (n=4) and AP2+VLN: 33.28 ± 3.04 seconds (n=5) arteries in response to $3x10^{-5}$M noradrenaline; (controls vs AP2, NS) (controls vs AP2+VLN, NS)).

AP2 or AP2+VLN arterial treatment had no effect on the time for the maximal increase in the F_{400}/F_{500} Ca^{2+} emission ratio to $3x10^{-5}$M noradrenaline (time for maximal increase in F_{400}/F_{500} Ca^{2+} emission ratio upon noradrenaline stimulation =

controls: 146.50 ± 8.19 seconds (n=4), AP2: 147.70 ± 21.13 seconds (n=4) and AP2+VLN: 148.32 ± 9.58 seconds (n=5), (controls vs AP2, NS) (controls vs AP2+VLN, NS) (figure 3.11.4.2); or on the time observed for arteries to reach maximum constriction (i.e. T constriction) (T constriction to $3x10^{-5}$M noradrenaline = controls: 182.20 ± 11.64 seconds (n=4), AP2: 183.80 ± 20.61 seconds (n=4) and AP2+VLN: 184.16 ± 18.02 seconds (n=5); (controls vs AP2, NS) (controls vs AP2+VLN, NS)) (figure 3.11.4.2).

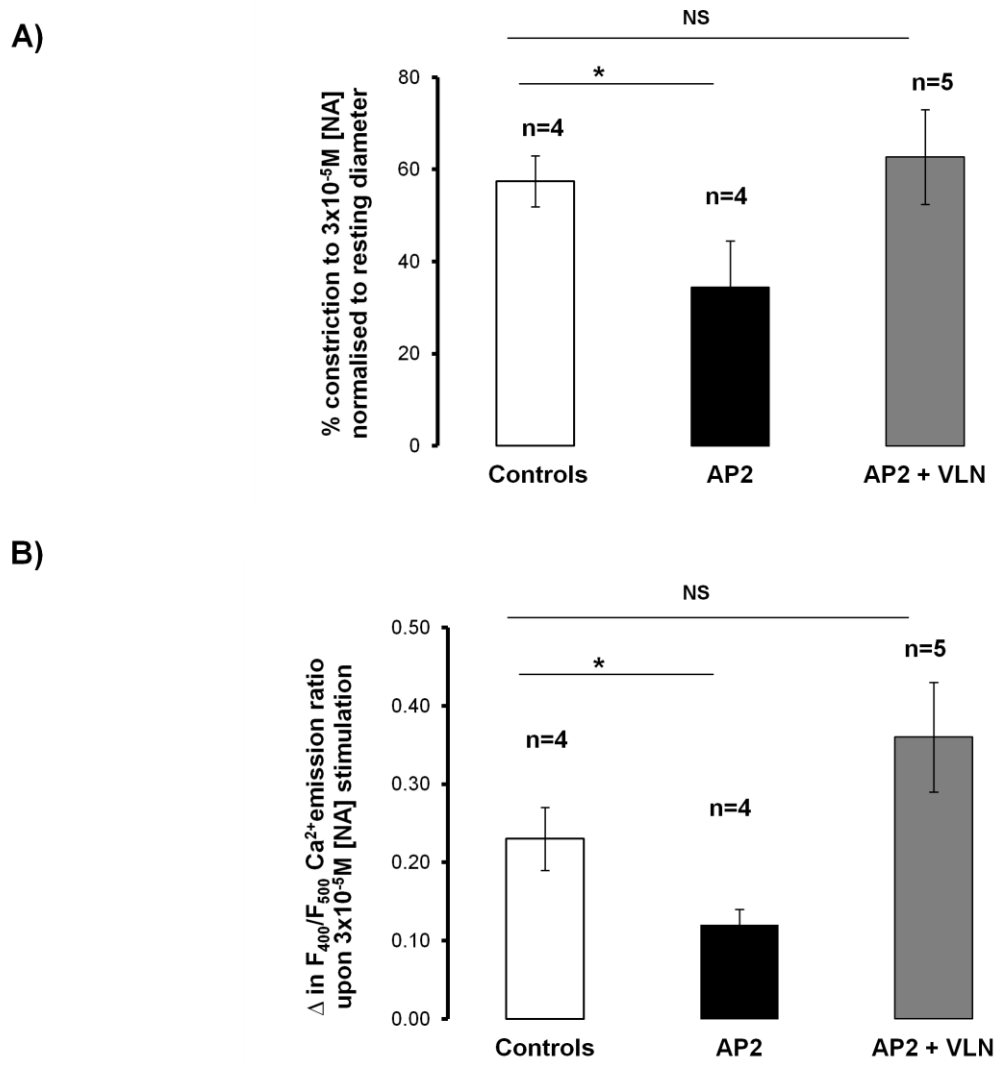

Figure 3.11.4.1: Effects of AP2 and AP2+Vinyl-L-Nio (VLN) on arterial constrictions and on the F_{400}/F_{500} Ca^{2+} emission responses to noradrenaline. A) Constrictions (as % of resting diameter) displayed by pressurised mesenteric resistance arteries obtained from WT $^{(+/+)}$ mice and in the same vessels B) the change i.e. increase, in the F_{400}/F_{500} Ca^{2+} emission ratio (representative of $[Ca^{2+}]_i$) to $3x10^{-5}$M noradrenaline. Arteries were incubated in PSS (controls) or with 10µM AP2 or 10µM AP2 in presence of 10µM VLN. AP2 incubated arteries showed significant reductions in A) constriction and B) change in the F_{400}/F_{500} Ca^{2+} emission ratio. On the figure NS, is not significantly different and * is $p<0.05$, unpaired student's t test. Data expressed as mean ± SEM.

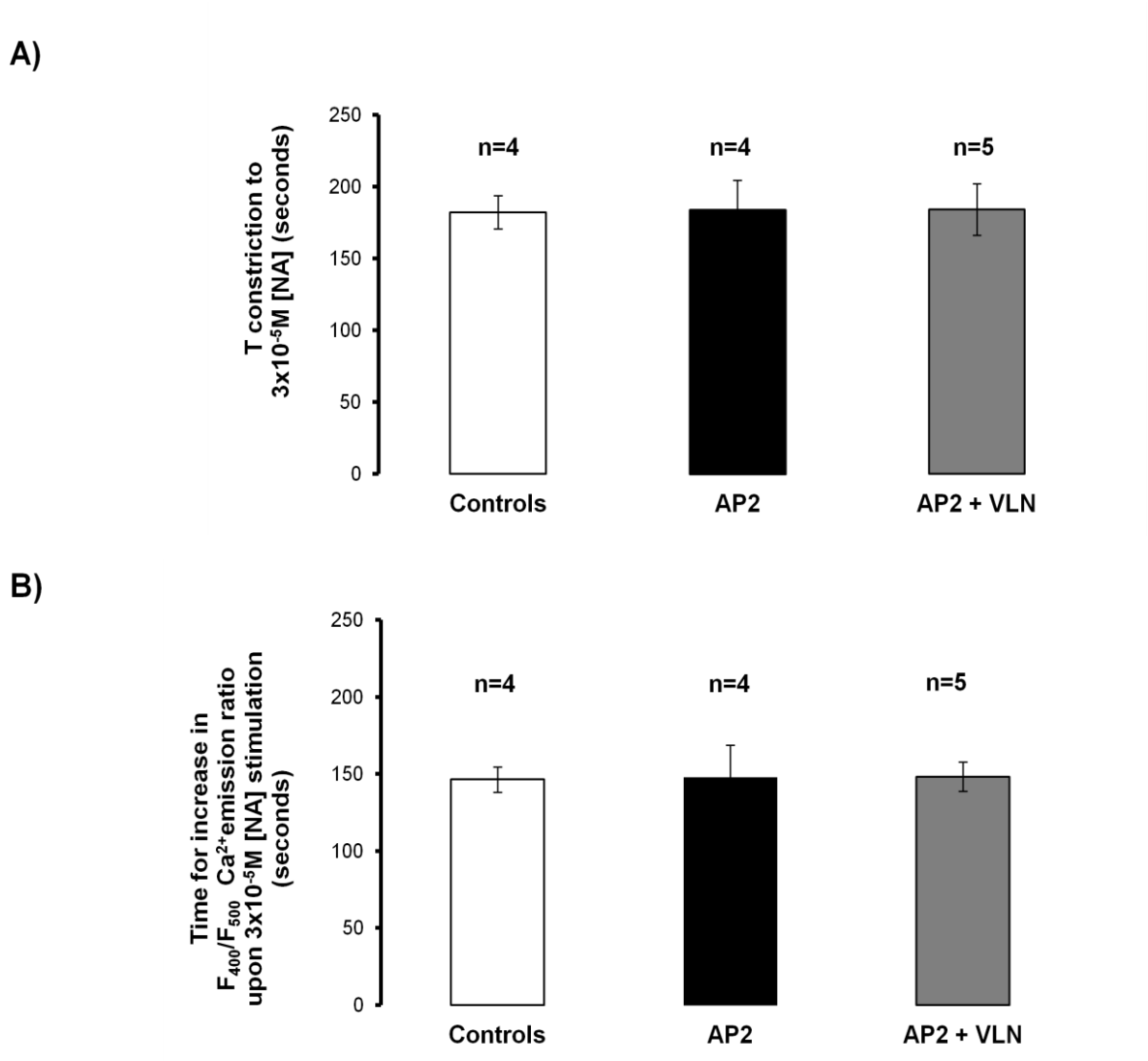

Figure 3.11.4.2: Effects of AP2 and AP2+Vinyl-L-Nio (VLN) on the constriction time and on the time for increase in the F_{400}/F_{500} Ca^{2+} emission responses of arteries to noradrenaline. A) Time pressurised arteries obtained from WT $^{(+/+)}$ mice achieved the maximum constriction and B) increased the F_{400}/F_{500} Ca^{2+} emission ratio to maximum in response to $3x10^{-5}$M noradrenaline when incubated in PSS (controls) or with 10µM AP2 or 10µM AP2 in presence of 10µM VLN. Data presented as mean ± SEM. No significant difference between AP2 or AP2+VLN treated and control's, unpaired student's t test.

Relaxation times (i.e. the T and $T_{1/2}$ relaxation times) noted in arteries from WT $^{(+/+)}$ mice following $3x10^{-5}$M noradrenaline washout were not significantly modulated by AP2 or by simultaneous AP2+VLN incubation (T relaxations = controls: 268.30 ± 31.55 seconds (n=4), AP2: 259.40 ± 44.0 seconds (n=4) and AP2+VLN: 288.08 ± 17.26 seconds (n=5); and for the $T_{1/2}$ relaxations = controls: 111.0 ± 18.70 seconds (n=4), AP2: 107.87 ± 18.66 seconds (n=4) and AP2+VLN: 101.28 ± 7.65 seconds (n=5); (controls vs AP2, NS) (controls vs AP2+VLN, NS)) after washout of $3x10^{-5}$M noradrenaline) ($T_{1/2}$ relaxation times shown in figure 3.11.4.3). Similarly, there were no significant alterations caused by AP2 or by AP2+VLN treatment of arteries in the time for maximal decrease in F_{400}/F_{500} Ca^{2+} emission ratio upon $3x10^{-5}$M noradrenaline washout (time for decrease in F_{400}/F_{500} Ca^{2+} emission ratio = controls: 271.30 ± 17.35 seconds (n=4), AP2: 235.70 ± 38.18 seconds (n=4) and AP2+VLN: 270.08 ± 15.16 seconds (n=5); and the $T_{1/2}$ (i.e. time taken for the maximum F_{400}/F_{500} Ca^{2+} emission ratio to decrease by 50%) upon noradrenaline washout = controls: 120.58 ± 22.16 seconds (n=4), AP2: 109.53 ± 4.36 seconds (n=4) and AP2+VLN: 121.08 ± 13.73 seconds (n=5); (controls vs AP2, NS) (controls vs AP2+VLN, NS)) (figure 3.11.4.3).

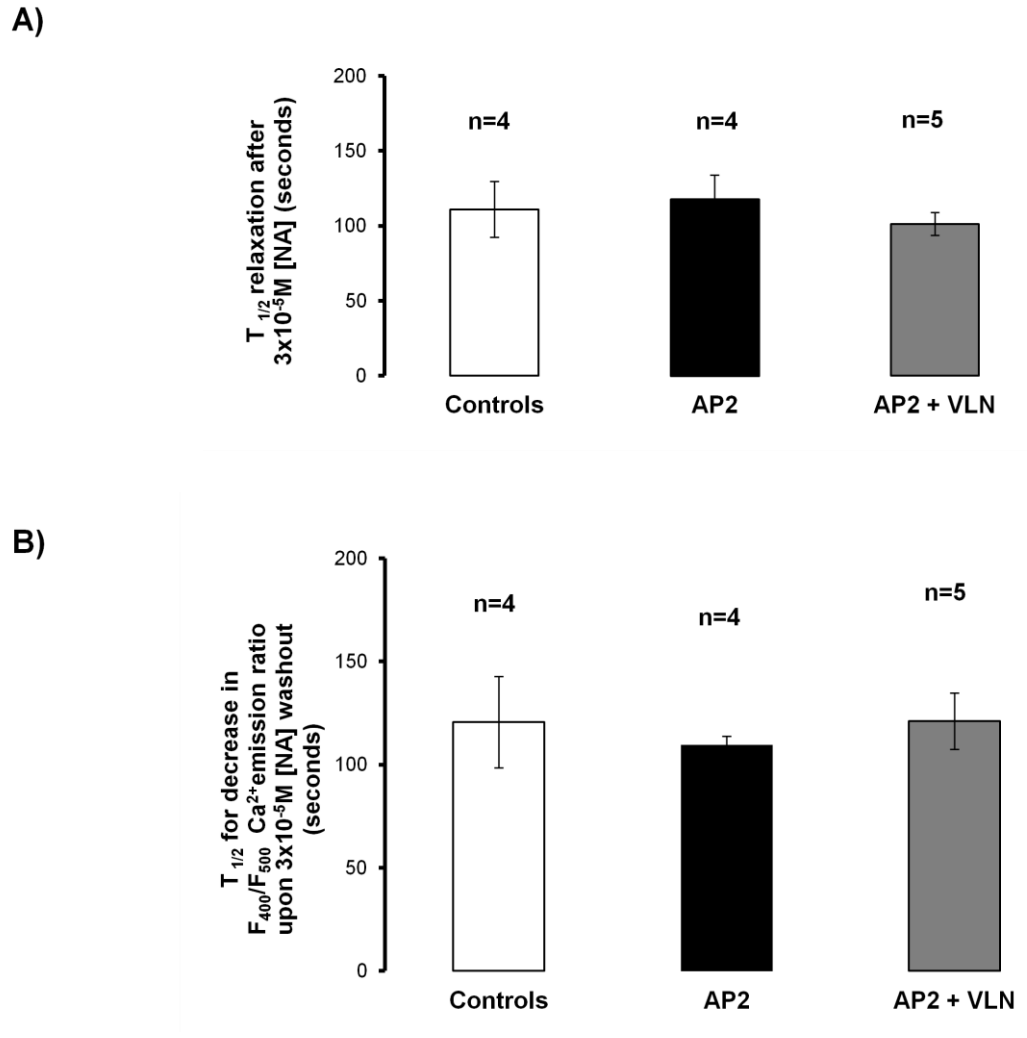

Figure 3.11.4.3: Effects of AP2 & AP2+Vinyl-L-Nio (VLN) on $T_{1/2}$ relaxation times and on the $T_{1/2}$ for decrease in the F_{400}/F_{500} Ca^{2+} emission responses of arteries upon washout of noradrenaline. A) $T_{1/2}$ relaxation (time in seconds for arteries pre-constricted to noradrenaline to relax by 50% upon PSS washout) and B) $T_{1/2}$ for decrease in the F_{400}/F_{500} Ca^{2+} emission response (i.e. time for the maximum F_{400}/F_{500} Ca^{2+} emission ratio to decrease by 50%) upon $3x10^{-5}$M noradrenaline washout, observed in the same vessels from WT $^{(+/+)}$ mice, after incubation in PSS (controls) or 10µM AP2 or 10µM AP2 + 10µM VLN. Data presented as mean ± SEM. Analysis by unpaired student's t test showed no significant difference between AP2 or AP2+VLN and control arteries.

3.12 Expression of nNOS in aortas of PMCA4 WT $^{(+/+)}$ and KO $^{(-/-)}$ mice and its colocalisation with PMCA4 in WT $^{(+/+)}$ mouse aortas

In order to investigate the expression of nNOS in aortas of PMCA4 WT $^{(+/+)}$ and KO $^{(-/-)}$ mice and whether it colocalised with PMCA4 (previously found to be present in VSM of these WT $^{(+/+)}$ mice), aortic sections were co-immunostained with antibodies against nNOS and against PMCA4 in immunohistochemistry experiments (figure 3.12.1). Sections cut from aortas were obtained from three PMCA4 WT $^{(+/+)}$ and from three KO $^{(-/-)}$ mice aged 3 months (n=3). This showed that nNOS expression was present in aortas from PMCA4 KO $^{(-/-)}$ mice and that it colocalised with PMCA4 within the walls of aortas obtained from PMCA4 WT $^{(+/+)}$ mice.

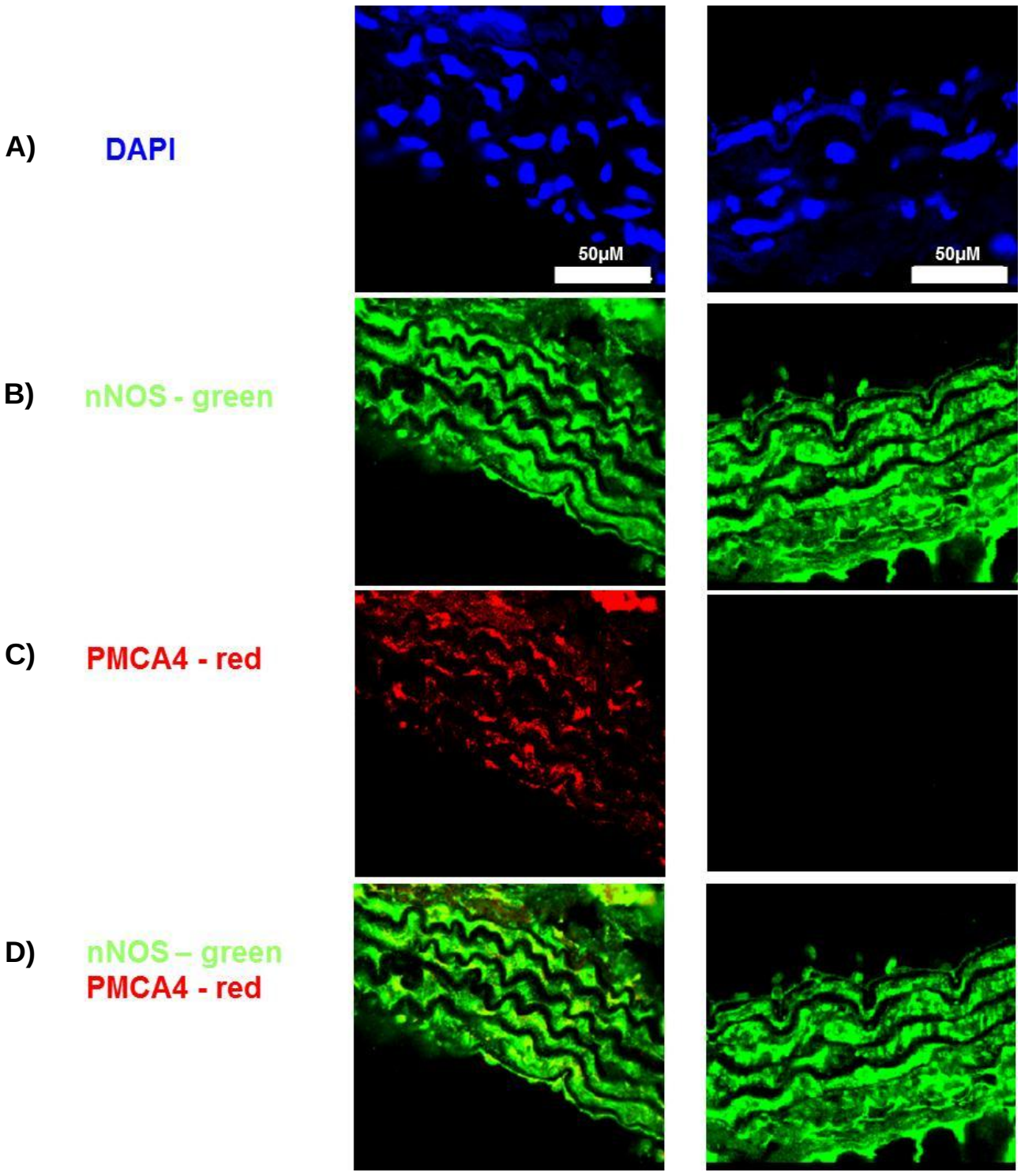

Figure 3.12.1: Detection of PMCA4 and nNOS expression in sectioned aortas obtained from PMCA4 WT $^{(+/+)}$ and KO $^{(-/-)}$ mice by immunofluorescence. Shown in A) are blue DAPI fluorescing cell nuclei within the vascular walls of aortic sections. In panel B) are immunofluorescence images of aortic sections following co-immunostaining with a nNOS antibody detected by FITC green and in panel C) with a PMCA4 antibody detected by texas red. In panel D) are the overlay images of nNOS and PMCA4 co-immunostained sections. All images were taken with a 60x objective after 70 seconds exposure time.

3.13 Does methyl-beta-cyclodextrin (mβcd) modulate the effects of AP2 on mouse mesenteric arterial contractility?

PMCA and nNOS are enriched in caveolae, plasma membrane microvesicle regions present in vascular smooth muscle cells (Fujimoto, 1993; Venema et al., 1997; Segal et al., 1999; Gros et al., 2003). The effects of methyl-beta-cyclodextrin (mβcd) (which has been previously shown to disrupt caveolae structure (Shaw *et al.*, 2006)), on arterial contractility in the presence and absence of PMCA4 inhibition by AP2 was examined. Isolated and pressurised mesenteric arteries form WT $^{(+/+)}$ mice were incubated for 30 minutes in 0.01M mβcd, or in PSS for controls.

Incubation of arteries with mβcd significantly decreased constrictions to KPSS or, in the case of 40mM KPSS almost abolished the contractile response (constrictions (as % of starting diameter) = to 40mM KPSS: 53.69 ± 4.43% (n=7) and 0.67 ± 0.42% (n=5) without and after mβcd treatment respectively, $p<0.05$ and to 100mM KPSS: 71.50 ± 3.02% (n=7) and 8.99 ± 0.98% (n=5) in the absence and presence of mβcd respectively, $p<0.05$) (figure 3.13.1).

The contractile response of arteries from WT $^{(+/+)}$ mice to noradrenaline were significantly attenuated as a result of mβcd incubation. (The % constrictions of arteries, to the maximum noradrenaline dose, Log [NA]-4.5M were 76.67 ± 1.58% (n=7) in the absence and 32.51 ± 9.54% (n=5) in the presence of mβcd, $p<0.05$) (figure 3.13.2).

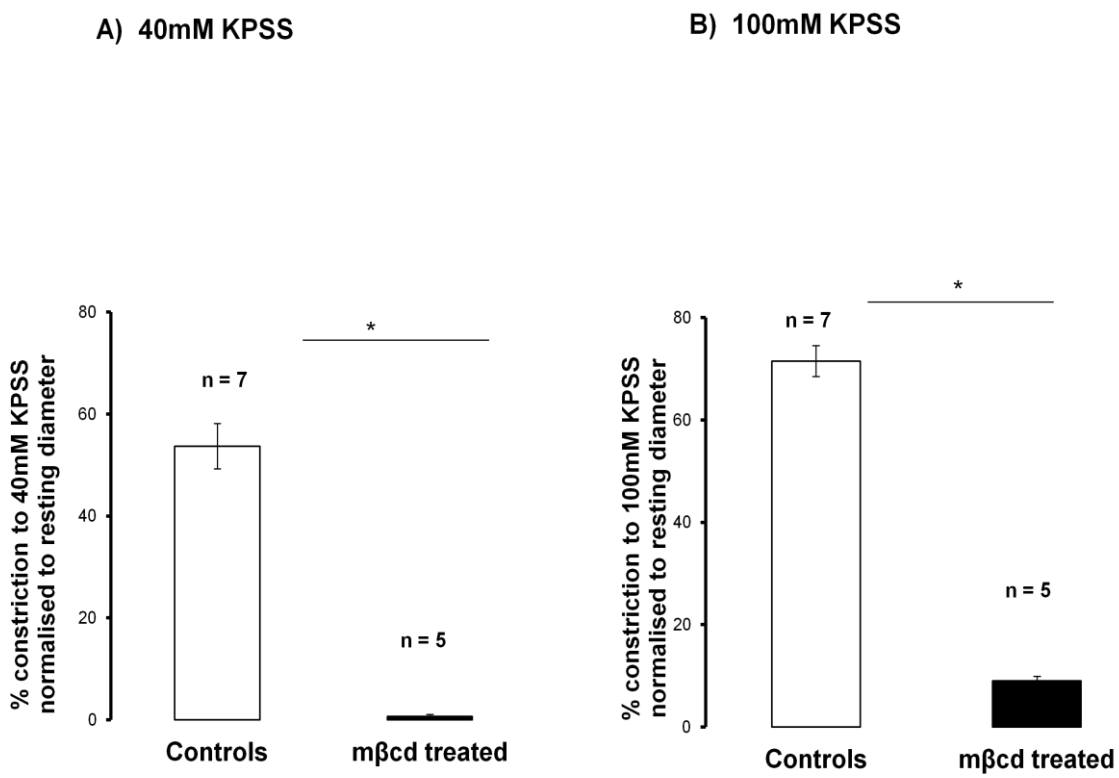

Figure 3.13.1: Effects of methyl-β-cyclodextrin (mβcd) on mesenteric arterial constrictions in response to 40mM & 100mM KPSS. Constrictions (as % of starting diameter) of mesenteric resistance arteries from WT $^{(+/+)}$ mice following incubation without and with 0.01M mβcd to A) 40mM and to B) 100mM KPSS. Data expressed as mean ± SEM and * is $p<0.05$. Constrictions to 40mM or to 100mM KPSS were significantly reduced, after arterial incubation with mβcd, compared to controls according to an unpaired student's t test.

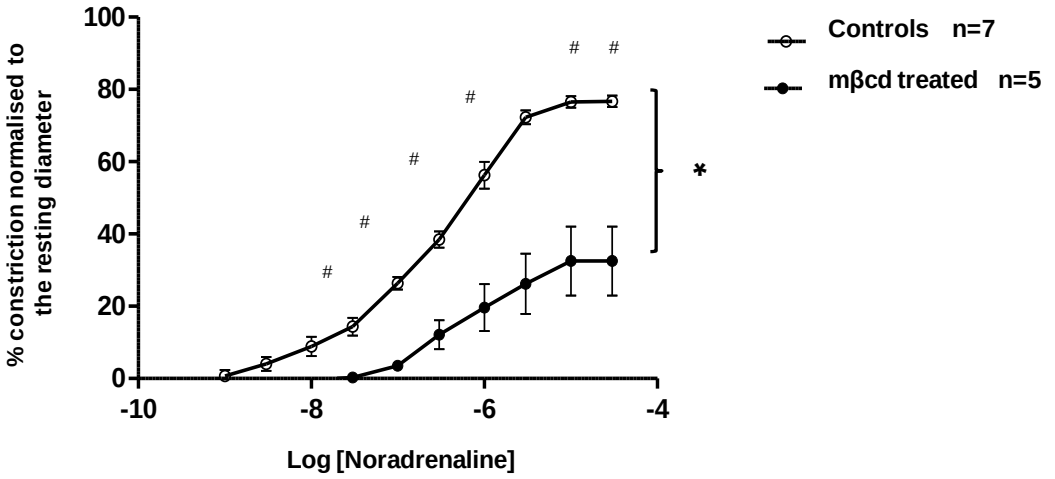

Figure 3.13.2: Effect of methyl-β-cyclodextrin (mβcd) on mesenteric arterial constrictions in response to noradrenaline. Constrictions of pressurised mesenteric arteries from WT $^{(+/+)}$ mice to noradrenaline (Log [NA] -9.0 to -4.5 M) after incubation without and with 0.01M mβcd. Data expressed as mean ± SEM. Analysis by repeated measures, ANOVA (* is $p<0.05$). Bonferroni post test revealed significant differences (# is $p<0.05$) at specific concentrations of noradrenaline.

Further investigations examined the effects of PMCA4 inhibition with AP2 in the presence of mβcd. Mesenteric resistance arteries obtained from WT $^{(+/+)}$ mice were incubated with/without 0.01M mβcd in the presence of and absence of 10μM AP2.

The contractile function of arteries in response to 40mM or to 100mM KPSS was not significantly changed as a result of AP2 incubation in the presence of mβcd. Constrictions (as % of starting diameter) induced by 40mM KPSS after arterial incubation with mβcd = 0.67 ± 0.42% (n=5) and after incubation with AP2+mβcd = 0.81 ± 0.54% (n=5); and induced by 100mM KPSS = 8.99 ± 0.98% (n=5) and 11.39 ± 1.31% (n=5) after mβcd and AP2+mβcd incubation respectively (NS) (figure 3.13.3).

AP2 did not modulate the effect of mβcd on contractile response of mouse mesenteric arteries to stimulation by noradrenaline with dose response curves to noradrenaline being similar between mβcd treated and AP2+mβcd treated arteries (constrictions (as % of starting diameter) to the maximum noradrenaline dose, Log [NA]-4.5M = 32.51 ± 9.54% (n=5) and 35.51 ± 8.41% (n=5), in the presence of mβcd and AP2+mβcd respectively) (figure 3.13.4).

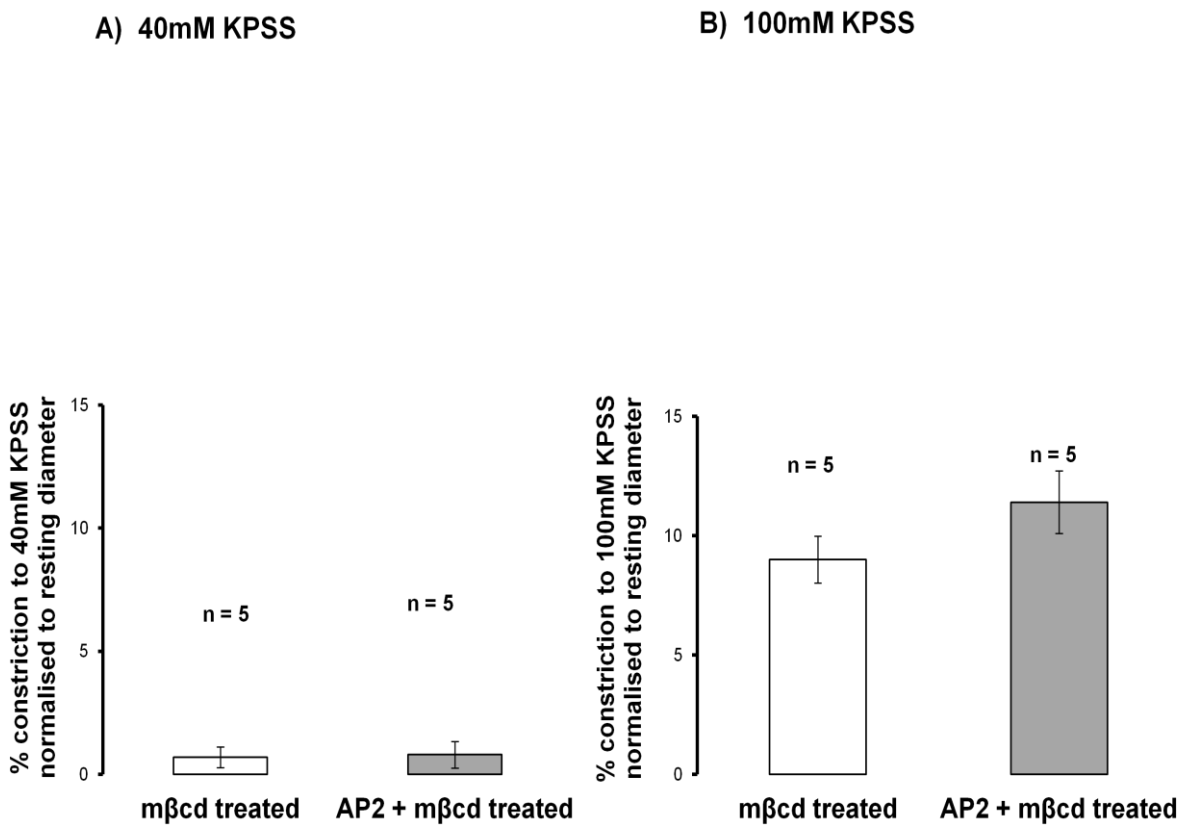

Figure 3.13.3: Effects of AP2+methyl-β-cyclodextrin (mβcd) on mesenteric arterial constrictions in response to 40mM & 100mM KPSS. Constrictions (as % of starting diameter) of mesenteric resistance arteries from WT $^{(+/+)}$ mice following incubation with 0.01M mβcd compared to incubation with 10µM AP2 in the presence of 0.01M mβcd to A) 40mM and to B) 100mM KPSS stimulations. Data presented as mean ± SEM, no significant difference according to unpaired student's t test.

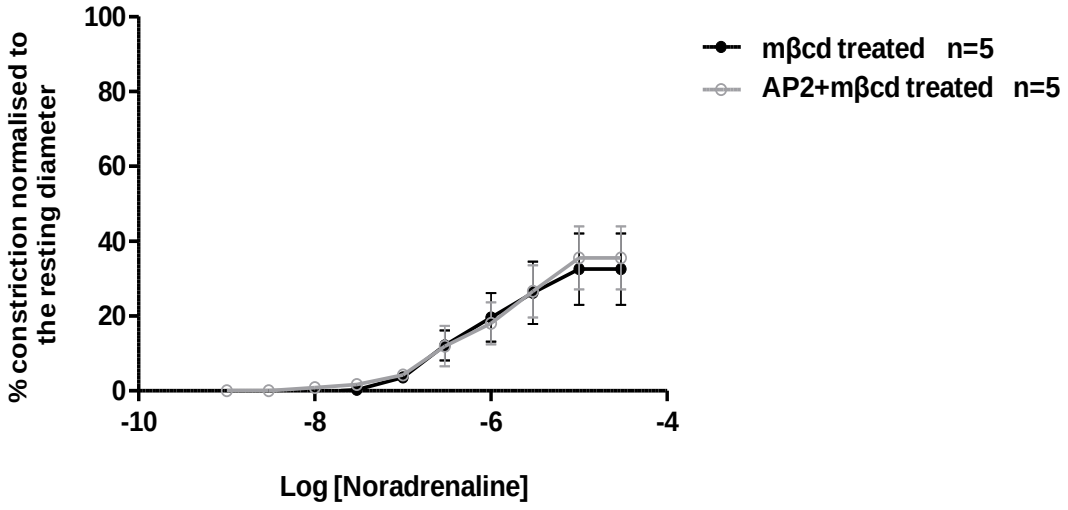

Figure 3.13.4: Effect of AP2+methyl-β-cyclodextrin (mβcd) on mesenteric arterial constrictions in response to noradrenaline. Contractile function of arteries from WT $^{(+/+)}$ mice to noradrenaline (Log[NA] -9.0 to -4.5 M), after incubation with 0.01M mβcd compared to incubation with 10µM AP2 in the presence of 0.01M mβcd. Data expressed as mean ± SEM. Analysis by repeated measures, ANOVA showed no significant difference.

3.14 What are the effects of caloxin 1b1 on arterial contractility?

3.14.1 In response to high potassium solution (KPSS)

Further studies were undertaken to investigate the effect of an alternate PMCA4 inhibitor caloxin 1b1 (Pande *et al.*, 2006). Vessels obtained from WT $^{(+/+)}$ mice were isolated, pressurised and incubated with 100µM caloxin 1b1 for 30 minutes and subjected to high potassium solutions. Control arteries were incubated for 30 minutes in PSS. Experiments were carried out on separate arteries from different mice and these were not paired experiments. While it is acknowledged that the use of equal n numbers would have been advantageous unfortunately limitations in both time and financial resources did not permit this.

Incubation with caloxin 1b1 significantly enhanced constrictions of arteries to 40mM KPSS (constrictions as % of starting diameter = 38.16 $\pm$ 3.23% (n=4) and 55.24 $\pm$ 5.09% (n=3), in the absence and presence of caloxin 1b1 respectively, $p<0.05$) (figure 3.14.1.1). Caloxin 1b1 also resulted in the significant augmentation of the contractile function of arteries isolated from WT $^{(+/+)}$ mice in response to 100mM KPSS (constrictions as % of starting diameter = 59.11 $\pm$ 6.24% (n=4) and 82.21 $\pm$ 3.76% (n=3), in the absence and presence of caloxin 1b1 respectively, $p<0.05$) (figure 3.14.1.1) in contrast to the effects of AP2.

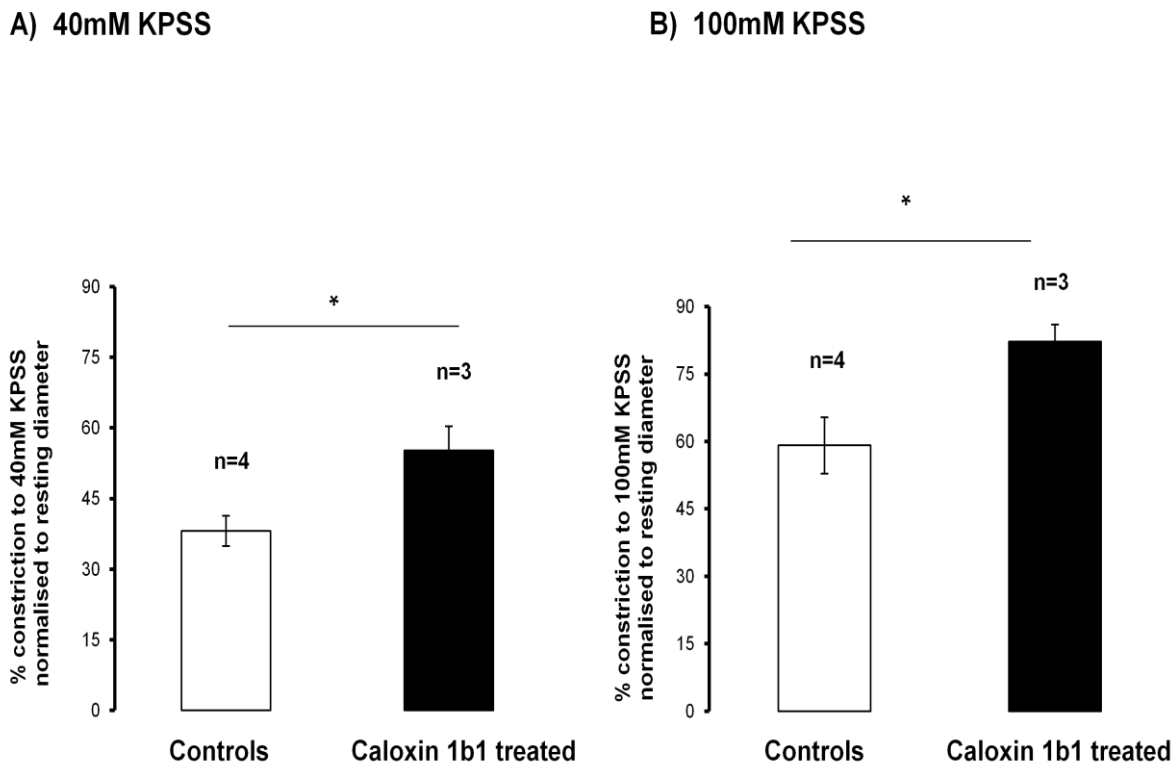

Figure 3.14.1.1: Effects of caloxin 1b1 on mesenteric arterial constrictions in response to 40mM & 100mM KPSS. Constrictions (as % of starting diameter) of isolated, pressurised mesenteric resistance arteries from WT $^{(+/+)}$ mice to A) 40mM and to B) 100mM KPSS stimulations following incubations in PSS (controls) and with100µM caloxin 1b1. Data expressed as mean ± SEM and * is $p<0.05$. Arterial contractile responses to 100mM or 40mM KPSS were significantly augmented, after incubation with 100µM caloxin 1b1 according to an unpaired student's t test.

Caloxin 1b1 was used to further examine mesenteric resistance arterial contractility of vessels isolated from PMCA4 KO $^{(-/-)}$ mice. Pressurised arteries from PMCA4 KO $^{(-/-)}$ were incubated with 100μM caloxin 1b1 for 30 minutes and alternatively in PSS for controls, then subjected to vasoconstrictor stimulants.

Interestingly, caloxin 1b1 treated arteries from PMCA4 KO $^{(-/-)}$ also displayed significantly enhanced constrictions to both 40mM and 100mM KPSS in comparison to untreated arteries (constrictions as % of starting diameter to 40mM KPSS= 48.86 $\pm$ 4.25% (n=7) in the absence of caloxin 1b1 and 62.72 $\pm$ 2.49% (n=4), in presence of caloxin 1b1, $p<0.05$; and constrictions as % of starting diameter to 100mM KPSS= 73.01 $\pm$ 2.49% (n=7) and 84.21 $\pm$ 1.63% (n=4), in the absence and presence of caloxin 1b1 respectively, $p<0.05$) (figure 3.14.1.2).

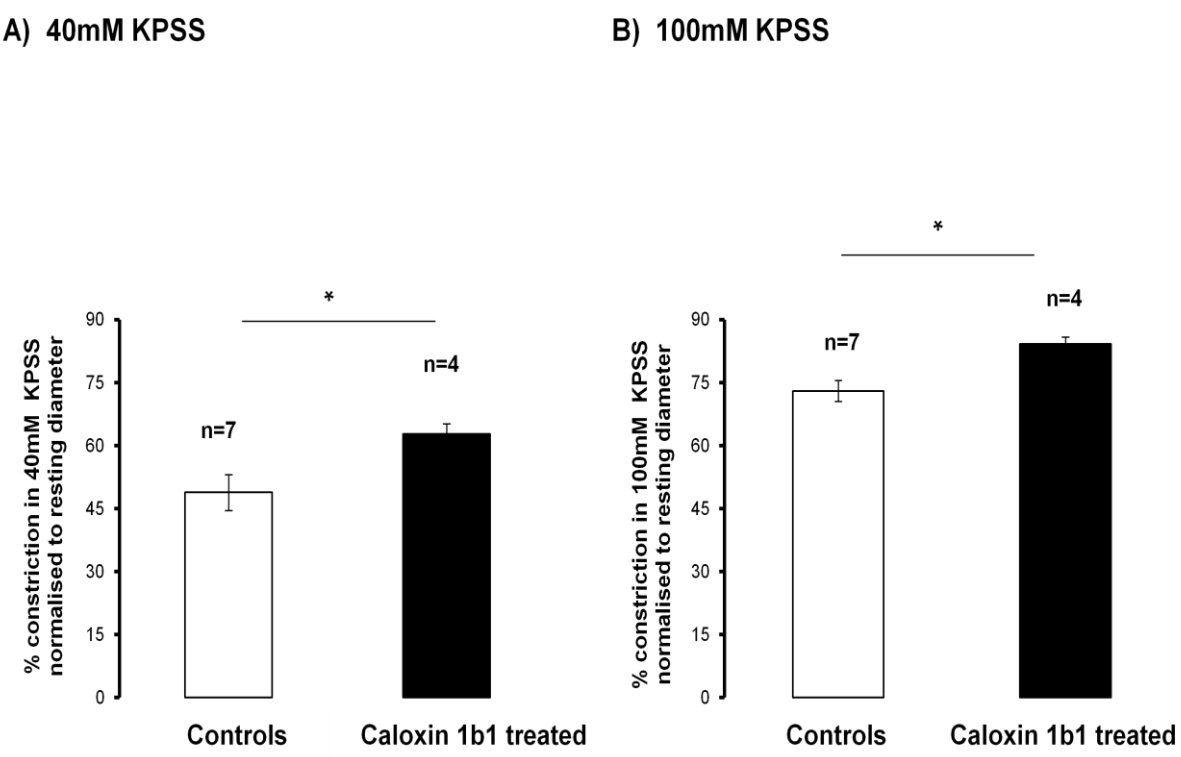

Figure 3.14.1.2: Effects of caloxin 1b1 on the contractility of mesenteric arteries from PMCA4 KO $^{(-/-)}$ mice in response to 40mM & 100mM KPSS. Arterial contractile response (as % of starting diameter) of pressurised mesenteric resistance arteries from PMCA4 KO $^{(-/-)}$ mice to A) 40mM and to B) 100mM KPSS stimulations after incubations in PSS (controls) and with 100µM caloxin 1b1. Data expressed as mean ± SEM and * is $p<0.05$. Constrictions to 100mM or to 40mM KPSS displayed by arteries treated with 100µM caloxin 1b1 were significantly increased, according to an unpaired student's t test.

3.14.2 In response to noradrenaline (NA)

Calxonin1b1 (100µM) significantly increased contractility of arteries from WT $^{(+/+)}$ mice in response to noradrenaline (maximal response to noradrenaline (as a % of starting diameter); 63.10 ± 4.75% (n=4) and 81.23 ± 1.22% (n=3) in the absence and presence of caloxin 1b1 respectively, $p<0.05$) (figure 3.14.2.1).

Caloxin 1b1 also significantly augmented the arterial constriction of arteries from PMCA4 KO $^{(-/-)}$ mice (maximal response to noradrenaline (as a % of starting diameter); 70.30 ± 2.98% (n=4) and 81.56 ± 2.14% (n=4) in the absence and presence of caloxin 1b1 respectively, $p<0.05$) (figure 3.14.2.1).

A) WT (+/+)

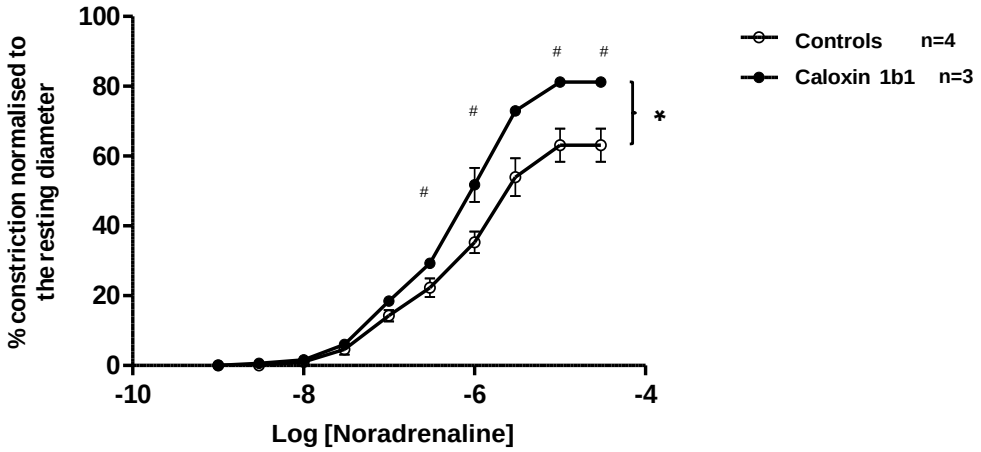

B) PMCA4 KO (-/-)

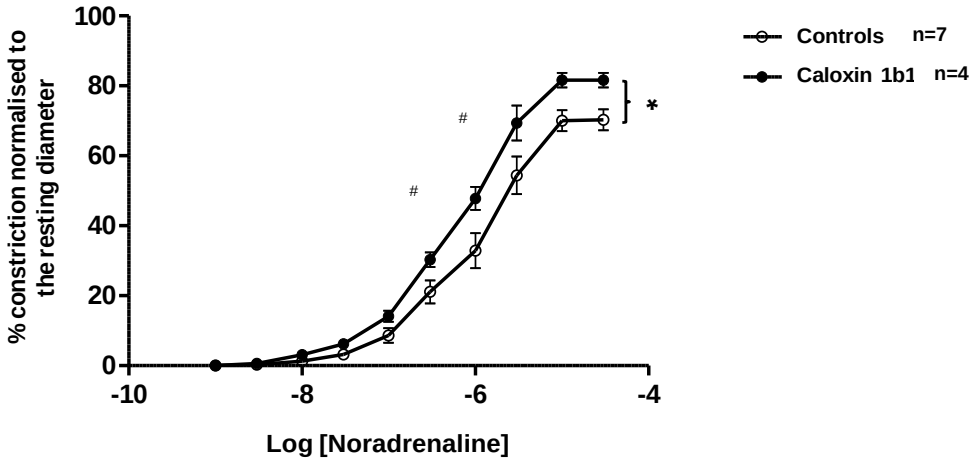

Figure 3.14.2.1: Effects of caloxin 1b1 on the contractility of mesenteric arteries from WT (+/+) and PMCA4 KO (-/-) mice in response to noradrenaline. Constrictions of pressurised mesenteric arteries from A) WT (+/+) mice and from B) PMCA4 KO (-/-) mice in response to cumulative doses of noradrenaline (Log[NA] -9.0 to -4.5 M) in the presence and absence of 100μM caloxin 1b1. Data expressed as mean ± SEM. Analysis by repeated measurements, ANOVA (* is $p<0.05$). Bonferroni post test showed significant differences (# is $p<0.05$) at specific Log concentrations of noradrenaline.

Chapter 4

Discussion

The physiological contribution of PMCA4 to vascular function is still under consideration and this study has employed PMCA4 KO $^{(-/-)}$ mice and a newly identified PMCA4 inhibitor, AP2 to address this conundrum in isolated mouse arteries. One of the main findings emerging from this study was, while PMCA4 ablation had no effect on the functional responses of pressurised mesenteric resistance arteries to different exogenously added vasoconstrictors, inhibition with AP2 significantly reduced arterial contractility an effect attributed to a nNOS-dependent mechanism. Global assessments of $[Ca^{2+}]_i$, within intact pressurised mesenteric arteries (using the Ca^{2+} indicator, indo-1) demonstrated no effect of PMCA4 ablation on resting or stimulated (KPSS or noradrenaline) $[Ca^{2+}]_i$, however, the rise in global $[Ca^{2+}]_i$ in response to vasoconstrictors was significantly attenuated by PMCA4 inhibition with AP2. The results of this study have also demonstrated that vasoconstrictor-mediated constrictions of arteries from both PMCA4 WT $^{(+/+)}$ and KO $^{(-/-)}$ mice were significantly enhanced by the presence of caloxin 1b1 (a commercially available PMCA4 inhibitor) an effect which is opposite to that of AP2 in arteries from WT $^{(+/+)}$ mice. Finally, a reduction in arterial wall distensibility was found in mesenteric resistance arteries from PMCA4 KO $^{(-/-)}$ mice in comparison to those obtained from PMCA4 WT $^{(+/+)}$ mice.

4.1 Confirmation of the presence and absence of PMCA4 in WT $^{(+/+)}$ an KO $^{(-/-)}$ mouse tissues and localisation of PMCA4 in mouse aortas

The presence of PMCA4 has previously been demonstrated in smooth muscles of mammalian non-vascular tissues including bladder, uterine, intestine and heart (El-Yazbi *et al.*, 2008; Hammes *et al.*, 1998; Hammes *et al.*, 1994; Liu *et al.*, 2007; Liu *et al.*, 2006; Matthew A *et al.*, 2004; Stauffer *et al.*, 1993). Additionally, the presence of PMCA4 has also been widely reported in VSM cells (Afroze *et al.*, 2003; Husain *et al.*, 1997; Pande *et al.*, 2006; Pande *et al.*, 2008; Schuh *et al.*, 2003; Szewczyk *et al.*, 2007). In the present study immunohistochemical analysis carried out on aortic sections confirmed that PMCA4 was present in the mouse vasculature and further showed that it was absent in the vasculature of PMCA4 KO $^{(-/-)}$ mice. Due to the ubiquitous expression of PMCA4 in most mammalian tissues and its abundance in the brain (Guerini, 1998; Sepulveda *et al.*, 2006; Stahl *et al.*, 1992; Stahl *et al.*, 1994; Stauffer *et al.*, 1995; Zylinska *et al.*, 2000) whole brain preparations were selected in this study for further analysis by Western blotting. This showed that while PMCA4 was abundant in brains from PMCA4 WT $^{(+/+)}$ mice it was not present in whole brain preparations from PMCA4 KO $^{(-/-)}$ mice. Coupled with PCR genotyping, these studies confirmed successful PMCA4 ablation in tissues from PMCA4 KO $^{(-/-)}$ mice. This is in keeping with previous results obtained by other members of the research group who also demonstrated PMCA4 was ablated in mouse testis and sperm (Schuh *et al.*, 2004) as well as in cardiac tissue and cardiomyocytes of PMCA4 KO $^{(-/-)}$ mice (analysed via Western blotting and immunofluorescence respectively) (Cartwright *et al.*, 2011a; Mohamed *et al.*, 2011b).

In the present study, co-immunostaining of isolated aortic sections from PMCA4 WT $^{(+/+)}$ and KO $^{(-/-)}$ mice with antibodies against PMCA4 and smooth muscle α-actin /CD34 (the endothelial marker) showed localisation of PMCA4 to the VSM but not to the endothelium of arteries from PMCA4 WT $^{(+/+)}$ mice. These results are consistent with previous RT-PCR analysis in cultured endothelial cells which failed to demonstrate the presence of PMCA4 (Pande *et al.*, 2006; Szewczyk *et al.*, 2007) and with previous studies which have shown, using both RT-PCR and immunohistological examination, that PMCA4 is expressed in mammalian aortic smooth muscle (Pande *et al.*, 2006; Schuh *et al.*, 2003), as well as in other smooth muscles namely that of the bladder (Liu *et al.*, 2006). Although the aim of my original study was to examine the presence and distribution of PMCA4 in sections of mouse mesenteric resistance arteries by immunohistochemistry this was not possible due to the technical difficulties encountered (as described in methods) and time constraints, hence aortic sections were used as an alternative. While it is accepted that one cannot be totally sure of the distribution of PMCA4 within the resistance vasculature the similar arrangement of the intima layer (containing the endothelium) in large and small resistance arterial walls (Martinez-Lemus *et al.*, 2009; Megens *et al.*, 2007; Rhodin *et al.*, 1980), and previous observations by others (Pande *et al.*, 2006; Schuh *et al.*, 2003) support our findings that PMCA4 is abundant in VSM and not endothelial cells.

4.2 Effects of PMCA4 ablation on arterial contractility and global $[Ca^{2+}]_i$

The results presented in this study have shown that ablation of PMCA4 had no effect on the contractile responses to KPSS/noradrenaline neither did this affect the levels of global $[Ca^{2+}]_i$ in resting and in KPSS/noradrenaline-stimulated mesenteric arteries. There have been no other studies which have investigated the effects of PMCA4 ablation on contractile responses of VSM however there have been assessments of smooth muscle contractility and $[Ca^{2+}]_i$ in the bladder smooth muscle from PMCA4 KO $^{(-/-)}$ mice towards carbachol and KCl (80mM) (Liu *et al.*, 2007; Liu *et al.*, 2006). In agreement with the responses observed in PMCA4 ablated mesenteric arteries to KPSS in this study, the contractile responses of PMCA4 ablated bladder smooth muscles to KCl were also not significantly different to those from WT $^{(+/+)}$ mice as were the KCl stimulated rises in global $[Ca^{2+}]_i$ (Liu *et al.*, 2007). However, the rise in global $[Ca^{2+}]_i$ and the contractile responses elicited by bladders from PMCA4 KO $^{(-/-)}$ mice to carbachol were reduced compared to those from WT $^{(+/+)}$ controls (Liu *et al.*, 2007). Even though carbachol has not been used in the present study, arterial responses to a different type of receptor-mediated agonist, noradrenaline were shown to be unaffected by the ablation of PMCA4. The reasons for these differences are unknown but may suggest that the ablation of PMCA4 may have differing effects on contractile responses elicited by different smooth muscle tissues and this may depend on the type of contractile stimuli. In the present study PMCA4 ablation had no effect on the fall in force and decline in global $[Ca^{2+}]_i$ upon PSS washout of pre-constricted mesenteric arteries (relaxation). This is not consistent with a previous study which observed prolonged relaxation times in PMCA4 ablated bladder smooth muscles following washout of pre-constricted bladders (to KCl) with Ca^{2+}-free PSS suggesting that PMCA4 plays a role in Ca^{2+}

extrusion in this tissue (Liu *et al.*, 2006). Indeed previous studies using different smooth muscles from PMCA4 KO $^{(-/-)}$ mice have reported that PMCA4 contributes significantly to Ca^{2+} efflux in bladder and uterine smooth muscles respectively (Liu *et al.*, 2006; Matthew *et al.*, 2004). These previous data are in contrast to the results generated in this study which do not support a role for PMCA4 as an extruder of gross Ca^{2+} in the vasculature. Thus, the observed effect of genetic ablation of PMCA4 on the rate of Ca^{2+} decay and/or on Ca^{2+} efflux may be distinct in vascular and non-vascular smooth muscle types.

An alternative approach previously taken to investigate the physiological relevance of PMCA4 in the vasculature has been with PMCA4 inhibitor peptides called caloxins (1b1 and 1c2) (Pande *et al.*, 2006; Pande *et al.*, 2008). Previous studies using caloxin peptides showed these inhibitors enhanced contractile responses of isolated rat aorta and porcine coronary arteries to exogenous addition of KCl (Pande *et al.*, 2006; Pande *et al.*, 2008) which was attributed to increased global $[Ca^{2+}]_i$ in VSM cells (Pande *et al.*, 2006). These data do seem to reflect the expectations of inhibiting a Ca^{2+} extrusion pump in the vasculature and may be consistent with PMCA4 functioning as a Ca^{2+} extrusion pump. A role for PMCA in Ca^{2+} extrusion in rat cerebral arteries has previously been suggested but there has been no direct evidence to support this (Kamishima *et al.*, 1998). Hence, the results achieved with PMCA4 inhibition by caloxin peptides in the vasculature are completely different to those we have demonstrated following the ablation of PMCA4.

Thus far, the only other approach to have addressed the effects of modulating PMCA4 expression on vascular function has been by *in vitro* studies of isolated mouse aortas and mesenteric arteries from mice overexpressing PMCA4 in the VSM (Gros *et al.*, 2003; Schuh *et al.*, 2003). This has been performed by two different

research groups who have demonstrated that overexpression of PMCA4 in mice caused an increase in arterial constrictions to KCl (Schuh *et al.*, 2003) as well as in vascular sensitivity to phenylephrine and in the myogenic contractile responses to elevations in intravascular pressure (Gros *et al.*, 2003). Although it must be acknowledged that effects on myogenic responsiveness were not investigated in the present study, the functional consequences of PMCA4 overexpression are clearly not opposite to the effects of ablating PMCA4 in mesenteric arteries. Overexpression of PMCA4 however, did not modulate basal $[Ca^{2+}]_i$ in isolated aortic smooth muscle cells (Gros *et al.*, 2003) supporting the results of the present study that modulation of PMCA4 expression does not influence global $[Ca^{2+}]_i$.

After a series of *in vitro* experiments in which nNOS/NOS activity was depressed the effects of PMCA4 overexpression on arterial contractility were attributed to the regulatory role of PMCA4 on nNOS activity (Gros *et al.*, 2003; Schuh *et al.*, 2003). Aortic rings from WT $^{(+/+)}$ mice treated with the NOS inhibitor (N^G-nitro-L-arginine methyl ester (L-NAME)) or the nNOS selective inhibitor N^{ω}-propyl-$_L$-arginine and those from nNOS knockout mice showed significant increases in contractility indicating that nNOS can modulate arterial contractility (Schuh *et al.*, 2003); (Gros *et al.*, 2003). NOS inhibition had no effect on the contractile activity of arteries from PMCA4 overexpressing mice (Gros *et al.*, 2003; Schuh *et al.*, 2003) indicating that nNOS activity (i.e. NO synthesis) was depressed in PMCA4 overexpressing mice. This gives strength to the hypothesised signal transduction role for PMCA4 in downregulating nNOS activity by the formation of a PMCA4-PDZ mediated complex with nNOS which has been identified in kidney and neuronal cellular systems as well as the heart (Cartwright *et al.*, 2007; Cartwright *et al.*, 2005; DeMarco *et al.*, 2001; Mohamed *et al.*, 2009; Oceandy *et al.*, 2007; Williams *et al.*,

2006). In the present study, inhibition of all NOS isoforms by LNNA had no effect on the KPSS/noradrenaline-stimulated arterial constrictions of mesenteric arteries obtained from both PMCA4 KO $^{(-/-)}$ and WT $^{(+/+)}$ mice. The lack of significant effect of LNNA on agonist-induced constrictions of mesenteric arteries from WT $^{(+/+)}$ mice is consistent with previous reports by our group and others (Cooke *et al.*, 2003; Hausman *et al.*, 2011). Thus, unlike overexpression of PMCA4, inhibition of NOS has no effect on contractile responses of arteries from PMCA4 KO $^{(-/-)}$ mice.

PMCA4 has been localised to VSM not endothelial cells (results of the present study; (Pande *et al.*, 2006; Szewczyk *et al.*, 2007)), but nNOS has been reported in both endothelial and VSM cells (Bachetti *et al.*, 2004; Boulanger *et al.*, 1998; Cheah *et al.*, 2002; Segal *et al.*, 1999), thus the effects of PMCA4 ablation on endothelial-dependent responses were investigated. The results of the present study show no differences between the endothelial-dependent dilations to acetylcholine displayed by mesenteric arteries from WT $^{(+/+)}$ mice in comparison to those from PMCA4 KO $^{(-/-)}$ mice. Even though, NO modulated the KCl-induced contractile responses of arteries from transgenic mice overexpressing PMCA4, it had no effect on the endothelium dependent responses of aortic rings to acetylcholine (Schuh *et al.*, 2003). This would suggest that nNOS does not normally contribute to acetylcholine-dependent dilation. We acknowledge that in the present study all mesenteric arteries obtained from both PMCA4 WT $^{(+/+)}$ and KO $^{(-/-)}$ mice exhibited small endothelium dependent dilations (under 35%) to acetylcholine. Although the reasons for this are uncertain it is possible that the delicate endothelial layer may have been damaged during the vessel mounting stages of the protocol, because other *in vitro* pressure myography studies have achieved larger acetylcholine dependent dilations in mouse mesenteric arteries (Beleznai *et al.*, 2011; Stoyanova *et al.*, 2012; Waldron *et al.*,

1999). However the level of dilation observed in the present study was similar to that reported by other colleagues in our group using mouse mesenteric arteries even when an endothelial layer was established by electron microscopy (Hausman *et al.*, 2011). As a preliminary control, one was able to obtain larger acetylcholine-dependent dilations (>35%) in isolated, pressurised mesenteric resistance arteries obtained from wistar rats, showing that I was able to mount small arteries whilst maintaining endothelial integrity. Since, this study and others have shown PMCA4 expression was localised in the VSM (Pande *et al.*, 2006; Schuh *et al.*, 2003) and not the endothelium of the mouse vasculature (Pande *et al.*, 2006) this did not interfere with the assessments of the effects of PMCA4 on arterial smooth muscle contractile function. In the present study the results have also showed similar dilations in arteries from PMCA4 KO $^{(-/-)}$ and WT $^{(+/+)}$ mice in response to exogenous NO donation by sodium nitroprusside thus suggesting that PMCA4 ablation does not alter the sensitivity of VSM to NO. Previously it has also been demonstrated that the overexpression of PMCA4 does not modulate endothelium-independent dilations of arteries to sodium nitroprusside (Schuh *et al.*, 2003) again suggesting that modulation of PMCA4 expression does not change the sensitivity of VSM to NO. Hence the results of the present study and those in the literature suggest that genetic ablation of PMCA4, inhibition with caloxins and alternatively transgenic overexpression of PMCA4 in mammalian arteries have distinct effects on vascular contractility and may modulate contractility by either changes in global $[Ca^{2+}]_i$ or by modulation of nNOS signal transduction. The reasons for these differences are unclear, however one possibility could be that modulation of the expression of PMCA4 changes the expression or activity of other calcium regulatory proteins in the vasculature.

In the present study, Western blotting demonstrated that ablation of PMCA4 had no significant effects on the protein expression levels of PMCA1, SERCA and NCX in mouse aortic preparations (from PMCA4 KO $^{(-/-)}$ mice versus WT $^{(+/+)}$ mice). It is acknowledged that the expression of other Ca^{2+} handling proteins such as IP_3R and L-type Ca^{2+} channels have not been investigated mainly because of time and financial restrictions of the project. Previous studies by our group have also demonstrated that the expression of PMCA1, SERCA2, NCX and L-type Ca^{2+} channel were not modified in the myocardium of the PMCA4 KO $^{(-/-)}$ mice developed by our group (Mohamed et al 2011). Western blot analysis of bladder smooth muscles also showed the expression of PMCA1, SERCA and NCX were unchanged in bladders obtained from PMCA4 KO $^{(-/-)}$ mice (Liu *et al.*, 2006). Therefore knocking out PMCA4, is not associated with any changes in the expression of other Ca^{2+} extrusion proteins as demonstrated in this study and in (Liu *et al.*, 2006). It is acknowledged that in this study the activity of these Ca^{2+} handling proteins were not investigated and indeed their expressions have been investigated in aortic tissue rather than in mesenteric arteries. Although the original aim was to use mesenteric arteries for Western blotting I experienced significant problems relating to the limited amount of protein which could be extracted. Due to time limitations it was decided to use aortic tissues which provided more protein and indeed detection of Ca^{2+} regulatory proteins including NCX1 and IP_3R1 (by Western blotting or quantitative PCR) have revealed similar expression patterns in both aortas and mesenteric arteries (Grayson *et al.*, 2004; Zhang *et al.*, 2010a). If time had permitted an alternative approach would have been to examine the mRNA expression levels of namely PMCA1, SERCA and NCX, (as well as other Ca^{2+}-regulatory genes) in freshly isolated aortas and/or in cultured VSM cells of PMCA4 KO $^{(-/-)}$ mice via the

real time PCR (RT-PCR) technique similar to the protocol used in previously study (Gros *et al.*, 2003). Currently, as the evidence suggests that ablation of PMCA4 does not modulate the expression of other Ca^{2+} handling proteins, it is unlikely that the differing effects observed due to ablating and inhibiting PMCA4 with caloxins can be explained by this. An alternative explanation relates to the specificity of caloxins, the only previously used selective inhibitors of PMCA4 to investigate its effects in the vasculature.

4.3 Effects of PMCA4 inhibition with AP2 on arterial contractility and on global $[Ca^{2+}]_i$

There have been very few studies which have investigated the effect(s) of PMCA4 inhibition on arterial function. This has mainly been because of the very limited availability of commercial inhibitors selective for PMCA4 (with the exception of caloxins), hence there is a need for the development of more inhibitors specific to PMCA4. Ongoing research in Ludwig Neyses's group has identified a novel pharmacological inhibitor of PMCA4 called AP2. This was recently identified during an extensive library screening process of medically optimised drugs in a colorimetric ATPase assay and is known to have an IC_{50} of 0.15µM for PMCA4 and 5µM for SERCA (Abou-Leisa *et al.*, 2011; Cartwright *et al.*, 2011a; Mohamed *et al.*, 2011a). Inhibition profiling of AP2 showed that, at this IC_{50} concentration, AP2 inhibited SERCA, PMCA1 and NKA by less than 20% (Abou-Leisa *et al.*, 2011; Mohamed *et al.*, 2011a). Due to the incompletion of the patenting process of AP2 there are currently few published data on this PMCA4 inhibitor. Nevertheless, the Neyses group have performed several preliminary analysis of AP2 to support its selectivity for PMCA4 over PMCA1 some of which can be disclosed. AP2 has been shown to cause sperm immotility in male wild type mice (unpublished data by Ludwig Neyses and Elizabeth Cartwright group, University of Manchester, UK), a classic phenotype present in both generated strains of male PMCA4 KO $^{(-/-)}$ mice which are infertile (Okunade *et al.*, 2004; Schuh *et al.*, 2004). Furthermore, injection of AP2 in mice has an anti-hypertrophic effect as was observed in PMCA4 ablated mice (Abou-Leisa *et al.*, 2011; Cartwright *et al.*, 2011a; Mohamed *et al.*, 2011a). The present study investigated, for the first time, the effects of AP2 on mesenteric resistance arterial contractility.

The results presented in this study revealed that the PMCA4 inhibitor AP2 (10µM) significantly reduced the constrictions of mesenteric arteries obtained from WT $^{(+/+)}$ mice in response to both KPSS (100mM) and noradrenaline. Further assessments of global $[Ca^{2+}]_i$ within intact pressurised mesenteric arteries also revealed AP2 (10µM) significantly decreased the rise in global $[Ca^{2+}]_i$ in response to KPSS (100mM) or noradrenaline, which align with the aforementioned attenuation in arterial contractility due to AP2. It is acknowledged that the effects of AP2 on arterial constrictions and on stimulated $[Ca^{2+}]_i$ in response to 40mM KPSS observed in this study did not reach a statistical level of significance, however the significant effects of AP2 in arteries responding to 100mM KPSS and noradrenaline show that AP2 and inhibition of PMCA4, reduces arterial contractility. These findings are in direct contrast to the earlier studies which have used the caloxin peptides (1b1 and 1c2) to inhibit PMCA4 which demonstrated significant increases in arterial contractile responses (Pande *et al.*, 2006; Pande *et al.*, 2008; Szewczyk *et al.*, 2008) associated with enhanced levels of global $[Ca^{2+}]_i$ in VSM cells (Pande *et al.*, 2006). Thus inhibition of PMCA4 with AP2 has a different effect on arterial contractility than inhibition of PMCA4 with caloxins. The reasons for these differences are unclear but differences in the specificity and mechanism of action of these inhibitors are possible reasons.

To date there have been three different caloxin peptides reported as selective PMCA4 inhibitors, namely peptide 2a1, 1b1 and 1c2 which are known to act on an extracellular domain of PMCA4 (Pande *et al.*, 2006; Pande *et al.*, 2008; Szewczyk *et al.*, 2008). Out of the caloxin peptides currently commercially available the most specific for PMCA4 is peptide 1b1, considered to be 10x more potent than the earliest discovered 2a1 (Pande *et al.*, 2006). In the present study the effects of

caloxin 1b1 on the constriction of mesenteric arteries obtained from WT $^{(+/+)}$ mice was investigated. As has been previously reported (Pande *et al.*, 2006), caloxin 1b1 (100µM) significantly increased the constriction of mesenteric arteries from PMCA4 WT $^{(+/+)}$ to noradrenaline, however, caloxin 1b1 had a similar effect in arteries from PMCA4 KO $^{(-/-)}$ mice therefore suggesting that its effects on contractility were independent of PMCA4. Caloxin 1b1 has been shown to inhibit the activity of PMCA4 at a K_i of approximately 46µM in erythrocytes and PMCA1 at around 105µM, in embryonic kidney cells (Pande *et al.*, 2006). However, the significant increases $[Ca^{2+}]_i$ shown in both endothelial and VSM cells and arterial contractility were with experimental use of caloxin 1b1 at 200µM (Pande *et al.*, 2006). It is possible that the effect seen with caloxin 1b1 at 200µM may be due to effects on PMCA1. While PMCA4 has been shown to have a prominent role in signal transduction (Cartwright *et al.*, 2007; Gros *et al.*, 2003; Liu *et al.*, 2007; Oceandy *et al.*, 2007; Oceandy *et al.*, 2011; Schuh *et al.*, 2003), PMCA1 is believed to play a more important role in Ca^{2+} clearance and/or modulation of $[Ca^{2+}]_i$ (Kobayashi *et al.*, 2012; Liu *et al.*, 2007). Moreover, studies that have reported a link between PMCA and enhanced Ca^{2+} efflux and/or decreased $[Ca^{2+}]_i$ within VSM cells have attributed these effects to increased mRNA and/or protein expression levels of PMCA1 (Husain *et al.*, 1997; Monteith *et al.*, 1996; Monteith *et al.*, 1997). Most recently, characterisation of the newly developed VSM specific PMCA1 knockout mice showed increased contractile responses in the isolated arteries and increased $[Ca^{2+}]_i$ under basal and agonist-stimulated conditions in cultured VSM cells of this model (Kobayashi *et al.*, 2012). These phenotypes are clearly similar to the observed effects of caloxins in the vasculature of WT $^{(+/+)}$ mice (Pande *et al.*, 2006; Pande *et al.*, 2008). Thus, if the caloxin PMCA4 inhibitors were also acting on PMCA1 (the more

significant Ca^{2+} clearance isoform in smooth muscle (Liu *et al.*, 2007)), this could offer an explanation for the increased contractile responses elicited by arteries treated with caloxins as was observed by others (Pande *et al.*, 2006; Pande *et al.*, 2008; Szewczyk *et al.*, 2008) and in this study. Though, it must be acknowledged that the caloxin 1b1 peptide used in our experiments is not currently considered to be the most specific for PMCA4 it is the only one commercially available and thus accessible to us. Caloxin 1c2 is now thought to be the most specific of the peptides and has a 20x higher affinity for PMCA4 than 1b1 (with a K_i for PMCA4 corresponding to 2.3μM), though it had a similar effect on vascular contractile function to caloxin 1b1, when it was used on coronary arteries. (Pande *et al.*, 2008).

In the present study it was demonstrated that AP2 (10μM) did not have any effects on KPSS and noradrenaline-induced constrictions of mesenteric arteries from PMCA4 KO $^{(-/-)}$ mice. This would suggest that AP2 does not modulate arterial contractility by affecting the activity of other ATPases present in the vasculature independent of its effects on PMCA4. Although, it must be acknowledged that the precise site of action of AP2 on the PMCA4 protein is currently unknown and that the AP2 dose utilised in this study was greater than its IC_{50} value for PMCA4 it was chosen as this was similar to that which has been previously used in cardiac tissues in our laboratory that showed an antihypertrophic effect in cardiomyocytes (Abou-Leisa *et al.*, 2011; Mohamed *et al.*, 2011a). However, additional investigations with a lower concentration of AP2 (1μM) also resulted in a significant reduction in arterial constrictions of arteries from WT $^{(+/+)}$ mice in response to noradrenaline, complimentary to the results achieved with the higher AP2 concentration (10μM) and the lack of effect of AP2 on arteries from PMCA4 KO $^{(-/-)}$ mice. Thus, the results of the present study support the notion that AP2 modulates arterial contractility via

effects on PMCA4. In contrast, caloxin 1b1 appears to modulate arterial contractility by PMCA4-independent mechanisms.

Furthermore in this study global assessments of $[Ca^{2+}]_i$ within intact pressurised mesenteric arteries from WT $^{(+/+)}$ mice after PMCA4 inhibition by AP2, showed that AP2 had no effect on the level of basal $[Ca^{2+}]_i$. This effect was similar to that seen in the PMCA4 ablated mesenteric arteries as previously described and also to the effect of PMCA4 overexpression on basal $[Ca^{2+}]_i$ levels in unstimulated aortic smooth muscle cells (Gros *et al.*, 2003). In addition, this study has shown PMCA4 inhibition by AP2 had no significant effect on the decline in force and in global $[Ca^{2+}]_i$, following PSS washout of KPSS or noradrenaline in pre-constricted arteries. AP2 also had no effect on the relaxation times elicited by pre-constricted arteries following agonist washout. Collectively these data are similar to the effects seen in the PMCA4 ablated mesenteric arteries supporting the notion that alteration of PMCA4 either by ablation or inhibition with AP2 does not directly modulate the rate of Ca^{2+} decay or decline in contractile force exhibited by pre-constricted arteries in response to vasoconstrictor washout. The ablation, inhibition and overexpression of PMCA4 had no effects on basal levels of global $[Ca^{2+}]_i$ in VSM cells (as shown in the present study and (Gros *et al.*, 2003)), therefore implying that PMCA4 may not contribute substantially to the bulk regulation of global $[Ca^{2+}]_i$ in VSM cells. This is similar to cardiac cells where PMCA4 has been shown not to play a significant role in the removal of global Ca^{2+} (Hammes *et al.*, 1998; Mohamed *et al.*, 2011b).

As studies in mice overexpressing PMCA4 showed that PMCA4 could modulate arterial constriction by a signal transduction role in regulating nNOS (Gros *et al.*, 2003; Schuh *et al.*, 2003) the present study examined whether the effects of AP2 on arterial constriction were also mediated via nNOS. It was found that AP2 had no

effect on arterial constrictions in the presence of the nNOS or NOS inhibitors (VLN and LNNA respectively) implying that the effects of PMCA4 inhibition were indeed due to modulation of nNOS activity. Indeed the potential PMCA4-nNOS modulation is now well supported by studies in a number of different cellular systems and tissues (Cartwright *et al.*, 2007; Gros *et al.*, 2003; Oceandy *et al.*, 2007; Schuh *et al.*, 2003; Schuh *et al.*, 2001; Williams *et al.*, 2006). Immunohistochemical analyses have shown that both PMCA4 and nNOS are found in vascular smooth muscle of aortas from our mice as has also been shown previously by other vascular researchers (Schuh *et al.*, 2003). Therefore the results of the present study suggest that AP2 modulates arterial constriction by modulation nNOS activity and thereby NO bioavailability. Previous studies show that NO sourced from nNOS is physiologically important in regulating microvascular tone in both human arteries (Melikian *et al.*, 2009; Seddon *et al.*, 2009) and mouse mesenteric arteries (Gros *et al.*, 2003). The precise mechanism by which PMCA4 modulates nNOS activity is not yet fully understood however, it has been hypothesised that PMCA4 activity may decrease local (or sub-cellular) $[Ca^{2+}]_i$ closely apposed to nNOS (which is Ca^{2+}-dependent), and thus downregulate its activity (Cartwright *et al.*, 2007; Oceandy *et al.*, 2007; Oceandy *et al.*, 2011). Interestingly in the present study the decrease in constrictions to both KPSS and noradrenaline in the presence of AP2 were accompanied by a reduction in the rise of global $[Ca^{2+}]_i$. No such changes were observed when nNOS was inhibited (with VLN), hence suggesting that the effects of AP2 on global $[Ca^{2+}]_i$ in response to vasoconstrictors were due to NO rather than any Ca^{2+} regulatory properties of PMCA. NO can modulate vascular constriction in numerous ways with the underlying mechanism of action being primarily through NO interacting with soluble guanylyl cyclase (sGC), which activates the enzyme to

increase cyclic GMP (cGMP) production (Cary *et al.*, 2006; Gao, 2010; Hall *et al.*, 2009; Morgado *et al.*, 2012; Orallo, 1996). Elevated levels of cGMP activate the cGMP-dependent protein kinase (PKG) which reduces VSM tone mainly by the inhibition of Ca^{2+} mobilisation mechanisms, including Ca^{2+} entry across the plasma membrane and/or Ca^{2+} release by IP_3Rs on internal SR stores, in VSM cells (Francis *et al.*, 2005; Gao, 2010; Morgado *et al.*, 2012; Rembold, 1992; Schlossmann *et al.*, 2000). Increased levels of cGMP can also desensitise the contractile myofilaments in VSM cells towards $[Ca^{2+}]_i$ due to effects on MLCK and MLCP activity in favour of a decrease in vascular tone (Morgado *et al.*, 2012; Orallo, 1996; Woodrum *et al.*, 2001). Furthermore, in VSM of various blood vessels cGMP has been shown to inhibit L-type Ca^{2+} channel activity (Ishikawa *et al.*, 1993; Liu *et al.*, 1997; Taguchi *et al.*, 1997), thought to be the most important route for Ca^{2+} influx into VSM cells. Thus, NO/cGMP signalling events can reduce global $[Ca^{2+}]_i$ levels of VSM cells and thereby lead to inhibition of VSM contractility in response to contractile stimuli (Cary *et al.*, 2006; Gao, 2010; Hall *et al.*, 2009; Morgado *et al.*, 2012; Orallo, 1996). NO itself also has the capacity to exert an anti-contractile effect on arteries independently of NO/cGMP signalling, mainly via pathways ending in the decrease of $[Ca^{2+}]_i$ in VSM cells. One pathway is via enhancing BK_{Ca} activity, resulting in VSM cell membrane hyperpolarisations, which reduces Ca^{2+} influx through VOCCs and the other is by stimulating Ca^{2+} uptake through SERCA into SR stores, both having adverse effects on levels of $[Ca^{2+}]_i$ (Adachi *et al.*, 2004; Bolotina *et al.*, 1994; Gao, 2010). One may hypothesise that augmentation of at least one/all of these NO-mediated signalling mechanisms may have been triggered by increased NOS activity (mediated by the PMCA4-nNOS complex) in VSM cells of arteries treated with AP2 and may contribute to the decrease in global $[Ca^{2+}]_i$ elevations and arterial

constrictions in response to contractile stimuli. In the future the use of appropriate enzyme assay technique(s) to check the levels of cGMP and/or nNOS activity (i.e. NO production) in mouse arteries after AP2 treatment would be important in expanding this project further.

In summary the results of the present study show that inhibition of PMCA4 with AP2 can modulate arterial contractility by effects on nNOS activity as has been reported in PMCA4 overexpressing mice (Gros *et al.*, 2003; Schuh *et al.*, 2003). It has also demonstrated that the different effects of caloxin 1b1 on arterial contractility are most likely due to non-specific effects of the peptide. In contrast, ablation of PMCA4 had no effect on vascular constrictions. The reasons why ablation and inhibition of PMCA4 with AP2 differentially affect vascular constriction are unknown but one possibility relates to the localisation of PMCA4-nNOS complex within the VSM cells.

4.4 Disruption of caveolae does not modulate the anti-contractile effect of AP2 on arterial contractility

Studies on cardiac muscle have proposed that the PMCA4-nNOS complex is mainly restricted to sub-cellular compartments (i.e. to plasma membrane microdomains) (Cartwright *et al.*, 2007; Mohamed *et al.*, 2011b; Oceandy *et al.*, 2011). In VSM, cyclic nucleotides (important mediators of NO-signalling cascades) have also been reported to be compartmentalised (Ostrom *et al.*, 2002; Rybalkin *et al.*, 2003). This restricts their signalling to specific sub-cellular regions, for example, to caveolin-rich domains following local increases in cyclic nucleotides (Ostrom *et al.*, 2002; Rybalkin *et al.*, 2003). Caveolae are caveolin-rich domains of small membraneous invaginations and due to their enrichment in a variety of other proteins, receptors and channels including those involved in Ca^{2+} regulation, are believed to participate in co-ordinating various cellular signal transduction pathways such as those involved in arterial contraction (Bergdahl *et al.*, 2004; Brainard *et al.*, 2005; El-Yazbi *et al.*, 2008; Floyd *et al.*, 2007; Fujimoto, 1993; Fujimoto *et al.*, 1992; Je *et al.*, 2004). PMCA4 and its associating proteins (including nNOS) have previously been localised to this caveolae plasma membrane microdomain (Beigi *et al.*, 2009; Cheah *et al.*, 2002; El-Yazbi *et al.*, 2008; Fujimoto, 1993; Hammes *et al.*, 1998; Schuh *et al.*, 2003; Segal *et al.*, 1999; Venema *et al.*, 1997). Furthermore in a previous study it was shown by immunohistochemistry that PMCA4 colocalised with caveolin-1 (an integral protein in caveolae) in smooth muscles of mouse intestinal and bovine tracheal tissues (El-Yazbi *et al.*, 2008). The same study also demonstrated that disruption of caveolae either by pharmacological means or in caveolin-1 knockout mice resulted in the loss of the effects of PMCA4 on smooth muscle contractile function of mammalian intestinal and tracheal tissues (El-Yazbi *et al.*, 2008). This

suggests that PMCA4 activity in smooth muscle cells is dependent on its presence within intact caveolae. Thus, the effects of caveolae disruption on the effect of AP2 on vascular contractile function were investigated in the present study. Functional analysis of mouse mesenteric arteries showed that incubation with methyl-β-cyclodextrin (mβcd) markedly decreased contractile responses to both KPSS and noradrenaline. Mβcd is a cholesterol binding agent which has been shown to disrupt caveolae structure in several muscle types (Cristofaro *et al.*, 2007; Dreja *et al.*, 2002; Ekman *et al.*, 2012; Lloyd *et al.*, 2001; Shaw *et al.*, 2006; Sun *et al.*, 2012). In mesenteric arterial smooth muscle cells mβcd was reported to cause flattened plasma membranes with few caveolae after electron microscopy analysis (Shaw *et al.*, 2006). The observed impairment in arterial contractility by mβcd observed in this study has also been previously demonstrated in rat mesenteric and tail arteries, (Dreja *et al.*, 2002; Shaw *et al.*, 2006) and in ferret aortas (Je *et al.*, 2004) implying that intact caveolae is important for the regulation VSM contractile function. A reduced contractile function was also observed in mesenteric arteries from caveolin-1 knockout mice which showed the absence of caveolae in their VSM (Hausman *et al.*, 2011) further supporting the concept that intact caveolae is required for regulating VSM contractile function.

In this study the PMCA4 inhibitor AP2 had no effect on arterial contractility after incubation with mβcd. It is acknowledged that mβcd reduced arterial contractility by a significant amount i.e. below the level to which AP2 decreased vascular constriction when mβcd was not present and we cannot exclude the possibility that that this may have prevented AP2 from having any noticeable effect on arterial contractility. However, the results of the present study are consistent with the requirement for sub-cellular localisation of PMCA4 and nNOS within caveolae

plasma membrane microdomains (figure 4.4.1). This supports the idea that PMCA4 has a structural role in tethering nNOS to a highly compartmentalised plasma membrane domain, as has previously been demonstrated in cardiac cells (Mohamed *et al.*, 2009; Mohamed *et al.*, 2011b; Oceandy *et al.*, 2007). It is likely that this highly compartmentalised plasma membrane domain may be caveolae (rich in lipid-rafts) as this is the only membrane fraction to which PMCA4 was localised in homogenates of both intestinal and tracheal smooth muscles (El-Yazbi *et al.*, 2008). It has also been shown in tracheal smooth muscle that caveolae disruption with mβcd led to the loss of PMCA4b immunoreactivity in lipid-raft rich fractions (i.e. caveolae) (El-Yazbi *et al.*, 2008). This data in concert with other results from the same study has suggested that the activity PMCA4 in smooth muscles is dependent upon its presence in intact caveolae (El-Yazbi *et al.*, 2008).

Thus one can hypothesise that in WT $^{(+/+)}$ mice the PMCA4-nNOS complex is localised to caveolae microdomains (figure 4.4.1), therefore any change in the activity of PMCA4, due to either inhibition or overexpression of PMCA4, can modulate nNOS activity. It has previously been shown, however, in cultured cardiomyocytes from PMCA4 KO $^{(-/-)}$ mice that, despite no apparent changes to total nNOS protein, more than 36% of membrane associated nNOS activity was translocated to the cytosol of these PMCA4 ablated cardiac cells (Mohamed *et al.*, 2011b). It is believed that this is due to the collapse of the functional PMCA4-nNOS complex in PMCA4 KO $^{(-/-)}$ mice which would likely lead to a removal of the modulation of nNOS by PMCA4. If a similar translocation of nNOS were evident in VSM from PMCA4 KO mice this may explain why ablation of PMCA4 had no effect on arterial contractility. However, in the inhibition experiments (with AP2) using arteries from WT $^{(+/+)}$ mice and in those from PMCA4 overexpressing mice it

is plausible that nNOS would still exist in a complex with PMCA4 localised to caveolae. Thus changes in the activity/expression of PMCA4 can modulate nNOS activity as seen in this study and that by Gros *et al* (2003) and by Schuh *et al* (2003).

However, further experimentation is required to determine whether the translocation of nNOS activity from plasma membrane domains to the cytosol is evident in VSM cells of the PMCA4 KO $^{(-/-)}$ mice as was found in cardiomyoctes (Mohamed *et al.*, 2011b). Until then one must be cautious in using this as a reason why ablating PMCA4 had no effect on arterial contractility as was seen in this study.

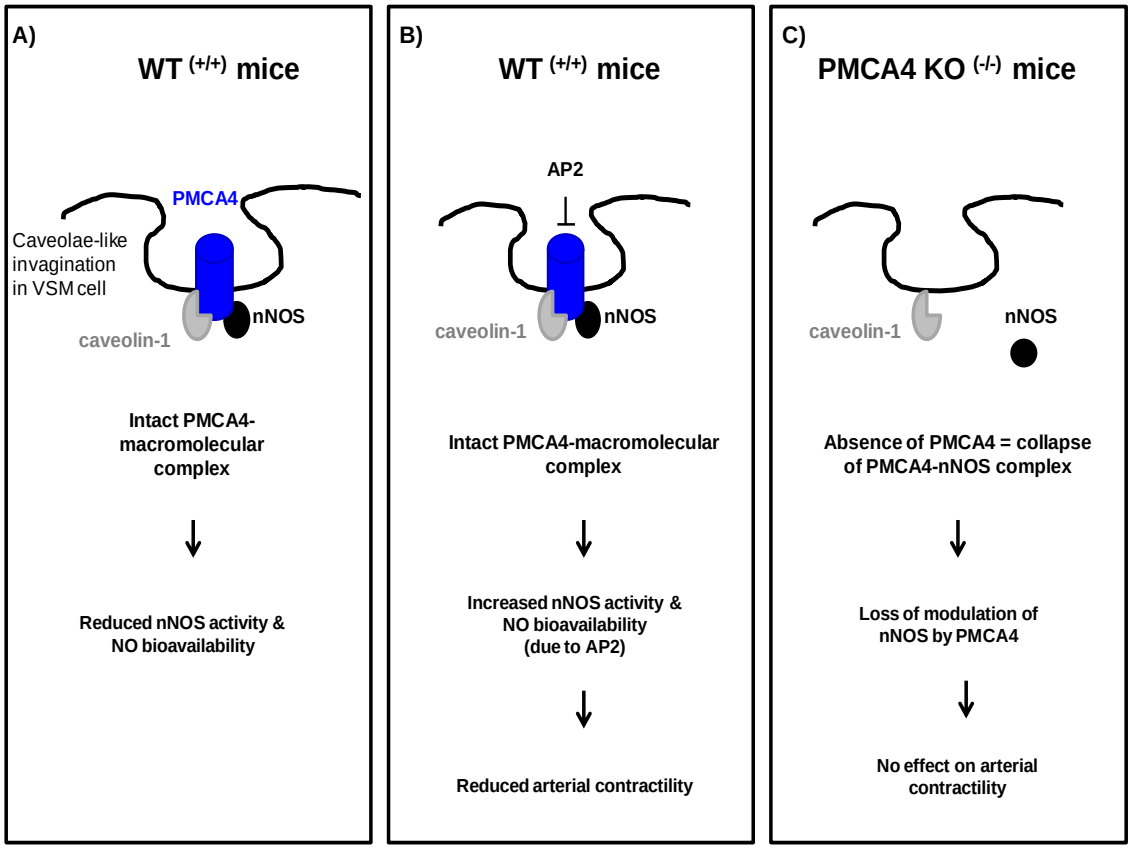

Figure 4.4.1: An illustration of the hypothesised significance of PMCA4 in the caveolae plasma membrane domain of VSM cells. Shown in A) is a representation of a caveolae-like invagination in the VSM cell membrane of WT $^{(+/+)}$ mice. Whereas B) represents a caveolae-like invagination in the VSM cell membrane of WT $^{(+/+)}$ mice upon treatement with AP2 and C) represents that in a VSM cell of PMCA4 KO $^{(-/-)}$ mice.

4.5 Effects of PMCA4 ablation on the passive arterial properties

In the present study structural *in vitro* assessments of isolated pressurised mesenteric arteries fully dilated under passive conditions revealed no significant differences in wall thicknesses, wall:lumen ratio and wall cross sectional area (CSA) of isolated arteries from PMCA4 KO $^{(-/-)}$ mice compared with those from WT $^{(+/+)}$ mice. These results were perhaps not surprising as the PMCA4 KO $^{(-/-)}$ mice have normal blood pressure (Cartwright *et al.*, 2011a); hypertension being the major disease state associated with vascular remodelling (Mulvany, 2008; Mulvany, 1999; Rizzoni *et al.*, 1996; Rizzoni *et al.*, 2001). The present study has also shown that histology of H&E stained mesenteric arterial sections from the PMCA4 KO $^{(-/-)}$ and WT $^{(+/+)}$ mice did not depict any visible changes to the gross structure of arterial walls due to knocking out PMCA4. Thus the data has revealed that ablation of PMCA4 in mice has no effect on the structural morphology of mesenteric arteries.

The results of the present study also demonstrate a leftward shift in the stress, strain relationship along with a significantly greater mean elastic modulus (β) found in isolated mesenteric arteries from PMCA4 KO $^{(-/-)}$ mice compared with those from WT $^{(+/+)}$ mice. These changes are indicative of a reduced arterial distensibility. Reduction in arterial distensibility has been previously associated with hypertension although both increases and decreases have also been reported (Bund, 2001; Giannattasio *et al.*, 2003; Hajdu *et al.*, 1994; Intengan *et al.*, 1999; Izzard *et al.*, 2005; Schofield *et al.*, 2002).

As the mice used in this study were aged three months it is yet to be established whether this change in arterial distensibility may contribute to a hypertensive phenotype in aged PMCA4 KO $^{(-/-)}$ mice. Reduced arterial distensibility or increased

arterial stiffness has an independent predictive value for cardiovascular morbidity as well as mortality (Duprez *et al.*, 2007; Laurent *et al.*, 2001; Laurent *et al.*, 2005). Increased arterial stiffness evident in hypertension has been proposed to be a consequence of alterations in extracellular matrix (ECM) proteins (Arribas *et al.*, 2006; Briones *et al.*, 2010; Briones *et al.*, 2003; Intengan *et al.*, 2000; Martinez-Lemus *et al.*, 2009). Vascular ECM is comprised of different constituents mainly collagen, elastin, glycoproteins and proteoglycans which are essential to the mechanical integrity of the vessel wall (Briones *et al.*, 2010; Wagenseil *et al.*, 2009). Abnormalities in the principal ECM components namely, collagen and elastin including excessive collagen deposition and altered spatial organisation of elastic fibres, have been shown in arteries in association with increased vessel stiffness (or compromised vascular elasticity) (Briones *et al.*, 2010; Briones *et al.*, 2003; Intengan *et al.*, 1999; Jimenez-Altayo *et al.*, 2007; Rizzoni *et al.*, 2006). To date the specific mechanisms underlying changes in vascular stiffness remain to be elucidated. In future, a closer inspection of the ECM components, collagen and elastin specifically in the walls of mesenteric arteries from PMCA4 KO $^{(-/-)}$ mice would be essential to clarify the reasons behind the reduced distensibility observed in this study. Due to the time restriction of the project this has regrettably not been investigated by this study and so the potential mechanisms underlying the reduced distensibility seen in PMCA4 ablated arteries remain incompletely understood but the underlying mechanisms are speculated below.

Previous studies carried out on caveolin-1 knockout mice have demonstrated that the ablation of caveolin-1 reduces distensibility of mesenteric arteries (Hausman *et al.*, 2011) similar to the effects seen after knocking out PMCA4 in mice during this study. As PCMCA4 co-localises and interacts with caveolin-1, an integral protein of

caveolae (El-Yazbi *et al.*, 2008; Fujimoto, 1993; Hammes *et al.*, 1998) and caveolae ablation has been shown to modify PMCA4 activity in non-vascular smooth muscle (El-Yazbi *et al.*, 2008), it is plausible that the effects of PMCA4 and caveolae ablation on arterial distensibility arise from a similar mechanistic signalling pathway. Unfortunately final conclusions cannot be drawn without further inspections of the elastin/collagen balance in vascular wall layers of arteries from both PMCA4 KO $^{(-/-)}$ and caveolin-1 knockout mice.

It is known that PMCA4 acts as an anchoring protein, tethering several proteins (including nNOS, calcineurin dystrophin and α-1 syntrophin) to form a macromolecular complex within compartmentalised domains of cardiomyocyte plasma membranes (Mohamed *et al.*, 2011b). Therefore potentially altering PMCA4 may have functional consequences on the signalling of its tethered proteins (e.g. nNOS) which has been previously shown to cause modifications in muscle contraction as seen in cardiac and VSM after PMCA4 overexpression (Gros *et al.*, 2003; Mohamed *et al.*, 2009; Oceandy *et al.*, 2007; Schuh *et al.*, 2003). Though it is unknown whether altering PMCA4 may modulate structural properties, there is evidence of anti-hypertrophic effects seen in cardiomyocytes as a result of knocking out PMCA4 or inhibition with AP2 in cardiomyocytes (Abou-Leisa *et al.*, 2011; Cartwright *et al.*, 2011a; Mohamed *et al.*, 2011a). This effect was associated with a reduction in PMCA4-mediated calcineurin signalling in microdomains of cardiomyocytes (Abou-Leisa *et al.*, 2011), however it must be noted that this project is still being investigated by the Ludwig Neyses group. Thus it is possible that altering PMCA4 may also have consequences on the tethered proteins dystrophin and α-1 syntrophin, which are clearly associated with pathological muscular dystrophies (Ahn *et al.*, 1994; Compton *et al.*, 2005; Lai *et al.*, 2009; Nakamori *et*

al., 2011). One may speculate that the absence of PMCA4 from the complex may potentially have adverse effects on the functional signalling pathways of these tethering proteins, possibly resulting in the modified mechanical properties observed in mesenteric arteries of PMCA4 KO $^{(-/-)}$ mice. Although one must acknowledge that as yet there is no evidence currently available to suggest this notion and therefore this idea remains a speculation.

Conclusion

This study concludes that while PMCA4 ablation had no effect on the contractile function and on global $[Ca^{2+}]_i$ elicited by KPSS and noradrenaline-stimulated mouse arteries, inhibition of PMCA4 with the novel AP2 inhibitor significantly impaired arterial constrictions and the rise in global $[Ca^{2+}]_i$ in response to KPSS (100mM) or noradrenaline. This effect of AP2 on arterial contractility has been established as nNOS dependent. Thus the present study has identified a signal transduction role for PMCA4 in modulating nNOS in the vasculature which compliments earlier studies addressing the role of PMCA4 in the mammalian vasculature (Gros *et al.*, 2003; Schuh *et al.*, 2003) (figure 4.6.1) and in the heart (Cartwright *et al.*, 2007; Mohamed *et al.*, 2009; Oceandy *et al.*, 2007; Oceandy *et al.*, 2011; Williams *et al.*, 2006). One may also conclude that altering PMCA4 by either ablation, overexpression (Gros *et al.*, 2003; Schuh *et al.*, 2003) or inhibition (with AP2/the caloxins (Pande *et al.*, 2006; Pande *et al.*, 2008)) all have differing effects on the contractile function of mammalian arteries and can mediate changes in vascular contractility by either modifying nNOS activity or global $[Ca^{2+}]_i$ levels in VSM cells (figure 4.6.1). However, this study has found evidence to suggest that the effects of the commercially available caloxin 1b1 inhibitor on agonist-mediated constrictions may be independent of PMCA4. Finally ablating PMCA4 led to a significant reduction in the distensibility of mesenteric resistance arteries which was not accompanied by any changes to vessel lumen diameter, wall thickness, wall:lumen ratio and cross sectional area though however the reasons for this are not yet clear and require further investigation.

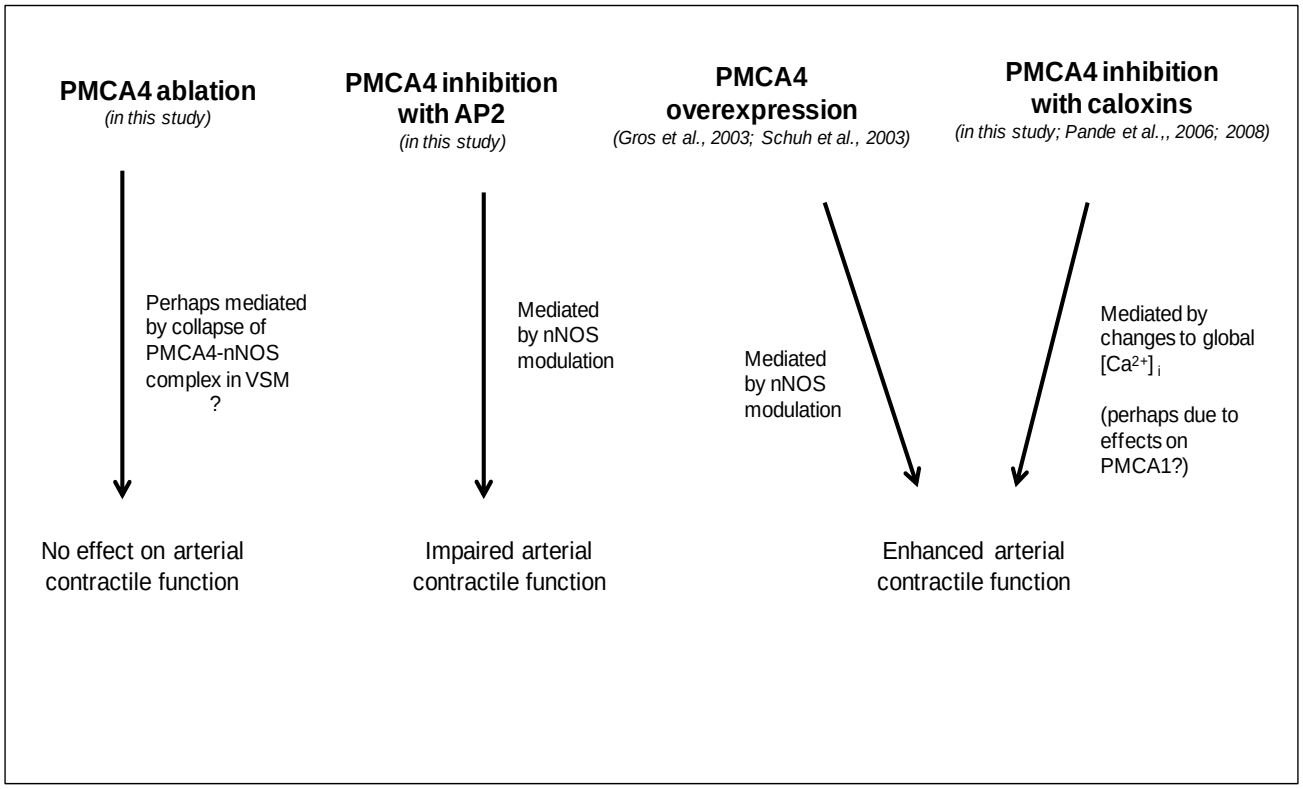

Figure 4.6.1: Schematic summarising the effects observed on mammalian arterial constrictions after the expression/activity of PMCA4 had been modulated and the postulated mechanisms thought to be responsible. Modulating PMCA4 can exert changes on the contractility of mammalian arteries which be may be dependent on either nNOS or on $[Ca^{2+}]_i$ modulations.

Future Studies

This study has given significant insight into the importance of PMCA4 in mesenteric arterial function. However in order to fully understand PMCA4's contribution to mesenteric arterial functionality there are several aspects of this project that must be expanded on in the future, as these could not be addressed in this report regrettably due to time and financial restrictions. These include:

- Testing whether the activity of nNOS is indeed translocated from membrane to cytoplasmic fractions in extracts of whole arteries/VSM cells obtained from PMCA4 KO $^{(-/-)}$ mice, as was previously shown in the cardiomyocytes of these mice (Mohamed *et al.*, 2011b). Such experiments will test the hypothesis proposed in this study, that the absence of PMCA4 in VSM cells may result in the loss of PMCA4 modulation of nNOS activity in the plasma membrane.

- Investigating the levels of nNOS activity/cGMP in VSM cells from WT $^{(+/+)}$ mice after treatment with AP2 by a suitable nNOS/sGC assay technique. This will determine the effect of PMCA4 inhibition with AP2 on NO-mediated signalling in the context of an *in vitro* VSM cellular system.

- In order to conclusively determine whether other Ca^{2+} handling proteins specific to VSM cells (including L-type Ca^{2+} channels, IP_3R which have not been tested in this study) are unaffected/affected by PMCA4 ablation; their protein and/or mRNA expression levels must be closely examined in VSM cells derived from PMCA4 KO $^{(-/-)}$ and WT $^{(+/+)}$ mice via molecular biology techniques such as Western blotting and RT-PCR respectively. Also required will be the use of suitable enzyme assay techniques to investigate whether the

activity of the Ca^{2+}-extrusion enzymes specific to VSM cells (i.e. PMCA1, NCX and SERCA) are modified in the vasculature of PMCA4 KO $^{(-/-)}$ compared to those of WT $^{(+/+)}$ mice. Only Ca^{2+} handling proteins specific to VSM cells (such as L-type Ca^{2+} channels, IP_3R, PMCA1, NCX and SERCA) will be investigated.

- Investigations that will employ collagen and elastin histological staining of mesenteric arterial sections obtained from PMCA4 KO $^{(-/-)}$ and WT $^{(+/+)}$ mice. These will assess for visible abnormalities in the arrangement of the collagen/elastin balance in the arterial wall structure of PMCA4 KO $^{(-/-)}$ mice and may explain why arterial distensibility was reduced in this model.

- Studying the effect of PMCA4 ablation on arterial contractility in response to other types of contractile stimuli (which have not been used in this study) using arteries from PMCA4 KO $^{(-/-)}$ and WT $^{(+/+)}$ mice, via pressure myography. For e.g. increasing intravascular pressure to assess myogenic constrictions or phenylephrine to assess agonist-induced constrictions. The use of other contractile stimuli different to those used in this study will provide more evidence of the effect(s) of PMCA4 ablation on contractile function of mouse arteries.

- Immunohistochemical analysis of PMCA4 and nNOS expression in mouse mesenteric arterial sections obtained from both PMCA4 KO $^{(-/-)}$ and WT $^{(+/+)}$ mice. Similar to that which was performed on mouse aortic sections in this study as PMCA4 and nNOS expression in the resistance vasculature is currently unknown.

References

(American Heart Association (AHA) 2008). (American Heart Association) International cardiovascular statistics. Statistical fact sheet - populations (2008 update)

(Health Survey for England 2010). NHS information centre for health & social care;Trend tables; National Centre for Social Research. *Department of Epidemiology & Publich Health* **http://www.ic.nhs.uk/webfiles/publications/003_Health_Lifestyles/HSE2010_REPORT/HSE2010_Trends_commentary.pdf**.

(World Health Organisation (WHO)). Statistical Information System. Mortality data for ICD 10 codings www.who.int/whosis/database/mort/download/ftp/morticd10.zip.

Aalkjaer C, Heagerty AM, Petersen KK, Swales JD, Mulvany MJ (1987). Evidence for increased media thickness, increased neuronal amine uptake, and depressed excitation--contraction coupling in isolated resistance vessels from essential hypertensives. *Circ Res* **61**(2)**:** 181-186.

Aarnoudse AJ, Newton-Cheh C, de Bakker PI, Straus SM, Kors JA, Hofman A*, et al.* (2007). Common NOS1AP variants are associated with a prolonged QTc interval in the Rotterdam Study. *Circulation* **116**(1)**:** 10-16.

Abe A, Karaki H (1992). Mechanisms underlying the inhibitory effect of dibutyryl cyclic AMP in vascular smooth muscle. *Eur J Pharmacol* **211**(3)**:** 305-311.

Abou-Leisa R, Cartwight E, Neyses L (2011). Identification of a novel specific PMCA4 inhibitor, a potential anti-hypertrophic agent. *University of Manchester, Cardiovascular research departmental showcase - personal communication* **http://spo.escardio.org/eslides/view.aspx?eevtid=48&fp=914**.

Adachi T, Weisbrod RM, Pimentel DR, Ying J, Sharov VS, Schoneich C*, et al.* (2004). S-Glutathiolation by peroxynitrite activates SERCA during arterial relaxation by nitric oxide. *Nat Med* **10**(11)**:** 1200-1207.

Afroze T, Yang LL, Wang C, Gros R, Kalair W, Hoque AN*, et al.* (2003). Calcineurin-independent regulation of plasma membrane Ca2+ ATPase-4 in the vascular smooth muscle cell cycle. *Am J Physiol Cell Physiol* **285**(1)**:** C88-95.

Agabiti-Rosei E (2003). [Structural and functional changes of the microcirculation in hypertension: influence of pharmacological therapy]. *Drugs* **63 Spec No 1:** 19-29.

Ahn AH, Yoshida M, Anderson MS, Feener CA, Selig S, Hagiwara Y*, et al.* (1994). Cloning of human basic A1, a distinct 59-kDa dystrophin-associated protein encoded on chromosome 8q23-24. *Proc Natl Acad Sci U S A* **91**(10)**:** 4446-4450.

Akata T (2007). Cellular and molecular mechanisms regulating vascular tone. Part 1: basic mechanisms controlling cytosolic Ca2+ concentration and the Ca2+-dependent regulation of vascular tone

Cellular and molecular mechanisms regulating vascular tone. Part 2: regulatory mechanisms modulating Ca2+ mobilization and/or myofilament Ca2+ sensitivity in vascular smooth muscle cells. *J Anesth* **21**(2)**:** 220-231.

Amberg GC, Navedo MF, Nieves-Cintron M, Molkentin JD, Santana LF (2007). Calcium sparklets regulate local and global calcium in murine arterial smooth muscle. *J Physiol* **579**(Pt 1)**:** 187-201.

Andresen J, Shafi NI, Bryan RM, Jr. (2006). Endothelial influences on cerebrovascular tone. *J Appl Physiol* **100**(1)**:** 318-327.

Arking DE, Pfeufer A, Post W, Kao WH, Newton-Cheh C, Ikeda M*, et al.* (2006). A common genetic variant in the NOS1 regulator NOS1AP modulates cardiac repolarization. *Nat Genet* **38**(6)**:** 644-651.

Armesilla AL, Williams JC, Buch MH, Pickard A, Emerson M, Cartwright EJ*, et al.* (2004). Novel functional interaction between the plasma membrane Ca2+ pump 4b and the proapoptotic tumor suppressor Ras-associated factor 1 (RASSF1). *J Biol Chem* **279**(30)**:** 31318-31328.

Arribas SM, Hinek A, Gonzalez MC (2006). Elastic fibres and vascular structure in hypertension. *Pharmacol Ther* **111**(3)**:** 771-791.

Aung CS, Kruger WA, Poronnik P, Roberts-Thomson SJ, Monteith GR (2007). Plasma membrane Ca2+-ATPase expression during colon cancer cell line differentiation. *Biochem Biophys Res Commun* **355**(4)**:** 932-936.

Aung CS, Ye W, Plowman G, Peters AA, Monteith GR, Roberts-Thomson SJ (2009). Plasma membrane calcium ATPase 4 and the remodeling of calcium homeostasis in human colon cancer cells. *Carcinogenesis* **30**(11)**:** 1962-1969.

Austin C, Wray S (1995). The effects of extracellular pH and calcium change on force and intracellular calcium in rat vascular smooth muscle. *J Physiol* **488 (Pt 2)**(Pt 2)**:** 281-291.

Babiluri EI (2009). [Endothelium-dependent vascular smooth muscle relaxation and contraction]. *Georgian Med News* **167**(167)**:** 89-92.

Bachetti T, Comini L, Curello S, Bastianon D, Palmieri M, Bresciani G*, et al.* (2004). Co-expression and modulation of neuronal and endothelial nitric oxide synthase in human endothelial cells. *J Mol Cell Cardiol* **37**(5)**:** 939-945.

Baek EB, Kim SJ (2011). Mechanisms of myogenic response: Ca(2+)-dependent and -independent signaling. *J Smooth Muscle Res* **47**(2)**:** 55-65.

Bakker EN, Buus CL, VanBavel E, Mulvany MJ (2004). Activation of resistance arteries with endothelin-1: from vasoconstriction to functional adaptation and remodeling. *J Vasc Res* **41**(2)**:** 174-182.

Baryshnikov SG, Pulina MV, Zulian A, Linde CI, Golovina VA (2009). Orai1, a critical component of store-operated Ca2+ entry, is functionally associated with Na+/Ca2+ exchanger and plasma membrane Ca2+ pump in proliferating human arterial myocytes. *Am J Physiol Cell Physiol* **297**(5)**:** C1103-1112.

Baumbach GL, Heistad DD (1989). Remodeling of cerebral arterioles in chronic hypertension. *Hypertension* **13**(6 Pt 2)**:** 968-972.

Beigi F, Oskouei BN, Zheng M, Cooke CA, Lamirault G, Hare JM (2009). Cardiac nitric oxide synthase-1 localization within the cardiomyocyte is accompanied by the adaptor protein, CAPON. *Nitric Oxide* **21**(3-4)**:** 226-233.

Beleznai T, Takano H, Hamill C, Yarova P, Douglas G, Channon K*, et al.* (2011). Enhanced K(+)-channel-mediated endothelium-dependent local and conducted dilation of small mesenteric arteries from ApoE(-/-) mice. *Cardiovasc Res* **92**(2)**:** 199-208.

Beny JL, Pacicca C (1994). Bidirectional electrical communication between smooth muscle and endothelial cells in the pig coronary artery. *Am J Physiol* **266**(4 Pt 2)**:** H1465-1472.

Bergdahl A, Sward K (2004). Caveolae-associated signalling in smooth muscle. *Can J Physiol Pharmacol* **82**(5)**:** 289-299.

Berra-Romani R, Mazzocco-Spezzia A, Pulina MV, Golovina VA (2008). Ca2+ handling is altered when arterial myocytes progress from a contractile to a proliferative phenotype in culture. *Am J Physiol Cell Physiol* **295**(3)**:** C779-790.

Berridge MJ (1995). Calcium signalling and cell proliferation. *Bioessays* **17**(6)**:** 491-500.

Berridge MJ (1993). Inositol trisphosphate and calcium signalling. *Nature* **361**(6410)**:** 315-325.

Berridge MJ, Lipp P, Bootman MD (2000). The versatility and universality of calcium signalling. *Nat Rev Mol Cell Biol* **1**(1)**:** 11-21.

Birenbaum A, Tesse A, Loyer X, Michelet P, Andriantsitohaina R, Heymes C*, et al.* (2008). Involvement of beta 3-adrenoceptor in altered beta-adrenergic response in senescent heart: role of nitric oxide synthase 1-derived nitric oxide. *Anesthesiology* **109**(6)**:** 1045-1053.

Bkaily G, Naik R, D'Orleans-Juste P, Wang S, Fong CN (1995). Endothelin-1 activates the R-type Ca2+ channel in vascular smooth-muscle cells. *J Cardiovasc Pharmacol* **26 Suppl 3**(3)**:** S303-306.

Blaustein MP, Lederer WJ (1999). Sodium/calcium exchange: its physiological implications. *Physiol Rev* **79**(3)**:** 763-854.

Boczek T, Kozaczuk A, Ferenc B, Kosiorek M, Pikula S, Zylinska L (2012). Gene expression pattern in PC12 cells with reduced PMCA2 or PMCA3 isoform: selective up-regulation of calmodulin and neuromodulin. *Mol Cell Biochem* **360**(1-2)**:** 89-102.

Boittin FX, Coussin F, Morel JL, Halet G, Macrez N, Mironneau J (2000). Ca(2+) signals mediated by Ins(1,4,5)P(3)-gated channels in rat ureteric myocytes. *Biochem J* **349**(Pt 1)**:** 323-332.

Bolotina VM, Najibi S, Palacino JJ, Pagano PJ, Cohen RA (1994). Nitric oxide directly activates calcium-dependent potassium channels in vascular smooth muscle. *Nature* **368**(6474)**:** 850-853.

Bolton TB (1979). Mechanisms of action of transmitters and other substances on smooth muscle. *Physiol Rev* **59**(3)**:** 606-718.

Boucher JL, Moali C, Tenu JP (1999). Nitric oxide biosynthesis, nitric oxide synthase inhibitors and arginase competition for L-arginine utilization. *Cell Mol Life Sci* **55**(8-9)**:** 1015-1028.

Boulanger CM, Heymes C, Benessiano J, Geske RS, Levy BI, Vanhoutte PM (1998). Neuronal nitric oxide synthase is expressed in rat vascular smooth muscle cells: activation by angiotensin II in hypertension. *Circ Res* **83**(12)**:** 1271-1278.

Bradley KK, Jaggar JH, Bonev AD, Heppner TJ, Flynn ER, Nelson MT*, et al.* (1999a). Kir2.1 encodes the inward rectifier potassium channel in rat arterial smooth muscle cells. *J Physiol* **515 (Pt 3)**(Pt 3)**:** 639-651.

Bradley KK, Jaggar JH, Bonev AD, Heppner TJ, Flynn ER, Nelson MT*, et al.* (1999b). Kir2.1 encodes the inward rectifier potassium channel in rat arterial smooth muscle cells. *J Physiol* **515 (Pt 3):** 639-651.

Brainard AM, Miller AJ, Martens JR, England SK (2005). Maxi-K channels localize to caveolae in human myometrium: a role for an actin-channel-caveolin complex in the regulation of myometrial smooth muscle K+ current. *Am J Physiol Cell Physiol* **289**(1)**:** C49-57.

Brandt P, Neve RL, Kammesheidt A, Rhoads RE, Vanaman TC (1992). Analysis of the tissue-specific distribution of mRNAs encoding the plasma membrane calcium-pumping ATPases and characterization of an alternately spliced form of PMCA4 at the cDNA and genomic levels. *J Biol Chem* **267**(7)**:** 4376-4385.

Brenner R, Perez GJ, Bonev AD, Eckman DM, Kosek JC, Wiler SW*, et al.* (2000). Vasoregulation by the beta1 subunit of the calcium-activated potassium channel. *Nature* **407**(6806)**:** 870-876.

Brini M (2009). Plasma membrane Ca(2+)-ATPase: from a housekeeping function to a versatile signaling role. *Pflugers Arch* **457**(3)**:** 657-664.

Briones AM, Arribas SM, Salaices M (2010). Role of extracellular matrix in vascular remodeling of hypertension. *Curr Opin Nephrol Hypertens* **19**(2)**:** 187-194.

Briones AM, Gonzalez JM, Somoza B, Giraldo J, Daly CJ, Vila E*, et al.* (2003). Role of elastin in spontaneously hypertensive rat small mesenteric artery remodelling. *J Physiol* **552**(Pt 1)**:** 185-195.

Broderick R, Somlyo AP (1987). Calcium and magnesium transport by in situ mitochondria: electron probe analysis of vascular smooth muscle. *Circ Res* **61**(4)**:** 523-530.

Brodin P, Falchetto R, Vorherr T, Carafoli E (1992). Identification of two domains which mediate the binding of activating phospholipids to the plasma-membrane Ca2+ pump. *Eur J Biochem* **204**(2)**:** 939-946.

Brueggemann LI, Markun DR, Henderson KK, Cribbs LL, Byron KL (2006). Pharmacological and electrophysiological characterization of store-operated currents and capacitative Ca(2+) entry in vascular smooth muscle cells. *J Pharmacol Exp Ther* **317**(2)**:** 488-499.

Buch MH, Pickard A, Rodriguez A, Gillies S, Maass AH, Emerson M*, et al.* (2005). The sarcolemmal calcium pump inhibits the calcineurin/nuclear factor of activated T-cell pathway via interaction with the calcineurin A catalytic subunit. *J Biol Chem* **280**(33)**:** 29479-29487.

Buchwalow IB, Podzuweit T, Bocker W, Samoilova VE, Thomas S, Wellner M*, et al.* (2002). Vascular smooth muscle and nitric oxide synthase. *FASEB J* **16**(6)**:** 500-508.

Buchwalow IB, Podzuweit T, Samoilova VE, Wellner M, Haller H, Grote S*, et al.* (2004). An in situ evidence for autocrine function of NO in the vasculature. *Nitric Oxide* **10**(4)**:** 203-212.

Bund SJ (2001). Spontaneously hypertensive rat resistance artery structure related to myogenic and mechanical properties. *Clin Sci (Lond)* **101**(4)**:** 385-393.

Busse R, Edwards G, Feletou M, Fleming I, Vanhoutte PM, Weston AH (2002). EDHF: bringing the concepts together. *Trends Pharmacol Sci* **23**(8)**:** 374-380.

Buus NH, Simonsen U, Pilegaard HK, Mulvany MJ (2000). Nitric oxide, prostanoid and non-NO, non-prostanoid involvement in acetylcholine relaxation of isolated human small arteries. *Br J Pharmacol* **129**(1)**:** 184-192.

Bylund DB, Eikenberg DC, Hieble JP, Langer SZ, Lefkowitz RJ, Minneman KP*, et al.* (1994). International Union of Pharmacology nomenclature of adrenoceptors. *Pharmacol Rev* **46**(2)**:** 121-136.

Capewell S, Allender S, Critchley J, Lloyd-Williams F, O'Flatherty M, Rayner M*, et al.* (2008). Modelling of the UK burden of CVD to 2020. *A research report for the Cardio & vascular coalition and the British Heart Foundation* **London, UK**.

Carafoli E (1994). Biogenesis: plasma membrane calcium ATPase: 15 years of work on the purified enzyme. *Faseb J* **8**(13)**:** 993-1002.

Cartwright E, Mohamed T., Oceandy D, Abou-Leisa R., Baudoin F, Zi. M*, et al.* (2011a). Treatment of cardiac hypertrophy with a novel pharmacological inhibitor of PMCA4 mimics the phenotype of the PMCA4 knockout mouse. *Animal models and their value in predicting drug efficacy and toxicity - Poster communication* **The New York Academy of Sciences**(Conference September 2011).

Cartwright EJ, Oceandy D, Austin C, Neyses L (2011b). Ca2+ signalling in cardiovascular disease: the role of the plasma membrane calcium pumps. *Sci China Life Sci* **54**(8)**:** 691-698.

Cartwright EJ, Oceandy D, Neyses L (2007). Plasma membrane calcium ATPase and its relationship to nitric oxide signaling in the heart. *Ann N Y Acad Sci* **1099:** 247-253.

Cartwright EJ, Schuh K, Neyses L (2005). Calcium transport in cardiovascular health and disease--the sarcolemmal calcium pump enters the stage. *J Mol Cell Cardiol* **39**(3)**:** 403-406.

Cary SP, Winger JA, Derbyshire ER, Marletta MA (2006). Nitric oxide signaling: no longer simply on or off. *Trends Biochem Sci* **31**(4)**:** 231-239.

Chalmers S, Nicholls DG (2003). The relationship between free and total calcium concentrations in the matrix of liver and brain mitochondria. *J Biol Chem* **278**(21)**:** 19062-19070.

Cheah LS, Gwee M, Das R, Ballard H, Yang YF, Daniel EE*, et al.* (2002). Evidence for the existence of a constitutive nitric oxide synthase in vascular smooth muscle. *Clin Exp Pharmacol Physiol* **29**(8)**:** 725-727.

Chen CC, Lamping KG, Nuno DW, Barresi R, Prouty SJ, Lavoie JL*, et al.* (2003). Abnormal coronary function in mice deficient in alpha1H T-type Ca2+ channels. *Science* **302**(5649)**:** 1416-1418.

Chen GF, Suzuki H (1989). Direct and indirect actions of acetylcholine and histamine on intrapulmonary artery and vein muscles of the rat. *Jpn J Physiol* **39**(1)**:** 51-65.

Chicka MC, Strehler EE (2003). Alternative splicing of the first intracellular loop of plasma membrane Ca2+-ATPase isoform 2 alters its membrane targeting. *J Biol Chem* **278**(20)**:** 18464-18470.

Cho YS, Go MJ, Kim YJ, Heo JY, Oh JH, Ban HJ*, et al.* (2009). A large-scale genome-wide association study of Asian populations uncovers genetic factors influencing eight quantitative traits. *Nat Genet* **41**(5)**:** 527-534.

Christensen KL, Mulvany MJ (1993). Mesenteric arcade arteries contribute substantially to vascular resistance in conscious rats. *J Vasc Res* **30**(2)**:** 73-79.

Christensen KL, Mulvany MJ (2001). Vasodilatation, not hypotension, improves resistance vessel design during treatment of essential hypertension: a literature survey. *J Hypertens* **19**(6)**:** 1001-1006.

Claing A, Bkaily G, Berthiaume N, Sirois P, Rola-Pleszczynski M, D'Orleans-Juste P (1994). Role of R-type calcium channels in the response of the perfused arterial and venous mesenteric vasculature of the rat to platelet-activating factor. *Br J Pharmacol* **112**(4)**:** 1202-1208.

Clark JH, Kinnear NP, Kalujnaia S, Cramb G, Fleischer S, Jeyakumar LH*, et al.* (2010). Identification of functionally segregated sarcoplasmic reticulum calcium stores in pulmonary arterial smooth muscle. *J Biol Chem* **285**(18)**:** 13542-13549.

Colella M, Grisan F, Robert V, Turner JD, Thomas AP, Pozzan T (2008). Ca2+ oscillation frequency decoding in cardiac cell hypertrophy: role of calcineurin/NFAT as Ca2+ signal integrators. *Proc Natl Acad Sci U S A* **105**(8)**:** 2859-2864.

Coleman RA, Smith WL, Narumiya S (1994). International Union of Pharmacology classification of prostanoid receptors: properties, distribution, and structure of the receptors and their subtypes. *Pharmacol Rev* **46**(2)**:** 205-229.

Collier ML, Ji G, Wang Y, Kotlikoff MI (2000). Calcium-induced calcium release in smooth muscle: loose coupling between the action potential and calcium release. *J Gen Physiol* **115**(5)**:** 653-662.

Compton AG, Cooper ST, Hill PM, Yang N, Froehner SC, North KN (2005). The syntrophin-dystrobrevin subcomplex in human neuromuscular disorders. *J Neuropathol Exp Neurol* **64**(4)**:** 350-361.

Cooke CL, Davidge ST (2003). Endothelial-dependent vasodilation is reduced in mesenteric arteries from superoxide dismutase knockout mice. *Cardiovasc Res* **60**(3)**:** 635-642.

Cox DA, Matlib MA (1993). Modulation of intramitochondrial free Ca2+ concentration by antagonists of Na(+)-Ca2+ exchange. *Trends Pharmacol Sci* **14**(11)**:** 408-413.

Crabtree GR (1999). Generic signals and specific outcomes: signaling through Ca2+, calcineurin, and NF-AT. *Cell* **96**(5)**:** 611-614.

Cristofaro V, Peters CA, Yalla SV, Sullivan MP (2007). Smooth muscle caveolae differentially regulate specific agonist induced bladder contractions. *Neurourol Urodyn* **26**(1)**:** 71-80.

Dalton AR, Soljak M, Samarasundera E, Millett C, Majeed A (2011). Prevalence of cardiovascular disease risk amongst the population eligible for the NHS Health Check Programme. *Eur J Cardiovasc Prev Rehabil*.

Dalziel HH, Westfall DP (1994). Receptors for adenine nucleotides and nucleosides: subclassification, distribution, and molecular characterization. *Pharmacol Rev* **46**(4)**:** 449-466.

Dargan SL, Parker I (2003). Buffer kinetics shape the spatiotemporal patterns of IP3-evoked Ca2+ signals. *J Physiol* **553**(Pt 3)**:** 775-788.

David G (1999). Mitochondrial clearance of cytosolic Ca(2+) in stimulated lizard motor nerve terminals proceeds without progressive elevation of mitochondrial matrix [Ca(2+)]. *J Neurosci* **19**(17)**:** 7495-7506.

De Jaegere S, Wuytack F, Eggermont JA, Verboomen H, Casteels R (1990). Molecular cloning and sequencing of the plasma-membrane Ca2+ pump of pig smooth muscle. *Biochem J* **271**(3)**:** 655-660.

Dedkova EN, Blatter LA (2008). Mitochondrial Ca2+ and the heart. *Cell Calcium* **44**(1)**:** 77-91.

DeMarco SJ, Strehler EE (2001). Plasma membrane Ca2+-atpase isoforms 2b and 4b interact promiscuously and selectively with members of the membrane-associated guanylate kinase family of PDZ (PSD95/Dlg/ZO-1) domain-containing proteins. *J Biol Chem* **276**(24)**:** 21594-21600.

Devine CE, Somlyo AV, Somlyo AP (1972). Sarcoplasmic reticulum and excitation-contraction coupling in mammalian smooth muscles. *J Cell Biol* **52**(3)**:** 690-718.

Di Leva F, Domi T, Fedrizzi L, Lim D, Carafoli E (2008). The plasma membrane Ca2+ ATPase of animal cells: structure, function and regulation. *Arch Biochem Biophys* **476**(1)**:** 65-74.

Dreja K, Voldstedlund M, Vinten J, Tranum-Jensen J, Hellstrand P, Sward K (2002). Cholesterol depletion disrupts caveolae and differentially impairs agonist-induced arterial contraction. *Arterioscler Thromb Vasc Biol* **22**(8)**:** 1267-1272.

Duprez DA, Cohn JN (2007). Arterial stiffness as a risk factor for coronary atherosclerosis. *Curr Atheroscler Rep* **9**(2)**:** 139-144.

Earley S, Straub SV, Brayden JE (2007). Protein kinase C regulates vascular myogenic tone through activation of TRPM4. *Am J Physiol Heart Circ Physiol* **292**(6)**:** H2613-2622.

Edwards G, Dora KA, Gardener MJ, Garland CJ, Weston AH (1998a). K+ is an endothelium-derived hyperpolarizing factor in rat arteries. *Nature* **396**(6708)**:** 269-272.

Edwards G, Weston AH (1998b). Endothelium-derived hyperpolarizing factor--a critical appraisal. *Prog Drug Res* **50:** 107-133.

Edwards G, Weston AH (2004). Potassium and potassium clouds in endothelium-dependent hyperpolarizations. *Pharmacol Res* **49**(6)**:** 535-541.

Eggermont JA, Wuytack F, Verbist J, Casteels R (1990). Expression of endoplasmic-reticulum Ca2(+)-pump isoforms and of phospholamban in pig smooth-muscle tissues. *Biochem J* **271**(3)**:** 649-653.

Ekman M, Rippe C, Sadegh MK, Dabestani S, Morgelin M, Uvelius B*, et al.* (2012). Association of muscarinic M(3) receptors and Kir6.1 with caveolae in human detrusor muscle. *Eur J Pharmacol* **683**(1-3)**:** 238-245.

El-Yazbi AF, Cho WJ, Schulz R, Daniel EE (2008). Calcium extrusion by plasma membrane calcium pump is impaired in caveolin-1 knockout mouse small intestine. *Eur J Pharmacol* **591**(1-3)**:** 80-87.

Ellis A, Triggle CR (2003). Endothelium-derived reactive oxygen species: their relationship to endothelium-dependent hyperpolarization and vascular tone. *Can J Physiol Pharmacol* **81**(11)**:** 1013-1028.

Emerson GG, Segal SS (2000). Electrical coupling between endothelial cells and smooth muscle cells in hamster feed arteries: role in vasomotor control. *Circ Res* **87**(6)**:** 474-479.

Eto M, Ohmori T, Suzuki M, Furuya K, Morita F (1995). A novel protein phosphatase-1 inhibitory protein potentiated by protein kinase C. Isolation from porcine aorta media and characterization. *J Biochem* **118**(6)**:** 1104-1107.

Falchetto R, Vorherr T, Brunner J, Carafoli E (1991). The plasma membrane Ca2+ pump contains a site that interacts with its calmodulin-binding domain. *J Biol Chem* **266**(5)**:** 2930-2936.

Falchetto R, Vorherr T, Carafoli E (1992). The calmodulin-binding site of the plasma membrane Ca2+ pump interacts with the transduction domain of the enzyme. *Protein Sci* **1**(12)**:** 1613-1621.

Falloon BJ, Heagerty AM (1994). In vitro perfusion studies of human resistance artery function in essential hypertension. *Hypertension* **24**(1)**:** 16-23.

Feihl F, Liaudet L, Levy BI, Waeber B (2008). Hypertension and microvascular remodelling. *Cardiovasc Res* **78**(2)**:** 274-285.

Feletou M, Vanhoutte PM (2009). EDHF: an update. *Clin Sci (Lond)* **117**(4)**:** 139-155.

Feletou M, Vanhoutte PM (2006a). EDHF: the complete story. *Boca Raton, Taylor & Francis CRC press***:** 1-298.

Feletou M, Vanhoutte PM (2006b). Endothelium-derived hyperpolarizing factor: where are we now? *Arterioscler Thromb Vasc Biol* **26**(6)**:** 1215-1225.

Ficarella R, Di Leva F, Bortolozzi M, Ortolano S, Donaudy F, Petrillo M*, et al.* (2007). A functional study of plasma-membrane calcium-pump isoform 2 mutants causing digenic deafness. *Proc Natl Acad Sci U S A* **104**(5)**:** 1516-1521.

Firth AL, Remillard CV, Platoshyn O, Fantozzi I, Ko EA, Yuan JX (2011). Functional ion channels in human pulmonary artery smooth muscle cells: Voltage-dependent cation channels. *Pulm Circ* **1**(1)**:** 48-71.

Flower RJ (2006). Prostaglandins, bioassay and inflammation. *Br J Pharmacol* **147 Suppl 1:** S182-192.

Floyd R, Wray S (2007). Calcium transporters and signalling in smooth muscles. *Cell Calcium* **42**(4-5)**:** 467-476.

Folkow B (1956). Structural, myogenic, humoral and nervous factors controlling peripheral resistance. *Harington M (ed.). Hypotensive Drugs.* **Pergamon, London:** 163-174.

Folkow B, Grimby G, Thulesius O (1958). Adaptive structural changes of the vascular walls in hypertension and their relation to the control of the peripheral resistance. *Acta Physiol Scand* **44**(3-4)**:** 255-272.

Forstermann U, Gath I, Schwarz P, Closs EI, Kleinert H (1995). Isoforms of nitric oxide synthase. Properties, cellular distribution and expressional control. *Biochem Pharmacol* **50**(9)**:** 1321-1332.

Forstermann U, Gorsky LD, Pollock JS, Ishii K, Schmidt HH, Heller M*, et al.* (1990). Hormone-induced biosynthesis of endothelium-derived relaxing factor/nitric oxide-like material in N1E-115 neuroblastoma cells requires calcium and calmodulin. *Mol Pharmacol* **38**(1)**:** 7-13.

Forstermann U, Pollock JS, Schmidt HH, Heller M, Murad F (1991). Calmodulin-dependent endothelium-derived relaxing factor/nitric oxide synthase activity is present in the particulate and cytosolic fractions of bovine aortic endothelial cells. *Proc Natl Acad Sci U S A* **88**(5)**:** 1788-1792.

Francis SH, Blount MA, Zoraghi R, Corbin JD (2005). Molecular properties of mammalian proteins that interact with cGMP: protein kinases, cation channels, phosphodiesterases, and multi-drug anion transporters. *Front Biosci* **10:** 2097-2117.

Fujimoto T (1993). Calcium pump of the plasma membrane is localized in caveolae. *J Cell Biol* **120**(5)**:** 1147-1157.

Fujimoto T, Nakade S, Miyawaki A, Mikoshiba K, Ogawa K (1992). Localization of inositol 1,4,5-trisphosphate receptor-like protein in plasmalemmal caveolae. *J Cell Biol* **119**(6)**:** 1507-1513.

Furchgott RF (1983). Role of endothelium in responses of vascular smooth muscle. *Circ Res* **53**(5)**:** 557-573.

Furchgott RF, Carvalho MH, Khan MT, Matsunaga K (1987). Evidence for endothelium-dependent vasodilation of resistance vessels by acetylcholine. *Blood Vessels* **24**(3)**:** 145-149.

Furchgott RF, Vanhoutte PM (1989). Endothelium-derived relaxing and contracting factors. *FASEB J* **3**(9)**:** 2007-2018.

Furchgott RF, Zawadzki JV (1980). The obligatory role of endothelial cells in the relaxation of arterial smooth muscle by acetylcholine. *Nature* **288**(5789)**:** 373-376.

Furuta H, Luo L, Hepler K, Ryan AF (1998). Evidence for differential regulation of calcium by outer versus inner hair cells: plasma membrane Ca-ATPase gene expression. *Hear Res* **123**(1-2)**:** 10-26.

Ganitkevich V, Hasse V, Pfitzer G (2002). Ca2+-dependent and Ca2+-independent regulation of smooth muscle contraction. *J Muscle Res Cell Motil* **23**(1)**:** 47-52.

Gao Y (2010). The multiple actions of NO. *Pflugers Arch* **459**(6)**:** 829-839.

Garland JG, McPherson GA (1992). Evidence that nitric oxide does not mediate the hyperpolarization and relaxation to acetylcholine in the rat small mesenteric artery. *Br J Pharmacol* **105**(2)**:** 429-435.

Giacomello M, De Mario A, Primerano S, Brini M, Carafoli E (2012). Hair cells, plasma membrane Ca(2)(+) ATPase and deafness. *Int J Biochem Cell Biol* **44**(5)**:** 679-683.

Giannattasio C, Failla M, Corsi D, Capra A, Meles E, Gentile G*, et al.* (2003). [Study of arterial distensibility in man. Modulating mechanisms, pathological conditions and effects of treatment]. *Ital Heart J Suppl* **4**(6)**:** 467-476.

Girard JP, Gillot I, De Renzis G, Payan P (1991). Calcium pools in sea urchin eggs: roles of endoplasmic reticulum and mitochondria in relation to fertilization. *Cell Calcium* **12**(4)**:** 289-299.

Gomez-Pinilla PJ, Pozo MJ, Baba A, Matsuda T, Camello PJ (2007). Ca2+ extrusion in aged smooth muscle cells. *Biochem Pharmacol* **74**(6)**:** 860-869.

Gomez-Varela D, Schmidt M, Schoellerman J, Peters EC, Berg DK (2012). PMCA2 via PSD-95 Controls Calcium Signaling by alpha7-Containing Nicotinic Acetylcholine Receptors on Aspiny Interneurons. *J Neurosci* **32**(20)**:** 6894-6905.

Gonzalez-Cobos JC, Trebak M (2010). TRPC channels in smooth muscle cells. *Front Biosci* **15:** 1023-1039.

Gonzalez JM, Briones AM, Starcher B, Conde MV, Somoza B, Daly C*, et al.* (2005). Influence of elastin on rat small artery mechanical properties. *Exp Physiol* **90**(4)**:** 463-468.

Gonzalez JM, Jost LJ, Rouse D, Suki WN (1996). Plasma membrane and sarcoplasmic reticulum Ca-ATPase and smooth muscle. *Miner Electrolyte Metab* **22**(5-6)**:** 345-348.

Gordienko DV, Greenwood IA, Bolton TB (2001). Direct visualization of sarcoplasmic reticulum regions discharging Ca(2+)sparks in vascular myocytes. *Cell Calcium* **29**(1)**:** 13-28.

Grassi G, Seravalle G, Scopelliti F, Dell'Oro R, Fattori L, Quarti-Trevano F*, et al.* (2010). Structural and functional alterations of subcutaneous small resistance arteries in severe human obesity. *Obesity (Silver Spring)* **18**(1)**:** 92-98.

Grayson TH, Haddock RE, Murray TP, Wojcikiewicz RJ, Hill CE (2004). Inositol 1,4,5-trisphosphate receptor subtypes are differentially distributed between smooth muscle and endothelial layers of rat arteries. *Cell Calcium* **36**(6)**:** 447-458.

Greeb J, Shull GE (1989). Molecular cloning of a third isoform of the calmodulin-sensitive plasma membrane Ca2+-transporting ATPase that is expressed predominantly in brain and skeletal muscle. *J Biol Chem* **264**(31)**:** 18569-18576.

Gros R, Afroze T, You XM, Kabir G, Van Wert R, Kalair W*, et al.* (2003). Plasma membrane calcium ATPase overexpression in arterial smooth muscle increases vasomotor responsiveness and blood pressure. *Circ Res* **93**(7)**:** 614-621.

Grover AK, Khan I (1992). Calcium pump isoforms: diversity, selectivity and plasticity. Review article. *Cell Calcium* **13**(1)**:** 9-17.

Guerini D (1998). The significance of the isoforms of plasma membrane calcium ATPase. *Cell Tissue Res* **292**(2)**:** 191-197.

Guerrero-Hernandez A, Gomez-Viquez L, Guerrero-Serna G, Rueda A (2002). Ryanodine receptors in smooth muscle. *Front Biosci* **7**(7)**:** d1676-1688.

Haddy FJ, Vanhoutte PM, Feletou M (2006). Role of potassium in regulating blood flow and blood pressure. *Am J Physiol Regul Integr Comp Physiol* **290**(3)**:** R546-552.

Hajdu MA, Baumbach GL (1994). Mechanics of large and small cerebral arteries in chronic hypertension. *Am J Physiol* **266**(3 Pt 2)**:** H1027-1033.

Hall CN, Garthwaite J (2009). What is the real physiological NO concentration in vivo? *Nitric Oxide* **21**(2)**:** 92-103.

Hammes A, Oberdorf-Maass S, Rother T, Nething K, Gollnick F, Linz KW*, et al.* (1998). Overexpression of the sarcolemmal calcium pump in the myocardium of transgenic rats. *Circ Res* **83**(9)**:** 877-888.

Hammes A, Oberdorf S, Strehler EE, Stauffer T, Carafoli E, Vetter H*, et al.* (1994). Differentiation-specific isoform mRNA expression of the calmodulin-dependent plasma membrane Ca(2+)-ATPase. *FASEB J* **8**(6)**:** 428-435.

Hatanaka Y, Hobara N, Honghua J, Akiyama S, Nawa H, Kobayashi Y*, et al.* (2006). Neuronal nitric-oxide synthase inhibition facilitates adrenergic neurotransmission in rat mesenteric resistance arteries. *J Pharmacol Exp Ther* **316**(2)**:** 490-497.

Hausman N, Martin J, Taggart MJ, Austin C (2011). Age-related changes in the contractile and passive arterial properties of murine mesenteric small arteries are altered by caveolin-1 knockout. *J Cell Mol Med* **5**(10)**:** 1582-4934.

Hayoz D, Rutschmann B, Perret F, Niederberger M, Tardy Y, Mooser V*, et al.* (1992). Conduit artery compliance and distensibility are not necessarily reduced in hypertension. *Hypertension* **20**(1)**:** 1-6.

Heagerty AM, Aalkjaer C, Bund SJ, Korsgaard N, Mulvany MJ (1993). Small artery structure in hypertension. Dual processes of remodeling and growth. *Hypertension* **21**(4)**:** 391-397.

Heidenreich PA, Trogdon JG, Khavjou OA, Butler J, Dracup K, Ezekowitz MD*, et al.* (2011). Forecasting the future of cardiovascular disease in the United States: a policy statement from the American Heart Association. *Circulation* **123**(8)**:** 933-944.

Hevel JM, White KA, Marletta MA (1991). Purification of the inducible murine macrophage nitric oxide synthase. Identification as a flavoprotein. *J Biol Chem* **266**(34)**:** 22789-22791.

Himpens B, Matthijs G, Somlyo AP (1989). Desensitization to cytoplasmic Ca2+ and Ca2+ sensitivities of guinea-pig ileum and rabbit pulmonary artery smooth muscle. *J Physiol* **413:** 489-503.

Hirano K (2007). Current topics in the regulatory mechanism underlying the Ca2+ sensitization of the contractile apparatus in vascular smooth muscle. *J Pharmacol Sci* **104**(2)**:** 109-115.

Hobbs AJ, Higgs A, Moncada S (1999). Inhibition of nitric oxide synthase as a potential therapeutic target. *Annu Rev Pharmacol Toxicol* **39:** 191-220.

Hofmann F, James P, Vorherr T, Carafoli E (1993). The C-terminal domain of the plasma membrane Ca2+ pump contains three high affinity Ca2+ binding sites. *J Biol Chem* **268**(14)**:** 10252-10259.

House SJ, Potier M, Bisaillon J, Singer HA, Trebak M (2008). The non-excitable smooth muscle: calcium signaling and phenotypic switching during vascular disease. *Pflugers Arch* **456**(5)**:** 769-785.

Huang A, Sun D, Shesely EG, Levee EM, Koller A, Kaley G (2002). Neuronal NOS-dependent dilation to flow in coronary arteries of male eNOS-KO mice. *Am J Physiol Heart Circ Physiol* **282**(2)**:** H429-436.

Hughes AD (1995). Calcium channels in vascular smooth muscle cells. *J Vasc Res* **32**(6)**:** 353-370.

Husain M, Jiang L, See V, Bein K, Simons M, Alper SL*, et al.* (1997). Regulation of vascular smooth muscle cell proliferation by plasma membrane Ca(2+)-ATPase. *Am J Physiol* **272**(6 Pt 1)**:** C1947-1959.

Ichihara A, Inscho EW, Imig JD, Navar LG (1998). Neuronal nitric oxide synthase modulates rat renal microvascular function. *Am J Physiol* **274**(3 Pt 2)**:** F516-524.

Iino M, Kasai H, Yamazawa T (1994). Visualization of neural control of intracellular Ca2+ concentration in single vascular smooth muscle cells in situ. *EMBO J* **13**(21)**:** 5026-5031.

Intengan HD, Deng LY, Li JS, Schiffrin EL (1999). Mechanics and composition of human subcutaneous resistance arteries in essential hypertension. *Hypertension* **33**(1 Pt 2)**:** 569-574.

Intengan HD, Schiffrin EL (2000). Structure and mechanical properties of resistance arteries in hypertension: role of adhesion molecules and extracellular matrix determinants. *Hypertension* **36**(3)**:** 312-318.

Ishikawa T, Hume JR, Keef KD (1993). Regulation of Ca2+ channels by cAMP and cGMP in vascular smooth muscle cells. *Circ Res* **73**(6)**:** 1128-1137.

Itoh T, Ikebe M, Kargacin GJ, Hartshorne DJ, Kemp BE, Fay FS (1989). Effects of modulators of myosin light-chain kinase activity in single smooth muscle cells. *Nature* **338**(6211)**:** 164-167.

Iwamoto T, Kita S, Zhang J, Blaustein MP, Arai Y, Yoshida S*, et al.* (2004). Salt-sensitive hypertension is triggered by Ca2+ entry via Na+/Ca2+ exchanger type-1 in vascular smooth muscle. *Nat Med* **10**(11)**:** 1193-1199.

Izzard AS, Horton S, Heerkens EH, Shaw L, Heagerty AM (2006). Middle cerebral artery structure and distensibility during developing and established phases of hypertension in the spontaneously hypertensive rat. *J Hypertens* **24**(5)**:** 875-880.

Izzard AS, Rizzoni D, Agabiti-Rosei E, Heagerty AM (2005). Small artery structure and hypertension: adaptive changes and target organ damage. *J Hypertens* **23**(2)**:** 247-250.

Jaggar JH, Wellman GC, Heppner TJ, Porter VA, Perez GJ, Gollasch M*, et al.* (1998). Ca2+ channels, ryanodine receptors and Ca(2+)-activated K+ channels: a functional unit for regulating arterial tone. *Acta Physiol Scand* **164**(4)**:** 577-587.

James P, Inui M, Tada M, Chiesi M, Carafoli E (1989). Nature and site of phospholamban regulation of the Ca2+ pump of sarcoplasmic reticulum. *Nature* **342**(6245)**:** 90-92.

James P, Maeda M, Fischer R, Verma AK, Krebs J, Penniston JT*, et al.* (1988). Identification and primary structure of a calmodulin binding domain of the Ca2+ pump of human erythrocytes. *J Biol Chem* **263**(6)**:** 2905-2910.

Je HD, Gallant C, Leavis PC, Morgan KG (2004). Caveolin-1 regulates contractility in differentiated vascular smooth muscle. *Am J Physiol Heart Circ Physiol* **286**(1)**:** H91-98.

Jimenez-Altayo F, Martin A, Rojas S, Justicia C, Briones AM, Giraldo J*, et al.* (2007). Transient middle cerebral artery occlusion causes different structural, mechanical, and myogenic alterations in normotensive and hypertensive rats. *Am J Physiol Heart Circ Physiol* **293**(1)**:** H628-635.

Jones S, Solomon A, Sanz-Rosa D, Moore C, Holbrook L, Cartwright EJ*, et al.* (2010). The plasma membrane calcium ATPase modulates calcium homeostasis, intracellular signaling events and function in platelets. *J Thromb Haemost* **8**(12)**:** 2766-2774.

Kamishima T, McCarron JG (1998). Ca2+ removal mechanisms in rat cerebral resistance size arteries. *Biophys J* **75**(4)**:** 1767-1773.

Kamishima T, Quayle JM (2002). Mitochondrial Ca2+ uptake is important over low [Ca2+]i range in arterial smooth muscle. *Am J Physiol Heart Circ Physiol* **283**(6)**:** H2431-2439.

Kamm KE, Stull JT (1989). Regulation of smooth muscle contractile elements by second messengers. *Annu Rev Physiol* **51:** 299-313.

Karaki H, Ozaki H, Hori M, Mitsui-Saito M, Amano K, Harada K*, et al.* (1997). Calcium movements, distribution, and functions in smooth muscle. *Pharmacol Rev* **49**(2)**:** 157-230.

Karashima E, Nishimura J, Iwamoto T, Hirano K, Hirano M, Kita S*, et al.* (2007). Involvement of Na+-Ca2+ exchanger in cAMP-mediated relaxation in mice aorta: evaluation using transgenic mice. *Br J Pharmacol* **150**(4)**:** 434-444.

Keeton TP, Burk SE, Shull GE (1993). Alternative splicing of exons encoding the calmodulin-binding domains and C termini of plasma membrane Ca(2+)-ATPase isoforms 1, 2, 3, and 4. *J Biol Chem* **268**(4)**:** 2740-2748.

Keeton TP, Shull GE (1995). Primary structure of rat plasma membrane Ca(2+)-ATPase isoform 4 and analysis of alternative splicing patterns at splice site A. *Biochem J* **306 (Pt 3)**(Pt 3)**:** 779-785.

Kerwin JF, Jr., Lancaster JR, Jr., Feldman PL (1995). Nitric oxide: a new paradigm for second messengers. *J Med Chem* **38**(22)**:** 4343-4362.

Kessler F, Falchetto R, Heim R, Meili R, Vorherr T, Strehler EE*, et al.* (1992). Study of calmodulin binding to the alternatively spliced C-terminal domain of the plasma membrane Ca2+ pump. *Biochemistry* **31**(47)**:** 11785-11792.

Kim E, DeMarco SJ, Marfatia SM, Chishti AH, Sheng M, Strehler EE (1998). Plasma membrane Ca2+ ATPase isoform 4b binds to membrane-associated guanylate kinase (MAGUK) proteins via their PDZ (PSD-95/Dlg/ZO-1) domains. *J Biol Chem* **273**(3)**:** 1591-1595.

Kobayashi Y, Hirawa N, Tabara Y, Muraoka H, Fujita M, Miyazaki N*, et al.* (2012). Mice lacking hypertension candidate gene ATP2B1 in vascular smooth muscle cells show significant blood pressure elevation. *Hypertension* **59**(4)**:** 854-860.

Korsgaard N, Aalkjaer C, Heagerty AM, Izzard AS, Mulvany MJ (1993). Histology of subcutaneous small arteries from patients with essential hypertension. *Hypertension* **22**(4)**:** 523-526.

Kozel PJ, Davis RR, Krieg EF, Shull GE, Erway LC (2002). Deficiency in plasma membrane calcium ATPase isoform 2 increases susceptibility to noise-induced hearing loss in mice. *Hear Res* **164**(1-2)**:** 231-239.

Kozel PJ, Friedman RA, Erway LC, Yamoah EN, Liu LH, Riddle T*, et al.* (1998). Balance and hearing deficits in mice with a null mutation in the gene encoding plasma membrane Ca2+-ATPase isoform 2. *J Biol Chem* **273**(30)**:** 18693-18696.

Kubis HP, Hanke N, Scheibe RJ, Meissner JD, Gros G (2003). Ca2+ transients activate calcineurin/NFATc1 and initiate fast-to-slow transformation in a primary skeletal muscle culture. *Am J Physiol Cell Physiol* **285**(1)**:** C56-63.

Kuga T, Kobayashi S, Hirakawa Y, Kanaide H, Takeshita A (1996). Cell cycle--dependent expression of L- and T-type Ca2+ currents in rat aortic smooth muscle cells in primary culture. *Circ Res* **79**(1)**:** 14-19.

Kuhr FK, Smith KA, Song MY, Levitan I, Yuan JX (2012). New mechanisms of pulmonary arterial hypertension: role of Ca(2)(+) signaling. *Am J Physiol Heart Circ Physiol* **302**(8)**:** H1546-1562.

Kukovetz WR, Holzmann S, Wurm A, Poch G (1979). Prostacyclin increases cAMP in coronary arteries. *J Cyclic Nucleotide Res* **5**(6)**:** 469-476.

Kumar B, Dreja K, Shah SS, Cheong A, Xu SZ, Sukumar P*, et al.* (2006). Upregulated TRPC1 channel in vascular injury in vivo and its role in human neointimal hyperplasia. *Circ Res* **98**(4)**:** 557-563.

Kuriyama H, Kitamura K, Nabata H (1995). Pharmacological and physiological significance of ion channels and factors that modulate them in vascular tissues. *Pharmacol Rev* **47**(3)**:** 387-573.

Kurnellas MP, Nicot A, Shull GE, Elkabes S (2005). Plasma membrane calcium ATPase deficiency causes neuronal pathology in the spinal cord: a potential mechanism for neurodegeneration in multiple sclerosis and spinal cord injury. *Faseb J* **19**(2)**:** 298-300.

Lai Y, Thomas GD, Yue Y, Yang HT, Li D, Long C*, et al.* (2009). Dystrophins carrying spectrin-like repeats 16 and 17 anchor nNOS to the sarcolemma and enhance exercise performance in a mouse model of muscular dystrophy. *J Clin Invest* **119**(3)**:** 624-635.

Lalli J, Harrer JM, Luo W, Kranias EG, Paul RJ (1997). Targeted ablation of the phospholamban gene is associated with a marked decrease in sensitivity in aortic smooth muscle. *Circ Res* **80**(4)**:** 506-513.

Lamont C, Wier WG (2004). Different roles of ryanodine receptors and inositol (1,4,5)-trisphosphate receptors in adrenergically stimulated contractions of small arteries. *Am J Physiol Heart Circ Physiol* **287**(2)**:** H617-625.

Lamping KG, Nuno DW, Shesely EG, Maeda N, Faraci FM (2000). Vasodilator mechanisms in the coronary circulation of endothelial nitric oxide synthase-deficient mice. *Am J Physiol Heart Circ Physiol* **279**(4)**:** H1906-1912.

Laporte R, Laher I (1997). Sarcoplasmic reticulum-sarcolemma interactions and vascular smooth muscle tone. *J Vasc Res* **34**(5)**:** 325-343.

Large WA (2002). Receptor-operated Ca2(+)-permeable nonselective cation channels in vascular smooth muscle: a physiologic perspective. *J Cardiovasc Electrophysiol* **13**(5)**:** 493-501.

Laurent S, Boutouyrie P, Asmar R, Gautier I, Laloux B, Guize L*, et al.* (2001). Aortic stiffness is an independent predictor of all-cause and cardiovascular mortality in hypertensive patients. *Hypertension* **37**(5)**:** 1236-1241.

Laurent S, Boutouyrie P, Lacolley P (2005). Structural and genetic bases of arterial stiffness. *Hypertension* **45**(6)**:** 1050-1055.

Laurent S, Caviezel B, Beck L, Girerd X, Billaud E, Boutouyrie P*, et al.* (1994). Carotid artery distensibility and distending pressure in hypertensive humans. *Hypertension* **23**(6 Pt 2)**:** 878-883.

Lee MR, Li L, Kitazawa T (1997). Cyclic GMP causes Ca2+ desensitization in vascular smooth muscle by activating the myosin light chain phosphatase. *J Biol Chem* **272**(8)**:** 5063-5068.

Lee WJ, Roberts-Thomson SJ, Holman NA, May FJ, Lehrbach GM, Monteith GR (2002). Expression of plasma membrane calcium pump isoform mRNAs in breast cancer cell lines. *Cell Signal* **14**(12)**:** 1015-1022.

Lee WJ, Roberts-Thomson SJ, Monteith GR (2005). Plasma membrane calcium-ATPase 2 and 4 in human breast cancer cell lines. *Biochem Biophys Res Commun* **337**(3)**:** 779-783.

Lesh RE, Nixon GF, Fleischer S, Airey JA, Somlyo AP, Somlyo AV (1998). Localization of ryanodine receptors in smooth muscle. *Circ Res* **82**(2)**:** 175-185.

Leung FP, Yung LM, Yao X, Laher I, Huang Y (2008). Store-operated calcium entry in vascular smooth muscle. *Br J Pharmacol* **153**(5)**:** 846-857.

Levy D, Ehret GB, Rice K, Verwoert GC, Launer LJ, Dehghan A*, et al.* (2009). Genome-wide association study of blood pressure and hypertension. *Nat Genet* **41**(6)**:** 677-687.

Levy D, Seigneuret M, Bluzat A, Rigaud JL (1990). Evidence for proton countertransport by the sarcoplasmic reticulum Ca2(+)-ATPase during calcium transport in reconstituted proteoliposomes with low ionic permeability. *J Biol Chem* **265**(32)**:** 19524-19534.

Lincoln TM, Komalavilas P, Cornwell TL (1994). Pleiotropic regulation of vascular smooth muscle tone by cyclic GMP-dependent protein kinase. *Hypertension* **23**(6 Pt 2)**:** 1141-1147.

Lingrel JB, Kuntzweiler T (1994). Na+,K(+)-ATPase. *J Biol Chem* **269**(31)**:** 19659-19662.

Liu H, Xiong Z, Sperelakis N (1997). Cyclic nucleotides regulate the activity of L-type calcium channels in smooth muscle cells from rat portal vein. *J Mol Cell Cardiol* **29**(5)**:** 1411-1421.

Liu L, Ishida Y, Okunade G, Pyne-Geithman GJ, Shull GE, Paul RJ (2007). Distinct roles of PMCA isoforms in Ca2+ homeostasis of bladder smooth muscle: evidence from PMCA gene-ablated mice. *Am J Physiol Cell Physiol* **292**(1)**:** C423-431.

Liu L, Ishida Y, Okunade G, Shull GE, Paul RJ (2006). Role of plasma membrane Ca2+-ATPase in contraction-relaxation processes of the bladder: evidence from PMCA gene-ablated mice. *Am J Physiol Cell Physiol* **290**(4)**:** C1239-1247.

Lloyd PG, Hardin CD (2001). Caveolae and the organization of carbohydrate metabolism in vascular smooth muscle. *J Cell Biochem* **82**(3)**:** 399-408.

Lorell BH, Carabello BA (2000). Left ventricular hypertrophy: pathogenesis, detection, and prognosis. *Circulation* **102**(4)**:** 470-479.

Luksha L, Agewall S, Kublickiene K (2009). Endothelium-derived hyperpolarizing factor in vascular physiology and cardiovascular disease. *Atherosclerosis* **202**(2)**:** 330-344.

Lytton J (2007). Na+/Ca2+ exchangers: three mammalian gene families control Ca2+ transport. *Biochem J* **406**(3)**:** 365-382.

Lytton J, Zarain-Herzberg A, Periasamy M, MacLennan DH (1989). Molecular cloning of the mammalian smooth muscle sarco(endo)plasmic reticulum Ca2+-ATPase. *J Biol Chem* **264**(12)**:** 7059-7065.

Mahaney JE, Thomas DD (1991). Effects of melittin on molecular dynamics and Ca-ATPase activity in sarcoplasmic reticulum membranes: electron paramagnetic resonance. *Biochemistry* **30**(29)**:** 7171-7180.

Mammano F (2011). Ca2+ homeostasis defects and hereditary hearing loss. *Biofactors* **37**(3)**:** 182-188.

Marchand A, Abi-Gerges A, Saliba Y, Merlet E, Lompre AM (2012). Calcium signaling in vascular smooth muscle cells: from physiology to pathology. *Adv Exp Med Biol* **740:** 795-810.

Marin J (1995). Age-related changes in vascular responses: a review. *Mech Ageing Dev* **79**(2-3)**:** 71-114.

Marin J (1993). Mechanisms involved in the increased vascular resistance in hypertension. *J Auton Pharmacol* **13**(2)**:** 127-176.

Marin J, Encabo A, Briones A, Garcia-Cohen EC, Alonso MJ (1999). Mechanisms involved in the cellular calcium homeostasis in vascular smooth muscle: calcium pumps. *Life Sci* **64**(5)**:** 279-303.

Martin R, Harvey NC, Crozier SR, Poole JR, Javaid MK, Dennison EM*, et al.* (2007). Placental calcium transporter (PMCA3) gene expression predicts intrauterine bone mineral accrual. *Bone* **40**(5)**:** 1203-1208.

Martinez-Lemus LA (2012). The dynamic structure of arterioles. *Basic Clin Pharmacol Toxicol* **110**(1)**:** 5-11.

Martinez-Lemus LA, Hill MA, Meininger GA (2009). The plastic nature of the vascular wall: a continuum of remodeling events contributing to control of arteriolar diameter and structure. *Physiology (Bethesda)* **24:** 45-57.

Mata AM, Berrocal M, Sepulveda MR (2011). Impairment of the activity of the plasma membrane Ca(2)(+)-ATPase in Alzheimer's disease. *Biochem Soc Trans* **39**(3)**:** 819-822.

Matchkov VV, Kudryavtseva O, Aalkjaer C (2012). Intracellular Ca(2)(+) signalling and phenotype of vascular smooth muscle cells. *Basic Clin Pharmacol Toxicol* **110**(1)**:** 42-48.

Matsumoto Y, Hof A, Baumlin Y, Muller M, Prescott MF, Hof RP (2003). Dynamics of medial smooth muscle changes after carotid artery transplantation in transgenic mice expressing green fluorescent protein. *Transplantation* **76**(11)**:** 1569-1572.

Matthew , Carwright E, Burdyga, Neyes L, S W (2004). The effect of knocking out isoform4 of the plasma membrane Ca-ATPase (PMCA) on force in mouse myometrium. *J. Physiol. Proc. Glasgow Meet. Physiol. Soc.***:** 557P C531.

Matthew A, Cartwright E, Burdyga, Neyes L, Wray S (2004). The effect of knocking out isoform4 of the plasma membrane Ca-ATPase (PMCA) on force in mouse myometrium. *J. Physiol. Proc. Glasgow Meet. Physiol. Soc.***:** 557P C531.

Matthew A, Shmygol A, Wray S (2004). Ca2+ entry, efflux and release in smooth muscle. *Biol Res* **37**(4)**:** 617-624.

McCarron JG, Chalmers S, Bradley KN, MacMillan D, Muir TC (2006). Ca2+ microdomains in smooth muscle. *Cell Calcium* **40**(5-6)**:** 461-493.

McGeown JG (2004). Interactions between inositol 1,4,5-trisphosphate receptors and ryanodine receptors in smooth muscle: one store or two? *Cell Calcium* **35**(6)**:** 613-619.

Means AR, VanBerkum MF, Bagchi I, Lu KP, Rasmussen CD (1991). Regulatory functions of calmodulin. *Pharmacol Ther* **50**(2)**:** 255-270.

Megens RT, Reitsma S, Schiffers PH, Hilgers RH, De Mey JG, Slaaf DW*, et al.* (2007). Two-photon microscopy of vital murine elastic and muscular arteries. Combined structural and functional imaging with subcellular resolution. *J Vasc Res* **44**(2)**:** 87-98.

Melikian N, Seddon MD, Casadei B, Chowienczyk PJ, Shah AM (2009). Neuronal nitric oxide synthase and human vascular regulation. *Trends Cardiovasc Med* **19**(8)**:** 256-262.

Missiaen L, De Smedt H, Droogmans G, Himpens B, Casteels R (1992). Calcium ion homeostasis in smooth muscle. *Pharmacol Ther* **56**(2)**:** 191-231.

Missiaen L, Wuytack F, Raeymaekers L, De Smedt H, Droogmans G, Declerck I*, et al.* (1991). Ca2+ extrusion across plasma membrane and Ca2+ uptake by intracellular stores. *Pharmacol Ther* **50**(2)**:** 191-232.

Mohamed T, Oceandy D, Abou-Leisa R, Zi M, Prehar S, Baudoin-Stanley F*, et al.* (2011a). Prevention and reversal of hypertrophy through a novel drug-like compund that inhibits PMCA4/calcineurin microdomain. *American Heart Association* **Circulation 2011:**(124: A9943).

Mohamed TM, Oceandy D, Prehar S, Alatwi N, Hegab Z, Baudoin FM*, et al.* (2009). Specific role of neuronal nitric-oxide synthase when tethered to the plasma membrane calcium pump in regulating the beta-adrenergic signal in the myocardium. *J Biol Chem* **284**(18)**:** 12091-12098.

Mohamed TM, Oceandy D, Zi M, Prehar S, Alatwi N, Wang Y*, et al.* (2011b). Plasma membrane calcium pump (PMCA4)-neuronal nitric-oxide synthase complex regulates cardiac contractility through modulation of a compartmentalized cyclic nucleotide microdomain. *J Biol Chem* **286**(48)**:** 41520-41529.

Molkentin JD, Lu JR, Antos CL, Markham B, Richardson J, Robbins J*, et al.* (1998). A calcineurin-dependent transcriptional pathway for cardiac hypertrophy. *Cell* **93**(2)**:** 215-228.

Mombouli JV, Vanhoutte PM (1999). Endothelial dysfunction: from physiology to therapy. *J Mol Cell Cardiol* **31**(1)**:** 61-74.

Moncada S (1982). Prostacyclin and arterial wall biology. *Arteriosclerosis* **2**(3)**:** 193-207.

Moncada S, Higgs EA (2006). The discovery of nitric oxide and its role in vascular biology. *Br J Pharmacol* **147 Suppl 1**(1)**:** S193-201.

Moncada S, Palmer RM, Higgs EA (1991). Nitric oxide: physiology, pathophysiology, and pharmacology. *Pharmacol Rev* **43**(2)**:** 109-142.

Moncada S, Vane JR (1979). The role of prostacyclin in vascular tissue. *Fed Proc* **38**(1)**:** 66-71.

Monteith GR, Kable EP, Chen S, Roufogalis BD (1996). Plasma membrane calcium pump-mediated calcium efflux and bulk cytosolic free calcium in cultured aortic smooth muscle cells from spontaneously hypertensive and Wistar-Kyoto normotensives rats. *J Hypertens* **14**(4)**:** 435-442.

Monteith GR, Kable EP, Kuo TH, Roufogalis BD (1997). Elevated plasma membrane and sarcoplasmic reticulum Ca2+ pump mRNA levels in cultured aortic smooth muscle cells from spontaneously hypertensive rats. *Biochem Biophys Res Commun* **230**(2)**:** 344-346.

Moore ED, Etter EF, Philipson KD, Carrington WA, Fogarty KE, Lifshitz LM*, et al.* (1993). Coupling of the Na+/Ca2+ exchanger, Na+/K+ pump and sarcoplasmic reticulum in smooth muscle. *Nature* **365**(6447)**:** 657-660.

Morgado M, Cairrao E, Santos-Silva AJ, Verde I (2012). Cyclic nucleotide-dependent relaxation pathways in vascular smooth muscle. *Cell Mol Life Sci* **69**(2)**:** 247-266.

Mulvany MJ (2002). Small artery remodeling and significance in the development of hypertension. *News Physiol Sci* **17:** 105-109.

Mulvany MJ (2012). Small artery remodelling in hypertension. *Basic Clin Pharmacol Toxicol* **110**(1)**:** 49-55.

Mulvany MJ (2008). Small artery remodelling in hypertension: causes, consequences and therapeutic implications. *Med Biol Eng Comput* **46**(5)**:** 461-467.

Mulvany MJ (1999). Vascular remodelling of resistance vessels: can we define this? *Cardiovasc Res* **41**(1)**:** 9-13.

Mulvany MJ (1987). Vascular structure and smooth muscle contractility in experimental hypertension. *J Cardiovasc Pharmacol* **10 Suppl 6:** S79-85.

Mulvany MJ, Aalkjaer C (1990). Structure and function of small arteries. *Physiol Rev* **70**(4)**:** 921-961.

Mulvany MJ, Baumbach GL, Aalkjaer C, Heagerty AM, Korsgaard N, Schiffrin EL*, et al.* (1996). Vascular remodeling. *Hypertension* **28**(3)**:** 505-506.

Nakamori M, Takahashi MP (2011). The role of alpha-dystrobrevin in striated muscle. *Int J Mol Sci* **12**(3)**:** 1660-1671.

Nakasaki Y, Iwamoto T, Hanada H, Imagawa T, Shigekawa M (1993). Cloning of the rat aortic smooth muscle Na+/Ca2+ exchanger and tissue-specific expression of isoforms. *J Biochem* **114**(4)**:** 528-534.

Nakata S, Tsutsui M, Shimokawa H, Suda O, Morishita T, Shibata K*, et al.* (2008). Spontaneous myocardial infarction in mice lacking all nitric oxide synthase isoforms. *Circulation* **117**(17)**:** 2211-2223.

Navedo MF, Amberg GC, Westenbroek RE, Sinnegger-Brauns MJ, Catterall WA, Striessnig J*, et al.* (2007). Ca(v)1.3 channels produce persistent calcium sparklets, but Ca(v)1.2 channels are responsible for sparklets in mouse arterial smooth muscle. *Am J Physiol Heart Circ Physiol* **293**(3)**:** H1359-1370.

Nazer MA, Van Breemen C (1998). A role for the sarcoplasmic reticulum in Ca2+ extrusion from rabbit inferior vena cava smooth muscle. *Am J Physiol* **274**(1 Pt 2)**:** H123-131.

Nelson MT, Cheng H, Rubart M, Santana LF, Bonev AD, Knot HJ*, et al.* (1995). Relaxation of arterial smooth muscle by calcium sparks. *Science* **270**(5236)**:** 633-637.

Nicot A, Ratnakar PV, Ron Y, Chen CC, Elkabes S (2003). Regulation of gene expression in experimental autoimmune encephalomyelitis indicates early neuronal dysfunction. *Brain* **126**(Pt 2)**:** 398-412.

Nixon GF, Mignery GA, Somlyo AV (1994). Immunogold localization of inositol 1,4,5-trisphosphate receptors and characterization of ultrastructural features of the sarcoplasmic reticulum in phasic and tonic smooth muscle. *J Muscle Res Cell Motil* **15**(6)**:** 682-700.

O'Donnell ME, Owen NE (1994). Regulation of ion pumps and carriers in vascular smooth muscle. *Physiol Rev* **74**(3)**:** 683-721.

Oceandy D, Cartwright EJ, Emerson M, Prehar S, Baudoin FM, Zi M*, et al.* (2007). Neuronal nitric oxide synthase signaling in the heart is regulated by the sarcolemmal calcium pump 4b. *Circulation* **115**(4)**:** 483-492.

Oceandy D, Mohamed TM, Cartwright EJ, Neyses L (2011). Local signals with global impacts and clinical implications: lessons from the plasma membrane calcium pump (PMCA4). *Biochim Biophys Acta* **1813**(5)**:** 974-978.

Ogletree ML (1987). Overview of physiological and pathophysiological effects of thromboxane A2. *Fed Proc* **46**(1)**:** 133-138.

Okunade GW, Miller ML, Pyne GJ, Sutliff RL, O'Connor KT, Neumann JC*, et al.* (2004). Targeted ablation of plasma membrane Ca2+-ATPase (PMCA) 1 and 4 indicates a major housekeeping function for PMCA1 and a critical role in hyperactivated sperm motility and male fertility for PMCA4. *J Biol Chem* **279**(32)**:** 33742-33750.

Oloizia B, Paul RJ (2008). Ca2+ clearance and contractility in vascular smooth muscle: evidence from gene-altered murine models. *J Mol Cell Cardiol* **45**(3)**:** 347-362.

Oltman CL, Weintraub NL, VanRollins M, Dellsperger KC (1998). Epoxyeicosatrienoic acids and dihydroxyeicosatrienoic acids are potent vasodilators in the canine coronary microcirculation. *Circ Res* **83**(9)**:** 932-939.

Ono K, Wang X, Han J (2001). Resistance to tumor necrosis factor-induced cell death mediated by PMCA4 deficiency. *Mol Cell Biol* **21**(24)**:** 8276-8288.

Orallo F (1996). Regulation of cytosolic calcium levels in vascular smooth muscle. *Pharmacol Ther* **69**(3)**:** 153-171.

Ostrom RS, Liu X, Head BP, Gregorian C, Seasholtz TM, Insel PA (2002). Localization of adenylyl cyclase isoforms and G protein-coupled receptors in vascular smooth muscle cells: expression in caveolin-rich and noncaveolin domains. *Mol Pharmacol* **62**(5)**:** 983-992.

Paisley AN, Izzard AS, Gemmell I, Cruickshank K, Trainer PJ, Heagerty AM (2009). Small vessel remodeling and impaired endothelial-dependent dilatation in subcutaneous resistance arteries from patients with acromegaly. *J Clin Endocrinol Metab* **94**(4)**:** 1111-1117.

Pande J, Mallhi KK, Sawh A, Szewczyk MM, Simpson F, Grover AK (2006). Aortic smooth muscle and endothelial plasma membrane Ca2+ pump isoforms are inhibited differently by the extracellular inhibitor caloxin 1b1. *Am J Physiol Cell Physiol* **290**(5)**:** C1341-1349.

Pande J, Szewczyk MM, Kuszczak I, Grover S, Escher E, Grover AK (2008). Functional effects of caloxin 1c2, a novel engineered selective inhibitor of plasma membrane Ca(2+)-pump isoform 4, on coronary artery. *J Cell Mol Med* **12**(3)**:** 1049-1060.

Park KM, Trucillo M, Serban N, Cohen RA, Bolotina VM (2008). Role of iPLA2 and store-operated channels in agonist-induced Ca2+ influx and constriction in cerebral, mesenteric, and carotid arteries. *Am J Physiol Heart Circ Physiol* **294**(3)**:** H1183-1187.

Patrono C, Ciabattoni G, Davi G (1990). Thromboxane biosynthesis in cardiovascular diseases. *Stroke* **21**(12 Suppl)**:** IV130-133.

Perez-Reyes E (1998). Molecular characterization of a novel family of low voltage-activated, T-type, calcium channels. *J Bioenerg Biomembr* **30**(4)**:** 313-318.

Perez-Reyes E (2003). Molecular physiology of low-voltage-activated t-type calcium channels. *Physiol Rev* **83**(1)**:** 117-161.

Pfitzer G (2001). Invited review: regulation of myosin phosphorylation in smooth muscle. *J Appl Physiol* **91**(1)**:** 497-503.

Philipson KD, Nicoll DA (2000). Sodium-calcium exchange: a molecular perspective. *Annu Rev Physiol* **62:** 111-133.

Plane F, Wiley KE, Jeremy JY, Cohen RA, Garland CJ (1998). Evidence that different mechanisms underlie smooth muscle relaxation to nitric oxide and nitric oxide donors in the rabbit isolated carotid artery. *Br J Pharmacol* **123**(7)**:** 1351-1358.

Poburko D, Kuo KH, Dai J, Lee CH, van Breemen C (2004a). Organellar junctions promote targeted Ca2+ signaling in smooth muscle: why two membranes are better than one. *Trends Pharmacol Sci* **25**(1)**:** 8-15.

Poburko D, Lee CH, van Breemen C (2004b). Vascular smooth muscle mitochondria at the cross roads of Ca(2+) regulation. *Cell Calcium* **35**(6)**:** 509-521.

Pohl U, Holtz J, Busse R, Bassenge E (1986). Crucial role of endothelium in the vasodilator response to increased flow in vivo. *Hypertension* **8**(1)**:** 37-44.

Pollock JS, Nakane M, Buttery LD, Martinez A, Springall D, Polak JM*, et al.* (1993). Characterization and localization of endothelial nitric oxide synthase using specific monoclonal antibodies. *Am J Physiol* **265**(5 Pt 1)**:** C1379-1387.

Post H, Schwarz A, Brandenburger T, Aumuller G, Wilhelm B (2010). Arrangement of PMCA4 in bovine sperm membrane fractions. *Int J Androl* **33**(6)**:** 775-783.

Pozzan T, Rizzuto R, Volpe P, Meldolesi J (1994). Molecular and cellular physiology of intracellular calcium stores. *Physiol Rev* **74**(3)**:** 595-636.

Prasad V, Okunade G, Liu L, Paul RJ, Shull GE (2007). Distinct phenotypes among plasma membrane Ca2+-ATPase knockout mice. *Ann N Y Acad Sci* **1099:** 276-286.

Pritchard TJ, Parvatiyar M, Bullard DP, Lynch RM, Lorenz JN, Paul RJ (2007). Transgenic mice expressing Na+-K+-ATPase in smooth muscle decreases blood pressure. *Am J Physiol Heart Circ Physiol* **293**(2)**:** H1172-1182.

Putney JW, Jr., Bird GS (1993). The signal for capacitative calcium entry. *Cell* **75**(2)**:** 199-201.

Quednau BD, Nicoll DA, Philipson KD (2004). The sodium/calcium exchanger family-SLC8. *Pflugers Arch* **447**(5)**:** 543-548.

Quednau BD, Nicoll DA, Philipson KD (1997). Tissue specificity and alternative splicing of the Na+/Ca2+ exchanger isoforms NCX1, NCX2, and NCX3 in rat. *Am J Physiol* **272**(4 Pt 1)**:** C1250-1261.

Quilley J, McGiff JC (2000). Is EDHF an epoxyeicosatrienoic acid? *Trends Pharmacol Sci* **21**(4)**:** 121-124.

Rapoport RM, Murad F (1983). Agonist-induced endothelium-dependent relaxation in rat thoracic aorta may be mediated through cGMP. *Circ Res* **52**(3)**:** 352-357.

Ratz PH, Miner AS, Barbour SE (2009). Calcium-independent phospholipase A2 participates in KCl-induced calcium sensitization of vascular smooth muscle. *Cell Calcium* **46**(1)**:** 65-72.

Reinhardt TA, Filoteo AG, Penniston JT, Horst RL (2000). Ca(2+)-ATPase protein expression in mammary tissue. *Am J Physiol Cell Physiol* **279**(5)**:** C1595-1602.

Reinhardt TA, Lippolis JD, Shull GE, Horst RL (2004). Null mutation in the gene encoding plasma membrane Ca2+-ATPase isoform 2 impairs calcium transport into milk. *J Biol Chem* **279**(41)**:** 42369-42373.

Rembold CM (1992). Regulation of contraction and relaxation in arterial smooth muscle. *Hypertension* **20**(2)**:** 129-137.

Ren D, Navarro B, Perez G, Jackson AC, Hsu S, Shi Q*, et al.* (2001). A sperm ion channel required for sperm motility and male fertility. *Nature* **413**(6856)**:** 603-609.

Rhodin J, D. B, A. S, H. S (1980). Rhodin J. :Archirtecture of the vessel wall in Handbook of Physiology. *The American Physiological Society* **2:** 1-29.

Ribiczey P, Tordai A, Andrikovics H, Filoteo AG, Penniston JT, Enouf J*, et al.* (2007). Isoform-specific up-regulation of plasma membrane Ca2+ATPase expression during colon and gastric cancer cell differentiation. *Cell Calcium* **42**(6)**:** 590-605.

Rizzoni D, De Ciuceis C, Porteri E, Semeraro F, Rosei EA (2012). Structural alterations in small resistance arteries in obesity. *Basic Clin Pharmacol Toxicol* **110**(1)**:** 56-62.

Rizzoni D, Muiesan ML, Porteri E, De Ciuceis C, Boari GE, Salvetti M*, et al.* (2009a). Vascular remodeling, macro- and microvessels: therapeutic implications. *Blood Press* **18**(5)**:** 242-246.

Rizzoni D, Paiardi S, Rodella L, Porteri E, De Ciuceis C, Rezzani R*, et al.* (2006). Changes in extracellular matrix in subcutaneous small resistance arteries of patients with primary aldosteronism. *J Clin Endocrinol Metab* **91**(7)**:** 2638-2642.

Rizzoni D, Porteri E, Castellano M, Bettoni G, Muiesan ML, Muiesan P*, et al.* (1996). Vascular hypertrophy and remodeling in secondary hypertension. *Hypertension* **28**(5)**:** 785-790.

Rizzoni D, Porteri E, Guelfi D, Muiesan ML, Valentini U, Cimino A*, et al.* (2001). Structural alterations in subcutaneous small arteries of normotensive and hypertensive patients with non-insulin-dependent diabetes mellitus. *Circulation* **103**(9)**:** 1238-1244.

Rizzoni D, Rosei EA (2009b). Small artery remodeling in diabetes mellitus. *Nutr Metab Cardiovasc Dis* **19**(8)**:** 587-592.

Rosei EA, Rizzoni D (2005). Pathophysiology and clinical meaning of small resistance artery remodeling. *Curr Hypertens Rep* **7**(2)**:** 79-80.

Rybalkin SD, Yan C, Bornfeldt KE, Beavo JA (2003). Cyclic GMP phosphodiesterases and regulation of smooth muscle function. *Circ Res* **93**(4)**:** 280-291.

Sachidanandam K, Hutchinson JR, Elgebaly MM, Mezzetti EM, Wang MH, Ergul A (2009). Differential effects of diet-induced dyslipidemia and hyperglycemia on mesenteric

resistance artery structure and function in type 2 diabetes. *J Pharmacol Exp Ther* **328**(1)**:** 123-130.

Sakurada S, Okamoto H, Takuwa N, Sugimoto N, Takuwa Y (2001). Rho activation in excitatory agonist-stimulated vascular smooth muscle. *Am J Physiol Cell Physiol* **281**(2)**:** C571-578.

Sakurada S, Takuwa N, Sugimoto N, Wang Y, Seto M, Sasaki Y*, et al.* (2003). Ca2+-dependent activation of Rho and Rho kinase in membrane depolarization-induced and receptor stimulation-induced vascular smooth muscle contraction. *Circ Res* **93**(6)**:** 548-556.

Sandow SL, Hill CE (2000). Incidence of myoendothelial gap junctions in the proximal and distal mesenteric arteries of the rat is suggestive of a role in endothelium-derived hyperpolarizing factor-mediated responses. *Circ Res* **86**(3)**:** 341-346.

Santiago-Garcia J, Mas-Oliva J, Saavedra D, Zarain-Herzberg A (1996). Analysis of mRNA expression and cloning of a novel plasma membrane Ca(2+)-ATPase splice variant in human heart. *Mol Cell Biochem* **155**(2)**:** 173-182.

Scarborough P, Bhatnagar P, Wickramasinghe K, Smolina K, Mitchell C, Rayner M (2010). Coronary heart disease statistics 2010 edition. *London, UK*.

Schiffrin EL, Deng LY, Larochelle P (1992). Blunted effects of endothelin upon small subcutaneous resistance arteries of mild essential hypertensive patients. *J Hypertens* **10**(5)**:** 437-444.

Schlossmann J, Ammendola A, Ashman K, Zong X, Huber A, Neubauer G*, et al.* (2000). Regulation of intracellular calcium by a signalling complex of IRAG, IP3 receptor and cGMP kinase Ibeta. *Nature* **404**(6774)**:** 197-201.

Schofield I, Malik R, Izzard A, Austin C, Heagerty A (2002). Vascular structural and functional changes in type 2 diabetes mellitus: evidence for the roles of abnormal myogenic responsiveness and dyslipidemia. *Circulation* **106**(24)**:** 3037-3043.

Schuh K, Cartwright EJ, Jankevics E, Bundschu K, Liebermann J, Williams JC*, et al.* (2004). Plasma membrane Ca2+ ATPase 4 is required for sperm motility and male fertility. *J Biol Chem* **279**(27)**:** 28220-28226.

Schuh K, Quaschning T, Knauer S, Hu K, Kocak S, Roethlein N*, et al.* (2003). Regulation of vascular tone in animals overexpressing the sarcolemmal calcium pump. *J Biol Chem* **278**(42)**:** 41246-41252.

Schuh K, Uldrijan S, Telkamp M, Rothlein N, Neyses L (2001). The plasmamembrane calmodulin-dependent calcium pump: a major regulator of nitric oxide synthase I. *J Cell Biol* **155**(2)**:** 201-205.

Schuhmann K, Groschner K (1994). Protein kinase-C mediates dual modulation of L-type Ca2+ channels in human vascular smooth muscle. *FEBS Lett* **341**(2-3)**:** 208-212.

Schultz JM, Yang Y, Caride AJ, Filoteo AG, Penheiter AR, Lagziel A*, et al.* (2005). Modification of human hearing loss by plasma-membrane calcium pump PMCA2. *N Engl J Med* **352**(15)**:** 1557-1564.

Schwab BL, Guerini D, Didszun C, Bano D, Ferrando-May E, Fava E*, et al.* (2002). Cleavage of plasma membrane calcium pumps by caspases: a link between apoptosis and necrosis. *Cell Death Differ* **9**(8)**:** 818-831.

Seddon M, Melikian N, Dworakowski R, Shabeeh H, Jiang B, Byrne J*, et al.* (2009). Effects of neuronal nitric oxide synthase on human coronary artery diameter and blood flow in vivo. *Circulation* **119**(20)**:** 2656-2662.

Segal SS, Brett SE, Sessa WC (1999). Codistribution of NOS and caveolin throughout peripheral vasculature and skeletal muscle of hamsters. *Am J Physiol* **277**(3 Pt 2)**:** H1167-1177.

Sepulveda MR, Berrocal-Carrillo M, Gasset M, Mata AM (2006). The plasma membrane Ca2+-ATPase isoform 4 is localized in lipid rafts of cerebellum synaptic plasma membranes. *J Biol Chem* **281**(1)**:** 447-453.

Shaheen MA, Cartwright E.J. Characterisation of the effect of the deletion of PMCA1 on cardiac structure and function. PhD PhD, 2010.

Shaw L, Ahmed S, Austin C, Taggart MJ (2003). Inhibitors of actin filament polymerisation attenuate force but not global intracellular calcium in isolated pressurised resistance arteries. *J Vasc Res* **40**(1)**:** 1-10; discussion 10.

Shaw L, Sweeney MA, O'Neill SC, Jones CJ, Austin C, Taggart MJ (2006). Caveolae and sarcoplasmic reticular coupling in smooth muscle cells of pressurised arteries: the relevance for Ca2+ oscillations and tone. *Cardiovasc Res* **69**(4)**:** 825-835.

Shelly DA, He S, Moseley A, Weber C, Stegemeyer M, Lynch RM*, et al.* (2004). Na(+) pump alpha 2-isoform specifically couples to contractility in vascular smooth muscle: evidence from gene-targeted neonatal mice. *Am J Physiol Cell Physiol* **286**(4)**:** C813-820.

Shimokawa H (1999). Primary endothelial dysfunction: atherosclerosis. *J Mol Cell Cardiol* **31**(1)**:** 23-37.

Shuai JW, Jung P (2002). Stochastic properties of Ca(2+) release of inositol 1,4,5-trisphosphate receptor clusters. *Biophys J* **83**(1)**:** 87-97.

Silver FH, Horvath I, Foran DJ (2001). Viscoelasticity of the vessel wall: the role of collagen and elastic fibers. *Crit Rev Biomed Eng* **29**(3)**:** 279-301.

Simonsen U, Aalkjaer C (2012). Small artery structure and function: a dual interaction with many players. *Basic Clin Pharmacol Toxicol* **110**(1)**:** 2-4.

Somlyo AP, Himpens B (1989). Cell calcium and its regulation in smooth muscle. *Faseb J* **3**(11)**:** 2266-2276.

Somlyo AP, Somlyo AV (2003). Ca2+ sensitivity of smooth muscle and nonmuscle myosin II: modulated by G proteins, kinases, and myosin phosphatase. *Physiol Rev* **83**(4)**:** 1325-1358.

Somlyo AP, Somlyo AV (1994a). Signal transduction and regulation in smooth muscle. *Nature* **372**(6503)**:** 231-236.

Somlyo AP, Somlyo AV (1994b). Smooth muscle: excitation-contraction coupling, contractile regulation, and the cross-bridge cycle. *Alcohol Clin Exp Res* **18**(1)**:** 138-143.

Stahl WL, Eakin TJ, Owens JW, Jr., Breininger JF, Filuk PE, Anderson WR (1992). Plasma membrane Ca(2+)-ATPase isoforms: distribution of mRNAs in rat brain by in situ hybridization. *Brain Res Mol Brain Res* **16**(3-4)**:** 223-231.

Stahl WL, Keeton TP, Eakin TJ (1994). The plasma membrane Ca(2+)-ATPase mRNA isoform PMCA 4 is expressed at high levels in neurons of rat piriform cortex and neocortex. *Neurosci Lett* **178**(2)**:** 267-270.

Stauffer TP, Guerini D, Carafoli E (1995). Tissue distribution of the four gene products of the plasma membrane Ca2+ pump. A study using specific antibodies. *J Biol Chem* **270**(20)**:** 12184-12190.

Stauffer TP, Hilfiker H, Carafoli E, Strehler EE (1993). Quantitative analysis of alternative splicing options of human plasma membrane calcium pump genes. *J Biol Chem* **268**(34)**:** 25993-26003.

Stoyanova E, Trudel M, Felfly H, Lemsaddek W, Garcia D, Cloutier G (2012). Vascular Endothelial Dysfunction in beta-Thalassemia Occurs Despite Increased eNOS Expression and Preserved Vascular Smooth Muscle Cell Reactivity to NO. *PLoS One* **7**(6)**:** e38089.

Strain WD, Chaturvedi N, Nihoyannopoulos P, Bulpitt CJ, Rajkumar C, Shore AC (2005). Differences in the association between type 2 diabetes and impaired microvascular function among Europeans and African Caribbeans. *Diabetologia* **48**(11)**:** 2269-2277.

Street VA, McKee-Johnson JW, Fonseca RC, Tempel BL, Noben-Trauth K (1998). Mutations in a plasma membrane Ca2+-ATPase gene cause deafness in deafwaddler mice. *Nat Genet* **19**(4)**:** 390-394.

Strehler EE, Filoteo AG, Penniston JT, Caride AJ (2007). Plasma-membrane Ca(2+) pumps: structural diversity as the basis for functional versatility. *Biochem Soc Trans* **35**(Pt 5)**:** 919-922.

Strehler EE, Zacharias DA (2001). Role of alternative splicing in generating isoform diversity among plasma membrane calcium pumps. *Physiol Rev* **81**(1)**:** 21-50.

Stuehr DJ, Cho HJ, Kwon NS, Weise MF, Nathan CF (1991a). Purification and characterization of the cytokine-induced macrophage nitric oxide synthase: an FAD- and FMN-containing flavoprotein. *Proc Natl Acad Sci U S A* **88**(17)**:** 7773-7777.

Stuehr DJ, Kwon NS, Nathan CF, Griffith OW, Feldman PL, Wiseman J (1991b). N omega-hydroxy-L-arginine is an intermediate in the biosynthesis of nitric oxide from L-arginine. *J Biol Chem* **266**(10)**:** 6259-6263.

Sugiyama T, Goldman WF (1995). Measurement of SR free Ca2+ and Mg2+ in permeabilized smooth muscle cells with use of furaptra. *Am J Physiol* **269**(3 Pt 1)**:** C698-705.

Sun J, Kohr MJ, Nguyen T, Aponte AM, Connelly PS, Esfahani SG*, et al.* (2012). Disruption of caveolae blocks ischemic preconditioning-mediated S-nitrosylation of mitochondrial proteins. *Antioxid Redox Signal* **16**(1)**:** 45-56.

Sweeney HL, Yang Z, Zhi G, Stull JT, Trybus KM (1994). Charge replacement near the phosphorylatable serine of the myosin regulatory light chain mimics aspects of phosphorylation. *Proc Natl Acad Sci U S A* **91**(4)**:** 1490-1494.

Szewczyk MM, Davis KA, Samson SE, Simpson F, Rangachari PK, Grover AK (2007). Ca2+-pumps and Na2+-Ca2+-exchangers in coronary artery endothelium versus smooth muscle. *J Cell Mol Med* **11**(1)**:** 129-138.

Szewczyk MM, Pande J, Grover AK (2008). Caloxins: a novel class of selective plasma membrane Ca2+ pump inhibitors obtained using biotechnology. *Pflugers Arch* **456**(2)**:** 255-266.

Tabara Y, Kohara K, Kita Y, Hirawa N, Katsuya T, Ohkubo T*, et al.* (2010). Common variants in the ATP2B1 gene are associated with susceptibility to hypertension: the Japanese Millennium Genome Project. *Hypertension* **56**(5)**:** 973-980.

Taggart MJ, Wray S (1997). Agonist mobilization of sarcoplasmic reticular calcium in smooth muscle: functional coupling to the plasmalemmal Na+/Ca2+ exchanger? *Cell Calcium* **22**(5)**:** 333-341.

Taguchi K, Ueda M, Kubo T (1997). Effects of cAMP and cGMP on L-type calcium channel currents in rat mesenteric artery cells. *Jpn J Pharmacol* **74**(2)**:** 179-186.

Takahashi K, Kitamura K (1999). A point mutation in a plasma membrane Ca(2+)-ATPase gene causes deafness in Wriggle Mouse Sagami. *Biochem Biophys Res Commun* **261**(3)**:** 773-778.

Takeuchi F, Isono M, Katsuya T, Yamamoto K, Yokota M, Sugiyama T*, et al.* (2010). Blood pressure and hypertension are associated with 7 loci in the Japanese population. *Circulation* **121**(21)**:** 2302-2309.

Tempel BL, Shilling DJ (2007). The plasma membrane calcium ATPase and disease. *Subcell Biochem* **45:** 365-383.

Testa JE, Chrastina A, Oh P, Li Y, Witkiewicz H, Czarny M*, et al.* (2009). Immunotargeting and cloning of two CD34 variants exhibiting restricted expression in adult rat endothelia in vivo. *Am J Physiol Lung Cell Mol Physiol* **297**(2)**:** L251-262.

Thakali KM, Kharade SV, Sonkusare SK, Rhee SW, Stimers JR, Rusch NJ (2010). Intracellular Ca2+ silences L-type Ca2+ channels in mesenteric veins: mechanism of venous smooth muscle resistance to calcium channel blockers. *Circ Res* **106**(4)**:** 739-747.

Touyz RM (2003). The role of angiotensin II in regulating vascular structural and functional changes in hypertension. *Curr Hypertens Rep* **5**(2)**:** 155-164.

Trebak M (2012). STIM/Orai signalling complexes in vascular smooth muscle. *J Physiol* **590**(Pt 17)**:** 4201-4208.

Tsien RW, Ellinor PT, Horne WA (1991). Molecular diversity of voltage-dependent Ca2+ channels. *Trends Pharmacol Sci* **12**(9)**:** 349-354.

Tsien RW, Tsien RY (1990). Calcium channels, stores, and oscillations. *Annu Rev Cell Biol* **6:** 715-760.

Ueda K, Valdivia C, Medeiros-Domingo A, Tester DJ, Vatta M, Farrugia G*, et al.* (2008). Syntrophin mutation associated with long QT syndrome through activation of the nNOS-SCN5A macromolecular complex. *Proc Natl Acad Sci U S A* **105**(27)**:** 9355-9360.

van Breemen C, Saida K (1989). Cellular mechanisms regulating [Ca2+]i smooth muscle. *Annu Rev Physiol* **51:** 315-329.

VanBavel E, Siersma P, Spaan JA (2003). Elasticity of passive blood vessels: a new concept. *Am J Physiol Heart Circ Physiol* **285**(5)**:** H1986-2000.

Vanhoutte PM (1989). Endothelium and control of vascular function. State of the Art lecture. *Hypertension* **13**(6 Pt 2)**:** 658-667.

Venema VJ, Ju H, Zou R, Venema RC (1997). Interaction of neuronal nitric-oxide synthase with caveolin-3 in skeletal muscle. Identification of a novel caveolin scaffolding/inhibitory domain. *J Biol Chem* **272**(45)**:** 28187-28190.

Voss J, Birmachu W, Hussey DM, Thomas DD (1991). Effects of melittin on molecular dynamics and Ca-ATPase activity in sarcoplasmic reticulum membranes: time-resolved optical anisotropy. *Biochemistry* **30**(30)**:** 7498-7506.

Wagenseil JE, Mecham RP (2009). Vascular extracellular matrix and arterial mechanics. *Physiol Rev* **89**(3)**:** 957-989.

Waldron GJ, Ding H, Lovren F, Kubes P, Triggle CR (1999). Acetylcholine-induced relaxation of peripheral arteries isolated from mice lacking endothelial nitric oxide synthase. *Br J Pharmacol* **128**(3)**:** 653-658.

Walker RL, Hume JR, Horowitz B (2001). Differential expression and alternative splicing of TRP channel genes in smooth muscles. *Am J Physiol Cell Physiol* **280**(5)**:** C1184-1192.

Wamhoff BR, Bowles DK, Owens GK (2006). Excitation-transcription coupling in arterial smooth muscle. *Circ Res* **98**(7)**:** 868-878.

Wheeler EC, Brenner ZR (1995). Peripheral vascular anatomy, physiology, and pathophysiology. *AACN Clin Issues* **6**(4)**:** 505-514.

Whittle BJ, Kauffman GL, Moncada S (1981). Vasoconstriction with thromboxane A2 induces ulceration of the gastric mucosa. *Nature* **292**(5822)**:** 472-474.

Widmann MD, Weintraub NL, Fudge JL, Brooks LA, Dellsperger KC (1998). Cytochrome P-450 pathway in acetylcholine-induced canine coronary microvascular vasodilation in vivo. *Am J Physiol* **274**(1 Pt 2)**:** H283-289.

Wilkins BJ, Dai YS, Bueno OF, Parsons SA, Xu J, Plank DM*, et al.* (2004). Calcineurin/NFAT coupling participates in pathological, but not physiological, cardiac hypertrophy. *Circ Res* **94**(1)**:** 110-118.

Williams JC, Armesilla AL, Mohamed TM, Hagarty CL, McIntyre FH, Schomburg S*, et al.* (2006). The sarcolemmal calcium pump, alpha-1 syntrophin, and neuronal nitric-oxide synthase are parts of a macromolecular protein complex. *J Biol Chem* **281**(33)**:** 23341-23348.

Withers SB, Taggart MJ, Baker P, Austin C (2009). Responses of isolated pressurised rat uterine arteries to changes in pressure: effects of pre-constriction, endothelium and pregnancy. *Placenta* **30**(6)**:** 529-535.

Woodrum DA, Brophy CM (2001). The paradox of smooth muscle physiology. *Mol Cell Endocrinol* **177**(1-2)**:** 135-143.

Wu KD, Lytton J (1993). Molecular cloning and quantification of sarcoplasmic reticulum Ca(2+)-ATPase isoforms in rat muscles. *Am J Physiol* **264**(2 Pt 1)**:** C333-341.

Wu X, Chang B, Blair NS, Sargent M, York AJ, Robbins J*, et al.* (2009). Plasma membrane Ca2+-ATPase isoform 4 antagonizes cardiac hypertrophy in association with calcineurin inhibition in rodents. *J Clin Invest* **119**(4)**:** 976-985.

Yagi S, Becker PL, Fay FS (1988). Relationship between force and Ca2+ concentration in smooth muscle as revealed by measurements on single cells. *Proc Natl Acad Sci U S A* **85**(11)**:** 4109-4113.

Yamamoto Y, Imaeda K, Suzuki H (1999). Endothelium-dependent hyperpolarization and intercellular electrical coupling in guinea-pig mesenteric arterioles. *J Physiol* **514 (Pt 2)**(Pt 2)**:** 505-513.

Yamazaki M, Stekiel TA, Bosnjak ZJ, Kampine JP, Stekiel WJ (1998). Effects of volatile anesthetic agents on in situ vascular smooth muscle transmembrane potential in resistance- and capacitance-regulating blood vessels. *Anesthesiology* **88**(4)**:** 1085-1095.

Yao A, Su Z, Nonaka A, Zubair I, Lu L, Philipson KD*, et al.* (1998). Effects of overexpression of the Na+-Ca2+ exchanger on [Ca2+]i transients in murine ventricular myocytes. *Circ Res* **82**(6)**:** 657-665.

Yogo K, Shimokawa H, Funakoshi H, Kandabashi T, Miyata K, Okamoto S*, et al.* (2000). Different vasculoprotective roles of NO synthase isoforms in vascular lesion formation in mice. *Arterioscler Thromb Vasc Biol* **20**(11)**:** E96-E100.

You J, Johnson TD, Marrelli SP, Bryan RM, Jr. (1999). Functional heterogeneity of endothelial P2 purinoceptors in the cerebrovascular tree of the rat. *Am J Physiol* **277**(3 Pt 2)**:** H893-900.

Young F, Capewell S, Ford ES, Critchley JA (2010). Coronary mortality declines in the U.S. between 1980 and 2000 quantifying the contributions from primary and secondary prevention. *Am J Prev Med* **39**(3)**:** 228-234.

Zarain-Herzberg A, MacLennan DH, Periasamy M (1990). Characterization of rabbit cardiac sarco(endo)plasmic reticulum Ca2(+)-ATPase gene. *J Biol Chem* **265**(8)**:** 4670-4677.

Zhang J, Berra-Romani R, Sinnegger-Brauns MJ, Striessnig J, Blaustein MP, Matteson DR (2007). Role of Cav1.2 L-type Ca2+ channels in vascular tone: effects of nifedipine and Mg2+. *Am J Physiol Heart Circ Physiol* **292**(1)**:** H415-425.

Zhang J, Lee MY, Cavalli M, Chen L, Berra-Romani R, Balke CW*, et al.* (2005). Sodium pump alpha2 subunits control myogenic tone and blood pressure in mice. *J Physiol* **569**(Pt 1)**:** 243-256.

Zhang J, Ren C, Chen L, Navedo MF, Antos LK, Kinsey SP*, et al.* (2010a). Knockout of Na+/Ca2+ exchanger in smooth muscle attenuates vasoconstriction and L-type Ca2+ channel current and lowers blood pressure. *Am J Physiol Heart Circ Physiol* **298**(5)**:** H1472-1483.

Zhang J, Wier WG, Blaustein MP (2002). Mg2+ blocks myogenic tone but not K+-induced constriction: role for SOCs in small arteries. *Am J Physiol Heart Circ Physiol* **283**(6)**:** H2692-2705.

Zhang Y, Wang QL, Zhan YZ, Duan HJ, Cao YJ, He LC (2010b). Role of store-operated calcium entry in imperatorin-induced vasodilatation of rat small mesenteric artery. *Eur J Pharmacol* **647**(1-3)**:** 126-131.

Zhi G, Herring BP, Stull JT (1994). Structural requirements for phosphorylation of myosin regulatory light chain from smooth muscle. *J Biol Chem* **269**(40)**:** 24723-24727.

Zvaritch E, James P, Vorherr T, Falchetto R, Modyanov N, Carafoli E (1990). Mapping of functional domains in the plasma membrane Ca2+ pump using trypsin proteolysis. *Biochemistry* **29**(35)**:** 8070-8076.

Zylinska L, Kozaczuk A, Szemraj J, Kargas C, Kowalska I (2007). Functional importance of PMCA isoforms in growth and development of PC12 cells. *Ann N Y Acad Sci* **1099:** 254-269.

Zylinska L, Soszynski M (2000). Plasma membrane Ca2+-ATPase in excitable and nonexcitable cells. *Acta Biochim Pol* **47**(3)**:** 529-539.